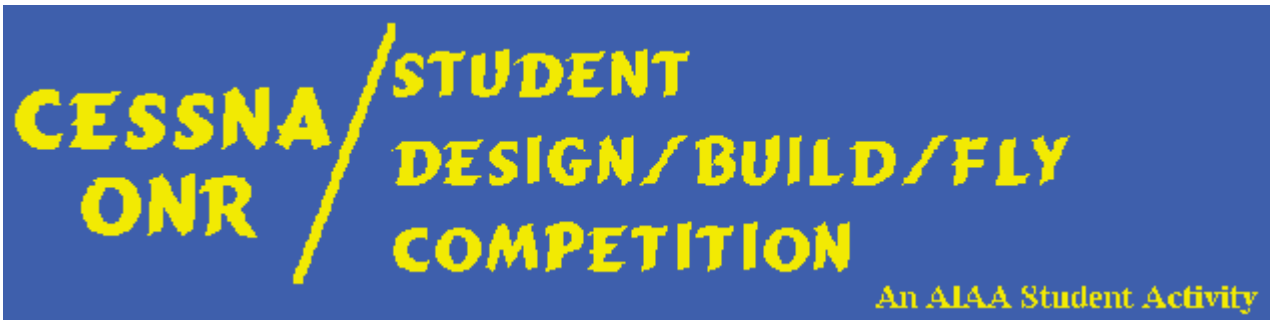

The 2005 Cessna/ONR Student Design/Build/Fly competition was held at the Webster Field annex of the Patuxent Naval Air Station in St. Inigoes Maryland over the weekend of 22-24 April. Thirty six teams from the United States, Canada, Italy, Israel and Turkey attended the contest fly-off weekend. Of the 36 teams attending the fly-off competition, 20 made at least one successful scoring flight attempt, with several teams completing all of their allowed five flight attempts during the two days of competition. The Saturday rain, which seems to be a DBF tradition, held off until after the end of the day's flying and only brief sprinkles on Sunday interfered with otherwise perfect flying weather.

The design objective for this years competition was to create an airplane that would fit in a 2 x 4 x 1 foot shipping container and was scored on the best two of three possible different missions. The 2005 missions included a simulated Sensor Deployment and repositioning mission; a Maximum Utilization and precision flight planning mission; and a Re-supply mission. Each mission was assigned its own Degree of Difficulty multiplier factor. The total score for each team is comprised of their flight performance on their best single flight of each of two different mission types, their score on a written report documenting their aircraft design and selection, and a "Rated Aircraft Cost" representing the complexity and manufacturing costs of their design.

Continuing this year the Design Engineering Technical Committee sponsored prizes for the top five teams in the form of copies of their Aerospace Design Engineering Guide handbook. This additional support, above and beyond their participation as one of the administering Technical Committees, is greatly appreciated.

The final results showed a very close battle between the two teams from Oklahoma State University, with Team Black the final victor. Oklahoma State University Team Orange placed second. The Washington State University team Wazzugar Flieger placed third. The highest written report score, 98.0, was the submission from the University of Illinois team (Un)Stable Mable. The aircraft with the lowest RAC which obtained at least one scoring flight was the tri-plane from Mississippi State University team Skeletor. The final positions and scores for all of the competing teams are listed in the table below.

First Place: Oklahoma State University, Team Black

Second Place: Oklahoma State University, Orange Team

Third Place: Washington State University, Wazzugar Fieiger

More details on the 2005 competition objectives and rules can be found at the contest web site at http://www.ae.uiuc.edu/aiaadbf .

The success of the competition required the efforts of many individuals. Our first thanks goes to the judges who assisted in the operation, technical inspections and scoring of the flight competition, and to the many judges who evaluated and scored the teams written reports. Thanks also go to the Applied Aerodynamics, Aircraft Design, Design Engineering, and Flight Test Technical committees of the AIAA who organized and manage the competition, and the AIAA Foundation for their administrative support. Thanks are also due to the competitions corporate supporters, the Cessna Aircraft Company and the Office of Naval Research. A special thanks goes to the Patuxent River Naval Air Station and Webster Field personnel for hosting this years event and providing access to their facilities and the flying field. A final thanks goes to VC-6 for providing the food service to 500 hungry college students.

Overall the 2005 Cessna/ONR Student Design/Build/Fly competition marked another very successful event, allowing the participating students to mix a highly enlightening educational experience with a good dose of fun. Congratulations to all the teams who participated for your great enthusiasm and achievement.

See you next year.

Greg Page
for the DBF Governing Committee

University	Entry Name	Paper Score	RAC	Flight Score	Total Score	Positions
Oklahoma State University	OSU Team Black	91.00	7.82	**25.84**	300.85	1
Oklahoma State University	OSU Orange Team	91.75	7.59	24.59	297.26	2
Washington State University	Wazzugar Flieger	88.15	7.12	20.36	252.19	3
Virginia Polytechnic University	Orange Effect	95.65	7.56	14.48	183.32	4
University of California, San Diego	TLARExtreme	72.50	9.51	23.53	179.43	5
Utah State University	Lady Satan	91.90	7.75	9.58	113.66	6
University of Southern California	Cardinal & Gold SChlager	86.75	8.16	9.51	101.05	7
University of Florida	Gator-Raid	79.50	9.10	10.63	92.85	8
Istanbul Technical University	Hezarfen	64.00	8.36	9.93	76.00	9
Technion	ALBATROS	87.50	7.41	5.84	69.04	10
Middle East Technical University	ANATOLIAN-CRAFT	89.25	9.47	7.20	67.80	11
University of California, Irvine	AntEaterOne	86.00	15.11	10.60	60.33	12
University of Illinois, Urbana-Champain	(Un)Stable Mable	**98.00**	7.06	2.00	27.77	13
West Virginia University	Sally II	61.65	11.94	4.00	20.65	14
Western Michigan University	FUBAR	86.63	9.76	2.00	17.76	15
Wichita State University	DCM-006	91.75	10.77	2.00	17.03	16
Mississippi State University	Skeletor	87.73	**6.23**	1.00	14.07	17
University of California, Los Angeles	Kamikaze	88.40	12.94	2.00	13.67	18
West Virginia University	Mindy	39.85	10.55	2.00	7.55	19
University of Texas at Arlington	Dawdling Pelican	39.00	16.33	2.00	4.78	20
University of Colorado at Boulder	Alpine Storm	82.07	6.76	0.00	0.121	21
Istanbul Technical University	ATA - 6	85.95	7.54	0.00	0.114	22
California State Polytechnic University, Pomona	Cal Poly Pomona, AeRecon	80.00	7.30	0.00	0.110	23
Georgia Institute of Technology	GT6	92.50	8.79	0.00	0.105	24
San Diego State University	Monty's Pride	84.25	9.87	0.00	0.085	25
University of Washington	HuskyWorks - Sirius	77.05	9.50	0.00	0.081	26
University of Texas at Austin	The Mother Shrew	88.50	12.16	0.00	0.073	27
Queen's University	Goose	78.75	10.95	0.00	0.072	28
University of Oklahoma	Gordo	72.75	10.66	0.00	0.068	29
University of Texas at Austin	Bevo XIV	83.25	12.42	0.00	0.067	30
Purdue University	Boilermaker Bomber	82.50	13.04	0.00	0.063	31
Università degli Studi di Napoli	Eracle	73.00	11.75	0.00	0.062	32
University of Arizona	Quit Stalling	80.25	13.15	0.00	0.061	33
University of Central Florida	The Reaper	60.00	18.23	0.00	0.033	34
US Military Academy	The Spicy Chicken	61.90	21.67	0.00	0.029	35
The State University of New York at Buffalo	Gilbird	42.50	20.59	0.00	0.021	36
University of Maryland, College Park	Turtle Dynamics	79.98	100.00	0.00	0.000	37
Syracuse University, NY	The Orange Knight	77.50	100.00	0.00	0.000	38
Case Western Reserve University	Project Mayhem	72.79	100.00	0.00	0.000	39
City College of New York	SPECIAL DELIVERY	72.25	100.00	0.00	0.000	40
University of Alabama-Tuscaloosa	BAMA B.A.L.D.	69.50	100.00	0.00	0.000	41
The State University of New York at Buffalo	SOBA Lawn Dart	52.00	100.00	0.00	0.000	42
Arizona State University	Air Devils	40.25	100.00	0.00	0.000	43
Columbia University, NY	Flyin' Lion	37.53	100.00	0.00	0.000	44

Highest Report Score

(Un)Stable Mable

Final Design Report

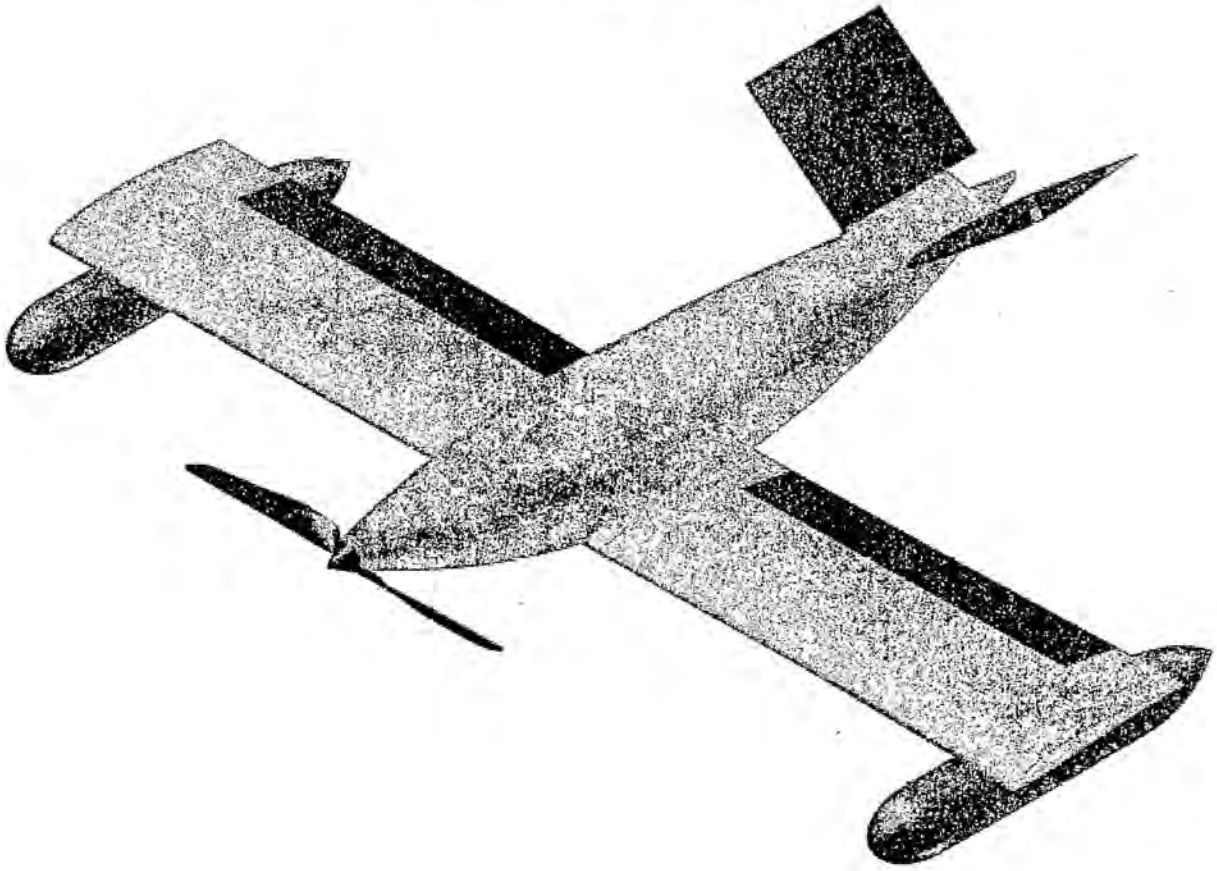

2004/2005 Cessna and ONR

AIAA Design/Build/Fly Competition

Webster Field

St. Inigos, Maryland

Submitted by

Department of Aerospace Engineering

University of Illinois at Urbana-Champaign

March 8, 2005

Table of Contents

1.0 Executive Summary

This report describes the process used to design (Un)Stable Mable, the University of Illinois' entry into the 2004-2005 AIAA Design/Build/Fly competition. The goal of the design was to maximize the competition score, which is a combination of the report score, the total flight score and the rated aircraft cost (RAC). Analysis of the mission requirements and estimates of the mission performance results showed that the competition score was maximized by optimizing the design of the airplane to fly only two of the three specified missions; the Sensor Reposition mission and the Re-Supply mission.

The conceptual design analysis focused on selecting the configuration that would maximize the competition score. The competition rules were analyzed to determine design requirements, and to identify the most important elements of the RAC equation. It was found that for all designs, the Sensor Reposition mission and Re-Supply mission outscored the Maximum Utilization mission. Therefore, the airplane was optimized to perform these two missions. The empty weight of the airplane was seen to be the most significant contributor the RAC, so minimizing the empty weight was a major objective throughout the design process. The ability to disassemble the airplane was also a factor since the airplane needed to be place in a 4 ft by 2 ft by 1 ft box at the end of each mission. A morphological chart was used to investigate thousands of possible airplane configurations. These were narrowed down through qualitative arguments to eight configurations that were analyzed using a figure of merit (FOM) analysis. These eight configurations were comprised of four variations on the conventional configuration, two flying wing configurations, a canard configuration and a joined wing configuration. The analysis included the RAC, predicted mission performance, qualitative scores for ground handling, internal payload storage, external payload storage, stability and control, and manufacturability for each configuration. Based on the FOM analysis, a flying wing configuration without vertical stabilizers was determined to provide the highest competition score. Initial preliminary design analyses of the flying wing design showed that this was not the case and that some of the assumptions made during the concept design were not valid. Wing tunnel testing showed that the expected maximum lift coefficients were not achievable. Stability and control analyses indicated that vertical stabilizing surfaces would be needed to provide adequate directional stability. Based on these considerations, the FOM results from the conceptual design study were revisited and the next highest scoring configuration, a conventional V-tail, was chosen. A tricycle landing gear with a steerable nose wheel and brakes was selected for its ground handling capabilities.

During the preliminary design analyses, the critical design variables were determined, an optimum design was developed, and the design was refined with detailed aerodynamic and stability and control analyses. The critical design variables were determined to be the propulsion system, wing area, aspect ratio, fuselage length, and cruise throttle setting. A performance code was used to integrate the flight path of the airplane over the specified missions. This code included aerodynamic, propulsion, weight and RAC models to allow evaluation of the competition score for a given set of design variables. An optimization code was used to analyze tens of thousands of designs and determine the optimum design. The results of the optimization led to an airplane with a wing area of 4 ft^2, an aspect ratio of 5.5, a

fuselage length of 3.5 ft and a propulsion system utilizing a Hacker B50-13S motor with a 6.7:1 gearbox, 16 GP1100 cells and a 17x13 propeller. The detailed aerodynamic analysis led to the selection of the SD7043 airfoil for the wing and the NACA0009 for the V-tail surfaces. Three degrees of washout were incorporated into the wings. The empennage and control surfaces were sized using static and dynamic stability and control analyses.

In the detailed design analyses the payload system design was finalized, the final components for the airplane were selected, and the manufacturing drawings of the airplane were generated. A computational fluid dynamics (CFD) analysis was used to design the payload fairings. Two release mechanisms were built and tested for the external payload release requirement. The final design weighed 5.65 lb and allowed for quick reloading of the payloads. The lightest flight control system components that met performance requirements were selected. A commercially available, hydraulic brake system was selected for its significant weight savings over pneumatic and magnetic alternatives. Rotary drive systems (RDS) were used for flight control surface actuation. These allowed for completely internal control surface actuators, reducing drag and improving durability. A molded composite construction method was selected for the wing, V-tail and fuselage because it had superior shape fidelity and provided a very light structure.

The predicted empty weight for (Un)Stable Mable was 5.65 lb which gives a greater than 50% payload fraction. The final RAC for the design was 5.98 and the predicted total flight score was 29.06. The airplane was expected to finish the Sensor Reposition mission in 201 seconds and the Re-Supply mission in 250 seconds. The airplane can be disassembled and placed in the box in less than 10 seconds by simple removal of the wings and V-tail surfaces.

2.0 Management Summary

2.1 Architecture of the Design Team

The Design/Build/Fly team at the University of Illinois consisted of undergraduate and graduate students from the Aerospace Engineering and the Electrical and Computer Engineering departments. There were 10 returning members to the design team and approximately 10 new members recruited. The team was split into a number of technical groups with a designated leader for each. At a higher level, the team was under the direction of four experienced members; the team leader (TL), chief design engineer (CDE), assistant chief manufacturing engineer (ACME) and chief manufacturing engineer (CME). The team leader was responsible for running meetings, fundraising, procurement and other administrative tasks. The chief design engineer kept the airplane design progressing and delegated tasks to the various technical groups. The assistant and chief manufacturing engineers were responsible for construction and flight testing of the airplane. Each member of the design team belonged to at least one technical group. Table 2.1 shows personnel assignments and each individual's level of participation.

2.2 Technical Groups

Each technical group was assigned a leader who was responsible for getting the group to meet the deadlines set forth by the CDE and the rest of the team. Each group consisted of anywhere between 2 and 15 team members. The aerodynamic group was responsible for evaluating the lift and drag of the

airplane. They were also tasked with selecting the airfoils for the wing and V-tail and setting the wing twist. The CAD Modeling group modeled the external shape, structure and systems of the airplane using a solid modeling program. Another group built and ran a CNC router acquired by the team. The configuration selection group consisted of all the team members who were present at the first few meetings. The goal of this group was to select the best airplane configuration to complete the specified missions.

Table 2.1 Personnel Assignment Chart

Member Name	Year	Technical Group: Aerodynamics	CAD Modeling	CNC Router	Configuration Selection	Flight Testing	Fundraising	Manufacturing	Payload Design	Performance and Optimization	Propulsion Selection	Report Writing	Stability and Control	Structural Analysis and Testing	Systems Selection and Testing	Telemetry System	Website Design
Bhamidipati, Keerti (CME)	SR		2	3	2	1	2	1	2		3	3	2	3	1	3	2
Bower, Geoffrey (TL)	SR	2		3	2	3	1	2	3	2	1	2		2	2		
Chew, Ethan (ACME)	JR		1		2	3		2	3			3		1	3		1
Franzen, Andrea	JR		3		2							2		2			2
Huckshold, Kevin	SO		2											3			
Joye, Keven	JR										2			3			
Kacmar, Tim	GRAD				2		3			1		2	3				
Kim, Amos	SR	1			2	3			2			2	3				
Krauss, JP	JR			2	2	2		2				3			2	1	
Lee, Calvin	FR	3						2	3					2			
Lee, Vincent	GRAD	2			2	3			1			3					2
Morii, Daisuke	SR	2			2	3		2	3			3					
Ogura,Hidetoshi	JR	3		2		3		2					2	2			
Pattenaude, Jim	SR		2	1	2	2		2				3			3		
Quek, Janice	FR				2			3			2	3					
Shaffer, Dustin	FR	2			2	3		3						2			
Spellman, Charles	FR			3	2	3		3									2
Tehrani, Kian	GRAD				2					2		2					
Wang, John	JR		2					2						2		3	2
Warrenburg, Sean (CDE)	SR				1	3		2				1	1		3		

Key: 1 = Group Leader, 2 = Major Contributor, 3 = Minor Contributor

The flight testing group was in charge of all testing of the system test bed airplane and the competition airplane. A very successful fundraising drive was run by the fundraising group, securing approximately $15000 for use on the project from various university and external sources. The manufacturing group was tasked with construction of the competition airplane and other test articles. The payload design group worked to optimize the payload fairing design and performed a CFD analysis. The performance and optimization group analyzed the performance of the airplane and optimized the design to obtain the highest contest score. The propulsion selection group was responsible for identifying and modeling candidate propulsion systems to be applied to the airplane and analyzed by the performance and optimization group. The report writing group was responsible for documenting the design and writing

the report. The stability and control group was in charge of analyzing the static and dynamic stability characteristics of the airplane and sizing the control surfaces. Structural design, analysis, and testing of the airplane were carried out by the structural analysis and testing group. The systems selection and testing group selected all of the sub-systems included on the airplane, including the servos, radio, landing gear and brakes. The telemetry group was in charge of developing a real-time telemetry and inertial navigation system to aid in flight testing of the airplane. Lastly, the website design group developed and maintained the team's website.

2.3 Scheduling, Configuration and Document Control

The first task for the team was to set an aggressive, yet achievable schedule. From previous experience in these projects, it was clear that there was a strong correlation between placing in the contest and the amount of flight testing conducted with the competition airplane. In order to meet the aggressive schedule, two team meetings were held each week from September through April. In addition, each technical group met at least once a week when it had an approaching deadline. Figure 2.1 shows the milestone chart for the design, construction and testing of (Un)Stable Mable.

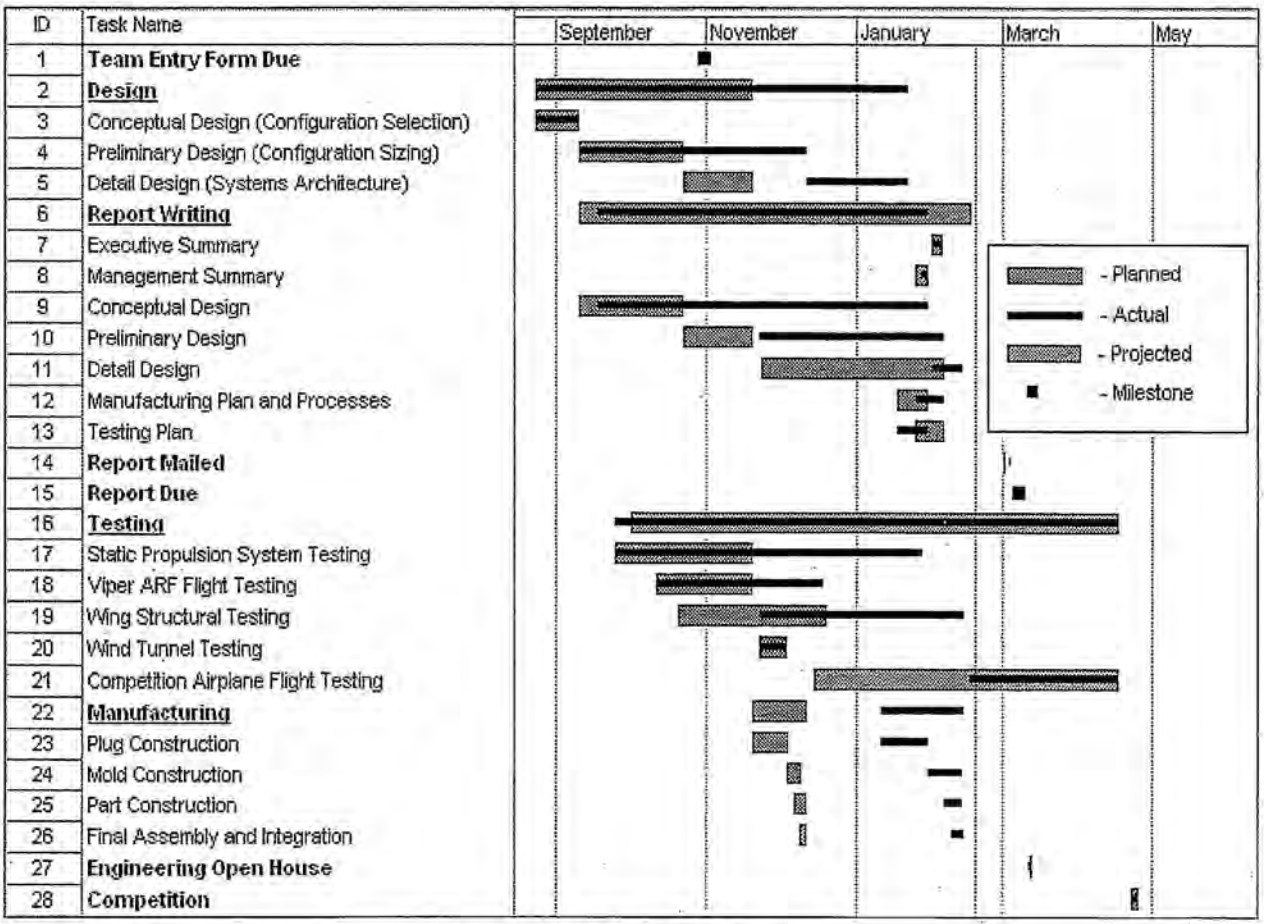

Figure 2.1 Milestone Chart

To facilitate easy communication and document control, an email newsgroup was set up for the design team members. In addition, the minutes of each meeting were typed up and sent to members of the team for a record of what was discussed. Storage space was also set aside on the Aerospace Engineering Department's network for storing team computer programs, documents, and drawings.

3.0 Conceptual Design

This section discusses the details of the conceptual design studies for (Un)Stable Mable. To begin these studies, a morphological chart of possible airplane configurations was developed. Many of these configurations were qualitatively eliminated based on feasibility considerations. The remaining eight configurations were analyzed based on figures of merit. The missions were analyzed to determine which two out of the three gave the highest single flights cores. The highest scoring configuration was selected to be refined in the preliminary design.

3.1 Mission and Design Requirements

There were a number of payload, structural, performance and propulsion system requirements the airplane had to meet. The 2004/2005 Design/Build/Fly competition includes three missions, two of which must be completed. The single flight scores (SFS) for the two highest scoring missions are used to determine the total flight score (TFS).

3.1.1 Payload Requirement

The airplane is required to carry two 3 lb payloads in two configurations; internally within the fuselage and externally on hard points within three inches of the wing tips. The payloads must be based on a 12 inch long section of 3 inch diameter PVC pipe. The PVC pipe must be capped, but may be faired. The payloads must be mechanically secured in both configurations, and capable of being remotely dropped in the external configuration.

3.1.2 Sensor Reposition Mission (SR)

This mission requires the airplane to fly three laps with a single 360° degree turn during the downwind leg of the flight pattern outlined in the rules.[1] The first lap requires the two payloads to be in their external configuration. Upon landing the airplane is to deploy each payload at prescribed locations on the runway, before taking off to fly the second lap unloaded. Upon landing, the airplane must come to a complete stop before the flight crew reloads the payloads. The final lap is then flown with the payloads in their external configuration. The airplane must cross the starting line upon landing and come to a complete stop before the flight crew can retrieve and disassemble the airplane. This mission has a difficulty factor of 2.0.

3.1.3 Re-Supply Mission (RS)

For this mission, the airplane needs to fly four laps. During the first and third laps, the payloads are in the internal configuration. After these laps, the airplane lands and the payloads are removed by the ground crew. The second and fourth laps are flown without payloads. After the second lap, the payloads are reloaded into the airplane by the ground crew. After the fourth lap, the airplane is disassembled and placed in the box by the ground crew. This mission has a difficulty factor of 1.5.

3.1.4 Maximum Utilization Mission (MU)

This mission requires the airplane to fly with the payloads in the internal configuration. The airplane must fly as many laps as possible within a six-minute time period. Each lap flown requires two 360° turns during the downwind leg. Six minutes is the maximum time for the mission. The mission time ends once the airplane comes to a complete stop and the flight crew disassembles the airplane and places it in the box. This mission has a difficulty factor of 1.0.

3.1.5 Structural Requirements

The airplane maximum weight may not exceed 55lb. During technical inspection the airplane must undergo upright and inverted wing tip tests at the maximum payload capacity without failure. This test generates root bending moments that are approximately equivalent to a 2.5g turn.

3.1.6 Airplane Storage Requirement

At the end of each mission the airplane must be disassembled and placed within a 1ft x 2ft x 4ft box. The disassembly time is counted in the mission times, which don't end until the box is closed and latched.

3.1.7 Takeoff Requirement

The maximum takeoff distance for each mission is 150 feet. The wheels must be off the runway in under this distance.

3.1.8 Propulsion System Requirements

The airplane must be powered by an electric propulsion system. The maximum current is limited to 40 Amps by means of a 40 Amp fuse. The motor(s) must be brushed or brushless commercial electric motor(s). The battery packs must consist of over-the-counter NiCad or NiMH cells. The battery pack must weigh less than 3lb. The propeller(s) must be commercially available and may not be modified, with the exception of balancing.

3.2 Competition Score and Rated Aircraft Cost Analyses

To obtain the highest competition score it was necessary analyze the three missions and the Rated Aircraft Cost (RAC) equation to find the elements that were the most important to the competition score. The competition score depends on three elements; the report score, the TFS, and the RAC.

$$\text{SCORE} = (\text{Written Report Score} * \text{TFS}) / \text{RAC} \tag{3.1}$$

3.2.1 Total Flight Score Analysis

The TFS is the sum of the two highest SFSs from two of the three different missions. The three single flight scores are calculated using the mission times or number of laps flown, and the appropriate mission difficulty factors. The mission time is defined as the time in minutes from when the airplane first crosses the start line until the lid of the box is latched with the airplane inside. Equations 3.2 through 3.4 show how the single flight score is calculated each of the three missions.

$$\text{SR SFS} = 2.0 * (12 - \text{Mission Time}) \tag{3.2}$$

$$\text{MU SFS} = 1.0 * \text{Number of Laps} \tag{3.3}$$

$$\text{RS SFS} = 1.5 * (12 - \text{Mission Time}) \tag{3.4}$$

The RS mission SFS is reduced if all four sorties are not flown during the mission. If only three sorties are flown the 12 in Eq. (3.4) is replaced with 6, and if only two sorties are flown it is replaced with 3.

Upon inspection of the three SFS equations it appeared that the SR and RS missions would give the highest TFS. To verify this, approximate analyses were conducted on the SFSs. It was assumed that a lap in the MU mission would take 0.75 minutes; this was an optimistic assumption based on the fastest lap times at the competition last year.[2] It was also assumed that the lap times for the SR and RS missions would be about 1.5 minutes, which is comparatively slow. Next, it was assumed that the same airplane would be able to fly all three missions optimally, so the RAC would be the same for all three missions and the best missions could be identified from their SFSs alone. In reality this would not be the case, since it would require more total energy to fly the MU mission, increasing the propulsion battery weight and the RAC. Using these assumptions the SFS for the three missions were determined as shown in Table 3.1. Even with these assumptions that favor the MU mission; the two highest scoring missions would be the RS and SR. From this point forward, the focus of the design was to optimize for these two missions.

Table 3.1 Mission SFS Analysis

Mission	Lap Time (min)	Mission Time (min)	Number of Laps	SFS
SR	1.5	4.5	3	11
RS	1.5	6	4	9
MU	0.75	6	8	8

3.2.2 RAC Analysis

Next, the RAC equation was analyzed to determine what factors were the greatest contributors. Since the competition score is inversely related to the RAC, the goal was to reduce the RAC as much as possible. The formula for the RAC is described below:

RAC ($, thousands) = (A*MEW + B*REP + C*MFHR)/1000

- A = $500 / pound, the Manufacturer's Empty Weight Multiplier,
- B = $1000 / pound, the Rated Engine Power Multiplier,
- C = $20 / hour, the Manufacturing Cost Multiplier,
- MEW, the Manufacturer's Empty Weight, is the weight of the airplane and its systems without the payload,
- REP, the Rated Engine Power, is computed based on the equation
  REP = (1+0.25*(#engines – 1))*Total Battery Weight [lbs]
- MFHR, the Manufacturing Man Hours, is calculated based on the equation
  MFHR = 10hr/ft^2*wing span*maximum wing chord*# of wings
  + 5 hr*Control Surface Multiplier
  + 20 hr/ft^3 * Fuselage Length * Fuselage Width * Fuselage Height
  + 5 hr * # of vertical surfaces without control
  + 10 hr * # of vertical surfaces with control
  + 10 hr * # of horizontal surfaces
  + 5 hr * # of servos or controllers.

There were changes in the equation from past years, so it was likely that factors with the largest contribution to the RAC had changed. To gain an idea of the relative importance of the various areas, last year's UIUC contest entry[3] and the winning design from Oklahoma State University Black[4] were analyzed with the new RAC equation. The pie chart in Fig 3.1 indicates the percentage RAC breakdown for the two airplanes. From the chart it is obvious that the largest contributor to the RAC this year is the manufacturer's empty weight at around 50%. Keeping the empty weight low was a primary focus during the structural design and the selection of the manufacturing materials and processes.

The next most important contributions to the RAC are the battery weight and the size of the wing. It will be important to minimize weight of the propulsion batteries, a primary component of REP. Also, from the RAC equation it is evident that a 25% REP penalty is incurred for each additional motor used. Using more than one motor also increases the empty weight due to added structure and the weight of the motors themselves. Since there are motors available capable of providing enough power for all phases of flight, only one motor was considered. Keeping the wing area small is also important. It should be noted that since the wing MFHR is determined by the maximum chord and the span, tapering the wing increases the RAC for a given area. Controlling lift distribution with twist rather than taper helps minimize the RAC while helping mitigate tip stall and improve induced drag characteristics. The aspect ratio has no effect on the RAC for a given area wing.

Figure 3.1, also shows that the fuselage dimensions, empennage type and the number of servos and controllers have a relatively small effect on the RAC. Although it is important to minimize these contributions, they do not need as much attention. The fuselage dimensions are driven by the payload dimensions and stability and control requirements. The payloads determine the maximum cross section, and the length is primarily established by the tail size and location. The empennage contribution can be kept low for most configurations by using one vertical stabilizer and one horizontal stabilizer, or a V-tail. Using more stabilizing surfaces has a detrimental effect on the RAC. If the horizontal stabilizer exceeds the span limit of 25% of the wing span, then the RAC increase is large since the wing MFHR is doubled. The servo and controller contributions to the RAC are difficult to improve because the number of controllers is essentially fixed for most configurations. This is due to the need for a speed control, two aileron servos, two empennage servos, a ground steering servo and at least one payload release servo.

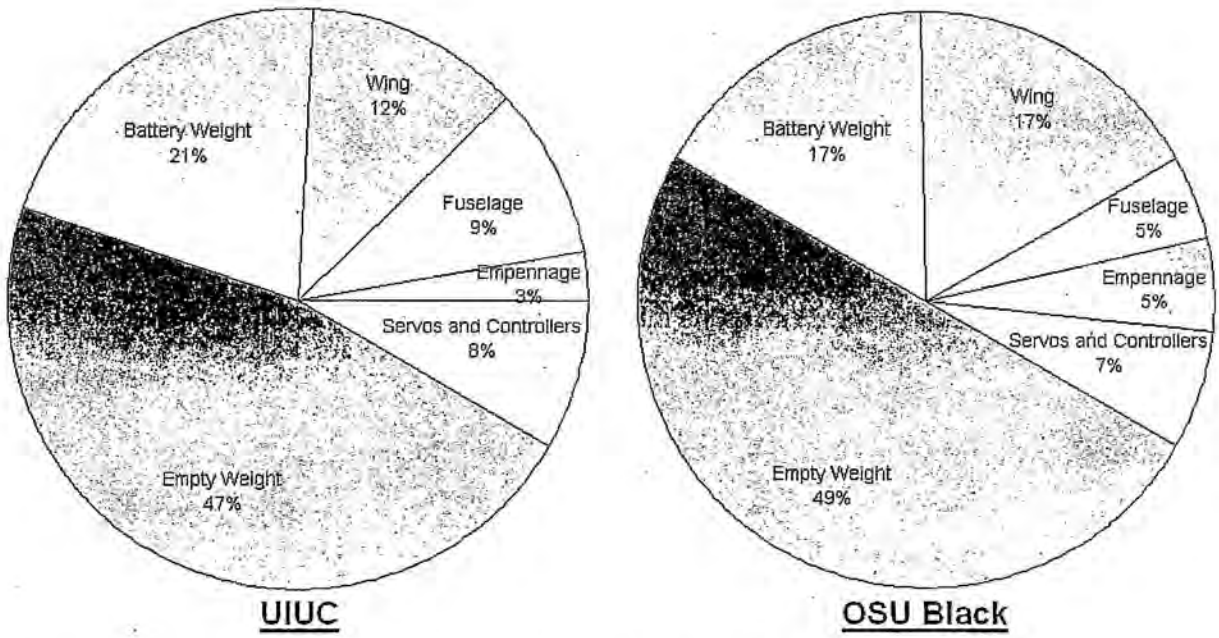

Fig. 3.1 Relative Importance of Various Factors in the RAC

3.3 Airplane Component Types Considered

For the first stage in selecting the configuration, a morphological chart of all possible airplane component types was generated. The initial morphological chart is shown in Table 3.2, and represents a total of 6480 configurations. The airplane components considered were the wing, fuselage, empennage, landing gear and propulsion system. Using this first morphological chart, the most radical and impractical component types were eliminated.

Table 3.2 Initial Morphological Chart

Component	Types				
Wing	Monoplane	Biplane	Joined	Ring	Gull
	Tandem	Tri (or greater) - wing		Annular	Channel
Fuselage	Lifting	Conventional	Pod-and-boom	Multiple	Blended
Empennage	V-tail	T-tail	Conventional	None	Canard
	Cruciform	H-tail	Vertical Only	Inverted V-tail	
Landing Gear	Tail Dragger	Bicycle	Mono-wheel	Tricycle	
Propulsion System	Pusher	Tractor	Multiple Pusher	Multiple Tractor	

3.3.1 Wing Types

Qualitative reasoning was used to eliminate some of the wing types because of their inherent structural complexity and manufacturing difficulties. The ring wing, annular wing, channel wing and gull wing were all eliminated because they created obvious structural problems with the spar, and this year the spar is very important given the requirement of carrying the payloads on the wing tips. The tandem wing and joined wing were grouped together since the joined wing is essentially a tandem with swept surfaces. The multi-wings beyond a biplane were eliminated due to added weight and complexity. The

monoplane, biplane and tandem wing were retained at this point and are shown in the revised morphological chart in Table 3.3.

3.3.2 Fuselage Types

The multiple fuselages were eliminated due to RAC and weight concerns. The pod-and-boom was eliminated since the fuselage would already be long because the payloads needed to be carried internally. The other fuselage types, lifting, conventional and blended were still considered and are shown in Table 3.3.

3.3.3 Empennage Types

The H-tail was eliminated due to the RAC penalty of having more than one vertical surface with control. It was decided to group the cruciform, T and conventional tails into the same group and refer to it as the conventional group. The V-tail and inverted V-tail were grouped as well, and the vertical only and the case of no empennage would be considered only in the event of selecting a flying wing configuration. The five remaining empennage types are shown in Table 3.3.

3.3.4 Landing Gear Types

From the mission description, it was evident that the airplane would need to have exceptional ground handling capabilities. Because of all the ground operations required during the missions it was decided to investigate the use of a braking system. The possible landing gear configurations considered were a tail dragger, bicycle, mono-wheel, and tricycle gear. Outrigger gear were also considered to support the plane after the first payload is dropped during the SR mission. None of these were eliminated since their feasibility depended on the overall size and configuration of the airplane. However, the landing gear was not included in the refined morphological chart; it was decided that it would be simpler to identify the best type of landing gear after the wing, fuselage, empennage, and propulsion types were determined.

3.3.5 Propulsion System

For the propulsion systems, either a pusher or tractor system was considered. In addition, multiple motors were considered, but quickly eliminated since sufficient power can be produced from one motor. The pusher and tractor propulsion systems were retained for further consideration and are shown in Table 3.3.

3.4 Morphological Chart

A new morphological chart was created to consider all of the possible airplane configurations that could be assembled from the remaining types of each component. This revised chart is shown in Table 3.3. There were three wing types, three fuselage types, five empennage types, and two propulsion types remaining. This resulted in 90 possible airplane configurations to investigate.

Each of the possible airplane configurations was examined to determine its feasibility and to identify any major technical problems. The main concerns that led configurations to be eliminated were potential stability problems, takeoff rotation problems, RAC concerns and problems with carrying the payload both internally and externally. For example, a biplane with a lifting fuselage was eliminated since

it would require an unreasonably tall fuselage which would hurt the RAC. Based on considerations such as these, eight configurations were selected to be evaluated quantitatively. These eight configurations were analyzed using figures of merit (FOM) and are shown in Table 3.4.

Table 3.3 Revised Morphological Chart

Component	Types				
Wing	 Monoplane	 Tandem	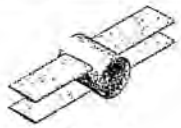 Biplane		
Fuselage	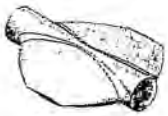 Blended	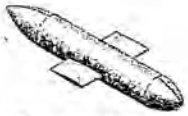 Conventional	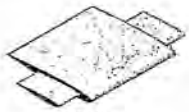 Lifting		
Empennage	 Conventional	 Canard	 Vertical Only	 V-tail	 No Tail
Propulsion	 Tractor	 Pusher			

Table 3.4 The Eight Configurations Analyzed with FOM's

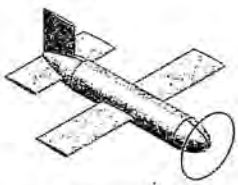 Conventional	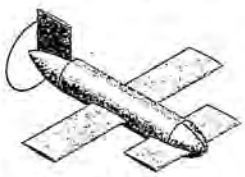 Canard	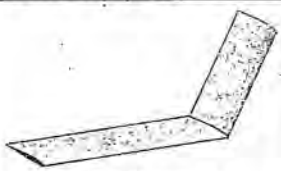 Flying Wing w/o Verticals	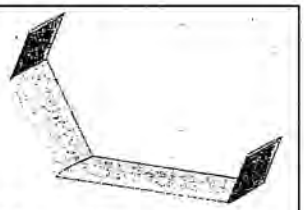 Flying Wing w/ Verticals
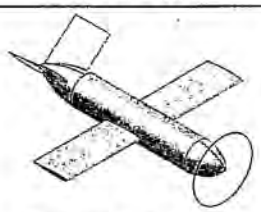 Conventional V-tail	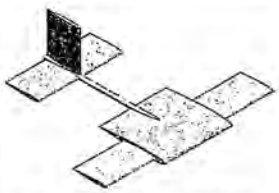 Lifting Conventional	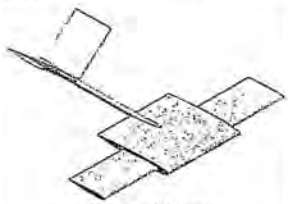 Lifting V-tail	 Joined Wing

3.5 Figures of Merit

The eight selected airplane configurations were analyzed with a number of qualitative and quantitative figures of merit. The qualitative FOM's were assigned a score between -1 and 1. These FOM's included: stability and control, ground handling, internal payload storage, external payload storage, and manufacturability. The quantitative figures of merit analyzed were the RAC and mission

performance. These were combined into a competition score by dividing the TFS by the RAC. The competition score was then normalized by dividing by the maximum competition score of the eight configurations. The normalized competition score was then used as the FOM. All of the FOM's were assigned weight factors that summed up to 100. Each FOM is related to a requirement in the rules or has a major impact on the competition score.

3.5.1 Stability and Control

In order to complete the required missions, it was essential that the airplane be both statically stable in all axes and be maneuverable enough to fly the course and withstand any wind conditions present at the contest. A stability and control figure of merit was qualitatively assigned to each configuration considered. Table 3.5 shows how the FOM scores were assigned to the configurations. The factors that were considered in applying this figure of merit were:

- Capability for robust longitudinal stability
- Inherent lateral and directional stability
- Adequate pitch control authority without excessive lift penalties
- Adequate lateral and directional control authority to allow the airplane to takeoff and land in a crosswind

This FOM was assigned a weight factor of 20 because of its effect on the overall mission performance. If the airplane is not stable or controllable, then no flight score would be posted.

Table 3.5 Stability and Control (S&C) FOM Criteria

Assigned Score	Configuration Characteristic
1	Exhibits positive S&C characteristics with respect to all criteria
0	Exhibits positive S&C characteristics with respect to two or three of the criteria
-1	Exhibits positive S&C characteristics with respect to one or zero of the criteria

3.5.2 Ground Handling

Another figure of merit that is important to the completion of the mission is the ground handling ability of the airplane. For the Re-Supply mission, the airplane will be required to taxi accurately and to stop precisely at each payload drop location. Therefore, brakes and nose wheel steering will play a very important role in the effective completion of the entire mission. In addition, having one payload mounted on a wing tip while taxing from the first drop location to the second, will require the airplane to have a wide landing gear stance to prevent the airplane from tipping. A score was qualitatively assigned to each configuration for its expected ground handling characteristics. The basis for assigning these scores is shown in Table 3.6. This FOM was given a weight factor of 8 because it influences how long the airplane will be on the ground during mission, which can be a major portion of the total mission time.

Table 3.6 Ground Handling FOM Criteria

Assigned Score	Configuration Characteristic
1	Nose wheel steering and brakes integrable
0	Tail wheel steering with brakes or Nose wheel steering without brakes
-1	Tail wheel steering without brakes

3.5.3 Internal Payload Storage

All missions require the payloads to be carried internally in the airplane. It was important that the airplane allow easy access to the payloads so that they could be quickly installed or removed. It was also important that the payload hatches not interfere with the primary load paths on the airplane. The scores were assigned as shown in Table 3.7. This FOM was given a weight factor of 5 because of its effect on the overall mission times and the integrity of the fuselage structure.

Table 3.7 Internal Payload Storage FOM Criteria

Assigned Score	Configuration Characteristic
1	Easy access and uninterrupted load paths
0	Difficult access or load paths disrupted
-1	Difficult access and load paths disrupted

3.5.4 External Payload Storage

Carrying the payloads externally near the wing tips is required by the SR mission. Some configurations would be easier than others for the integration of the required wing hard points. For some configurations, the payloads would induce undesirable twist and bending that would require additional structure. This added structure would add weight, increase the RAC and decrease performance. The basis for assigning these FOM scores is shown in Table 3.8. This FOM was given a weight factor 5 because it directly affects the ability of the airplane to perform the SR mission.

Table 3.8 External Payload Storage FOM Criteria

Assigned Score	Configuration Characteristic
1	Can hold the payloads on the wing tips without structural issues
0	Can hold the payloads on the wing tips, but requires some structural support
-1	Can hold the payloads on the wing tips with, but requires a lot of structural support

3.5.5 Manufacturability

For every airplane studied, a qualitative figure of merit was assigned based on its manufacturability. Each airplane's manufacturability is defined by the impact it has on the RAC, its airworthiness, and that the team has the ability and experience to construct the airplane in a reasonable amount of time. Based on these factors a score was qualitatively assigned to each of the eight configurations considered. Table 3.9 shows the criteria for assigning these scores. This FOM was given a weight factor of 7 due to its impact on the RAC.

Table 3.9 Manufacturability FOM Criteria

Assigned Score	Configuration Characteristic
1	Experience building, structurally simple
0	Little or no experience building or structurally complex
-1	Little or no experience building and structurally complex

3.5.6 Rated Aircraft Cost

One of the quantitative figures of merit was the RAC. The competition score for the airplane is computed using this value. It was important to reduce the RAC in order to maximize the competition score. For each of the eight airplane configurations considered, the RAC was computed. A spreadsheet-

based, weight-and-RAC model was developed to evaluate each of the configurations. The estimated weights helped to size the configurations and to determine the manufacturer's empty weight contribution to the RAC.

3.5.7 Estimated Mission Performance

The other quantitative figure of merit was the estimated mission performance of each configuration. This was an important FOM because it is directly used in the computation of the competition score. The performance of the different configurations was analyzed using a performance code written in MATLAB.[5] The code used to a fourth order Runge-Kutta method to integrate the airplane equations of motion over the SR and RS missions. The mission model used is described in Section 4.2. The code output distances, time and energy used during each time step. Using the times for the SR and RS missions enabled their single flight scores to be computed. These were then summed to determine the total flights score and divided by the RAC to get the competition score without the report contribution. This FOM was given a weight factor of 55 since it is representative of the actual competition score.

The eight selected configurations were sized using a common propulsion system so that the mission performance of the different configurations could be compared. Simplified weight and aerodynamic models were used to for determining the wing loadings and aerodynamic characteristics of the airplanes. All six of the non-flying wing configurations were sized to a wing loading of 3 lb/ft^2. The two flying wing configurations were sized to a wing loading of 2.5 lb/ft^2. This was done since the maximum lift coefficient of the flying wing designs would be less than for the conventional designs. This would enable the flying wing to takeoff in less than 150 ft while using the same propulsion system as the other configurations. Other assumptions were made to make a comparison of the designs. The aspect ratio was kept constant at 8, the spans of the horizontal empennage surfaces were kept under 25% of the wingspan, the fuselage length was set at 60% of the wingspan and the fuselage width and height were kept constant. The propulsion system modeled for this stage of the design was a Hacker B50 motor with a 14x10 propeller and 20 GP1100 cells (1.0 lb of batteries). This gave respectable performance, with static thrust of 6 lb and a pitch speed of 60 mph. The critical dimensions, weight, and RAC of the eight configurations are summarized in Table 3.10.

3.6 Initial Configuration Selection

The results of the FOM analysis are shown in Table 3.11. Equation (3.5) was used to determine the FOM scores:

$$TotalFOM = 55 \cdot \left[\frac{RS \cdot SFS + SR \cdot SFS}{RAC} \right] + \sum_{Qualitative\text{-}FOMs} (WeightFactor)(QuatitativeFOM) \qquad (3.5)$$

After the figures of merit were assigned, the results showed that the flying wing and the flying wing with verticals were the two leading configurations with the conventional V-tail and conventional close behind. The other four configurations scored much lower. It is interesting to note that the performance of the eight configurations was very comparable. This was likely due to the selection of a common propulsion system for all of the configurations.

Table 3.10 Sizing of Configurations for Performance Analysis

Configuration / Parameter	Conventional tractor	Conventional V-tail tractor	Flying Wing w/o Verticals	Flying Wing w/ Verticals	Lifting Conventional	Lifting body w/ V-tail	Joined Wing	Canard Pusher
Wing span(ft)	5.59	5.56	6.01	6.09	5.71	5.69	5.67	5.63
Wing chord(ft)	0.70	0.69	0.75	0.76	0.71	0.71	0.71	0.70
Stabilizer span(ft)	1.40	1.39	N/A	N/A	1.43	1.42	1.42	1.41
Stabilizer chord(ft)	0.81	0.81	N/A	N/A	0.83	0.83	0.47	0.68
Fuselage Length(ft)	3.35	3.34	3.60	3.65	3.43	3.41	3.40	3.38
Fuselage Width(ft)	0.60	0.60	0.60	0.60	0.60	0.60	0.60	0.60
Fuselage Height(ft)	0.46	0.46	0.46	0.46	0.46	0.46	0.46	0.46
Weight (lb)	5.71	5.59	5.28	5.59	6.24	6.14	6.14	5.90
RAC ($1000)	6.21	6.04	5.22	5.40	6.47	6.36	6.61	6.31

Table 3.11 FOM Results

Configuration	RAC	Resupply Time (min)	Resupply Flight Score	Sensor Reposition Time (min)	Sensor Reposition Flight Score	TFS	Score = TFS/RAC	Normalized Score	Stability & Control FOM	Ground Handling FOM	Internal Payload FOM	External Payload FOM	Manufacturing FOM	**Total FOM**
	Weight Factor							*55*	*20*	*8*	*5*	*5*	*7*	
Conventional	6.21	4.21	11.69	3.27	17.45	29	4.69	0.73	1	1	0	0	0	**68.33**
Conventional V-tail	6.04	4.21	11.69	3.27	17.46	29	4.83	0.75	1	1	0	0	0	**69.48**
Flying Wing (no vert)	4.55	4.22	11.67	3.28	17.44	29	6.40	1.00	0	1	1	0	1	**75.00**
Flying Wing (w/ vert)	4.90	4.23	11.66	3.28	17.43	29	5.94	0.93	0	1	1	0	1	**71.04**
Canard	6.32	4.21	11.68	3.28	17.44	29	4.61	0.72	0	1	-1	-1	0	**37.61**
Lifting Conventional	6.52	4.22	11.67	3.29	17.43	29	4.46	0.70	0	0	0	0	0	**38.36**
Lifting V-tail	6.36	4.22	11.67	3.28	17.43	29	4.58	0.72	0	0	0	0	0	**39.33**
Joined Wing	6.77	4.22	11.68	3.28	17.44	29	4.30	0.67	-1	-1	-1	1	-1	**1.97**

The flying wing without verticals was the first choice. However, a further analysis was conducted in order to validate the superiority of the flying wing configuration. The aerodynamics proved to be worse than originally predicted. The wing loading would have to have been lower than 2.5 lb/ft^2 to meet the takeoff requirement, or a more powerful propulsion system would have had to be used. The placement of the payloads ahead of the wing tips in the external configuration presented some structural challenges. The stability and control analysis showed that it would be very difficult to stabilize the airplane in yaw without using vertical surfaces. Based on the refined analysis and consultation with the team advisors, the flying wing configuration was eliminated in favor of a conventional V-tail design. This is the reason for the

delay between the planned and actual events in the milestone chart presented in Section 2.3. In addition, the team, collectively, is more experienced with designing and building a conventional airplane design.

3.7 Final Configuration Selection

After the flying wing configurations, the next best total FOM score was for the conventional V-tail configuration. The V-tail resulted in a slightly higher total FOM score than the conventional tail design due to its slight RAC advantage. The V-tail counted as a horizontal surface with control and a vertical surface without control. It was decided that the payloads should be placed side by side within the fuselage. This allowed easy access to both of them at the same time, reducing loading and reloading time. The total fuselage height was also lower, simplifying the placement of the airplane in the box later on. A low wing was chosen in order to keep the spar out of the way of loading and unloading the payloads. This also simplified the transfer of the payload weight to the wing spar. A tricycle landing gear configuration was selected. Depending on the selected wing span, an outrigger gear to support the wing tips after the first payload is dropped in the SR mission might be needed. It was also decided that brakes should be used to improve ground handling. If the ground handling contribution to the total mission time could be decreased by 2%, it would more than offset the RAC penalty of the added servo and weight. The concept sketch for the selected design is shown in Fig. 3.2.

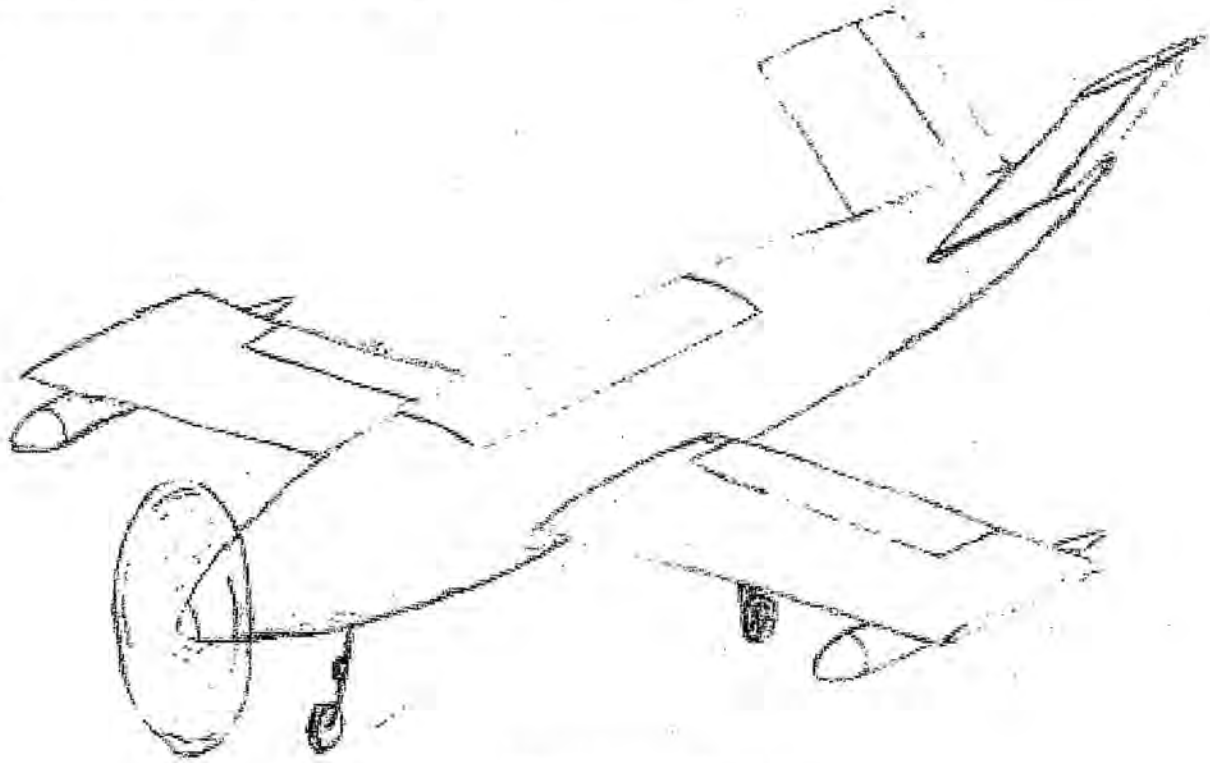

Fig. 3.2 Final Concept Design

4.0 Preliminary Design

The goal of the preliminary design studies was to optimize the sizing of the conventional V-tail configuration and to determine its general layout. As identified in the conceptual design phase, the airplane needed to be designed to complete the Re-Supply and Sensor Reposition missions in as short a time as possible with the lowest possible RAC. This was accomplished through the use of a multi-disciplinary design optimization code (MDO). The MDO code included a detailed performance code that modeled both missions. Critical design variables were identified and used to investigate the design space. More detailed aerodynamic trade studies and a stability and control analysis were then conducted to refine the design.

4.1 Design Variable Selection

To optimize the airplane, the first step was to select the variables that would be used to describe a given design. The goal was to minimize the number of design variables necessary to describe the airplane and to determine its propulsion, aerodynamic, weight, performance and cost characteristics. The selected configuration, contest rules and intuition guided the selection of the design variables. As determined in the conceptual design phase, the selected configuration was a conventional tractor V-tail with side-by-side internal payload positioning. Sweep and taper were not considered due to the operating flight speeds and the RAC concerns, respectively. This left the wing area and aspect ratio as the variables to describe the wing geometry. The fuselage length was chosen as another design variable since it relates directly to the payload storage volume and to the empennage sizing. For RAC reasons, the V-tail span was kept under 25% of the wing span. Historical horizontal and vertical tail volume coefficients were used to size the empennage as a conventional tail. The V-tail area and dihedral angle were then determined using Drela's quick V-tail sizing relations.[6]

A propulsion system can be described by its four major components; motor, gearbox, propeller and battery pack. Due to computer program interface limitations, individual elements of the propulsion system were not able to be used as design variables. Instead, the propulsion system as a whole was taken to be a design variable.

Two other variables were considered to be needed during the mission simulation. The first was the cruise throttle setting. Maximum power would be needed for takeoff and, possibly, for the climb out, but it would not be required during cruise. By throttling back during cruise, battery energy would be conserved and potentially the capacity of the battery pack could be reduced. The other variable that has an effect on the mission performance is the turn load factor. This was initially used as a design variable, but initial runs of the performance code indicated that a load factor of about 3 was optimal. This value was then fixed and decreased the computational requirements later on. Table 4.1 lists the chosen design variables and the ranges over which they were investigated. Table 4.2 show the relationships used to determine other geometrical characteristics from the design variables.

Table 4.1 Design Variables and Their Ranges

Variable	Minimum Value	Maximum Value
Wing Area (S)	2 ft^2	10 ft^2
Aspect Ratio (AR)	2	15
Fuselage Length (FL)	3 ft	5 ft
Cruise Throttle (CT)	50 %	100 %

Table 4.2 Relationships for Determining Geometrical Characteristics

Parameter	Value	Notes
Horizontal Tail Volume Coefficient	0.5	Used to determine effective horizontal tail area (S_H)
Vertical Tail Volume Coefficient	0.055	Used to determine effective vertical tail area (S_V)
V-tail area (S_{Vtail})	= $S_H + S_V$	Total V-tail area
V-tail angle (θ_{Vtail})	= arctan((Sv/Sh)^0.5)	V-tail angles from horizontal
V-tail span (b_{Vtail})	= 0.25*(S*AR)^0.5	25% of wing span
V-tail chord (C_{Vtail})	= S_{Vtail} / (b_{Vtail} *sec(θ_{Vtail}))	
Landing Gear length	Prop Diameter/2 -3	For necessary prop clearance
Wing X_{ac} Location	14 in. from nose	Based on most motor and payload dimensions
Payload Length	20 in.	From payload detail design

4.2 Mission Model

The three missions were modeled using seven different segments; takeoff, climb, 180 degree turn, cruise, descent, landing and ground operations. Table 4.3 shows the number of times each segment was used for each mission. Each segment contained different assumptions that were needed for an efficient computational model of the mission. The time to taxi and to change the payloads was estimated at 15 sec for each landing. The estimated time to disassemble and pack the airplane was 20 sec. The Maximum Utilization mission was modeled to verify the conclusions reached in Section 3.2.1.

Table 4.3 Segment Types for Each Mission

Mission Segment	Number of Segments in			Notes
	SR mission	RS mission	MU mission	
Take-off roll	3	4	1	<150 ft
Acceleration and climb out	3	4	1	From takeoff to first turn
500 ft Level Cruise	6	8	4n - 2	n = # of laps
180 degree turn	6	8	2n	n = # of laps
360 degree turn	3	4	2n	n = # of laps, on downwind leg
Landing Approach	3	4	1	
Ground Roll	3	4	1	From touchdown until start line
Reload/Unload	2	3	0	Assumed 15 seconds
Disassembly	1	1	1	Assumed 20 seconds

During takeoff, the throttle was assumed to be at 100%. A rolling coefficient of friction of 0.1 was used based on test data.[7] A rolling lift coefficient of 0.1 was also assumed. The ground acceleration phase of the takeoff continued until the airplane reached 110% of the stall speed, at which point rotation was assumed to occur in 0.5 seconds.

Starting with the takeoff distance calculated from the takeoff segment, the distance to the first turn was calculated. With a desired altitude of 50 feet at the beginning of the turn, as specified by the pilot, a constant climb angle was calculated. A throttle setting of 100% was assumed.

During the turn segments, a constant load factor was assumed, unless C_{Lmax} was exceeded at the specified load factor. If C_{Lmax} was exceeded, the load factor was decreased until the C_L was decreased to C_{Lmax}. The radius of the turn might not remain constant, but that aspect was neglected since the variations were assumed to be minimal. The cause of the radius change was due to the variation of the velocity and possibly load factor throughout the turn. The altitude was held constant throughout the turn. The throttle setting in the turn was specified by the cruise throttle (CT) variable.

In the cruise segments of the mission, the altitude remained constant at 50 ft and the cruise throttle was specified by the CT variable.

Information about the descent was gathered by assuming a constant descent angle and from the existing boundary conditions. The velocity and altitude at the end of the final turn, along with the velocity and altitude at landing were known. The landing/braking distance was calculated before the descent phase. Since the distance from the end of the last turn to where the airplane stops was 500 feet, if the landing distance was subtracted from that value, the descent distance was obtained. The use of spoilers was simulated by incrementally adding drag and iterating until the speed of the airplane matched the landing speed.

For the final segment of the mission, the landing, the touch-down speed was assumed to be 110% of the stall speed. For the landing roll, a braking coefficient of 0.3, and a rolling lift coefficient of 0.1 were used in the analysis.

4.3 Analysis Methods Used

There were a number of tools used to analyze and size the airplane. The performance code, written for the conceptual design studies was updated to more accurately model the missions. The MDO code was then used to find the optimal set of design variable values to maximize the competition score. Since there were a small number of design variables used to describe each design in the MDO code, further preliminary design work was carried out to refine the optimum design. Trade studies were conducted external to the MDO framework to select the wing airfoil, wing twist distribution and the V-tail airfoil. A stability-and-control analysis was performed to refine the empennage and control surface sizing as well.

4.3.1 Performance Code

The same performance code that was used in the conceptual design was used in these studies. It was written in MATLAB to integrate the airplane equations of motion (EOM) using a fourth order Runge-Kutta method. It was updated to include the effects of wind and more accurate drag and propulsion predictions. The code accounted for Reynolds number effects and for the additional aerodynamic forces when the payloads were in their external configuration. The effect of head and tail winds were also incorporated into the model. The code output time, distance, true velocity, ground velocity, current, thrust,

and load factor at each time step. It also output the takeoff and landing distances, total energy used, and mission times.

4.3.2 MDO Code

The multi-disciplinary optimization (MDO) code was created to incorporate several design tools to enable the selection of the design variable values that maximized the competition score. The MDO code evaluated thousands of sets of design variable values to find the set that maximized the competition score. The melding of many design and analysis tools into a single design tool that allowed an "ultimate trade study" to be performed among the MDO design variables. The tools incorporated into the MDO code included RAC calculation, propulsion, aerodynamic and weight models, and the performance code.

Since the propulsion system as whole was taken to be a design variable, an optimum design was determined for each selected propulsion system. These optimums were then compared to determine the overall optimum design. This introduces some risk in that the best propulsion system might not have selected as one of the candidate propulsion systems. A strategy to overcome this was developed and will be discussed in section 4.4.1.

4.3.3 Stability and Control Analysis

Using fundamental stability equations, the dimensions of the V-tail configuration were refined and the flying qualities of the airplane were determined.[8] The dynamic stability was analyzed using a MATLAB code. The ruddervators and ailerons were sized to provide control authority in all payload configurations.

4.4 Elements of MDO Code

The MDO code consisted of six major components that were written in and tied together using MATLAB. The propulsion model provided the thrust and current for a given combination of motor, gearbox, battery and propeller as a function of velocity and throttle setting. The aerodynamic model determined the drag of the airplane as a function of the design variables (as shown in Table 4.1), payload configuration, lift coefficient and Reynolds number. The weight model predicted the airplane weight as a function of the design variables. The RAC model determined the RAC given the design variables. The performance code predicted the time and energy required to complete the various missions. Finally, the objective function tied all of the other elements together to determine the MDO score. The MDO score was taken to be the total flight score divided by the RAC with penalties added for constraint violations.

4.4.1 Propulsion Model

Since the interactions between the elements of the propulsion system are complex, the propulsion system as a whole was taken to be a discrete design variable in the MDO code. In order to predict the propulsion system performance throughout the missions, a model was developed that provided the thrust and current as functions of the flight velocity and throttle setting. A commercial software program, MotoCalc,[9] was used to obtain the thrust and current predictions for a given motor, gearbox, battery and propeller combination. From propulsion system testing it was found that these predictions did not always correlate with the experimentally obtained performance; thrust and current tended to be lower than predicted. Based on this testing, the thrust was assumed to be 80% of that

predicted by MotoCalc, but the current was not changed to provide a safety factor on the battery energy. A MATLAB script was written to curve fit the data generated by MotoCalc and to output it to the rest of the MDO code.

Due to the large number (millions) of possible propulsion systems, it was impractical to optimize the design for all of them to find the best overall design. To ensure that the best possible propulsion systems were run with the optimization code without wasting too many resources, a two phase approach was taken. The initial runs of the performance code showed that the mission performance of a propulsion system was primarily a function of its static thrust and pitch speed. The first goal was to optimize the design for each of a matrix of 25 propulsion systems with pitch speeds between 40 mph and 80 mph (in increments of 10 mph) and static thrust between 4 lb and 8 lb (in increments of 1 lb). These systems were selected using MotoCalc's filtering abilities to find the lowest battery weight that could give the desired performance. After running the optimization code on these 25 systems, an additional 19 systems were selected with pitch speeds and static thrust near the maximums from the first batch. The second set of propulsion systems explored more motors as well as changes in cell count and propeller geometry. The following paragraphs describe the criteria used to select the individual components for the 44 propulsion systems.

The motors for these systems were all brushless and selected from a few of the major brands. Brushed motors were quickly ruled out due to their low power-to-volume and power-to-weight ratios, lower efficiencies and their cost. For the thrust and pitch speeds mentioned above it was determined that the motor would have to handle about 500 W and 40A. The motor search was limited to the Hacker B40 and B50 series, the Kontronik Fun 480 series, the Mega 22/10/xx and 16/25/xx series, and the Aveox 27/26/xx and 27/39/xx series. Plettenberg motors were initially considered as well, but ruled out due to their higher cost. The gear ratios that were available for each of these motor types were identified.

A database of carbon folding propellers was generated for use in the MotoCalc runs. Carbon folders were selected primarily for their lighter weight and better durability as compared to APC glass filled or wooden propellers. Propellers with diameters between 12 and 20 inches and pitches between 8 and 20 inches were included from three product lines; RFM, Aeronaut and Graupner.

A database of battery cell types along with their energy densities and maximum currents was generated. Table 4.4 presents these data. It is clear that the NiMH cells vastly outperform the NiCd cells. To identify the cell capacity needed to complete the missions, two assumptions were made. The first was that the maximum current would be limited to 40 A as allowed by the rules and the second was that the maximum battery run time for each lap would be about 45 seconds. Based on these assumptions, a maximum of 2000 mAh would be needed if the propulsion system drew a constant 40 A. This eliminated the need for cells with a capacity greater than 2000 mAh. This left the GP1100 and Sanyo 4/5FAUP 1950 as the best remaining cells that could handle the necessary currents. If the total energy usage could be kept under 1100 mAh, the GP1100 cells presented an opportunity to cut the battery weight by 45%

compared to the Sanyo 4/5FAUP 1950 cells. The optimization code was left to determine if using the GP1100 cells would be feasible.

Table 4.4 Battery Energy Densities and Maximum Currents

Cell Type	Chemistry	Capacity (mAh)	Weight (oz)	Energy Density (mAh/oz)	Maximum Current (A)
Sanyo RC 3300 HV	NiMH	3300	2.12	1557	30
Kan 1800 4/5A	NiMH	1800	1.2	1500	Less than GP2200
GP-3300	NiMH	3300	2.2	1500	100+
GP-1100	**NiMH**	**1100**	**0.75**	**1467**	**35+**
Sanyo 4/5FAUP 1950	**NiMH**	**1950**	**1.37**	**1423**	**40+**
GP-2200	NiMH	2200	1.55	1419	60+
Sanyo 4/5AUP 1700	NiMH	1700	1.2	1417	30
Kan 1300	NiMH	1300	0.92	1413	20+
Kan 1050	NiMH	1050	0.75	1400	Less than GP1100
CP 2400 SCR	NiCd	2300	2.05	1122	???
CP 1700 SCR	NiCd	1700	1.63	1043	50+
CP 1300 SCR	NiCd	1100	1.16	948	35+

4.4.2 Aerodynamic Model

The role of the aerodynamic model was to generate a drag polar to be used in the performance code. The drag coefficient for the airplane was calculated as a function of Reynolds number and lift coefficient by using a method that included a build up of wing profile drag, wing induced drag, fuselage drag, empennage drag, payload drag and interference drag. The airfoil profile drag was calculated using PROFILI[10] (a GUI for XFOIL) that generated drag polars for a range of Reynolds numbers and lift coefficients. These data were curve fit to obtain a function which output c_d as a function of c_l and Re. At this stage, a candidate airfoil was selected for the purposes of the design variable optimization. The SD7043 was selected because it has a high c_{lmax} of 1.4, a pitching moment greater than -0.1 and low profile drag at low Reynolds numbers. A more detailed airfoil trade study was conducted after the MDO code found the optimum using this airfoil.

The induced drag was calculated using span efficiency estimates, aspect ratio, and C_L.[11] The fuselage drag was estimated using the method outlined by Raymer.[12] The empennage drag was estimated using average skin friction coefficients and assuming a tail C_L of 0.2 to calculate its induced drag. The payload drag was estimated at this stage by using data from Hoerner[13] for the drag of bodies of revolution given a fineness ratio and Reynolds number. The final drag build-up incorporated the parasite drag including interference drag estimates and the induced drag, as well as potential payload drag depending on the mission. Next, C_{Lmax} was estimated at 90% of c_{lmax} as estimated from Eq 12.15 in Raymer.[12] Lastly, the aerodynamic center was calculated based on the wing and empennage areas and lift-curve slopes.

4.4.3 Weight Model

The weight model estimated the total weight of the airplane based on the design variables and a number of assumptions based on manufacturing methods and materials. The code used volumetric assumptions along with material densities to determine the weight of the components. It used basic Euler-

Bernoulli formulas for bending and torsion on the wing to determine skin and spar cap thicknesses given specified deflections and twist under maximum loads. The wing, empennage and fuselage were assumed to be hollow molded composite parts utilizing fiberglass and balsa sandwich skins with carbon fiber reinforcements. Following the weight calculations, the code estimated the possible range of the center of gravity of the airplane based on movable internal components. This served as a method of deciding on the feasibility of a given set of design variables based on the center of gravity range that is compared to the aerodynamic center location calculated by the aerodynamic model.

4.4.4 Rated Aircraft Cost Model

The RAC model consisted of the RAC equation from the competition rules. For each set of design variables, the RAC was determined using the contest supplied equation.[1] The details of the RAC calculation were discussed in Section 3.2.

4.4.5 Performance Code

The performance code was developed using MATLAB software to predict the airplane performance over the three missions. This was done by integrating the airplane equations of motion through the mission model described in section 4.2.1 using a fourth order Runge-Kutta method. The parameters obtained from the code are mission time, velocity, distance, lift coefficient, thrust, current, and energy for each time step.

4.4.6 Optimization and Objective Functions

The goal of the MDO was to maximize the objective function that is the competition score with added penalties. The code could evaluate any set of design variables and output a competition score. The flow of the objective function was as follows:

1. Load propulsion data
2. Evaluate drag polar
3. Evaluate weight
4. Evaluate RAC
5. Integrate flight path with performance code
6. Determine total flight score (TFS) as sum of two best single flight scores
7. Determine if airplane takes off in 130 ft, if not penalize according to: $P_{TO} = (S_{TO} - 130)/10$
8. Determine if airplane exceeds battery pack energy limit, if so penalize according to :
   $P_{mAh} = (mAh_{used} - mAh_{battery} - 100)/50$
9. Determine if airplane climbs to 50ft by first turn, if not penalize according to:
   $P_{climb} = (h_{actual} - 50)/5$
10. Determine if CG range is feasible, if not penalize according to: $P_{CG} = 1$
11. Compute final objective function value according to: $G = TFS/RAC - P_{TO} - P_{mAh} - P_{Climb} - P_{CG}$

The takeoff distance cutoff was put at 130 ft to give a 20 ft safety factor. The battery energy cutoff was placed at the battery mAh rating minus 100 mAh as indicated by propulsion testing. The 50 ft climb requirement was set as a minimum altitude that the airplane should be able to reach by the first turn.

Lastly, if the CG range did not allow for a static margin between 5% and 15% a penalty was added for infeasibility. These penalties allowed the optimization function to automatically search back into the design space if a solution constraint was violated without starting over. A final check was made that final optimum designs did not violate any of the solution constraints imposed.

In order to optimize the design, a point search optimization function was used. First, the range of each design variable was split into 5 subdivisions. Each of these 625 (four continuous design variables = 5^4) possibilities was then evaluated. By observing the best performing designs, the range for each design variable could be decreased and the process repeated until a maximum objective function value converged. This process was repeated for 44 different propulsion systems and required about 50 hours of computation time.

4.5 MDO Results

After running the optimization code, there was a wealth of data to sift through. It quickly became evident that there were a number of designs that lay within one percent of the optimum. This provided some flexibility in selection of the design point to enhance the versatility and adaptability of the airplane. First, some general trends were identified. Next, the data were processed and the design point was selected. Finally, a sensitivity study was performed to verify that the selected design point did not stray too far from the optimum.

4.5.1 General Trends

There were a number of trends evident in the results of the optimization. For most of the propulsion systems, the values for the design variables converged to within fairly small ranges. The wing aspect ratio was almost always between about 5 and 6. This likely occurred for two reasons. The first is the tradeoff between increased profile drag due to smaller Reynolds numbers and decreased induced drag due to increasing aspect ratio. In past years, the optimum designs tended to converge upon an aspect ratio of about 8 for this same reason.[3] However, this year, the aspect ratio tended to converge to between 5 and 6 because of the structural requirement of placing the payloads on the wing tips. In the weight model, the wing spar and skin were sized to handle a 5g landing with a specified wing tip deflection with the payloads in their external configuration.

The optimum wing areas varied between 3.5 ft^2 and 5.5 ft^2 depending on the empty weight. This corresponded to wing loadings between 2.75 and 3.25 lb/ft^2, the lower values for the propulsion systems with lower thrust to weight ratios. The empty weight of the optimum designs for each propulsion system varied between about 5.3 lb and 6.5 lb. As expected, the main driver on the wing loading was the takeoff distance. It was thought that the turn load factor might be a driver for the wing loading as well, but it turned out to be not as important as the takeoff requirement. The fuselage length for the optimum designs varied between 3.2 ft and 3.9 ft depending on the wing area. Smaller wings favored shorter fuselage lengths.

The propulsion systems also produced some interesting trends. Figure 4.1 presents the optimum objective function value for each propulsion system. In the interest of space, details are not presented on

all of the propulsion systems. Table 4.5 lists the values of the design variables and propulsion system components for some of the best designs. The best performing propulsion systems seemed to favor two motors; the Hacker B50-13S and the Mega cAn 16/25/4. All the top systems had a maximum static thrust on the order of 6 lb to 7 lb and a pitch speed of 80 to 90 ft/s. These systems presented a good balance between low battery weight (low RAC), thrust-to-weight ratio (over 0.5) and a pitch speed of about 60 mph. The RAC increase from increasing the battery weight to increase the static thrust did not offset the RAC decrease of a smaller wing. Also, the RAC increase from increasing the battery weight to increase the pitch speed did not offset the decreased mission time. The GP1100 battery cells proved capable of completing the missions and outperformed the Sanyo 4/5FAUP 1950 cells for every propulsion system. For the missions to be completed with the GP1100's, the cruise throttle had to be reduced to roughly 70%, which corresponds to about half of the maximum power available. It was observed that the mission score increased as the throttle was increased, until the energy limits of the battery were reached. The 17 x 11 and 17 x 13 propellers seemed to fit the mission best. The gear ratios depended on the motor; 6.7:1 for the Hacker B50-13S and the 3:1 for the Mega cAn 16/25/4.

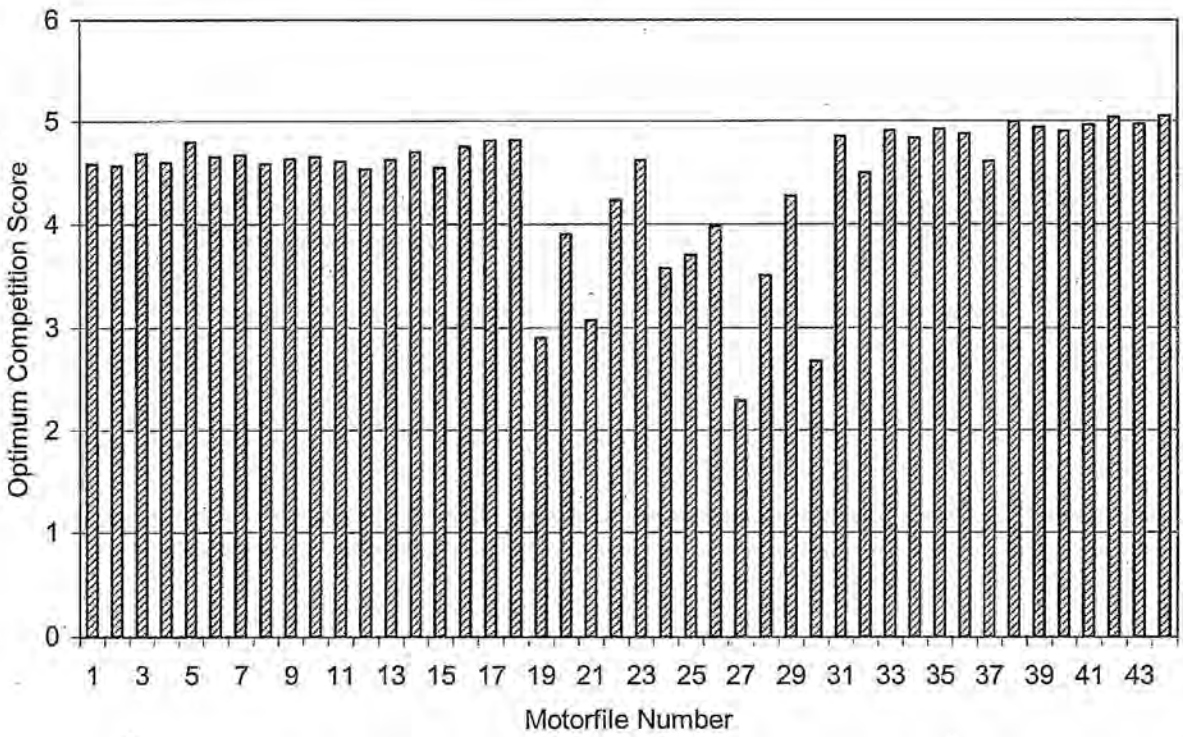

Fig. 4.1 Optimum Competition Score for Each Propulsion System

Table 4.5 Optimum Competition Score and Design Variables for Select Propulsion Systems

Motorfile Number	Optimum Competition Score	Motor	Gear Ratio	Number of Cells	Type of Cell	Propeller	S (ft^2)	AR	FL (ft)	CT (%)
44	5.05	Mega cAn 16/25/4	3	17	GP1100	17 x 11	3.5	5	3.1	75
42	5.04	Mega cAn 16/25/4	3	17	GP1100	17 x 13	3.5	5	3.1	65
38	5.00	Mega cAn 16/25/4	3	15	GP1100	17 x 13	4	5.5	3.3	70
43	4.97	Mega cAn 16/25/4	3	16	GP1100	17 x 11	3.75	5	3.2	75
41	4.97	Mega cAn 16/25/4	3	16	GP1100	17 x 13	4	5.25	3.3	67.5
39	4.94	Hacker B50-13S	6.7	16	GP1100	17 x 13	3.75	5.5	3.3	67.5
35	4.92	Mega cAn 16/25/4	3	14	GP1100	17 x 13	4.5	5.75	3.55	75
33	4.91	Hacker B50-13S	6.7	15	GP1100	17 x 13	4	5.5	3.3	70
40	4.90	Hacker B50-13S	6.7	17	GP1100	17 x 13	3.75	5.5	3.3	65
36	4.87	Mega cAn 16/25/4	3	15	GP1100	17 x 11	4.25	5.25	3.45	77.5
31	4.85	Hacker B50-13S	6.7	14	GP1100	17 x 13	4.25	5.5	3.55	72.5
18	4.81	Hacker B50-15S	6.7	18	GP1100	16 x 13	3.95	5.2	3.35	72.5
17	4.80	Hacker B50-16S	6.7	19	GP1100	16 x 13	4.1	5.1	3.3	80
10	4.65	Mega cAn 16/25/4	2.5	16	GP1100	14 x 9	5	6	3.75	80
9	4.63	Hacker B40-13L	4.4	16	GP1100	14 x 9	4.85	6.1	3.8	77.5
22	4.23	Hacker B50-13S	6.7	13	GP1100	16 x 13	5.4	6.4	3.95	80

4.5.2 Design Variable and Propulsion System Selection

It was observed from the best scoring propulsion systems, that there were a lot of common trends and that a large degree of flexibility could be introduced by properly selecting the design point. There were some doubts about the ability of the Mega 16/25/4 because the 3:1 inner driven gearbox could not handle the predicted 600 to 700 W power output. For this reason, it was decided that the chosen design would be selected for the Hacker B50-13S motor with a 6.7:1 gearbox, but that the Mega would still be investigated during flight testing since it appeared to provide a slight edge in performance. The propulsion system selected at this point was Motorfile Number 39. It used the Hacker B50-13S with 16 GP1100 cells and the 17 x 13 propeller. All of the other top performing systems utilized either the Aeronaut 17 x 11 or 17 x 13 carbon folding propellers and between 14 and 17 GP1100 cells. The dimensions of the airplane were chosen to provide a good score, while still maintaining some flexibility in being able to apply the other propulsion systems to suit conditions. Table 4.6 shows the selected design point. A wing area of 4.004 ft^2 and an aspect ratio of 5.5 were selected. This represented a rectangular wing with a 0.854 ft chord and 4.69 ft span. The fuselage length was selected at 3.5 ft. The empty weight was predicted at 5.65 lb. The cruise throttle might vary depending on conditions, but would be around 70%. This design was analyzed with the performance code and gave a competition score of 4.90, only 3% lower than the overall optimum identified and less than 1% lower than that specified by the optimum design for Motorfile Number 39. The slightly larger wing area provided a further margin on the takeoff distance should C_{Lmax} decrease due to building inaccuracies or if the empty weight exceeded the predicted value.

Table 4.6 Selected Design Point

Motor	Hacker B50-13S	Wing Area	4.00 ft^2
Gear Ratio	6.7:1	Aspect Ratio	5.5
Battery Type	GP1100	Span	4.69 ft
Number of cells	16	Chord	0.854 ft
Propeller	Aeronaut 17 x 13	Fuselage Length	3.5 ft
Empty Weight	5.65 lb	Cruise Throttle	67.5%

4.5.3 Sensitivity Analysis

To verify that the selected design point did not shift too far from the optimum, a sensitivity analysis was performed. The affect of changing the wing area, aspect ratio, fuselage length, cruise throttle, and cell count were identified. Figure 4.2 shows the results of this analysis by plotting the normalized parameters versus the score normalized to the selected design point. It is clear from this plot that the throttle and number of cells are near their optimums. The other three variables have small gradients, indicating that while the design is not optimum it is very nearly so. Reducing the wing area slightly would improve the score, but it was deemed more important to maintain a safety factor for the takeoff distance. The design is very insensitive to aspect ratio, so increasing it will have very little impact on the score. Lastly, the fuselage length also has a low sensitivity. The score appears to increase slightly as the fuselage length decreases. The insensitivity of this variable means that overall score will not be greatly effected if the fuselage length had to change for stability and control reasons.

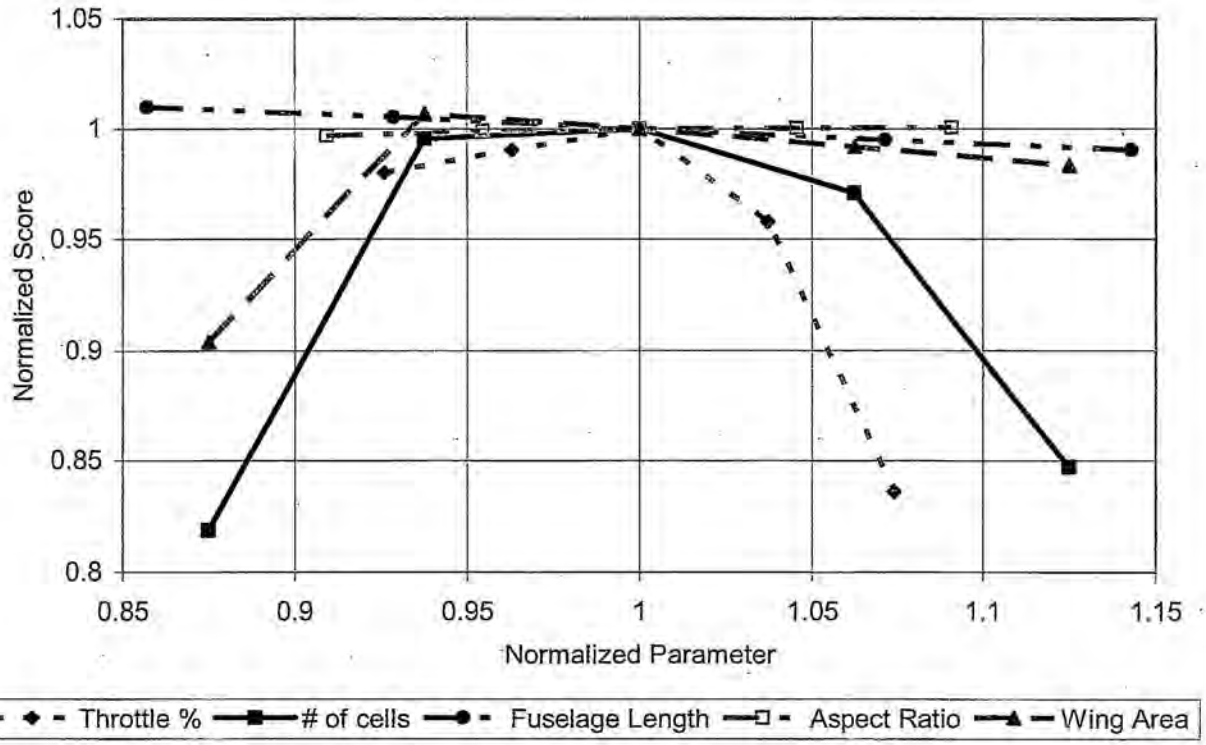

Fig. 4.2 Sensitivity Plot of Design Point

4.6 Refined Aerodynamic Design

After the MDO results were compiled, a more detailed aerodynamic analysis was performed to optimize the aerodynamic performance of the wing and V-tail. Airfoils were selected for the wing and V-tail and a twist distribution was specified for the wing.

4.6.1 Airfoil Selection

As stated previously, the SD7043 was initially chosen for the airplane sizing and configuration optimization. Next, a more detailed analysis was performed in selecting the optimum airfoil for the design. There were many considerations that had to be taken into account. $c_{l_{max}}$ was a major driver for the takeoff requirement and turn performance. Low profile drag was important for cruise efficiency and minimizing the energy expended during the mission. The wing pitching moment was important for empennage sizing and minimizing trim drag. Lastly, the airfoil thickness ratio was structurally important, driving the wing weight necessary to support the given loads. The following criteria were used for selecting candidate airfoils:

- $c_{l_{max}} > 1.4$ at Re = 300,000
- c_d @ $C_L = 0.3 < 0.0125$ at Re = 300,000
- c_d @ $C_L = 1.0 < 0.0125$ at Re = 300,000
- $c_{m,c/4} > -0.15$
- $(t/c)_{max} > 0.09$

There were six candidate airfoils chosen that met these criteria. Data for the airfoils were generated by PROFILI at Re = 300,000 and are presented in Figs. 4.3 and 4.4.

Based on the data, the airfoil chosen for the wing was the SD7043. This airfoil had the lowest profile drag over the c_l range of 0.35 to 0.8, the cruise c_l range of the airplane. Also, it met the $c_{l_{max}}$ and thickness requirements with $c_{l_{max}}$ = 1.46 and a t/c = 0.091. It also had a fairly low negative pitching moments of -0.10.

The V-tail airfoil was selected to minimize profile drag while providing adequate thickness to accommodate the tail servos and to keep the spar light. To trim the airplane in steady flight, a tail C_L between approximately -0.2 and 0.2 is required. The set of NACA 00xx series airfoils was considered. The general trend exhibited at Re = 300,000 was for the minimum drag to increase with increasing thickness ratio. The best compromise between low profile drag and thickness requirements was seen to occur for the NACA 0009, which was chosen for the V-tail airfoil.

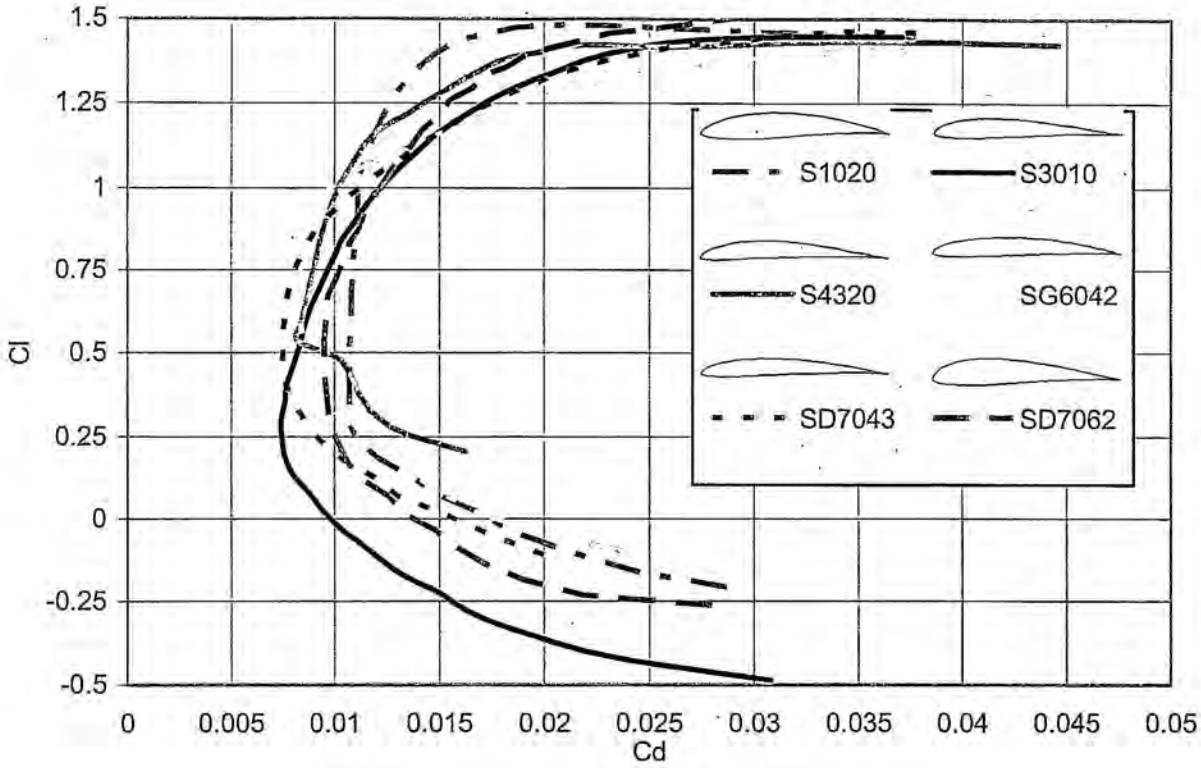

Fig. 4.3 Drag Polars for Candidate Wing Airfoils

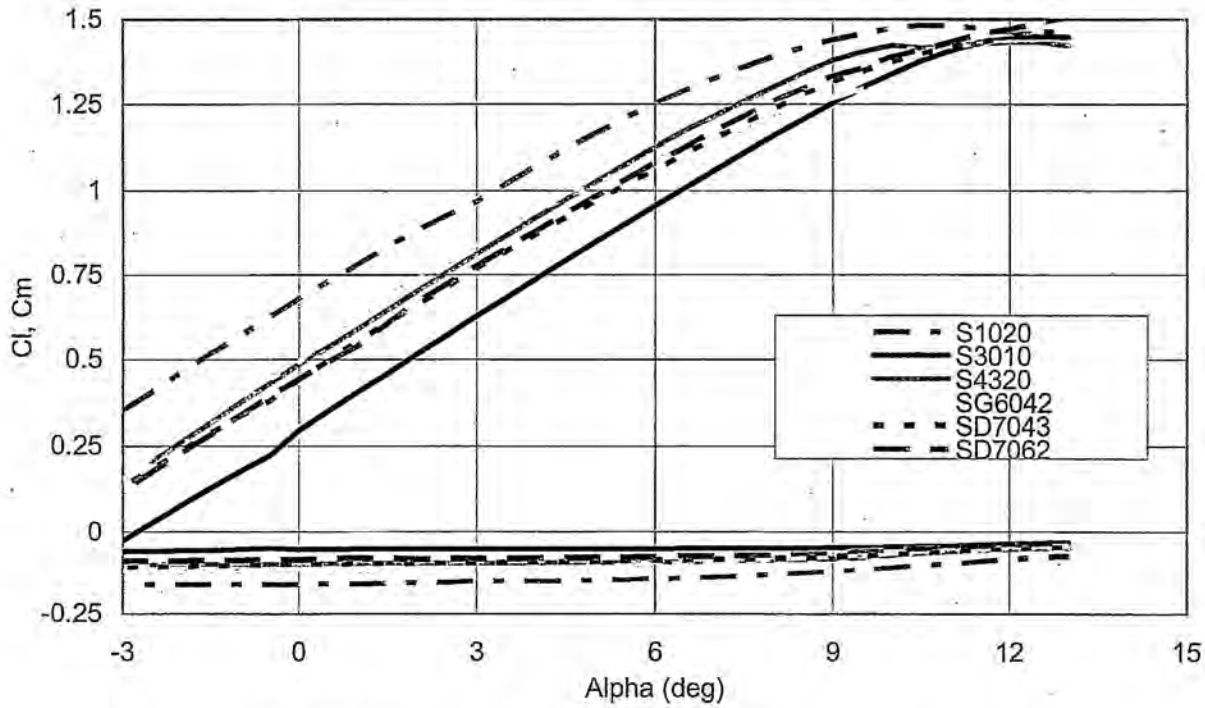

Fig. 4.4 Lift and Moment Curves for Candidate Wing Airfoils.

4.6.2 Twist Trade Study

A trade study was conducted to determine the ideal amount of twist to include in the wing. By washing out the tips, the lift distribution can be improved to more closely approximate an elliptical distribution and decrease the induced drag. This also has the added benefit of causing the root of the wing to stall earlier than the tips, maintaining some aileron authority even if the root of the wing is stalled. The twist can either be geometric, aerodynamic or a combination of the two. To simplify construction and analysis, only a linear geometric twist from root to tip was considered. A lifting line code[14] was used to determine the span efficiency for varying amounts of twist over a range of lift coefficients. From the performance code output, it was determined that the airplane primarily operated in the C_L range between 0.2 and 1.2, with a majority of the time spent between 0.35 and 0.8. Figure 4.5 shows the span efficiency as a function of tip washout for varying lift coefficients. Based on this plot, a linear geometric twist of -3 deg was chosen. This amount of twist maximizes the span efficiency at higher C_L values while still providing a higher span efficiency than the untwisted case at a $C_L = 0.2$.

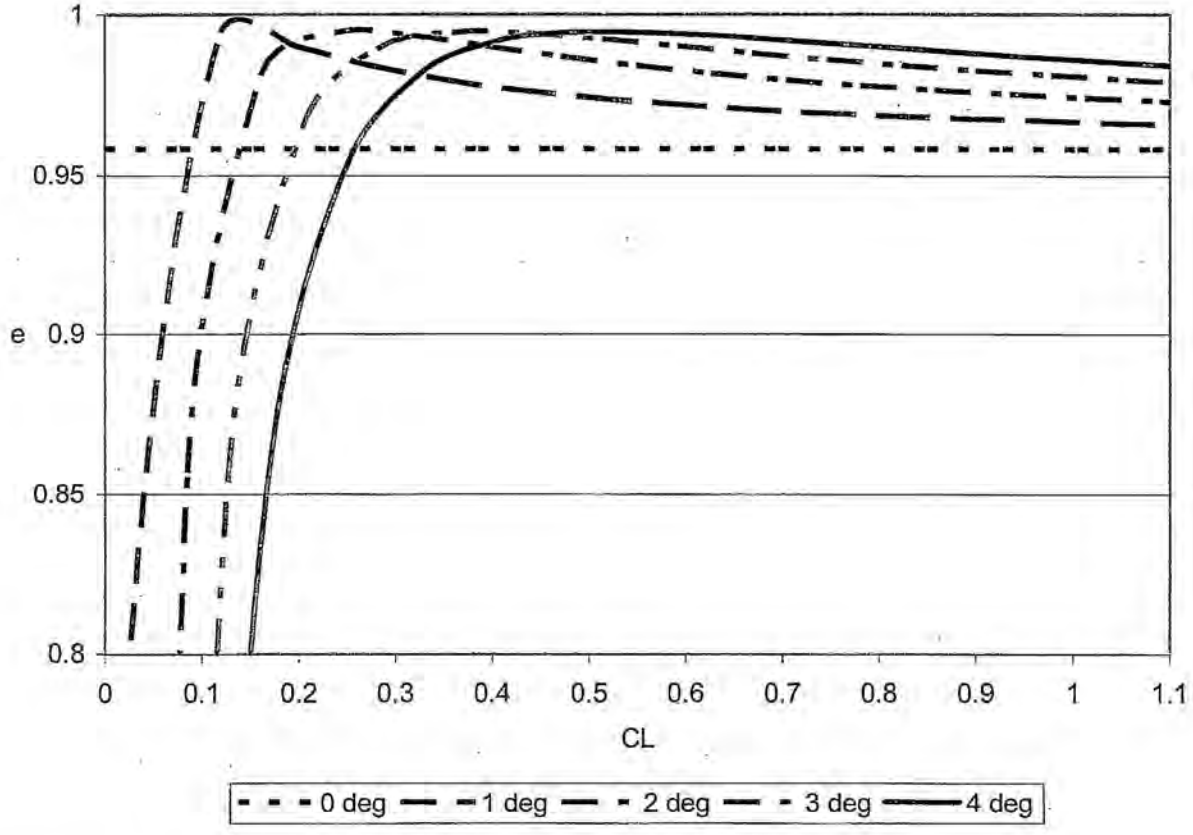

Fig. 4.5 Wing Twist Trade Study

4.7 Stability and Control

Using the MATLAB code mentioned in Section 4.3.3, the empennage and control surface sizes were determined taking static and dynamic stability into account. An experienced RC pilot qualified the resulting flying qualities.

4.7.1 Dynamic Stability Analysis

With the aerodynamics, geometry, inertial characteristics, and static margin specified, the longitudinal and lateral/directional dynamics modes of the airplane were evaluated. The flying qualities of the airplane in both the longitudinal and lateral/directional modes were carefully explored. Conventional flying quality standards are not directly applicable to model airplanes. The flying quality "levels" prescribed in Nelson[8] are too conservative for model airplanes since the pilot can visually reference the airplane's orientation at all times. This is why, after consultation with an experienced RC airplane pilot, the flying quality standards were relaxed.

4.7.2 Empennage Sizing

For a given static margin and tail moment arm, the dynamic stability characteristics of the airplane were evaluated for various effective horizontal and vertical tail areas. Many iterations were performed until a good compromise between satisfactory dynamic characteristics and other requirements was obtained. The projected V-tail span needed to be less than 25% of the wingspan, and the fuselage length needed to be as short as possible to keep the RAC low and minimize the fuselage wetted area. The resulting projected horizontal tail area was 0.8 ft^2 and the projected vertical tail area was 0.65 ft^2. Using formulas for converting a conventional tail to a V-tail produced an eight-inch chord and a dihedral angle of 38° for the V-tail surfaces.[6]

4.7.3 Control Surface Sizing

Based on experience and historical data, the ailerons and ruddervators were sized to 30% of the chord length to ensure adequate roll authority, proper pitch control, and trim ability in all flight conditions.

4.7.4 Static Trim Analysis

Figure 4.6 presents a pitch trim diagram for the airplane with the static margin set at 2%. Trim lines for ruddervator deflections of +20, 0 and -30 degrees are shown. The figure shows that the ruddervators can trim the airplane over the range of lift coefficients from 0 to C_{Lmax}.

4.7.5 Stability and Control Predictions

Table 4.7 presents a brief description of the flying quality levels used in these studies. Table 4.8 presents the characteristics of each of the dynamic modes and the steady-state roll rate of the airplane for each payload configuration for both cruise and terminal flight phases. The cruise phase has a higher airspeed and a lower C_L, and the terminal phase is slower and has a higher C_L. Although the phugoid and spiral instability modes are at their worst during terminal flight phases, it was agreed upon that a pilot in visual reference flight should be able to handle the airplane. The steady-state roll rate demonstrates more than enough roll authority even in the loaded airplane configurations. In addition, the small time constant values show the system will respond very rapidly to disturbances. The short period is well damped and the Dutch roll, while not ideal, is acceptable for all payload configurations.

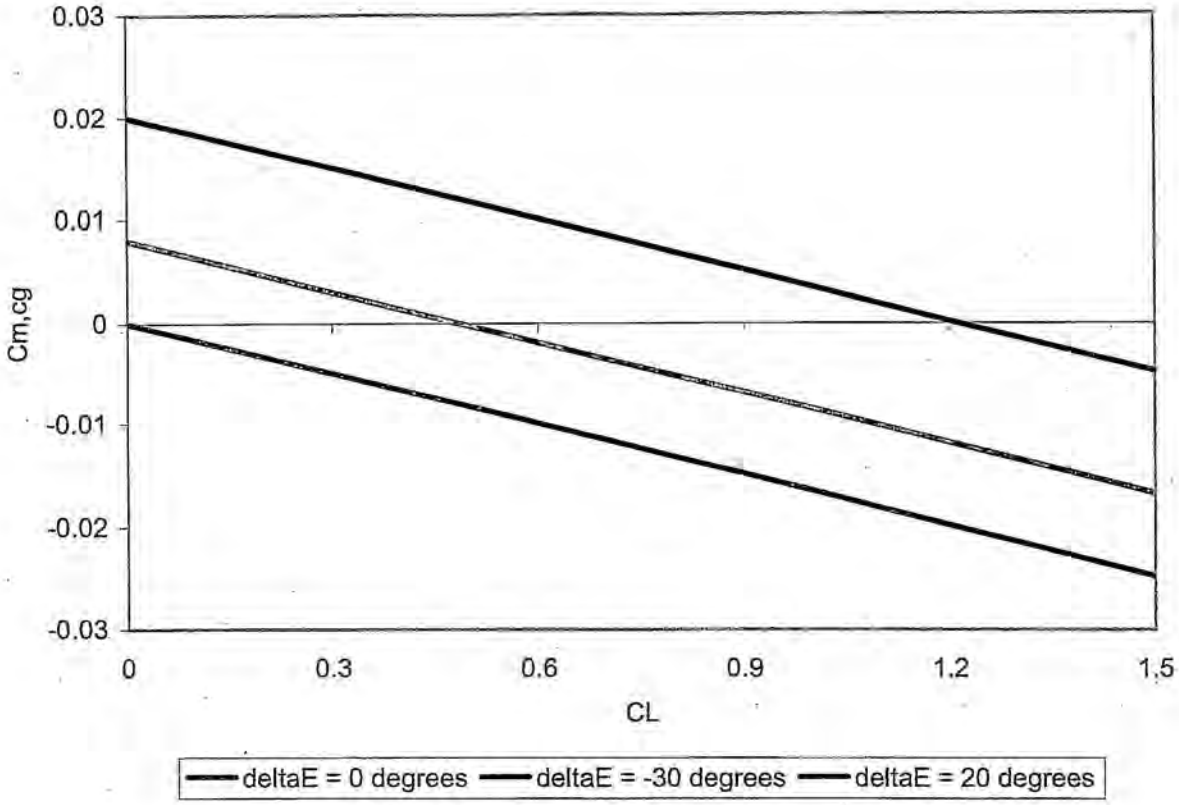

Fig. 4.6 Trim Plot for 2% Static Margin

Table 4.7 Description of Flight Quality Levels

Flying Quality Levels	
Good	1
Acceptable	2
Marginal	3

Table 4.8 Characteristics of Dynamic Modes and Roll Rate

		Longitudinal						Lateral							
		Phugoid			Short Period			Roll		Spiral		Dutch Roll			Rates
Flight Phase	Airplane Configuration	Damping	Frequency, (rad/s)	Flight Quality Levels	Damping	Frequency, (rad/s)	Flight Quality Levels	Time Constant, tau (sec)	Flight Quality Levels	Time to Double, (sec)	Flight Quality Levels	Damping	Frequency, (rad/s)	Flight Quality Levels	Steady Roll (deg/s) (da = 20 degrees)
Cruise	Empty	0.10	0.54	1.00	0.82	9.81	1.00	0.05	1.00	15.89	1.00	0.09	4.19	2.00	280.74
	Internal	0.04	0.99	2.00	0.55	5.34	1.00	0.09	1.00	12.03	2.00	0.26	2.73	1.00	167.78
	External	0.04	0.99	2.00	0.55	5.34	1.00	0.57	1.00	2.37	2.00	0.14	1.40	2.00	167.78
Terminal	Empty	0.11	1.13	3.00	0.81	4.73	1.00	0.10	1.00	1.93	3.00	0.25	2.09	1.00	128.14
	Internal	0.08	1.26	3.00	0.56	4.18	1.00	0.11	1.00	1.21	3.00	0.52	2.62	1.00	128.14
	External	0.08	1.26	3.00	0.56	4.18	1.00	0.75	1.00	1.57	3.00	0.20	1.29	1.00	128.14

4.8 Preliminary Design Results

Based on the MDO results, the aerodynamic trade studies, and the stability and control analysis, the component sizes of (Un)Stable Mable were finalized.

4.8.1 Component Sizing

Table 4.9 details the final component sizes for the airplane.

Table 4.9 Component Sizes

Dimension	Value
Wing Area	4.004 ft^2
Wing Aspect Ratio	5.5
Wing Span	4.69 ft
Wing Chord	0.854 ft
Wing Airfoil	SD7043
Aileron Chord	1.5 ft
Aileron Span	0.25 ft
Dihedral	0 deg
Washout	3 deg
Wing X_{ac}	1.17 ft from nose
Wing Taper Ratio	1.0
Motor	Hacker B50-13S
Gear Ratio	6.7:1
Propeller Diameter	17 in
Propeller Pitch	13 in
Empty Weight	5.65 lb

Dimension	Value
V-tail Span	1.17 in
V-tail Height	0.52 ft
V-tail Chord	0.67 ft
Ruddervator Chord	0.21ft
Ruddervator Span	0.60 ft
V-tail Airfoil	NACA0009
V-tail Angle (from horizontal)	38 deg
Fuselage Length	3.5 ft
Fuselage Width	0.583 ft
Fuselage Height	0.375 ft
V-tail Taper Ratio	1.0
V-tail Aspect Ratio (horizontal projection)	1.75
Battery Type	GP1100
# of cells	16
Battery Weight	0.75 lb
Gross Weight	11.65 lb

4.8.2 Airplane Performance Predictions

Table 4.10 shows various performance parameters that were calculated for the airplane in its three main configurations; empty, internal payload and external payload. Power required curves for all three configurations are presented along with power available curves at 100% and 70% throttle in Fig 4.7.

Table 4.10 (Un)Stable Mable Performance Parameters

Parameter	Empty	Internal Payload	External Payload
Gross Takeoff Weight	5.65 lb	11.65 lb	11.65 lb
Takeoff Distance	20 ft	119 ft	119 ft
Maximum L/D	8.53	8.66	8.20
Cruise L/D	3.99	7.78	7.41
Maximum Climb Rate	2000 ft/s	850 ft/s	820 ft/s
Minimum Turn Radius	16 ft	32 ft	32 ft
C_{Lmax}	1.26	1.26	1.26
Turn Load Factor	3	3	3
Maximum Turn Rate	132 deg/s	97 deg/s	97 deg/s
Maximum Speed	96 ft/s	95 ft/s	93 ft/s
Stall Speed	31 ft/s	44 ft/s	44 ft/s
Cruise Speed	71 ft/s	67 ft/s	65 ft/s
Maximum Battery Current	50 A	50 A	50 A
Static Thrust	6.8 lb	6.8 lb	6.8 lb

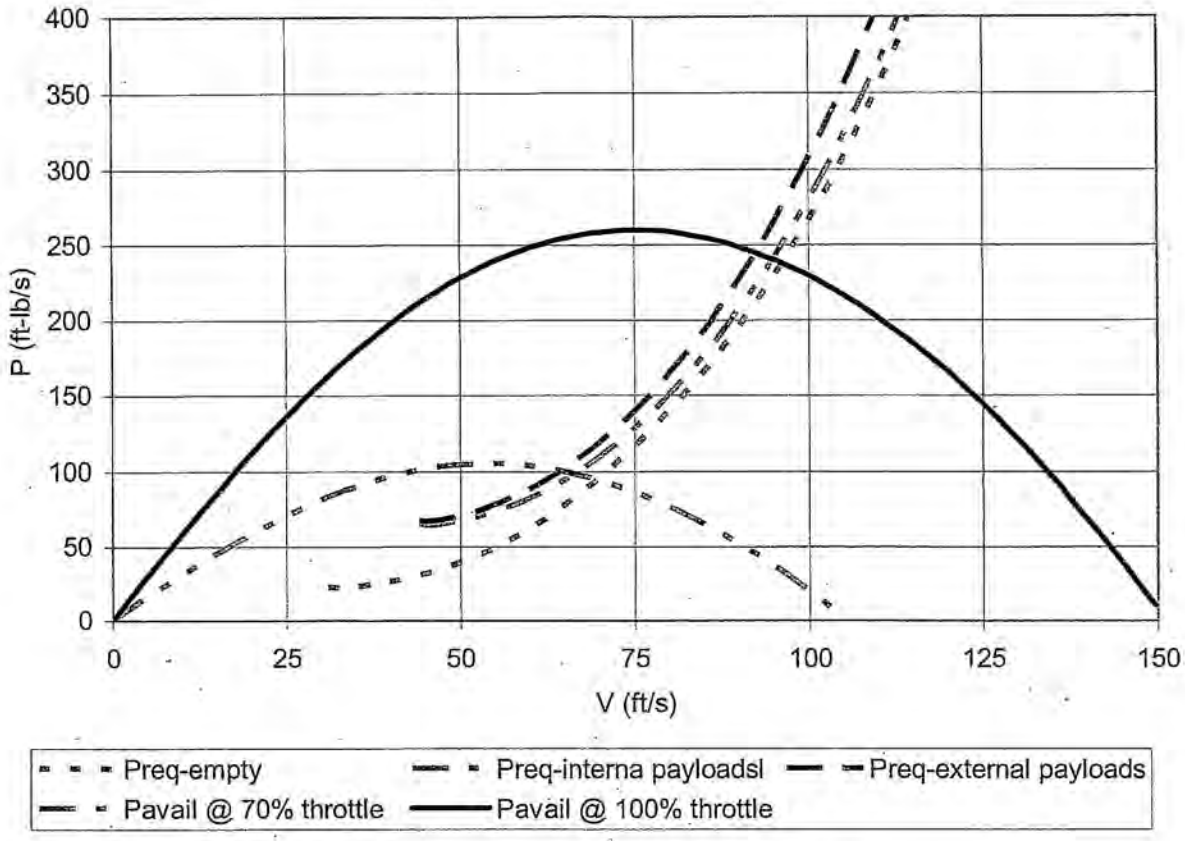

Fig. 4.7 Power Required and Power Available

4.8.3 Mission Performance Predictions

Mission times, takeoff distances and energy requirements in still air were predicted for the airplane over all three missions. The results are summarized in Table 4.11. Since the aerodynamic and/or weight parameters change between the sorties of the Sensor Reposition and Re-Supply missions, multiple values are given. For both missions, the parameters are the same during the first and third sorties. For the Re-Supply mission, the parameters are the same for the 2nd and 4th sorties, and for the Sensor Reposition mission the 2nd sortie is different than the 1st and 3rd. The predicted RAC is 5.98 and the predicted single flight scores for the three missions are 17.3 for the Sensor Reposition mission, 11.75 for the Re-Supply mission, and 3 for the Maximum Utilization mission. The energy required for the Sensor Reposition and Re-Supply missions was the driving factor in selecting the battery capacity. This limited the number of laps that could be completed in the Maximum Utilization mission to three, even though there was time remaining. The sum of the two best SFSs divided by the RAC give a competition score without the report contribution of 4.86.

Table 4.11 Mission Performance Predictions

Mission Parameter	Re-supply Mission	Sensor Reposition Mission	Maximum Utilization Mission
Takeoff distance (1st & 3rd sorties)	119 ft	119 ft	119 ft
Takeoff distance (2nd & 4th sorties)	20 ft	20 ft	N/A
Time to takeoff (1st & 3rd sorties)	3.8 s	3.8 s	3.8 s
Time to takeoff (2nd & 4th sorties)	1.4 s	1.4 s	N/A
Time to climb (1st & 3rd sorties)	5.6 s	5.6 s	5.6 s
Time to climb (2nd & 4th sorties)	5.7 s	5.7 s	N/A
Time to turn 180 deg (1st & 3rd sorties)	3.1 s	3.2 s	3.1 s
Time to turn 180 deg (2nd & 4th sorties)	2.6 s	2.6 s	N/A
Time to cruise downwind (1st & 3rd sorties)	15.2 s	15.4 s	15.2 s
Time to cruise downwind (2nd & 4th sorties	13.6 s	13.6 s	N/A
Time to cruise upwind	N/A	N/A	14.8 s
Time to descend and land (1st & 3rd sorties)	11.4 s	11.6 s	11.7 s
Time to descend and land (2nd & 4th sorties)	11.2 s	11.2 s	N/A
Time on ground	65 s	55 s	20 s
Total mission time	250 s	201 s	190 s
Energy used for takeoff (1st & 3rd sorties)	61 mAh	61 mAh	61 mAh
Energy used for takeoff (2nd & 4th sorties)	25 mAh	25 mAh	N/A
Energy used for climb (1st & 3rd sorties)	81 mAh	82 mAh	81 mAh
Energy used for climb (2nd & 4th sorties)	74 mAh	74 mAh	N/A
Energy used for 180 deg turn (1st & 3rd sorties)	13 mAh	16 mAh	13 mAh
Energy used for 180 deg turn (2nd & 4th sorties)	8 mAh	8 mAh	N/A
Energy used to cruise downwind (1st & 3rd sorties)	65 mAh	70 mAh	65 mAh
Energy used to cruise downwind (2nd & 4th sorties)	52 mAh	52 mAh	N/A
Energy used to cruise upwind	N/A	N/A	65 mAh
Energy used to descend and land (1st & 3rd sorties)	0 mAh	0 mAh	0 mAh
Energy used to descend and land (2nd & 4th sorties)	0 mAh	0 mAh	N/A
Energy used for complete mission	1000 mAh	851 mAh	868 mAh
# of laps	4	3	3
Single Flight Score	11.75	17.3	3

5.0 Detail Design

The goals of the detail design process were to select and size all of the internal components and to integrate all aspects of the design. This included selection of all the avionics equipment, a detailed weight breakdown, design of the payload system, structural sizing, and 3D solid modeling of the airplane.

5.1 Component Selection and Systems Architecture

5.1.1 Payload Design

The dimensions of the payload must be at least 12 inches long not including any fairings, fins, or other aerodynamic devices. The payload section must be constructed from PVC pipe of at least 3 inches inside diameter. The payloads must weigh at least 3 lb each. The payloads were made of PVC pipe with an outside diameter of 3.25 in and an inside diameter of 3.03 in.

The main design objective for the payload was to minimize the drag in the external configuration (i.e. mounted below the wing tips). The skin friction and pressure drag components were considered

during the fairing design. To minimized drag, the fairing designs were streamlined and blended into the main body of the payload to prevent sharp pressure gradients that would contribute to the pressure drag.

The main design parameter investigated for the payload design was the fineness ratio, f = l/d, where l is the characteristic length of the payload, and d is the diameter of the maximum cross-section. In the initial design phase, the payload was modeled with a half-ellipsoid as the front fairing, a cylinder as the main section, and a right circular cone for the rear fairing. Estimates for the drag were built up using values obtained from formulations for the flat-plate turbulent skin-friction coefficient and the pressure drag, and as a function of the fineness ratio. Initial design results showed that the minimum drag occurred for a fineness ratio of 6.6 (or a payload length of about 20 inches) with a drag coefficient of ~0.162 based on frontal area.[13]

A second design phase to further refine the geometry of the fairings was conducted using CFD. Based on a 20-inch overall length, the design parameters chosen for the second phase were the ratio of the forward and rear fairing lengths and the amount of curvature of each fairing. A series of 2D C-grid meshes of the payload profile halves were constructed with variations of these parameters in the program GRIDGEN using geometry from the modeling software Rhinoceros. The fairings themselves were modeled as cubic splines where a curvature (ρ) was specified.

Solutions were computed on these meshes with FLUENT using an axi-symmetric flow assumption and boundary conditions consistent with those encountered during the cruise phase of the airplane's mission profile. The free-stream flow conditions used were a Mach number of 0.07, and total pressure and temperature of 1 atm and 300 K respectively. The results of the second phase showed that a forward fairing with a length of 2.9 inches and a curvature (ρ) of 0.3, and a rear fairing with a length of 5.1 inches and a curvature of 0.3 produced the smallest drag coefficient. Figure 5.1 shows the mesh and velocity distribution for the selected payload fairing design. The pressure drag, neglecting viscous effects, was computed by integrating the pressure forces across the surface of the payload. CFD results of this geometry computed a drag coefficient (neglecting viscous effects) of ~0.11, a result consistent with and on the same order as the rough initial estimates. The pressure distribution, shown in Fig. 5.2, appears consistent with the distributions expected for streamlined bodies of revolution. The "dip" in the distribution is characteristic for flow over the mid-section of such bodies as well. Some interesting phenomena are the pressure spikes observed where the fairing meets the main section, both in the front and in the rear. This is the expected result of the flow "turning" at that point of the body due to the fact that the geometry of the payload is not that of a pure streamline. These spikes may be an indication of the presence of small regions of separated flow. However, the favorable pressure gradient downstream of the nose fairing (x = 4 to 14 in) in Fig. 5.2 suggests that the extent of this flow separation is limited.

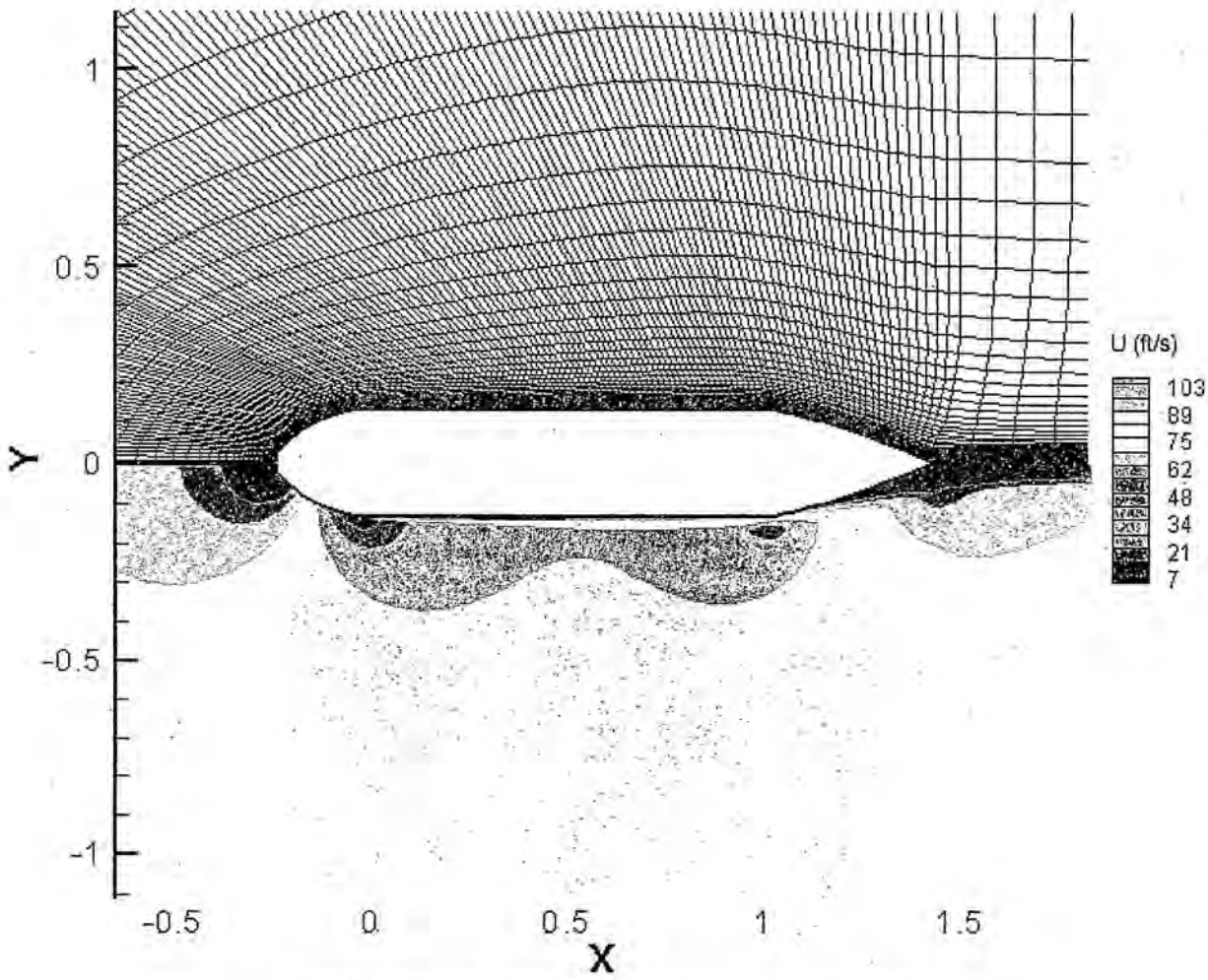

Fig. 5.1 Payload CFD Mesh and Velocity Distribution

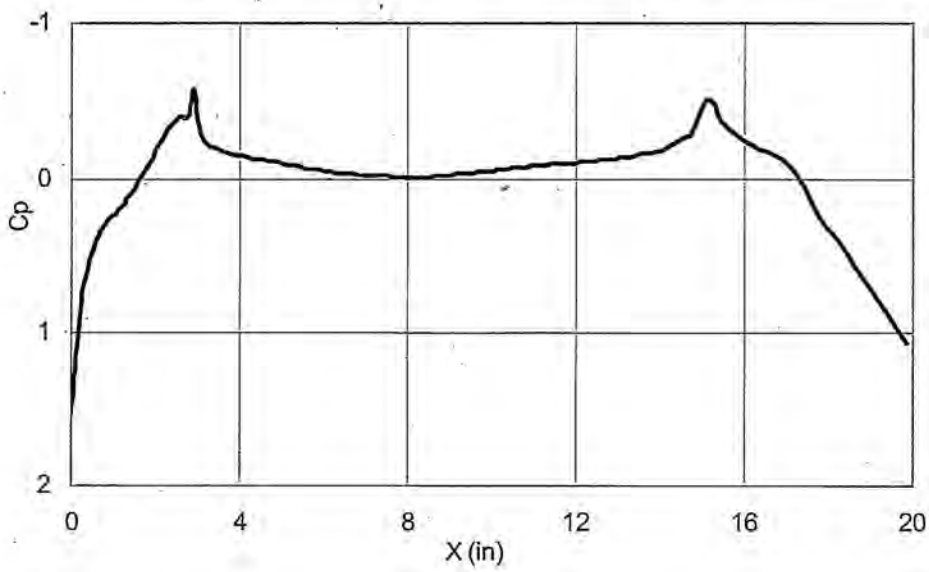

Fig. 5.2 Pressure Distribution over Payload Length

5.1.2 Structural System

The structural system of the airplane was designed based on the selected manufacturing processes described in Section 6. The goal was to design the lightest structure that could handle the necessary flight and ground handling loads. The primary components sized during this stage were the wing spar and skin, empennage spar and skin, and the fuselage longerons, bulkheads, and skin. Integration of the landing gear, design of the payload release system and sizing and location of access hatches also had to be considered.

5.1.2.1 Spar, Longeron and Skin Sizing

As is discussed in more detail in Section 6, molded composite construction methods were selected for the primary components. Table 5.1 details the component sizes along with the critical load cases, critical failure methods and safety factors.

Table 5.1 Structural Component Sizing

Part	Materials and Sizes	Critical Load Case	Critical Failure Method	Safety Factor
Wing Spar Caps	0.5" wide, 0.06" thick unidirectional carbon fiber	5 g landing w/ external payloads	Tip deflection exceeds payload ground clearance	2.0
Wing Skins	2 layers of 1.45 oz/yd^2 fiberglass separated by 1/32" balsa wood core	Ground handling of wings	Shear-buckling	1.5
Wing Ribs	1/8" plywood for root and payload ribs, 1/8" balsa for others	Maximum aileron deflection at V_{max}	Shear	2.5
V-tail Spar Caps	0.25" wide, 0.03" thick unidirectional carbon fiber	Maximum elevator deflection at V_{max}	Spar Cap Buckling	3.0
V-tail Skins	2 layers of 1.45 oz/yd^2 fiberglass separated by 1/32" balsa wood core	Ground Handling of tails	Shear-buckling	2.0
V-tail Ribs	3/32" balsa wood	Maximum elevator deflection at V_{max}	Shear	2.5
Fuselage Longerons	0.01" thick, 0.5" wide unidirectional carbon fiber	5 g landing w/ payloads	Buckling	2.0
Fuselage Bulkheads	Firewall – 1/8" birch plywood, others 1/8" Liteply	Maximum opposite ruddervator (rudder) deflection at Vmax	Shear	2.5
Fuselage Skins	2 layers of 1.45 oz/yd^2 fiberglass separated by 1/32" balsa wood core	Maximum opposite ruddervator (rudder) deflection at Vmax	Shear-Buckling	1.75

The spars were sized using Euler-Bernoulli beam bending theory and strength of materials theory. The worst-case loading scenario was expected to be a 5g landing with the payloads in the external configuration. The spar was assumed to be made out of unidirectional carbon fiber caps with a balsa core and wrapped with Kevlar tow. The smallest commercially available carbon fiber caps were selected that gave a wingtip deflection of less than one inch for the worst-case loading scenario. A one-inch maximum deflection was selected to prevent the payloads from contacting the ground under these loads with a suitable safety factor.

The wing skins were sized to keep wing twist under one degree for the worst-case loading condition; 5 ft-lb of torque, approximately equal to a full down aileron deflection at cruise velocity. This required a skin thickness thinner than commercially available fiberglass. The critical loads for the skins were in plate buckling. To counter this, the skins have a balsa wood core 1/32 in thick between two layers of 1.4 oz/yd^2 fiberglass.

The longerons were sized using Euler-Bernoulli beam bending theory and strength of materials theory. Like the wing spars, the worst-case loading scenario was expected to be a 5g landing. The longerons were assumed to be made of 2 layers of unidirectional carbon fiber (0.005 inches thick) integrated in the fuselage skin. The safety factor for longeron failure was two.

The fuselage skins were sized to keep nose and tail from twisting more than one degree. The worst-case scenario torque load was expected to be a 5 ft-lb nose-to-tail torque. This corresponds to full ruddervator deflection for yaw at maximum cruise velocity. Again, this required a skin thickness thinner than commercially available fiberglass. The critical loads for the skins were only plate buckling. To counter this, the skins have a balsa wood core 1/32 in thick between two layers of 1.4 oz/yd^2 fiberglass.

5.1.2.2 Landing Gear Design and Integration

The selected main landing gear is made by GraphTechRC and weighed 5.0 oz. The carbon fiber gear selected has a stance of 20 inches between the main wheels and a height from the ground to the bottom of the fuselage of 6.5 inches. The 20-inch stance allowed for the airplane to taxi with one external payload without tipping over. The landing gear is rated for model airplanes up to 15 lb. The landing gear will be attached by way of three bolts to a plywood plate in the bottom of the fuselage under the wing joiner tube. This will allow efficient load paths to the fuselage bulkheads and longerons. The nose gear will be fastened to the bulkhead at the front of the payloads.

5.1.2.3 Access Hatches

Access hatches needed to be located to facilitate easy maintenance of the airplane and to allow for the payloads to be quickly removed and re-loaded during the Re-Supply mission. The payload hatch is located on the top of the airplane and stretches between the front and rear payload bulkheads. It opens to the back, with a Kevlar skin hinge at the rear payload bulkhead. The payload door also provides access to a majority of the systems located in the fuselage including the propulsion batteries. Another hatch is located on top of the fuselage above the motor. This allows access to the motor, nose wheel steering mechanism and speed control. Finally, the wing and V-tail servos are mounted behind hatches that allow quick removal if they need to be accessed. The skins around all of the hatches are reinforced with 2.4 oz/yd^2 carbon fiber cloth. In addition, the fuselage structure around the payload hatch is reinforced with diagonal unidirectional carbon fiber bracing, 0.01" thick and 0.25" wide, to stiffen the cutout area for torsional loads.

5.1.2.4 External Payload Attachment and Release System

Since the loading of the payloads onto the wing hard-points is timed during the Senor Reposition mission, the payload reloading mechanism had to be quick. Mounting the payloads on the bottom of the

wings made the most sense since the payloads would need to be dropped at specific locations on the runway. The part of the payload mount attachment housed in the wing needed to be light to keep the airplane weight down. The part of the payload mount attachment fixed on the payload could be as heavy as need be as long as the total payload weight did not exceed three pounds. The entire mechanism needed to be reliable enough to be used many times without failing, and strong enough that the payloads would not break off the airplane or drop during flight or ground handling.

Of the many systems that were proposed, two showed promise and were tested. The two payload mechanisms considered are shown in Fig. 5.2. The first system incorporated two plywood tabs attached to the payload and corresponding guides for the tabs mounted in the wing underside. The guides contained a mechanism that locked onto the wooden tabs and held the payload in place. These locks could be released by a servo, allowing the payload to fall under the force gravity alone. During testing, this system worked approximately 75% of the time. The other 25% of the time the payload would get stuck in the wing mount and needed to be jiggled so that it would fall out. This system also had problems with the wooden payload tabs breaking if the payload rotated during the fall.

The second mounting method consisted of a six inch long section of 1/8" music wire that was attached to the payload. The payload was attached to the wing by inserting the music wire through the leading edge into a three inch long section of Teflon tubing which was placed at an angle of 15 degrees downward from the horizontal. A latch, controlled by a servo, held onto the music wire to lock the payload onto the wing. When released, the payload slides forward and falls out of the wing and onto the ground. Since this payload release method worked 100% of the time during testing, was harder to break, and weighed less, it was chosen for the competition airplane.

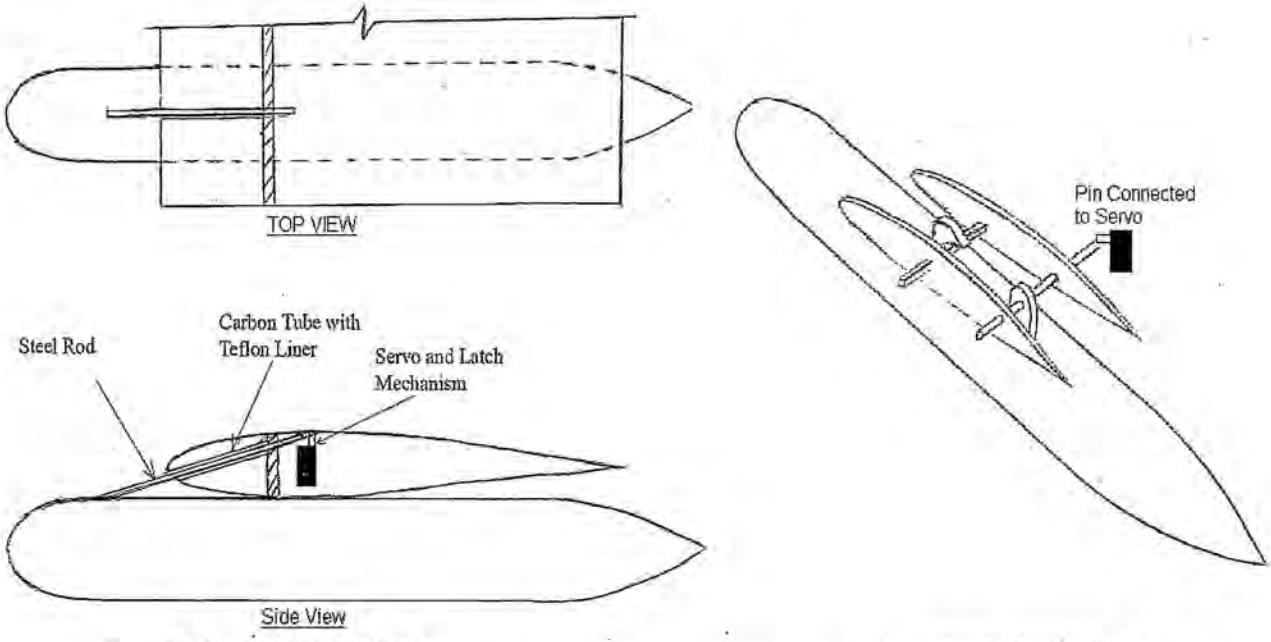

Fig 5.2 Payload Release Mechanism Sketches

5.1.3 Avionics System

The avionics system for the airplane needed to be as reliable as possible while having little negative effect on the performance of the airplane. This meant that the components needed to be light and be small so that they could fit inside airplane and not produce any unnecessary drag.

5.1.3.1 Servo Selection and Placement

The lightest servos that provided the required torque were chosen for each respective component. CS-12 MG servos were selected for the ailerons, ruddervators, and nose wheel steering mechanism, a Futaba S3102 servo for the brake actuator, and Futaba S3102 servos for the payload release mechanisms. The servos for the ailerons and ruddervators were placed inside the wings and tails respectively, and used a Rotary Drive System (RDS) to actuate the control surface. An RDS is contained completely inside the airplane; there are no control horns or servo linkages protruding out into the flow. As a result, no extra drag is produced. Since the RDS is built into the wing or tail during the construction process (see Fig. 6.2), the entire structure is stronger and provides for more reliable control surface actuation. The servos to actuate the ailerons and ruddervators were placed at the spanwise center of the control surfaces directly behind the spar.

5.1.3.2 Electronic Speed Control and Radios

The electronic speed control (ESC) and radio receiver needed to be as light as possible while providing the required performance. Since the airplane is powered by a brushless motor that draws approximately 40 amps out of 16 cells, the ESC needed to handle a steady 40 amp draw and bursts of up to 50 amps at the supplied voltage. The lightest ESC that fit these requirements was the Castle Creations Phoenix 45.

The receiver radio that was chosen was the Berg 6* DSP GIII with a 7-inch long Azarr micro receiver antenna. It is a six-channel FM receiver that has a programmable failsafe mode, as required by the contest. It was chosen because its weight is half of that of an equivalent PCM receiver with a full-length antenna, and because flight testing showed no noticeable loss of range. In addition, the 7-inch long antenna fits completely inside the fuselage and does not produce drag like a traditional receiver antenna by trailing behind airplane.

5.1.3.3 Landing Gear Systems

As mentioned in the conceptual design section of the report, a tricycle landing gear configuration with brakes was selected for its good ground handling characteristics. Since reliability was an issue, the decision was made to purchase brake and nose wheel steering systems rather than attempt to build them. Most of the available commercial brake systems would have been able to provide enough performance, but were too heavy since they were made for scale jets. The three lightest systems were a magnetic system made by Kavan, a pneumatic system made by BVM, and a hydraulic system made by Bob Fiorenze. Each Kavan brake hub weighed 2.3 oz and required a nine-volt battery for a power source. The BVM brakes system came preinstalled inside machined BVM wheels and required a master air cylinder as well as a proportional valve. The total system would have weighed 12.9 oz. The Bob Fiorenze

system consisted of two brake hubs and a master water cylinder which weighed a total of 1.1 oz. Including wheels and a servo for actuating the brake cylinder, the total system weighed 2.5 oz. The Bob Fiorenze brake system was chosen and mounted onto the carbon composite main gear.

A nose wheel steering system, instead of a differential braking one, was selected because of the reduced complexity. A differential braking system would have required two master cylinders, two high torque servos, and extremely precise calibration in order for the airplane to be able to track straight while braking. In addition, the high torque servos would weigh considerably more than the standard servos used throughout the rest of the airplane. The nose wheel gear selected was a dual strut system made by Fults out of 5/32" music wire that weighed 2.3oz. Adding a wheel and a standard servo for steering brought the total nose wheel steering system weight to 4.0 oz.

5.1.3.4 Telemetry System

In order to facilitate the collection of flight data for testing and monitoring during the competition, the telemetry system from last year was enhanced and integrated into the airplane. The system monitors propeller RPM, battery current, battery voltage, altitude and airspeed. The altitude and airspeed module was mounted in a payload for flight testing, but will be removed for the competition. A magnet is mounted on the propeller spinner, which along with a Hall-effect sensor on the fuselage measures the RPM. The transmitting antenna and power source are mounted within the fuselage along with the engine-monitoring package. A laptop is set up to download and display the real-time data during testing and the competition. This allows the team to monitor the amount of battery energy remaining in order to aid the pilot in flying the mission.

5.1.4 Disassembly Method

From the overall dimensions of the airplane, it was clear that it would not fit in the box in one piece. The goal was to minimize the number of pieces and connections that would be required, so that airplane could be disassembled quickly. Since the wing span is greater than 4 ft, it was determined that removing the right and left wing panels would be a logical disassembly step. There was still the issue of fitting the fuselage in the box; either the landing gear or the V-tail panels would have to be removed or folded so that the height would be less than 1 ft. A folding mechanism for the landing gear would be heavy, and removing the gear would require disconnecting the brake hydraulic lines. This led to the decision to remove the V-tail surfaces. The wing and V-tail halves will friction fit on carbon fiber joiner tubes and be restrained from rotating with carbon fiber anti-rotation pins. When removed, the V-tail halves will hang at the sides of the fuselage by their servo connector wires, which will not need to be disconnected. The wing electronic connections will be made with 4 pin connectors. This disassembly method will enable the airplane to be taken apart in under 10 seconds. There will be a total of 5 pieces, and two electrical connections that have to be unplugged.

5.2 Final Airplane Specifications

The final airplane specifications are given in the following tables. Table 5.1 shows the RAC breakdown for the airplane. Table 5.2 shows the final airplane specifications that will be posted in the

team's pit area as required by the contest rules. Table 5.3 is a detailed weight, balance, and moment of inertia breakdown for the airplane in all three configurations. The datum point is the projection of the tip of the spinner onto the ground plane. X is positive aft, Y is positive out the right wing and Z is positive up.

Table 5.1 RAC Table

Category	Parameter	Value	Computation	Cost ($)
MEW	Empty Weight (lb)	5.65	MEW * 500($/lb)	**2825**
REP	# of Engines	1	[1 + 0.25(# engines-1)] * Total Battery Weight (lb) * 1000 ($/lb)	**750**
	Total Battery Weight (lb)	0.75		
MFHR				(hr)
WBS 1.0 Wings	Wing Span (ft)	4.69	10 hr/ft^2 * Wing Span (ft) * Wing Chord (ft) * # of Wings	40.04
	Wing Chord (ft)	0.85		
	# of Wings	1		
	Control Function Multiplier	1	5 hr * Control Function Multiplier	5
WBS 2.0 Fuselage	Body Length (ft)	3.5	20 hr/ft^3 * Body Length (ft) * Body Width (ft) * Body Height (ft)	15.31
	Body Width (ft)	0.58		
	Body Height (ft)	0.38		
WBS 3.0 Empennage	# of Vertical Surfaces without Control	1	5 hr * # of Vertical Surfaces without Control	5
	# of Vertical Surfaces with Control	0	10 hr * # of Vertical Surfaces with Control	0
	# of Horizontal Surfaces	1	10 hr * # of Horizontal Surfaces	10
WBS 4.0 Flight Systems	# of Servos or Motor Controllers	9	5 hr * # of Servos or Motor Controllers	45
Total MFHR (hr) = Σ[WBS 1.0 Wing (hr), WBS 2.0 Fuselage (hr), WBS 3.0 Empennage (hr), WBS 4.0 Flight Systems (hr)]		120.352	20 ($/hr) * MFHR (hr)	**2407**
RAC			[MEW ($) + REP ($) + MFHR ($)] / $1000	**5.982**

5.3 Drawing Package

Drawings of the airplane were made in the Autodesk Inventor 3D modeling program. Page 46 shows a 3-view of the airplane. The next page shows the internal structure and the airplane disassembled in the box. The final page of the drawing package shows the layout of internal systems and a detail of the payload release mechanism.

Table 5.2 Airplane Specifications

University of Illinois - (Un)Stable Mable	
Geometry	
Span	4.69 ft
Length	3.5 ft
Height	1.21 ft
Wing Area	4.004 ft^2
Wing Aspect Ratio	5.5
Projected Horizontal Area	0.78 ft^2
Projected Vertical Area	0.60 ft^2
Horizontal Stabilizer Volume	1.43 ft^2
Elevator Volume	0.53 ft^2
Vertical Stabilizer Volume	1.10 ft^2
Rudder Volume	0.41 ft^2
Aileron Volume	0.88 ft^2
Wing Airfoil	SD7043
V-tail	NACA0009
Performance	
Clmax	1.26
L/D max	8.66
Maximum Rate of Climb	820 ft/min at gross weight
	2000 ft/min at empty weight
Stall Speed	44 ft/s at gross weight
	31 ft/s at empty weight
Maximum Speed	96 ft/s
Take-off Field Length Empty Weight	20 ft
Take-off Field Length Gross Weight	119 ft
Weight Statement	
Airframe Weight	3.5 lb
Propulsion System Weight	1.5 lb
Control System Weight	0.6 lb
Payload System Weight	0.1 lb
Payload Weight	6.0 lb
Empty Weight	5.7 lb
Gross Weight	11.7 lb
Systems	
Radio	Futaba 8UHFS
Reciever	Berg-6*G III
Aileron Servos	2 - Hobbico CS-12MG
Ruddervator Servos	2 - Hobbico CS-12MG
Payload Release Servos	Futaba S3108
Brake Actuator	Futaba S3102
Nose Wheel Steering Servo	Hobbico CS-12 MG
Battery Configuration	16 GP1100 Cells. 2 sets in 4x2 shotgun configuration
Motor	Hacker B50-13S
Gearbox	Maxon 6.7:1 Planetary
Propellers (nominal)	Aeronaut 17x13 folding carbon

Table 5.3 Weights, Balance, and Moments of Inertia

Part	Weight (oz)	X (in)	Y (in)	Z (in)	Ixx (oz in^2)	Iyy (oz-in^2)	Izz (oz in^2)
Right Wing Skin	4.0	16.0	16.0	6.5	1027	54	1079
Left Wing Skin	4.0	16.0	-16.0	6.5	1027	54	1079
Right Wing Spar	2.6	14.0	16.0	6.5	500	3	503
Left Wing Spar	2.6	14.0	-16.0	6.5	500	3	503
Right Aileron Servo	0.7	19.0	14.0	6.5	179	10	190
Left Aileron Servo	0.7	19.0	-14.0	6.5	179	10	190
Right Drop Servo	0.3	16.0	25.0	6.5	206	0	206
Left Drop Servo	0.3	16.0	-25.0	6.5	206	0	206
Right Drop Mechanism	0.3	12.0	25.0	6.5	156	1	157
Left Drop Mechanism	0.3	12.0	-25.0	6.5	156	1	157
Right Wing Ribs	1.3	16.0	16.0	6.5	276	13	289
Left Wing Ribs	1.3	16.0	-16.0	6.5	276	13	289
Wing Miscellaneous	6.8	16.0	0.0	6.5	2090	140	2230
Right V-tail Skin	0.9	43.0	4.0	13.0	65	448	447
Left V-tail Skin	0.9	43.0	-4.0	13.0	65	448	447
Right V-tail Spar	0.4	42.0	4.0	13.0	23	135	137
Left V-tail Spar	0.4	42.0	-4.0	13.0	23	135	137
Right Ruddervator Servo	0.7	44.0	3.0	12.0	32	318	322
Left Ruddervator Servo	0.7	44.0	-3.0	12.0	32	318	322
V-tail Miscellaneous	1.3	43.0	0.0	12.0	40	187	185
Fuselage Skins	8.0	19.0	0.0	8.5	70	1168	1168
Fuselage Longerons	1.2	20.0	0.0	8.5	8	191	193
Fuselage Bulkheads	1.7	16.0	0.0	8.5	10	208	202
Payload Hatch	1.7	16.0	0.0	10.0	6	40	35
Wing Joiner Tube	2.5	14.0	0.0	6.5	210	14	203
Landing Gear Attachment Plate	1.0	16.0	0.0	6.5	6	6	35
Main Landing Gear	5.7	17.0	0.0	5.0	343	148	240
Nose Landing Gear	3.3	5.0	0.0	4.0	23	363	342
Nose Wheel Steering Servo	0.7	5.0	1.0	9.0	0	72	72
Brake System	1.0	17.0	0.0	7.0	136	60	84
Brake Actuator	0.7	18.0	1.0	7.0	2	2	1
Motor	7.1	3.0	0.0	10.0	20	1077	1061
Gearbox	1.6	1.5	0.0	10.0	5	282	278
Propeller and Spinner	2.5	0.5	0.0	10.0	126	603	597
Propulsion Batteries	12.0	7.5	0.0	8.0	4	372	369
Electronic Speed Control	1.2	12.0	-1.0	9.0	3	103	101
Receiver	0.7	12.0	1.0	7.0	2	8	8
Receiver Battery	1.5	12.0	-0.5	7.0	5	18	16
Telemetry System	2.5	17.0	0.0	7.0	7	36	31
Telemetry Battery	1.5	17.0	0.0	7.0	3	12	11
Fuselage Miscellaneous	2.6	18.0	0.0	8.0	397	795	939
Right Internal Payload	48.0	14.5	1.6	9.0	285	1719	1815
Left Internal Payload	48.0	14.5	-1.6	9.0	285	1719	1815
Right External Payload	48.0	14.5	25.2	5.0	30928	1884	32295
Left External Payload	48.0	14.5	-25.2	5.0	30928	1884	32295
Total (Empty)	**91.2**	**14.49**	**0.00**	**7.73**	**8445**	**7872**	**15060**
Total (Internal Payload)	**187.2**	**14.50**	**0.00**	**8.38**	**9015**	**11310**	**18690**
Total (External Payload)	**187.2**	**14.50**	**0.00**	**6.33**	**70300**	**11640**	**79650**

6.0 Manufacturing Plan and Processes

The selection of the materials and processes for the manufacturing of the airplane were important throughout the design process. It was important that the airplane be built in a reasonable time with materials and methods that the team could afford and were familiar with. It was also important that the airplane be kept light and strong to increase its performance. A figure of merit and scheduling approach was used to develop the manufacturing plan to accomplish these goals.

6.1 Manufacturing Materials and Processes Investigated

There were a number of manufacturing materials and processes that were considered for each of the main components of the airplane. These materials and processes are described below for each of the main components.

6.1.1 Wing and Empennage Manufacturing Materials and Processes

There were a total of five manufacturing materials and processes considered for the wing and the empennage.

- A balsa, built-up structure with either a carbon fiber or wooden spar. This rib and spar structure would be covered in Monokote™ to provide a skin for the structure.
- A foam core covered in fiberglass that is vacuum bagged on. This method relies on the fiberglass to provide the torsional stiffness and unidirectional carbon fiber to provide bending stiffness.
- A molded composite wing. For this method, female molds would be constructed and from these the fiberglass and balsa wing skins would be formed and the internal structure added.
- A hybrid composite and built-up method. This method consists of a carbon fiber spar and leading edge D-tube edge and a built-up balsa structure covered with Monokote™ behind the spar.
- A foam core sheeted with balsa wood and covered with Monokote™

Also included in the figure of merit analysis was the material to be used for the joiner tube that connects the wing to the fuselage. The materials that were considered for the joiner tube were aluminum, carbon fiber, and steel.

6.1.2 Fuselage Manufacturing Materials and Processes

There were four manufacturing materials and processes considered for the construction of the fuselage.

- A molded structure where the shell of the fuselage is pulled from a female mold.
- Fiberglass vacuum bagged on a foam core. The foam would then be removed to make room for internal systems and payloads.
- Traditional sheeted balsa and plywood structure covered with Monokote™.
- A wooden truss structure covered in Monokote™.

6.1.3 Landing Gear

There were four options for the main landing gear struts. The first three were to buy aluminum, steel, or carbon fiber gear. The final method was to construct the landing gear from carbon fiber composites.

6.2 Figures of Merit

Figures of merit were used to logically rank the various materials and manufacturing processes used for the various parts of the airplane. These figures of merit were weighted with respect to their influence on the various aspects of the final score of the airplane and used to do eliminate all but the most appropriate material and processes. The sum of the weighting factors was 100 for each component considered. The seven figures of merit that were used are discussed below.

6.2.1 Strength-to-Weight Ratio

One of the major factors that determined the final competition score is the weight of the airplane. With this in mind, it was important that the materials used to construct the airplane be as light as possible while having the strength to satisfy the mission requirements. The materials and their corresponding manufacturing processes received scores ranging from -1 for low strength-to-weight ratios to 1 for high strength-to-weight ratios. The weighting factors, for the strength-to-weight ratio FOM, ranged from 20 to 80, depending on the airplane component being considered. These values were selected because of the weight's large impact on the RAC and performance of the airplane.

6.2.2 Skill Level Required

It was also important that the manufacturing materials and processes selected be within the set of skills possessed by the team. A skill matrix was developed to rate the team's experience and skills with the manufacturing materials and processes investigated, see Table 6.1. Manufacturing materials and processes that more than six team members had experience with were given a score of 1. Materials and processes that three to five team members had experience with were given a score of zero. Lastly, materials and processes that less than three members of the team had experience with were given a score of -1. The weighting factors, for the skill level FOM, ranged from 0 to 5, depending on the airplane component being considered.

Table 6.1 Skill Matrix

Skill	Wood-working	Monokote Covering	Foam Hotwiring	CNC Operation	Vacuum Bagging	Molded Construction	Soldering and Electronics	Metal Working
Number of Personnel with Experience	12	6	8	5	8	2	4	3
Score	1	0	1	0	1	-1	0	0

6.2.3 Cost and Availability

Another influencing factor used in the figure of merit analysis was the cost and availability of the materials and processes. The group had limited resources to manufacture the airplane, so inexpensive and readily accessible materials and processes would allow more resources to be applied to other areas. If the material or process was inexpensive and at hand it was given a score of 1. At the other end of the spectrum, if the material or process was expensive and/or would require a significant amount of time to acquire it was given a score of -1, with the others falling between these extremes. Since this FOM had

little impact in the overall performance of the airplane it was given lower weighting factors that ranged from 7 to 10, depending on the airplane component being considered

6.2.4 Time to Build

As with cost, the team had a limited budget of time to build the airplane. This produced a requirement for a figure of merit to take this into account. For this figure of merit, any manufacturing process that took a relatively short amount of time was given a score of 1 while a process that took a large amount of time was given a score of -1. This figure of merit was given an intermediate weighting factor of 13 because of the limited time that was available and, on the other hand, its limited impact to the final competition score of the airplane.

6.2.5 Internal Component Placement

Another important factor, taken into account for the figure of merit analysis, was the placement of the internal components, such as servos, in the airplane. For this figure of merit, manufacturing methods that allowed the internal components to be placed easily was given a score of 1. Methods that caused some difficulty in placing the internal components were given a score of 0, and those methods for which it would be extremely difficult or impossible to insert internal components were given a score of -1. The internal component placement FOM was given weighting factors ranging from 10 to 20 as it has some influence in the airplane's manufacturability.

6.2.6 Durability of Part

The next factor in the selection of the manufacturing materials was the durability of the component. The materials and manufacturing processes that would result in a part that would last through the lifetime of the airplane were given a score of 1. The materials and processes that would produce parts that would last through many flights were given a score of 0, and those that would result in a life of only a few flights were given a score of -1. This FOM was given weighting factors from 10 to 20 based on how hard it would be to replace the part and how critical the part is to the airplane.

6.2.7 Shape Fidelity

The final figure of merit selected for the analysis was the shape fidelity of the materials and manufacturing processes. The materials and processes that showed no deviation from the desired shape were given a score of 1. Materials and processes that exhibited limited deviation from the desired shape were given a score of zero, while ones that showed significant deviation were given a score of -1. This figure of merit was given a weight factor of 20 for the wing, empennage, and fuselage as it has a major effect on the aerodynamics of the airplane.

6.3 Figure of Merit Analysis Results

Table 6.2 shows the figures of merit that were used to select the manufacturing methods and materials for the major parts of the airplane. The weighting factors for each figure of merit are shown for each component. The figure of merit analysis resulted in the following manufacturing methods and materials being selected:

- Molded composite construction for the wing, fuselage, and empennage
- A carbon fiber wing joiner tube
- A purchased carbon fiber landing gear structure

Table 6.2 Manufacturing FOM's

	Figures of Merit	Strength to Weight Ratio	Internal Component Placement	Cost and Availability	Time to Build	Skill Level Required to Build	Durability of Part	Shape Fidelity	
Component	**Construction method**								**Score**
Wing	**Weight**	**30**	**15**	**7**	**13**	**5**	**10**	**20**	
	built-up monokote covered	0	1	1	1	1	-1	-1	10
	fiberglass covered foam core	0	0	0	1	1	0.5	0.5	33
	molded	***1***	***1***	***-1***	***-1***	***-1***	***1***	***1***	***50***
	hybrid	1	0	0	0	0	0.5	0.5	45
	wood sheeted on foam	0	0	1	1	1	0	0	25
Tail	**Weight**	**20**	**20**	**7**	**13**	**5**	**15**	**20**	
	built-up monokote covered	0	1	1	1	1	-1	-1	10
	foam core	0	0	0	1	1	0.5	0.5	35.5
	molded	***1***	***1***	***-1***	***-1***	***-1***	***1***	***1***	***50***
	hybrid	1	0	0	0	0	0.5	0.5	37.5
	wood sheeted on foam	0	0	1	1	1	-1	0	10
Fuselage	**Weight**	**25**	**10**	**7**	**13**	**5**	**20**	**20**	
	molded	***1***	***1***	***-1***	***-1***	***-1***	***1***	***1***	***50***
	fiberglass over foam plug	0	0	0	1	1	0	0	18
	built-up with monokote	1	1	1	0	1	-1	-1	7
	wood truss covered with monokote	-1	0	1	1	1	0	0	0
Wing Joiner Tube	**Weight**	**80**	**0**	**10**	**0**	**0**	**10**	**0**	
	aluminum	0	0	0	0	0	0	0	0
	carbon fiber	***1***	***0***	***-1***	***0***	***0***	***1***	***0***	***80***
	steel	-1	0	0	0	0	1	0	-70
Landing Gear	**Weight**	**60**	**0**	**7**	**13**	**0**	**20**	**0**	
	aluminum	0	0	1	1	0	0	0	20
	carbon fiber bought	***1***	***0***	***1***	***-1***	***0***	***1***	***0***	***100***
	steel	-1	0	0	1	0	1	0	-27
	carbon fiber made	1	0	1	0	0	1	0	87

6.4 Selected Manufacturing Processes

The selected materials and manufacturing processes will be described in more detail. The step-by-step processes required for creating the different molded parts and assembling the complete airplane are also detailed. A construction schedule was developed to keep construction on track and to maximize the time and other resources available to the team. The construction milestone chart is presented in Fig. 6.1. The construction schedule slipped due to the change from a flying wing to conventional configuration. In past years the team has always built over the predicted weight. To help prevent unwanted weight overruns, the team posted a checklist in the shop to detail where every gram in the airplane comes from. This running tally allowed the team to see which parts exceeded the predicted weights and locate any inconsistencies in the manufacturing processes.

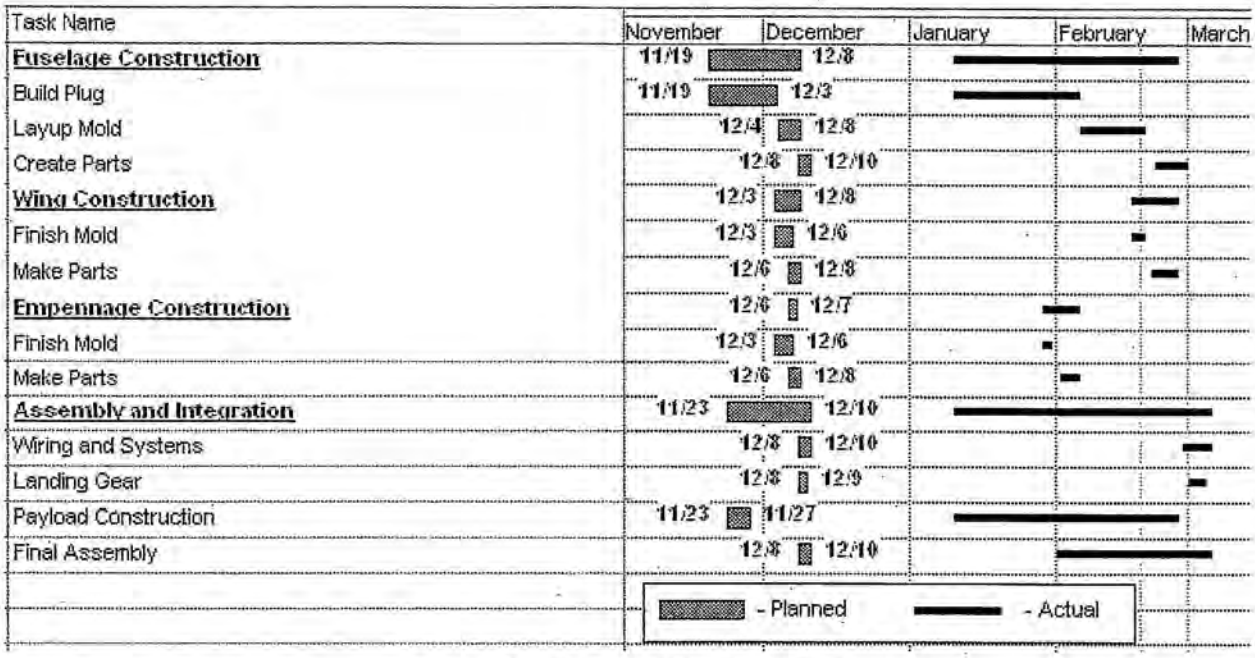

Fig. 6.1 Construction Milestone Chart

6.4.1 Wing and Empennage Manufacturing Process

The method selected for the manufacture of the wing and empennage was molding. The first step in these processes was the cutting of the mold. The mold for the wing was professionally cut with a CNC router out of Medium Density Fiberboard (MDF) to ensure accuracy and durability. The mold for the empennage was cut out of foam with a CNC foam cutter that was built by the group last year. The second step in the process was finishing the surface of the mold. The surface of the wing mold was sanded to ensure a smooth mold and then painted with multiple layers of automotive paint to harden the surface. The third step in the molding processes was the lay-up of the parts. First the mold was waxed to ensure that the parts would release from the mold. Next, the outer layer of 1.4 oz/yd^2 fiberglass was put into the mold and coated with epoxy. This was done for both the top and bottom halves of the wing and empennage. Following this, a layer of 1/32" contest grade balsa was laid on top of the fiberglass. After the balsa, the inner layer of 1.4 oz/yd^2 fiberglass was laid on top of the balsa, coated with epoxy and then both halves of the part were vacuum bagged. The fourth step in the construction of the wing or empennage was placing the internal structure and components into the part. This was done by removing the halves from the vacuum bag and, while keeping the part halves in the molds, trimming the excess material from the parts. Following this, internal components such as ribs, servos, and the spar were epoxied to the bottom half of the part. The placement of these parts was aided with the use of templates created earlier. With the internal components in place, the two halves were epoxied together. To do this, edges that were going to come into contact were covered with epoxy and then the mold halves were clamped together. After the epoxy had cured the part was taken from the mold and the joined edges were sanded smooth to complete the wing or empennage part.

6.4.2 Fuselage Manufacturing Process

The method selected for the construction of the fuselage also was molding, but unlike the wing and empennage, cutting a direct female mold of the fuselage from a single piece of material was not practical due to the amount of material that would have to be removed. Another approach was taken for the fuselage mold. The first step in this process was the construction of a mold plug. This was done by cutting twenty cross-section formers of the fuselage and mounting them to a centerline board of the plug. With the formers mounted every couple of inches they were then sheeted with balsa to provide a solid surface. This surface was sanded smooth and coated with fiberglass to provide a hard surface. The mold plug was painted with multiple layers of paint to make the surface even smoother. With the plug finished, a parting board was put vertically around the centerline of the plug to allow one half of the mold to be made at a time. The next step in the process was the lay-up of the first half of the mold. To do this the plug and parting board were both waxed on one side of the parting board to ensure that the mold would release from the plug. The plug was then coated with a graphite powder and epoxy mix to form the mold. After this cured the backside of the mold was built up with fiberglass to ensure that it maintained its shape. After the first half of the mold cured, the parting board was removed and the other half of the plug and the edge of the first mold half were waxed in preparation for the lay-up of the other half of the mold. The second half of the mold was laid up exactly the way that the first half was and cured. When the second half of the mold had cured, the mold halves were removed from the plug. Finally, the composite parts were created in the molds in the same way as the wing and empennage molds.

Figure 6.2 shows a photograph of the finished fuselage plug before the mold was built on it. The figure also includes a photograph of the empennage surfaces during construction. The servos and RDS internal control surface actuation system can be seen. Also included in the figure is a photograph of the mold surface coat being applied to the plug for the front payload fairing.

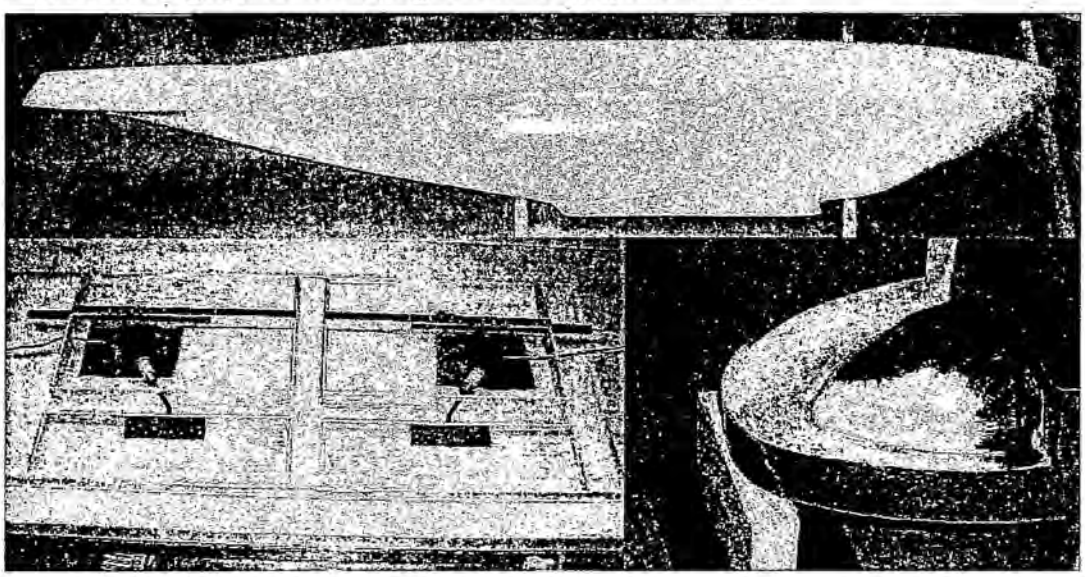

Fig. 6.2 Construction Photos (Clockwise from top: fuselage plug, making mold of front payload fairing, molded tail construction with RDS system installed)

7.0 Testing Plan

A detailed testing plan was carried out during the development of (Un)Stable Mable. Tests were performed at the sub-system level and will be performed on the competition airframe. Sub-system testing included structural testing, static and in-flight propulsion system testing, payload system testing, and wind tunnel testing of candidate airfoils. An Almost Ready to Fly (ARF) airplane was purchased for performing in-flight testing of the propulsion and payload drop systems. In addition, the ARF provided new members with experience in model airplane construction and operation. Testing on the competition airplane will include structural, ground handling, and flight tests. The objective of the tests are to verify the analytic models used in designing the airplane, and ensure to that the airplane meets the necessary performance requirements. The testing schedule is outlined in Fig. 7.1.

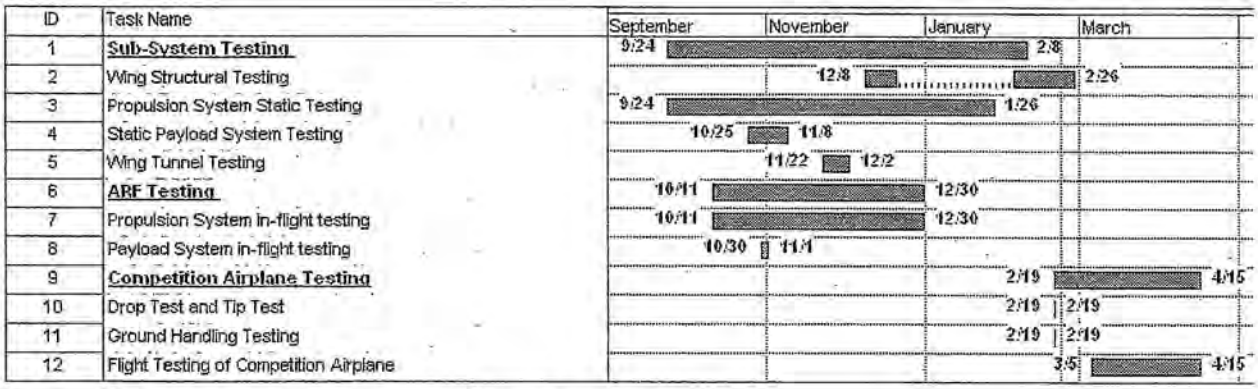

Fig. 7.1 Testing Schedule

7.1 Propulsion Testing

The objectives of propulsion testing were primarily to verify propulsion system predictions made by MotoCalc and to investigate the influence of real-world parameters on propulsion system performance.[9]

7.1.1 Static Testing

Initially, static tests were performed on a thrust stand built by the team. This setup allowed measurement of battery current, battery voltage, net thrust and propeller RPM. The top performing propulsion systems from the MDO code were tested. Table 7.1 indicates the propulsion systems tested, and compares the theoretical predictions from MotoCalc with the results obtained during testing. The results show that the actual thrust produced did not exactly match MotoCalc's thrust predictions. In general, the less current was drawn and 20% less thrust was produced. To account for these discrepancies when estimating mission performance, the thrust was taken to be 80% of MotoCalc's predicted thrust. Testing also showed that the actual GP1100 cell capacity was around 1000 mAh. This value was used as a solution constraint in the optimization code.

Table 7.1 Static Thrust Testing Results

Motor	Gear ratio	Battery Pack	Propeller	Actual Current (A)	Actual Voltage (V)	Actual Thrust (lb)	Actual RPM	Predicted Current (A)	Predicted Voltage (V)	Predicted Thrust (lb)	Predicted RPM
Hacker B50-13S	6.7:1	14 cell GP1100	17x11 Aeronaut	38	11.7	5.28	4800	44.1	13.0	6.81	5100
Hacker B50-13S	6.7:1	14 cell GP1100	17x13 Aeronaut	50	11.3	5.15	4600	48.6	12.6	6.65	4900
Hacker B50-13S	6.7:1	14 cell CP1300	17x13 Aeronaut	51	12.3	5.20	4700	44.6	12.1	6.12	4700
Hacker B50-13S	6.7:1	15 cell GP1100	17x13 Aeronaut	46	13.0	5.44	5100	52	13.6	7.19	5100
Hacker B50-13S	6.7:1	14 cell GP1100	18x11 Aeronaut	45	13.0	6.16	5200	50	12.5	7.62	4900
Mega ACn 16-25-4	3:1	14 cell GP1100	17x11 Aeronaut	33	12.7	4.80	4500	43	13.1	6.58	5000
Mega ACn 16-25-4	3:1	14 cell GP1100	17x13 Aeronaut	41	13.0	4.56	4800	47	12.8	6.39	4800
Mega ACn 16-25-4	3:1	15 cell GP1100	17x11 Aeronaut	40	14.6	5.60	4900	46	13.7	7.14	5200
Mega ACn 16-25-4	3:1	15 cell GP1100	17x13 Aeronaut	46	14.8	5.25	4700	50	13.4	6.88	5000

7.1.2 Flight Testing

To get a qualitative feel for the performance of the candidate propulsion systems, a series of flight tests were conducted with the Viper ARF kit. This ARF was selected due to its similarity in size and shape to the competition airplane being designed. It was setup to be outfitted with any of the expected propulsion systems and was capable of being loaded up to 11 lb. Initial testing in October showed very poor results. The airplane struggled to maintain altitude even when empty and crashed a couple of times. This was very perplexing since the static thrust testing indicated that the airplane should have been capable of a near vertical climb when empty with any of the propulsion systems.

The problem was resolved with on-site ground testing before the next set of flights, and through research on the Internet. The cool temperatures in Illinois in October (40's) were having a negative effect on the GP1100 battery performance. After pulsing the motor for 5 seconds at 10 second intervals on the ground, the static thrust increased from 2 lb to 6 lb over the course of two minutes. The current also increased from 14 A to 45 A. The temperature effect on battery performance was not as evident during static thrust testing since it occurred at room temperature. To alleviate the problem, it was ensured that the batteries were at least at room temperature before performing further flight tests.

Further testing of the Viper was conducted to verify that the propulsion systems could lift up to 11 lb and to investigate energy usage over the contest course. The testing indicated that each lap around the contest course averaged approximately 200 mAh of energy usage. This compared well with the predicted value of 220 mAh per lap from the performance code.

7.2 Wind Tunnel Testing

When investigating the feasibility of a flying wing design it was quickly observed that the airfoil c_{lmax} was going to be a major driver of the design. To keep the airplane as small as possible for RAC reasons it was desired to improve on the c_{lmax} of existing reflexed low-Reynolds number airfoils. A number of airfoils were designed using PROFOIL[15] and analyzed using XFOIL.[16] To verify the predictions of XFOIL, wind tunnel testing was conducted in the University of Illinois Low Speed Wind Tunnel. More information on the test setup is described by Lee.[17]

Results of the testing indicated that the airfoils did not reach the predicted c_{lmax} values. The shape fidelity and surface quality of the test wings were not very good, but they represented the manufacturing quality of the construction methods used by past UIUC DBF teams. The wind tunnel tests provided an approximation of the degradation in c_{lmax} that can be attributed to the building methods. This led to two conclusions that influenced the design and construction of the airplane. First, the flying wing design was no longer feasible. With the lower than expected c_{lmax}, the wing area would need to increase to meet the takeoff requirement, which in turn negated the RAC benefit of the flying wing design. Second, to approach the theoretical c_{lmax} values calculated with XFOIL, a building method that resulted in better shape fidelity needed to be used. This strongly influenced the decision to construct the wings using a hollow molded structure.

7.3 Payload System Testing

The two payload drop mechanisms developed during the detail design phase were constructed and tested (See Fig. 5.2). The latch and pin system was built in two versions. The first did not have a quick reloading mechanism and tended to jam during reloading. The second version utilized a quick reloading mechanism and worked over 75% of the time. Both versions were installed in the wing of the team's Spacewalker ARF from last year. During the airplane's only test flight with the payloads attached, the payloads and release mechanisms withstood dynamic flight maneuvers. The payloads pushed the center of gravity location too far aft, so the pilot had to jettison the payloads to land the airplane. Both payloads were successfully released 30 seconds into the flight.

The rod and tube release system was also constructed and tested statically in the shop. One concern was the tube angle which would be required for a successful release of the payload. Testing indicated that a 10° angle was sufficient to release the payload, which fell well under the 17° limit allowed by internal dimensions of the wing.

Both mechanisms worked successfully and allowed a quick reload. The rod and tube release system was selected due to its weight savings and the fact that it was more reliable. The rod and tube system weighed 1 oz versus 4 oz for the latch and pin system.

7.4 Structural Testing

In order to verify the structural integrity and sizing predictions made during the design of the airplane, a number of structural tests were performed. Since initially a flying wing was considered, a swept wing test article was constructed using a fiberglass and carbon fiber skin vacuum bagged on a

foam core. The wing was loaded approximately 7 inches ahead of the LE at the tip, where the payload CG would have been located. The resulting deflection and twist were measured and compared to predictions made using a beam bending and single cell torsion analysis. This test was used to help verify the accuracy of the methods used for structural calculations. The theoretical and actual results are shown in Fig 7.2. It can be seen that the torsional stiffness predictions were accurate up to about a 10 lb load. The bending predictions did not match with the experimental results. It was noticed that the skin spar began to delaminate from the foam where the mounting spar terminated as the initial loads were applied. This was responsible for the early failure and likely the decreased bending and torsional stiffness as compared to the theoretical results.

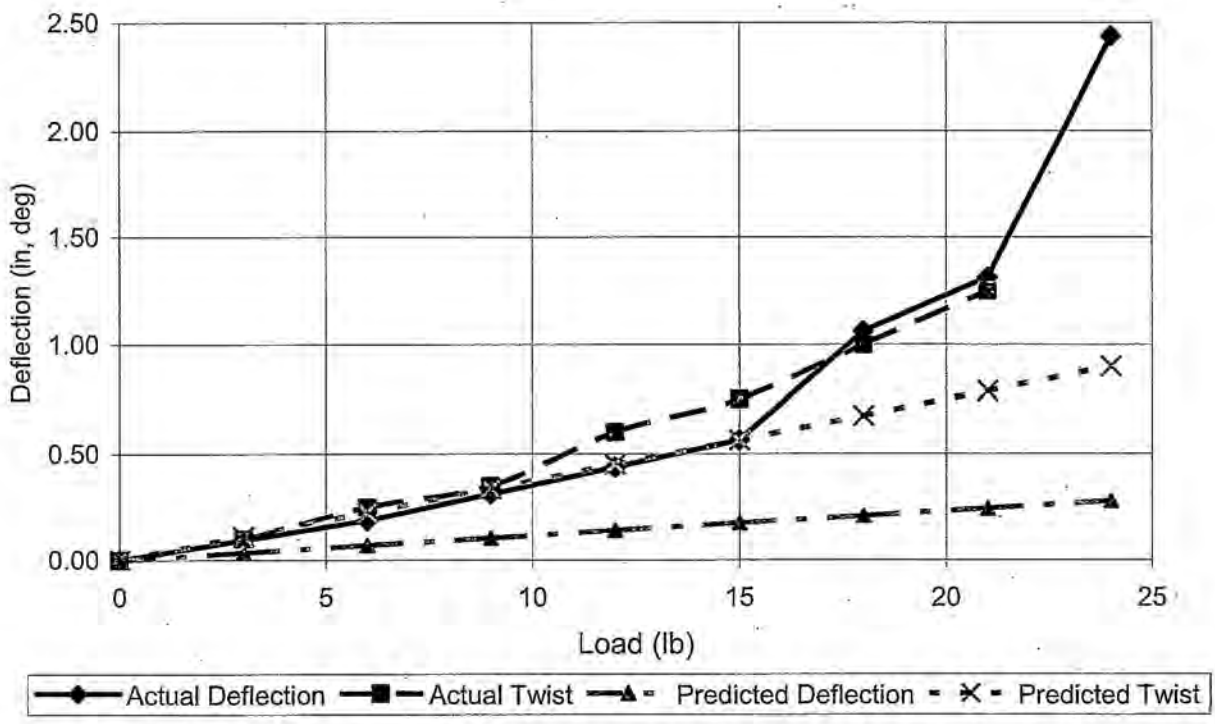

Fig. 7.2 Fiberglass on Foam Swept Wing Structural Test Results

After the conventional V-tail configuration was settled upon, the plan was for the first pre-production molded composite wing to be tested in bending to verify the predictions made during its design. With a 15 lb load applied at the payload external attachment point to simulate a 5g landing, the predicted deflection was 0.43 inches.

When construction is completed, the complete airframe will also undergo testing. First, the upright and inverted tip tests will be performed as required at the contest. A drop test will be conducted from 1 ft above the ground with the payloads first in their internal configuration, then in the external configuration. This will simulate the effect of a hard landing with a vertical velocity of about 8 ft/s. The torsional stiffness of the fuselage will also be tested. A torque of 5 ft-lb will be applied to the V-tail. The predicted twist for this test is less than three degrees.

7.5 Flight Test Plan

A detailed flight testing schedule was established to verify the performance of (Un)Stable Mable and to practice for the competition as time and weather permit. No flight tests were carried out before the submission of the report. Before flight testing begins, low and high speed taxi tests will be conducted with and without payloads. This will be done to familiarize the pilot with ground handling characteristics of the airplane, and to verify that the airplane can taxi with only one external payload. The flight testing schedule is shown in Table 7.2. A preflight checklist has been developed to verify the structural integrity of the airplane and to ensure that all of the electronic systems on the airplane are operating correctly. The preflight checklist is shown in Table 7.3.

Table 7.2 Flight Test Schedule

Flight #	Date(s)	Description	Goals
1	March 5, 2005	Takeoff, fly 2 laps and land. No payload.	Familiarize pilot with flight characteristics and identify and correct any problems before continuing.
2	March 5, 2005	Takeoff, perform coordinated and uncoordinated stalls, two high-speed passes, land. No payload.	Familiarize pilot, explore flight envelope and measure takeoff distance.
3	March 6, 2005	Takeoff, fly 2 laps and land. Payloads in internal configuration.	Familiarize pilot with flight characteristics and identify and correct any problems before continuing.
4	March 6, 2005	Takeoff, perform coordinated and uncoordinated stalls, high-speed pass, land. Payloads in internal configuration.	Familiarize pilot, explore flight envelope with internal payloads, and measure takeoff distance.
5	March 12, 2005	Takeoff, fly 2 laps and land. Payloads in external configuration.	Familiarize pilot with flight characteristics and identify and correct any problems before continuing.
6	March 12, 2005	Takeoff, perform coordinated and uncoordinated stalls, high-speed pass, land. Payloads in internal configuration.	Familiarize pilot, explore flight envelope with external payloads, and measure takeoff distance.
7-9	March 12, 2005	Takeoff, perform touch and goes, land. Repeat with 3 payload configurations.	Improve landings and low speed handling qualities
10	March 19, 2005	Takeoff, fly laps until the airplane is low on energy.	Verify battery capacity and gauge performance on Maximum Utilization Mission
11+	March 19 – April 15, 2005	Practice Re-Supply and Sensor Reposition Missions	Pilot and ground crew practice. Evaluate performance under various wind conditions.

7.6 Lessons Learned

The following list summarizes the lessons learned during propulsion, wind tunnel, payload system, and structural testing.

- MotoCalc over predicts thrust by about 20%
- The GP1100 battery capacity is actually ≈1000 mAh
- The GP1100 cells perform poorly in low temperature environments
- The optimal propulsion systems from the MDO provided ample in-flight performance

- The performance code energy predictions were close to measured values
- It is hard to achieve predicted c_{lmax} with previously used manufacturing methods
- The simpler payload release system is lighter and more reliable
- Skin spar buckling needs to be accounted for in bending predictions
- Twist predictions were accurate in the linear region
- Flight test early and often

Table 7.3 Preflight Checklist

	1. Check wing structural integrity		16. Check brake hydraulic pressure
	2. Check V-tail structural integrity		17. Unpowered aileron slop check
	3. Check fuselage structural integrity		18. Unpowered ruddervator slop check
	4. Check landing gear structural integrity		19. Powered aileron slop check
	5. Payload door latched properly		20. Powered ruddervator slop check
	6. Check right payload attachment		21. Check nosewheel steering mechanism
	7. Check left payload attachment		22. No-throttle range check
	8. Check that propeller is tightened		23. Range check with throttle advanced
	9. Verfiy that propulsion battery is charged		24. 5 sec full throttle run up
	10. Verify that propulsion battery is at least at room temperature		25. Check ground crew and cameraman readiness
	11. Verify that receiver battery is charged		26. Test right external payload deployment
	12. Verify that telemetry battery is charged		27. Test left external payload deployment
	13. Check telemetry radio link		28. Check spotter and pilot readiness
	14. Check wing and V-tail servo connections		29. Check that fuse is properly inserted
	15. Check that propulsion batteries are securely connected		30. Final inspection of all electrical and structural connections.

8.0 References

[1] "AIAA Design/Build/Fly Competition – 2005_Rules". Accessed: November 12th, 2004 at: http://www.ae.uiuc.edu/aiaadbf/

[2] "Terrabreak.org 2003/2004 Speed Comparison". Accessed: October 5th, 2004 at: http://www.terrabreak.org/groundloop/2004_speeds.shtml

[3] "Fiberglass Overcast Final Design Report" UIUC Design/Build/Fly Team, 2004.

[4] "OSU Black Final Design Report" Oklahoma State University Design/Build/Fly Team, 2004.

[5] MATLAB™. Version 6.5, Mathworks Inc., 2002.

[6] Drela, Mark, "Quick V-tail Sizing", http://www.charlesriverrc.org/articles/design/markdrela_vtailsizing.htm March 2000.

[7] "Phoenix Final Design Report" UIUC Design/Build/Fly Team, 2001.

[8] Nelson, Robert C., Flight Stability and Automatic Control, McGraw Hill, New York, NY, 1986.

[9] MotoCalc™. Version 7.01, Capable Computing Inc., 2004.

[10] PROFILI. Version 2.17, Stefano Duranti, 2004.

[11] Abbott, Ira H. & Von Doenhoff, E., Theory of Wing Sections, Dover Publications, Mineola, NY, 1980.

[12] Raymer, Daniel P., Aircraft Design: A Conceptual Approach, 3rd Edition, American Institute of Aeronautics and Astronautics, Reston, VA, 1999.

[13] Hoerner, Sighard F., Fluid-Dynamic Drag, 2nd Edition, Hoerner Fluid Dynamics, Bakersfield, CA, 1965.

[14] Simple Lifting Line Theory [computer program]. W.H. Mason, Department of Aerospace and Ocean Engineering, Virginia Tech, Blacksburg, VA.

[15] PROFOIL. Version 2.0, Michael Selig, 1999.

[16] XFOIL. Version 6.94, Mark Drela, 2001.

[17] Lee, S., "Effects of Supercooled Large-Droplet Icing on Airfoil Aerodynamics," Ph.D. Dissertation, Dept. of Aeronautical and Astronautical Eng., Univ. of Illinois, Urbana, IL, 2001.

2004/2005 AIAA Foundation
Cessna/ONR Student
Design Build Fly Competition

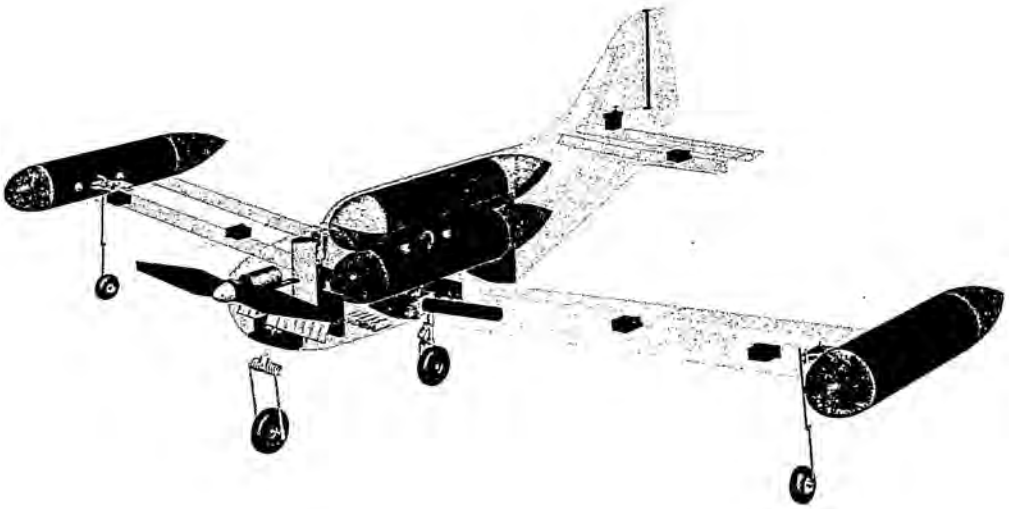

Design Report

"B-5 BLACKOUT"

OKLAHOMA STATE UNIVERSITY

BLACK TEAM

March 2005

Table of Contents

1.0 Executive Summary

This report presents the procedures and methods used to design and develop the Oklahoma State University Black Team aircraft entry for the 2004/2005 Cessna/ONR student Design/Build/Fly competition. The aircraft was designed to be competitive in each of the three possible mission profiles: Sensor Reposition, Maximum Utilization, and Re-Supply.

1.1 Design Development

The development of the Black Team's aircraft occurred in several key design stages. In order to maximize the effectiveness and productivity of the team, the members were divided into technical groups tasked with solving issues related to the primary aircraft categories of aerodynamics, propulsion, and structures. With efficient team organization and planning, the team stepped through the conceptual, preliminary, and detailed design phases of the project.

1.1.1 Conceptual Design

The first effort made during the conceptual design phase was to ensure that all members had a thorough knowledge of the contest rules and structure. This process allowed for the identification of critical aircraft design parameters associated with the contest and led to a streamlined conceptual design phase centered on developing an optimized aircraft. Initial contest sensitivity studies were performed to evaluate the impact that aircraft design parameters such as aircraft weight, propulsion system weight, and aircraft dimensions would have on the Rated Aircraft Cost (RAC) value and subsequently the Total Score.

Once the contest rules and structure were understood, a Figure of Merit (FOM) screening process was implemented in order to aid in making conceptual design decisions for aircraft and component configuration. The aircraft was divided into several categories, where alternative designs appropriate to the contest requirements were developed and screened. The conceptual design aircraft categories included overall aircraft configuration, payload systems configuration, landing gear systems and configuration, and propulsion system configuration. Many alternative designs were evaluated through the use of the FOM screening process. Using developed computer models, mission profile and design parameter sensitivities studies were performed to identify optimum aircraft design configurations capable of achieving high contest scores.

The efforts made during the conceptual design phase led to the optimum target aircraft design, which was an aircraft of conventional type with a low-wing design and the provision for "over-under" storage of the internal payload. Due to the complicated taxiing requirements of the Sensor Reposition mission, the aircraft landing gear configuration was chosen as a bicycle-type, complete with steering and braking systems.

1.1.2 Preliminary Design

During the preliminary design phase, the technical groups began further analysis into their respective areas of aircraft design. The chosen aircraft configuration was analyzed by the Aerodynamics and Propulsion groups using the developed mission profile and propulsion system computer models to determine target aircraft performance baselines such as mission flight times, rated aircraft cost, and contest score. Using iterative techniques, the groups used the computer models to determine the optimal airfoil selection, wing span, wing area, motor/battery/propeller selection, and propulsion system integration.

The Structures group began experimental testing of conceptual aircraft structural components such as payload release systems and landing gear components. Several payload release prototypes were developed and evaluated to determine the most simple and reliable solution. A similar landing gear configuration was tested on a prototype aircraft to identify problem areas associated with aircraft handling issues that arise while taxiing under an asymmetric loading condition during the Sensor Reposition mission. The aircraft internal structural layout was determined using finite element analysis and historical data. Tests were conducted to evaluate the structural integrity of the wings when the external payload was loaded. Using the results of these tests, it was possible to select appropriate wing spars capable of resisting static and dynamic deflection.

The results of the testing and analysis performed during the preliminary design phase were used to verify the FOM values determined during the conceptual design phase.

1.1.3 Detail Design

In the detail design phase, the technical groups worked closely to finalize all aspects of aircraft design. Component selections were made based upon preliminary design testing and optimal systems integration information gathered through the use of the computer models. Further testing was performed to ensure that each aspect of aircraft design had been optimized for the contest requirements. Prototype testing was performed to verify aircraft construction techniques and to minimize weight. The dynamic response and stability of the aircraft was studied and verified through flight simulation software. The propulsion system configuration was verified and optimized through mission profile wind tunnel testing. The tasks of the detail design phase led to an optimized aircraft capable of generating high contest scores.

1.2 Design Alternatives

During the conceptual design phase, many design alternatives were considered and screened using the developed FOMs for the aerodynamic, structural, and propulsive aircraft categories. The aerodynamic design categories included overall aircraft configuration, empennage configuration, wing mounting location, and payload mounting orientation. The overall configurations evaluated included conventional, canard, flying wing, blended wing, multiple wing, and dual fuselage. The conventional

configuration was chosen primarily due to stability reasons and the ability to maintain a constant center of gravity location regardless of payload mounting condition. Empennage configurations evaluated included conventional, V-tail, T-tail, split fin, and inverted V-tail. The conventional tail was chosen for its advantages in aerodynamic stability, ease of construction, and ease of box storage. High, low, and mid-wing mounting locations were studied. The low-wing configuration was chosen primarily for fast access to internal payload. The internal payload mounting configurations studied included horizontal (side-by-side) and vertical (over-under) storage. The vertical orientation was chosen to provide relatively short landing gear coupled with a high thrust line. The external payload mounting configurations studied included under-wing, wing-tip, and in-wing designs. The wing-tip mounting location was chosen for ease of manufacturability and to minimize disturbance in aerodynamic performance.

The structural design categories developed included the payload release mechanism, the landing gear configuration, the steering system, and the braking system. External payload release mechanism design alternatives included a kick-out latch, spring-loaded ejection latch, and a rare-earth magnet fixture. Several attempts were made to generate a simple and reliable rare-earth magnet payload release; however, the kick-out latch was chosen due to a much greater potential for simplicity. The landing gear configurations considered included tail-dragger, bicycle, tricycle, and quad layouts. The bicycle gear was chosen due to the asymmetric loading requirements of the Sensor Reposition mission. Steering methods investigated included nose wheel steering, differential braking, and aerodynamic steering using the rudder alone. Nose wheel steering was chosen due to a high demand for effective and precise ground handling characteristics along with a relatively low pilot workload requirement. The mission requirements necessitated effective aircraft braking. Braking system designs studied included pneumatic, mechanical, electro-mechanical, and reverse thrust. The pneumatic system was chosen based on proven historical reliable performance along with advantages in power efficiency.

Several propulsion system design alternatives were considered in the areas of motor, battery, and configuration selection. The Kontronic motor was chosen for superior performance and lighter weight when tested against several other motor types. NiMH batteries were selected based upon their increased charge density and fewer memory problems when compared to NiCd types. The propulsion system configuration chosen was a single motor with two battery packs as a result of computer modeling and system testing.

1.3 Design Process Highlights

Total flight score is based on the best scores from only two missions; therefore, in order to limit design considerations, the team focused on only two of the three missions. First, each mission had to be analyzed to determine which two have the most scoring potential. By using the scoring equations for each mission, it was decided that the maximum utilization sortie was an unnecessary design focus. As a result, the major design focus was in optimizing the aircraft for sensor Repositioning and Re-Supply.

The optimization program was adapted to the demands of the Sensor Reposition and Re-Supply missions. Iterating through the program revealed the aircraft configuration with the highest scoring potential, while helping to determine battery selection and count, propeller size, and gearing ratio. Additional analysis programs, decision matrices and calculations validated the output of the optimization programs and provided accurate mission times, velocities, takeoff distances, and power needs.

Fuselage sizing became a disassembly issue early in the design phase. Structural rigidity and construction complexity discouraged the use of a two-piece fuselage and resulted in a one-piece fuselage design limited by the four feet length of the box. It was also determined through static tests that a vertical tail placement allows the tail to be incorporated with the fuselage construction and fit within the box without subsequent disassembly.

Due to heavy concentration on the Sensor Reposition mission, center of gravity placement became the most pressing design concern. The wing-tip payloads create large moment arms on the aircraft and when one is dropped, the center of gravity (CG) shift is dramatic. Using conventional tricycle landing gear proved to be fool-hardy as the CG shift put the aircraft on its nose. Therefore, landing gear had to be designed to handle such changes without losing performance. In-flight performance must also be optimized with CG placement and designed so there is little change in flight characteristics between external and internal payload missions.

Payload release mechanisms are at the heart of the Sensor Repositioning mission and must be designed to be fast, light, reliable, and simple. Using wing-tip payload placement requires the mechanism to eject the payload, not just drop it. Several prototypes were constructed and analyzed for manufacturing simplicity and reliability; they revealed the kick-out latch as the most desirable.

Flight testing of a prototype allowed the team to finalize all design decisions. The propulsion group fine-tuned the battery selection and count while optimizing propeller performance to make use of all available power. The structures group tested aircraft stability and strength and located areas to shave weight.

2.0 Management Summary

The 2005 Oklahoma State University Black Team was comprised of students from both the Aerospace and Mechanical Engineering disciplines at various stages in their college careers, spanning from freshmen to seniors in their final semester of the program. The diverse background of the team allowed for broad distribution of design ideas and skills. In order to ensure that critical tasks were completed on time, a detailed management plan was developed early in the design process.

2.1 Design Team Architecture

The Black Team members were divided into technical groups tasked with addressing the three major areas of the aircraft design and construction. These areas include Aerodynamics / Stability and Control,

Propulsion, and Structures. Each technical group was headed by a Group Lead, who had the responsibility of organizing the group tasks and coordinating with the other Group Leads. The team was headed by a Chief Engineer, whose responsibility was to ensure effective communication between the technical groups and see to it that critical project deadlines were met. The design team architecture is shown in Figure 2.1 below.

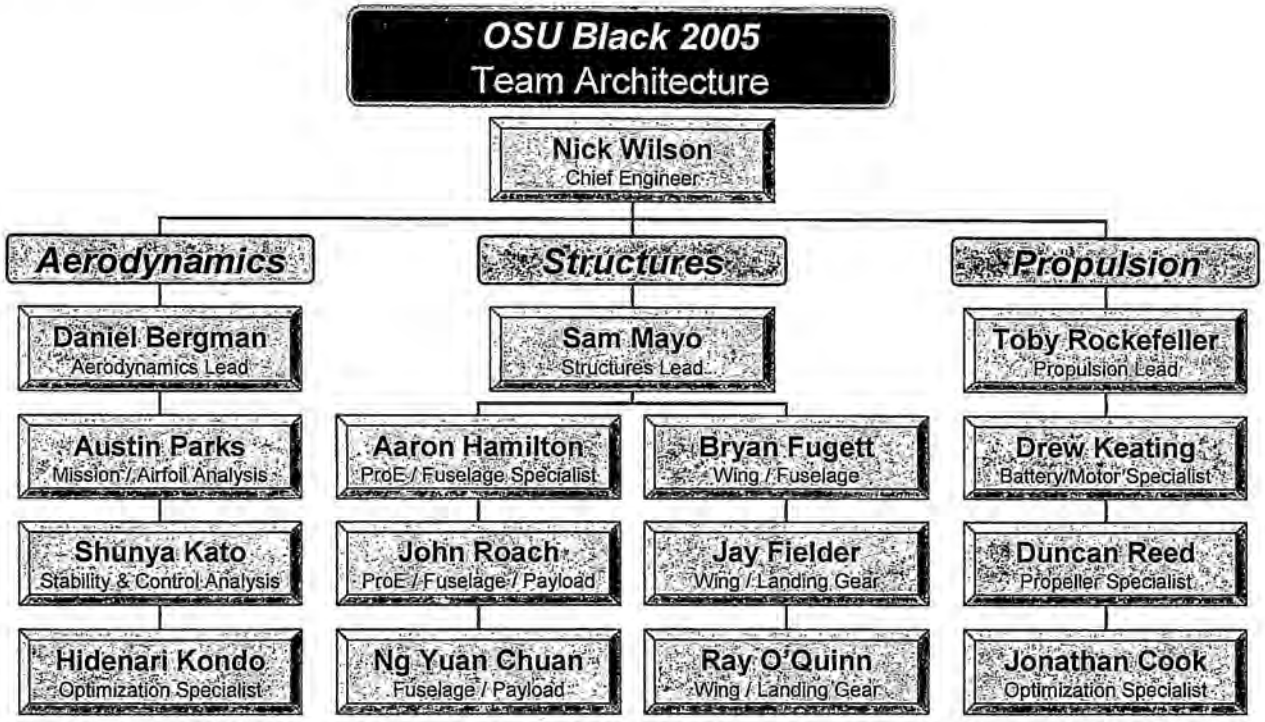

Figure 2.1 – Team Organizational Structure

The primary goal of the aerodynamics group was to provide the optimization of the aircraft in terms of mission performance. Optimization encompasses many features of the aircraft design such as the following: stability and control calculations, control surface sizing and selection, wing / airfoil selection, handling quality issues, external configuration and layout, and a full analysis of aircraft performance.

It was the responsibility of the propulsion group to manage the aircraft propulsion system. This includes the aircraft motor, batteries, propeller, and electrical systems. The structures team determined the best arrangement of off-the-shelf components to obtain the desired performance through the use of developed propulsion system computer models. The propulsion team was also responsible for mission profile testing of the selected propulsion system using the university wind tunnel and dynamometer.

The structures group was in charge of all the structural aspects of the aircraft, which includes internal aircraft design and construction. The group was responsible for conducting research to determine the best construction method; performing structural analysis for the entire aircraft; designing the sub-components such as release mechanisms and attachments; and, constructing the aircraft and sub-

components. The group was also responsible for integrating all of the designs, including those from the aerodynamics and propulsion groups, into the aircraft. For example, wing construction, battery placement, payload systems, and the landing gear and braking system were considered. Finally, the Structures group was also responsible for the technical drawings and prototype testing.

2.2 Schedule and Planning

The entire life of the design project occurred over the course of one semester. The fast-paced nature of the project necessitated the implementation of a detailed and efficient scheduling plan early in the design phase in order to develop a competitive aircraft. Based upon deadlines set at the onset of the project, a Gantt chart was created with projected schedules for critical design tasks. The progress of the team was continuously monitored in an effort to make certain that deadlines were met. Figure 2.2 shows the Gantt chart adhered to and tracked by the Black Team.

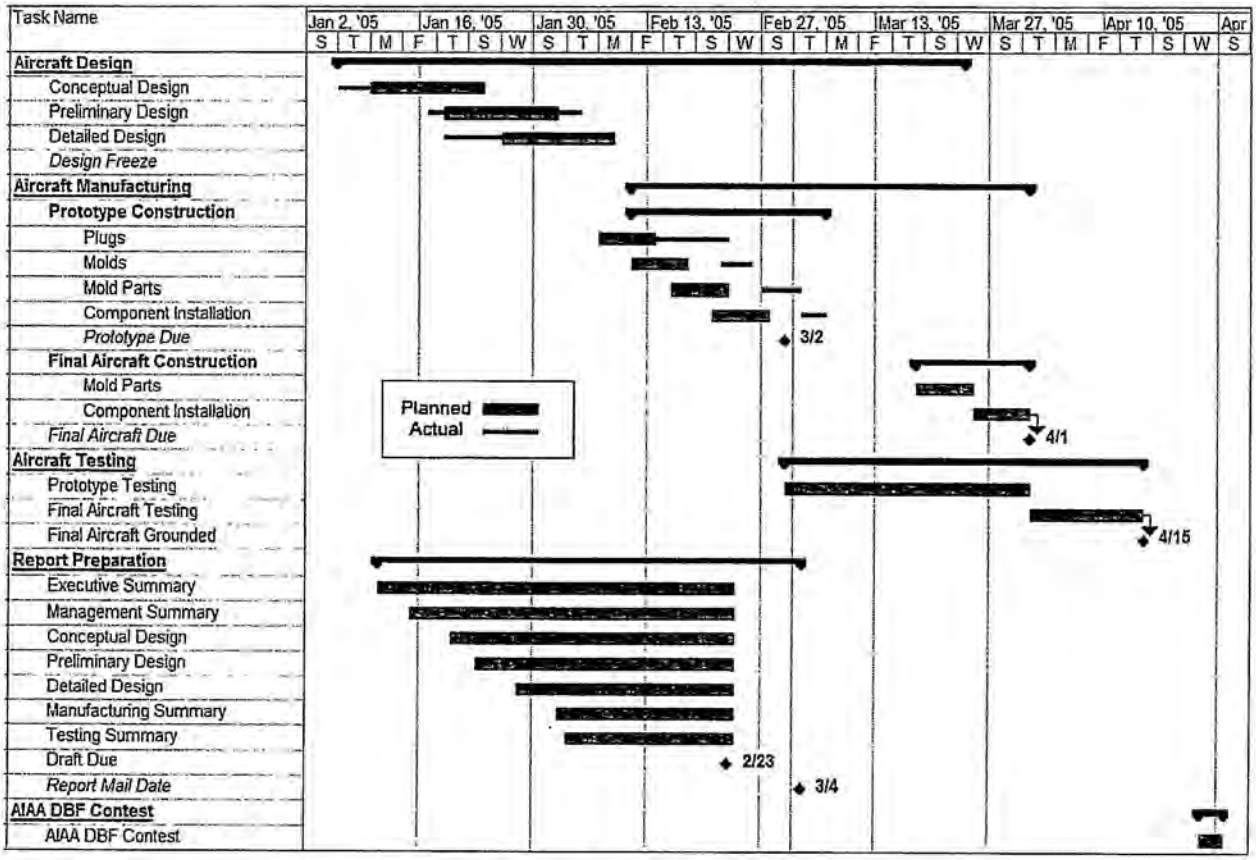

Figure 2.2 – Black Team Project Schedule

3.0 Conceptual Design

The team began the conceptual design phase of the project by first becoming familiar with the contest rules and structure. Effort was made to ensure that each team member had a thorough knowledge of the mission requirements in order to maximize the effectiveness of the conceptual design phase. The aircraft was then divided into categories that encompassed the important aspects of the design. Next, the key Figures of Merit (FOM) associated with each aircraft category were determined. Finally, with an understanding of the mission requirements and the important factors associated with the design, multiple design alternatives were developed and studied for each category.

3.1 Mission Requirements

The purpose of this project was to design an aircraft to compete in the 2005 Cessna/ONR Student Design/Build/Fly Competition. To ensure that a competitive aircraft was constructed, the conceptual design phase was focused on developing an aircraft equally capable of competing successfully for each mission. The aircraft's success is determined by the final score. The final score calculation is as follows:

$$FINAL\ \ SCORE = \frac{WRITTEN\ REPORT\ SCORE * TOTAL\ FLIGHT\ SCORE}{RATED\ AIRCRAFT\ COST}$$

Total Flight Score is a multiple in the final score calculation, so optimizing the missions flown is critical in scoring success. The team's "Total Flight Score" is the sum of the highest scores from two different missions performed by the aircraft. The team is given up to five attempts to increase their score through a combination of three available mission profiles, each with a different scoring function. "Laps" are completed in each mission with various payload configurations. Each mission involves a predefined flight profile that includes takeoff, climb, turns, cruise, and landing. These "Laps" are completed in each mission under various payload configurations.

Payload Description

In accordance with the rules, the payloads must be comprised of a 12-inch long PVC tube with a three inch diameter. Fairings or caps may be added to the ends of this tube, but the tube proper must remain twelve inches in length. Each end must be closed, but may be faired in any way. Each payload must weigh at least three pounds. The same payload must be used for both external and internal loadings without modification. For example, if a fin is attached to the payload for external carriage, the fin must be contained within the fuselage for internal carriage. External payload must be mounted within 3 inches of the wingtip using a hard-point, and the payload must be capable of remote-controlled release. Internal payload must be fully within the fuselage and symmetric to the fuselage centerline. In other words, the payloads cannot be staggered or placed in tandem within the fuselage.

Once the mission is completed, the aircraft must be disassembled and placed inside of a 4'x2'x1' box without damaging the aircraft. Mission time will stop once the box is closed and latched. Maximum mission time is ten minutes. It is imperative that a plan is established to evaluate mission performance and to analyze the pros and cons of each mission. Below are descriptions of each of the three mission profiles and their separate scoring functions.

3.1.1 Sensor Reposition

The aircraft will begin this mission by taking off and performing a lap with the wing-mounted (external) payload. Once the first lap is completed, the aircraft must taxi to a predetermined spot on the runway and release one of the external payloads. It will then taxi to another predetermined area and release the other payload. The aircraft performs a lap unloaded and then lands and taxis to a payload drop zone. The ground crew will go to the aircraft, "safe" the propulsion system, load the first external payload, re-engage the propulsion system, and return to the flight box. The craft then taxis to the next payload drop zone and the process is repeated. The aircraft then takes off and completes a lap loaded. Once the plane lands and comes to a complete stop, the ground crew will break down the aircraft and return it to the box. Time stops when the box is closed and latched. This mission has a Difficulty Factor (DF) of 2. Final Single Flight Score is calculated by:

$$SCORE = DF * (12 - Mission\ Time)$$

3.1.2 Maximum Utilization

In this mission, the aircraft will complete as many laps as possible in six minutes with the internal payload loaded. When performing a lap, the aircraft must make two 360° turns—as opposed to one—on the downwind leg. The aircraft must safely return to the box. Mission time stops when the box is closed and latched. This mission has a Difficulty Factor (DF) of 1. Final Single Flight Score is calculated by:

$$SCORE = DF * Number\ Of\ Laps$$

3.1.3 Re-Supply

In this mission, the aircraft will begin by flying a lap with the internal payload loaded. When the plane lands, the ground crew "safes" the plane, removes the payload, and arms the aircraft. The aircraft then flies a lap unloaded. The process is repeated for a total of four pattern flights. Next, the aircraft is loaded into the box. Time stops when the box is closed and latched. This mission has a Difficulty Factor (DF) of 1.5. Final Single Flight Score is calculated by the following equation:

$$SCORE = DF * (12 - Mission\ Time)$$

If only three of the four sorties are completed, the final score is calculated by the following equation:

$$SCORE = DF * (6 - Mission\ Time)$$

If only two of the four sorties are completed, the final score is calculated by:

$$SCORE = DF * (3 - Mission\ Time)$$

3.2 Alternative Configurations

The aircraft was divided into the following categories to allow for the systematic FOM screening process: overall aircraft configuration, wing location, empennage, payload systems, landing gear, and the propulsion system. To ensure that the screening process was consistent for each aircraft category, a standardized FOM decision matrix was developed. Within each category, the FOMs were assigned weight factors based upon their importance to the design criteria. A standard option was chosen among the designs and used as a baseline to score each alternative. Where applicable, the standard option was chosen as the most common design with sufficient historical data to use as a comparison to the remaining alternates. The alternates were then scored using a scale of -1 to 1, with -1 being worse, 0 being equal, and +1 being better than the standard option. The final scores were found through the summation of the product of the weight factors and scores for each alternative. The designs with positive scores were viewed to be better choices than the standard option, while negative scores indicated that the standard option was the best.

3.2.1 Overall Aircraft Configuration

The first category studied during the conceptual design phase was the aircraft's overall configuration, which has a profound influence on all subsequent aircraft categories.

Figures of Merit

The Figures of Merit developed for the overall aircraft configuration are shown below. Their implementation into the aircraft configuration decision matrix is shown in Table 3.1.

- **RAC:** The total available score for the aircraft is divided by the Rated Aircraft Cost (RAC). Therefore, efforts were made to choose a configuration capable of achieving a low RAC.
- **Stability & Control:** The aircraft must be capable of flying all of the mission profiles, which places it in three different loading conditions in the air. The chosen configuration must be capable of having similar aerodynamic stability and control characteristics for each flight condition.
- **Drag Efficiency:** Total aircraft efficiency is an important factor in the design. Also, the aircraft design should be capable of a high lift / drag ratio to allow for the fastest mission time possible. Any design with low drag efficiency has a negative impact on both of these aspects.
- **Complexity:** The aircraft design must ultimately be capable of being constructed multiple times with a small amount of uncertainty in the finished product. Therefore, design simplicity was factored into the overall configuration.

Design Alternatives

The following design alternatives were developed for the overall aircraft configuration as a result of the chosen Figures of Merit.

- **Bi-Plane:** The Bi-Plane configuration fared well in the stability and control and complexity categories. Since it was similar to a conventional configuration, it would be fairly easy to build and would be

predictably stable. However, the RAC and drag efficiency takes a hit due to increased wing area and increased wetted area, respectively.

- **Canard:** A canard or delta configuration would also fit well into the box and provide a short breakdown time at the end of a mission. However, stability and control problems arise when adding weights to the wings, which also introduce a center of gravity (CG) placement problem.
- **Conventional:** The conventional configuration was chosen as the standard option for the overall configuration decision matrix due to the high amount of historical data and experience with this aircraft type. This configuration fit very well into the RAC and complexity categories. The OSU facilities are very capable of building this configuration and it contributes the least to the RAC score out of all the other configurations considered. Stability and control is acceptable but drag efficiency suffers due to the moderate wetted area and sharp contours.
- **Flying Wing:** A flying wing fared very well in the drag efficiency category. With no empennage, wetted area was considerably reduced. However, past experience with the flying wing configuration has presented difficult handling qualities, and, hence, the option was quickly disregarded.
- **Blended Wing:** The blended wing configuration scored well in the Drag Efficiency category due to its smoothed lines and lessened wetted area. However, it is difficult to build and presents stability and control complexity. The RAC is also a negative issue due to its larger wing area.
- **Dual Fuselage:** A dual fuselage configuration was thought to fit into the box well. However, it struggles in terms of the RAC, stability and control, and drag efficiency.

Overall Aircraft Configuration							
Figure of Merit	***Weight Factor***	**Bi-Plane**	**Canard**	**Conventional**	**Flying Wing**	**Blended Wing**	**Dual Fuselage**
RAC	0.4	-1	-1	0	-1	-1	-1
Stability & Control	0.3	0	-1	0	-1	0	0
Drag Efficiency	0.1	-1	0	0	1	1	-1
Complexity	0.2	-1	-1	0	-1	-1	-1
Total:	**1.0**	**-0.7**	**-0.9**	**0**	**-0.8**	**-0.5**	**-0.7**

Table 3.1 – Overall Aircraft Configuration Decision Matrix

The conventional configuration was chosen to be the most suitable aircraft configuration as a result of the FOM screening process shown in Table 3.1. This configuration presents the best potential in nearly

every category. Its design simplicity and well documented historical data allow for a relatively low-risk design which is capable of competing well for all mission profiles.

3.2.2 Wing Location

Once the overall aircraft configuration was determined, the location of the wing attachment to the fuselage was evaluated. For the conventional overall configuration, high, mid and low-wing mounts were considered. The low-wing mount was chosen as the optimum configuration to be used in the aircraft design since it provides the fastest and most efficient way for reloading the internal payload by accessing the bay area from the top of the plane. The wing-supporting structure can then be located conveniently beneath the payload bay. Aerodynamic stability problems encountered by the low-wing configuration can be countered with wing dihedral.

3.2.3 Empennage

Once the conventional aircraft configuration was chosen, it was necessary to select the appropriate empennage configuration that would be optimum for the competition.

Figures of Merit

The FOMs implemented into the empennage configuration were chosen to be the same as those for the overall configuration aircraft category discussed in section 3.2.1. They are compared with alternative concepts in Table 3.2.

Design Alternatives

Several empennage design alternatives were generated and evaluated in the FOM screening process shown in Table 3.2.

- **V-Tail:** A V-tail configuration provides an excellent RAC score which is nearly a third less than the rest of the configurations considered. However, stability and control suffer due to dutch roll issues and complexity.
- **T-Tail:** A T-tail scored well in the stability and control category. The T-tail raises the horizontal stabilizer out of the vortex wake of the wing and thus increases its effectiveness. However, since controls would have to be routed through the vertical fin, the complexity score suffered.
- **Conventional:** The conventional tail configuration was again chosen as the standard option in the decision matrix because of experience with past aircraft. This configuration consists of a vertical fin and horizontal stabilizer. This configuration scored well in the complexity category when compared to the other options due to its ease of functionality.

Empennage				
Figure of Merit	***Weight Factor***	**V-Tail**	**T-Tail**	**Conventional**
RAC	0.35	1	0	0
Stability & Control	0.30	-1	0	0
Drag Efficiency	0.10	1	1	0
Complexity	0.25	-1	-1	0
Total:	**1.00**	**-0.10**	**-0.15**	**0.00**

Table 3.2 – Empennage Configuration Decision Matrix

After evaluating all of the design configurations, the conventional empennage was chosen as the best design. This design allows for the simplest method of production while still providing a reduced RAC.

3.2.4 Internal Payload

Based upon the contest rules, the two internal payloads must be mounted such that they are symmetric about the fuselage centerline. The rules also explicitly state that the payload cannot be tandem or staggered along the fuselage centerline. Based upon these restrictions, two feasible internal payload mounting methods were available.

Figures of Merit:

The following internal payload orientation FOMs were developed and implemented into the decision matrix in Table 3.3:

- **Reloadability:** Due to the timed nature of the Re-Supply mission, the aircraft must allow for quick and reliable internal payload storage and removal.
- **CG Location:** The aircraft must be capable of flying under three loading conditions: internal payload, external payload, and without payload. To ensure that changes in aircraft stability and control characteristics are kept at a minimum, the longitudinal CG location must remain the same for each flight condition. Also, the choice of internal payload mounting orientation directly affects the vertical CG of the aircraft, which subsequently affects the pitch stability of the aircraft in relation to the thrust line.
- **Ground Handling:** The choice of internal payload orientation directly affects the fuselage configuration of the aircraft. A taller, slender fuselage presents the option of using shorter landing gear which will improve the ground handling of the aircraft. Propeller ground clearance was also taken into consideration.

- **Directional Stability:** The aerodynamic characteristics of the aircraft will be affected by the orientation and cross-sectional area of the fuselage, which is in large part determined by the orientation of the internal payload.

Design Alternatives

Each of the chosen design alternatives are presented here and implemented into the decision matrix in Table 3.3.

- **Horizontal Storing:** The horizontal payload orientation provides a slight advantage with respect to ease of reloading due to the potential increase in the size of the access hatch. This configuration also requires a short and wide fuselage, which will require longer landing gear for propeller clearance. This in turn reduces the ground stability potential of the aircraft when landing gear of similar type and construction are used. The horizontal orientation was chosen as the standard option for the decision.
- **Vertical Storing:** This method is slightly more difficult to reload and also introduces a difficultly in maintaining a lower vertical CG location. However, the tall and slender nature of the fuselage will add to the directional stability of the aircraft, which will reduce the necessary volume of vertical stabilizer. The thrust line can also be raised to improve propeller clearance and ground stability and maneuverability.

Internal Payload Mounting Orientation			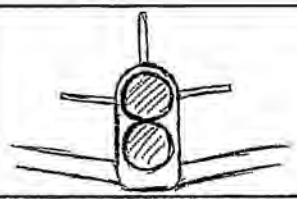
Figure of Merit	***Weight Factor***	**Horizontal Storing**	**Vertical Storing**
Reloadability	0.2	0	-1
CG Location	0.2	0	-1
Ground Handling	0.3	0	1
Directional Stability	0.3	0	1
Total:	**1.0**	**0**	**0.2**

Table 3.3 – Internal Payload Mounting Orientation Decision Matrix

Based upon the Figure of Merit evaluation for the two internal payload orientation types, the vertical payload storage orientation was chosen as the optimum configuration. Improved ground handling and directional stability served as the primary reasons for the choice.

3.2.5 External Payload Mount

The external payload mount and release mechanism must function properly in order to ensure the success of the aircraft. Several design alternatives were considered which included under-wing, wing-tip, and an incorporated wing fairing. After taking into consideration aerodynamic effects, the reliability and accuracy of the payload loading and ejection, and the effect of the payload on the weight and size of the wing, it was determined that loading the payloads to the end-tip of each wing would be most beneficial. This allows more effective use of the wing's lifting surface and allows gravity to aid in the removal of the payload. Another criterion used to make this decision was the ability to reduce the change in the vertical center of gravity, since the payloads would be mounted more vertical with respect to the fuselage.

3.2.6 External Payload Release

The external payload release mechanism is a critical aspect of the Sensor Repositioning mission. Once the payload mounting location was determined, a significant effort was made to generate concepts that would result in an efficient and reliable release system.

Figures of Merit

In order to develop and evaluate payload release system concepts, it was first necessary to develop the FOMs associated with a successful design. The following FOMs were developed for the external payload release system and implemented into the payload release decision matrix in Table 3.4.

- **Speed:** Due to the effect of time on the Sensor Reposition mission, the system must be capable of releasing the payload quickly.
- **Reliability:** The release system design must be reliable for two primary reasons. First, it must perform correctly to allow the aircraft to generate a score for the mission. Second, the system must be secure in order to prevent inadvertent payload ejection, a design failure that would likely result in the loss of the aircraft.
- **Weight:** Effort should be taken to ensure that the weight of the release system is minimized. It will be necessary to add weight to the payload to make it total three pounds, so designs that have more of their weight attached to the payload will be favorable.
- **Simplicity:** The release system must be designed to have a simple action, and it must be able to be produced with a minimal amount of effort.

Design Alternatives

Designs were selected based upon the decision to mount the external payload on the end of the wing tip. This decision results in the requirement that the system must release and then eject the payload. Also, due to the time constraints of the Sensor Reposition mission, a design constraint was developed that required each release system concept to be capable of being quickly loaded without the use of a servo. Many concepts were then developed for the payload release system. Once the payload system FOMs were determined, it was possible to narrow the list of conceptual designs to three systems that showed potential.

- **Kick-Out Latch:** This concept will allow for payload release and ejection in one simple action. The design is lightweight, and payload ejection is accomplished via the same latch. The kick-out latch was chosen as the standard option for the FOM evaluation.
- **Latch & Spring:** The latch & spring concept also proves to be a viable alternative. However, the design requires springs to enable payload ejection. Therefore, the design is both less reliable and more complex.
- **Rare-Earth Magnets:** This design concept could provide a simple and reliable release system. The system consists of three rare-earth magnets which will be appropriately sized. Payload attachment is provided by two magnets of opposite polarity, while ejection is accomplished through two magnets of similar polarity. The concept would have to be fully studied and tested to be effective at the contest.

Payload Release			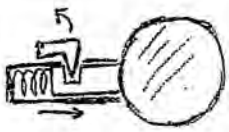	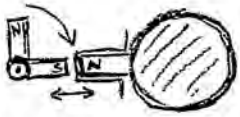
Figure of Merit	***Weight Factor***	**Kick-Out Latch**	**Latch & Spring**	**Rare Earth Magnets**
Speed	0.2	0	0	0
Reliability	0.4	0	0	-1
Weight / RAC	0.2	0	-1	0
Simplicity	0.2	0	-1	+1
Total:	**1.0**	**0**	**-0.4**	**-0.2**

Table 3.4 – Payload Release Decision Matrix

The kick-out latch was chosen as the optimal payload release mechanism using the information in Table 3.4. Its design reliability and low weight were the primary factors for this decision.

3.2.7 Landing Gear Configuration

The choice of landing configuration is very important due to the asymmetrical taxiing condition encountered during the Sensor Reposition mission.

Figures of Merit

Listed below are the FOMs which were developed for the overall landing gear configuration. These are used in the design alternative screening in Table 3.5.

- **Stability:** Ground stability is a very important requirement for the contest. This is especially important during the Sensor Reposition mission when the aircraft must taxi while loaded asymmetrically. The aircraft must resist tipping or be designed to tip without rendering it useless.
- **Ground Handling:** Due to the contest requirements, the aircraft must be capable of effective ground

maneuvering. The aircraft must be capable of taxiing very well without undue strain on the pilot to ensure consistent aircraft ground performance.

- **Weight:** Aircraft weight has a direct effect on the aircraft RAC, and thus should be minimized in order to maximize the potential aircraft score.
- **Ability to Remove:** The aircraft must be placed into the box before the timed mission ends. Therefore, the gear must be capable of stowing quickly.

Design Alternatives

These design alternatives were developed as viable landing gear configurations. Their implementation into the landing gear configuration is shown in Table 3.5.

- **Tail Dragger:** The tail dragger configuration was selected as the standard option for the landing gear selection matrix. It generally performs well in the area of landing performance. However, this configuration is difficult to maneuver on the ground and would be somewhat ineffective at accomplishing the contest requirements.
- **Quad:** The quad landing gear configuration has the potential to provide increased ground stability and handling. These benefits result at the expense of the added weight needed to provide wide front and main gear. The quad configuration also is more difficult to fit into the box.
- **Bicycle:** The bicycle landing gear enables the aircraft to have a very wide stance along the point where the CG will shift while taxiing with an asymmetric load. This significantly increases the ground stability of the aircraft. The bicycle configuration introduces a structural and ground handling disadvantage due to the placement of the wing landing gear.
- **Tricycle:** The tricycle gear configuration will provide the best ground stability and handling when the aircraft is evenly loaded. However, the stance must be significantly widened to allow for ground stability when the aircraft is asymmetrically loaded.

Landing Gear Stance			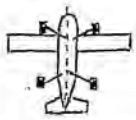		
Figure of Merit	***Weight Factor***	**Tail Dragger**	**Quad**	**Bicycle**	**Tricycle**
Stability	0.30	0	0	1	0
Ground Handling	0.25	0	1	1	1
Land Performance	0.20	0	0	0	0
Weight	0.15	0	-1	0	1
Ability to Remove	0.10	0	-1	0	-1
Total:	**1.00**	**0.00**	**0.00**	**0.55**	**0.3**

Table 3.5 – Landing Gear Stance Decision Matrix

From Table 3.5, the landing gear configuration best suited for the aircraft is the bicycle type. This design provides a compromise between complexity and ground stability.

3.2.8 Steering and Braking Methods

In order for the aircraft to successfully accomplish the mission requirements and be competitive, the aircraft design must allow for effective ground maneuvering. The aircraft will be required to taxi to multiple positions during the Sensor Reposition mission, which will require some form of aircraft steering control. The nose wheel steering method provides the most efficient ground handling. Counter-steering of the main gear may also provide better mobility.

Due to the contest requirements that involve large amounts of ground maneuvering during timed mission runs, it is necessary to incorporate a braking system into the aircraft design. A pneumatic braking system was found to be the most effective method based on experience from previous competitions. This method provides for high power efficiency as well as pleasing performance characteristics.

3.2.9 Propulsion System

The conceptual design of the propulsion system consisted of several different combinations of motors and battery packs. Depending on the importance of each FOM, the different configurations are compared below.

Figures of Merit

The following FOMs were developed for the propulsion system configuration. Their implementation into the selection matrix is shown in Table 3.6.

- **RAC:** The Rated Aircraft Cost incorporates both the number of engines and the weight of the system through the Rated Engine Power equation. Therefore, it must be minimized.
- **Ground Handling:** The aircraft must have balanced and reliable handling in both the air and on the ground. Special attention is placed on taxiing stability due to unique mission profiles. The selection of the propulsion system configuration can have an impact on the ground and aerodynamic stability of the aircraft.
- **Power:** The mission calls for the transportation of a six pound payload. Therefore, it is essential to have adequate power to takeoff and complete laps quickly.
- **Efficiency:** Since the weight of the battery packs strongly affects the RAC, it is vital to have an efficient system to minimize battery weight while maintaining performance.

Design Alternatives

Several propulsion system configurations were evaluated during the conceptual design phase. The design alternative descriptions are shown below followed by the selection process in Table 3.6.

- **Dual Motor – Dual Pack:** This configuration consists of two motors with two separate battery packs and would produce the most aircraft power. The dual motor configuration introduces an advantage in

taxiing performance due to the potential for using asymmetric thrust. Unfortunately, this configuration is punished harshly by the RAC due to the multiple motors and additional weight.

- **Dual Motor – Single Pack:** This configuration consists of two motors but is supplied by a single battery pack. As a result, this arrangement produces similar power but slightly reduces weight. On the other hand, the dual motors still bring a harsh punishment in the RAC.
- **Single Motor – Dual Pack:** This configuration only has one motor but derives power from two packs. This allows for more versatile battery placement, which increases stability. This also provides excellent power while greatly reducing RAC.
- **Single Motor – Single Pack:** This is the simplest and consequently most efficient arrangement, and therefore was chosen as the standard option. It also optimizes the RAC score while supplying ample power.

Propulsion System		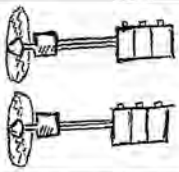	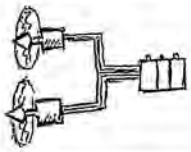	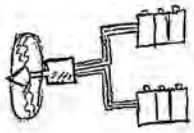	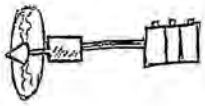
Figure of Merit	***Weight Factor***	**2 Motors / 2 Battery Packs**	**2 Motors / 1 Battery Pack**	**1 Motor / 2 Battery Pack**	**1 Motor / 1 Battery Pack**
RAC	0.3	-1	-1	0	0
Ground Handling	0.2	-1	-1	1	0
Power	0.2	1	1	0	0
Efficiency	0.3	-1	-1	0	0
Total:	**1.0**	**-0.6**	**-0.6**	**0.2**	**0**

Table 3.6 – Preliminary Propulsion Decision Matrix

Based on the decision matrix above it can be seen that the single motor arrangements are much more desirable than the dual motor. Considering the nearly identical performances of the two single motor arrangements, the versatility of the dual pack becomes the determining factor. Therefore, the single motor and double pack arrangement is selected with the confidence that the mission success is not compromised and scores are optimized. During the propulsion system testing and evaluation phase, the accuracy of the FOM assumptions will be verified along with the choice of propulsion.

3.2.10 Aircraft Disassembly Procedure

Due to the contest requirements that the aircraft must be stored in its box prior to the end of the mission time, it is very important to design the aircraft in such a manner as to allow for an efficient and

effective method of returning it to the box. A FOM screening process was used to determine that removing each wing and the main gear would allow for the fuselage and empennage to be stored in the box with minimal disassembly.

3.2.11 Conceptual Structural Design

Several structural methods were researched and evaluated to find the optimum approach to building the aircraft. These methods were screened using a detailed set of FOMs and implemented into a construction method selection matrix in Table 3.7.

Figures of Merit

Figures of Merit were developed after researching several construction methods and evaluating the contest rules. The aircraft construction method FOMs are as follows:

- **Build Time:** Time is a crucial factor in any project. A fast construction time will allow for more testing time and any replacement parts needed.
- **Repeatability:** In the event that an aircraft malfunctions or is damaged, it will be necessary to either rebuild or repair, so each method is evaluated on how easily the plane can be fixed or reproduced.
- **Cost:** Aircraft cost is a vital factor that must be evaluated when choosing a construction method.
- **Weight:** A process that allows for lightweight aircraft components is critical. The lighter the aircraft, the better the RAC, which translates to a higher overall score.
- **Strength:** The construction method must provide the needed strength and structural integrity for the plane to perform all of the desired functions.

Construction Method Alternatives

The following design alternatives were considered as a result of a literature survey of construction methods. They are screened in Table 3.6 in order to determine the best method.

- **Basic Balsa:** The basic balsa construction method is a popular and inexpensive approach to building small-scale aircraft, and was therefore chosen as the standard option. The balsa wood pieces can be shaped to any dimension desired and the materials are widely available. However, balsa wood construction is heavy and requires a high level of skill to maintain precision consistently during the construction process.
- **Foam Core:** The advantages of using the foam core method include a short build time, decent strength and stiffness, and ease of manufacturing. The major disadvantages of using foam core is that it is very heavy, it is difficult to incorporate hard points on the wings, and it is difficult to repair.
- **Monocoque:** A monocoque, or reinforced skin fuselage, can produce strong and stiff aircraft through the use of lightweight composite structures. The most common way to develop a monocoque aircraft is by foremost building molds. The molds allow the exact outer shape to be consistently controlled. The monocoque method typically takes longer than the other alternates to produce the first aircraft; however, subsequent aircraft can be developed much more quickly.

Construction Methods			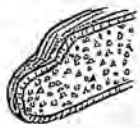	
Figure of Merit	***Weight Factor***	**Basic Balsa**	**Foam Core**	**Monocoque**
Build Time	0.1	0	-1	-1
Repeatability	0.2	0	1	1
Cost	0.1	0	1	0
Weight	0.3	0	0	1
Strength	0.3	0	0	1
Total:	**1.0**	**0.0**	**0.2**	**0.7**

Table 3.7 – Construction Method Decision Matrix

As a result of the FOM screening process shown in Table 3.7, the decision was made to pursue the monocoque construction method for the aircraft. Other factors contributing to the decision included the proven successful history and experience with the method.

3.3 Conceptual Design Summary

The efforts of the conceptual design phase led to the selection of the conceptual aircraft configuration, shown in Figure 3.8.

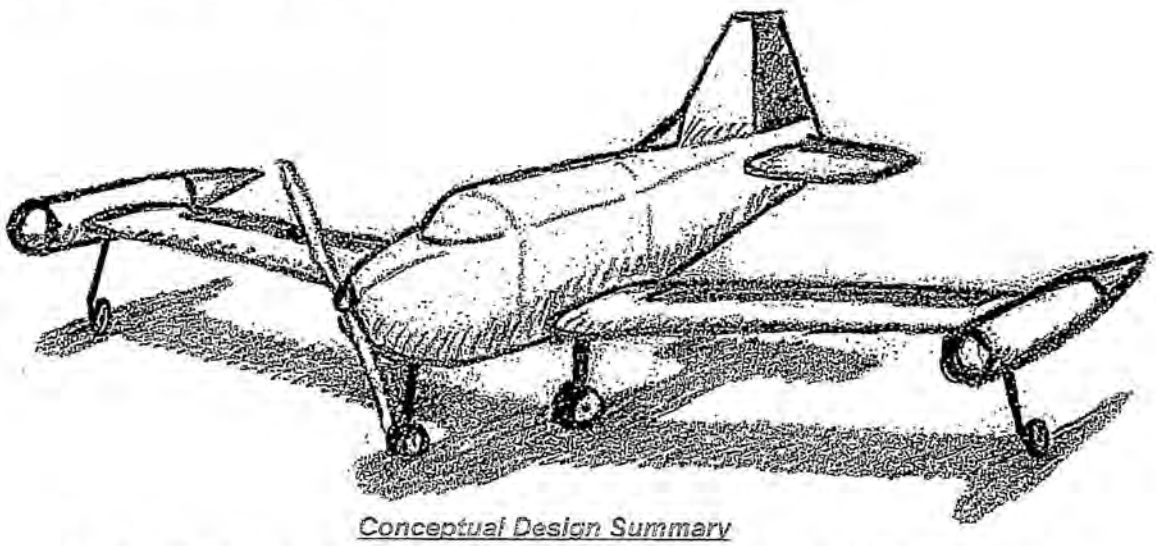

Conceptual Design Summary

- Conventional Low-Wing Design
- Bicycle Type Landing Gear
- Remove-able Wings and Main Gear
- Wing-Tip Mounted External Payload
- Vertical Internal Payload Storage
- Kick-Out Latch Payload Release System

Figure 3.8 – Conceptual Aircraft Design.

4.0 Preliminary Design

The Black Team immediately transitioned into the preliminary design phase once the conceptual configuration of the aircraft had been determined. This section describes the critical aspects of the preliminary design and the analysis methods used to optimize the aircraft.

4.1 Design Parameters and Sizing Trades Summary

Before the technical groups began optimization procedures for the aircraft, a detailed list of critical contest design parameters was generated and reviewed. These parameters were used to ensure that aircraft sizing and component selection decisions were made on the basis of maximizing the potential mission score. The design parameters associated with each group are presented here.

4.1.1 Aerodynamic Design Parameters

- **Wing Area and Wingspan:** This involves several important aspects, including aspect ratio and chord length. The design of all flight systems is dependent on wing geometry. In addition, the performance of the aircraft will be strongly affected by the lift and drag produced by the wing for a variety of flight conditions.
- **Wing Airfoil:** An appropriate airfoil is required for optimum performance and adaptability to variable flight conditions. The airfoil must provide for all mission requirements and be versatile enough to allow for variable flight conditions. Airfoil selection also depends strongly on manufacturability and having enough internal space for flight and payload systems.
- **Fuselage Length and Empennage Size:** The length of the fuselage is limited by the interior dimensions of the storage box, which in turn limits the effective length of the empennage. The empennage must then be designed for optimum performance and drag efficiency.

4.1.2 Propulsion Design Parameters

- **Motor Selection:** Selection is based on performance both in the form of power and efficiency. The motor must be able to provide the necessary thrust, but it must also do so in an efficient manner. Brushless motors demonstrate superior efficiency and comparable power in a lighter weight construction than brushed. Nevertheless, all motors were evaluated for optimal performance in the given application.
- **Battery Selection:** Battery weight is severely punished in the RAC; therefore, high charge density is extremely important in order to produce the necessary power without adding unwanted weight. The capacity of a battery determines the flight time of the craft and should be designed precisely to ensure that no power is wasted. Arriving at the optimum voltage and capacity with the least amount of weight is paramount to the success of the plane.

- **Propeller Selection:** The propeller pitch and size is responsible for converting the torque and rpm of the motor into thrust and airspeed. Propeller pitch and size impact both the load of the motor and the efficiencies at various airspeeds; a high pitch-to-diameter ratio is more efficient at higher airspeeds, while a low pitch-to-diameter ratio creates more thrust. Therefore, a compromise must be found between take-off and flight performance.
- **Propulsive Power:** Due to the importance of battery weight on RAC, power demands must be met at an optimized efficiency. Takeoff drains most of the system's power due to large accelerations. The remaining power will be consumed during cruise where the craft simply needs to maintain flight. Since takeoff is characterized by high power demands, the flight section needs to avoid the maximum current draw of 40 amps. Airplane characteristics define the necessary power needs while propeller, gear, and battery selections determine the efficiency at which it is obtained.

4.2 Aircraft Mission Modeling

Once a thorough understanding of the necessary design parameters had been reached, the groups conducted an analysis of the aircraft mission profiles in order to select aircraft components and geometry that would produce the highest scoring potential.

4.2.1 Aerodynamics

The Aerodynamics group used the overall aircraft configuration, which was developed through conceptual design, along with optimization software, to analyze the mission profiles and conduct a sensitivity analysis on key mission parameters.

Mission Profile Model

A computer code was used in studies comparing potential competition scores to various major design considerations. This code simulated the Re-Supply mission and outputted many results and parameters of the mission, including the predicted score. Operating conditions (i.e. wind) and operating equipment (i.e. batteries) could be set as constants and the code would generate a multitude of scores for various aircraft configurations. Functions in the code would calculate various efficiencies, mission performance parameters, and propulsion performance parameters. The maximum possible score was then determined for the following design variables:

- Battery weight
- Cruise velocity without payload
- Cruise velocity with payload
- Wing area
- Wingspan.

The design could then be analyzed for a multitude of mission performance parameters, including:

- Time, power, and distance required for takeoff

- Time and power required for climb, flight mission, and descent
- Time and distance required for landing and coming to a stop
- Total mission time.

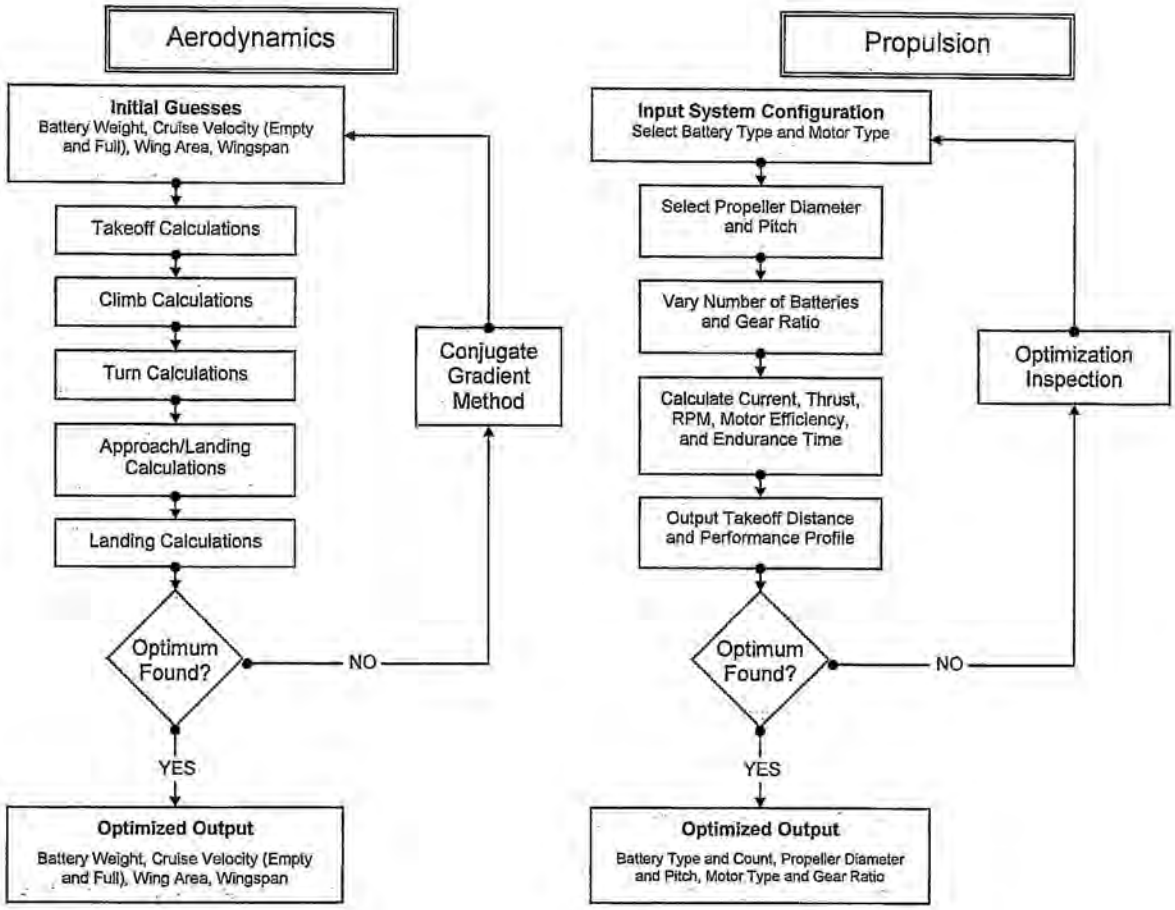

Figure 4.1 – Aerodynamic and Propulsion Optimization Program Flowcharts

Constraints were used to limit the search for optimum plane characteristics. Oklahoma State University competition RC planes with aspect ratios higher than 8 have a history of poor stall and spin performance; therefore, the upper limit for the wing aspect ratio was set at 8. The wingspan of the craft was limited to 8 feet due to storage of the disassembled plane within the box. The takeoff distance was limited to 150 feet due to competition rules. The number of battery cells was limited to between 7 and 18 based on past performance. Other constraints were made to ensure reasonable optimization of the score, such as having a positive wingspan and using less than 100% of available power.

Several assumptions were made during optimization. The weight model was based on measurements of Oklahoma State University planes from previous competitions. A standard weight was assumed for the fuselage, while additional weight was dependent on wing area and number of battery cells generated by the program. The drag model incorporated the build-up method used by Raymer (1999). Reynolds

number was kept above 150,000 and monitored for rationality to minimize laminar separation concerns. The propulsion model was developed in collaboration with the Propulsion team. The RAC model provided by the contest was also incorporated into the analysis program.

No single configuration could be specifically determined from one "run" of the score optimization code since many local maxima exist. However, by executing the code many times using randomly generated initial parameters and plotting the various outputs versus score, trends could be observed. Figure 4.1 above illustrates the progression of the program. These results were then used to develop a preliminary aircraft design.

Mission Score Sensitivity Studies

The program is not capable of simulating or predicting every possible scenario while accounting for every possible aircraft configuration. Therefore, sensitivity studies were required to determine the effects of major aircraft parameters on overall score. Utilizing our Mission Profile Program, a simplified VBA code written specifically for this purpose, and common sense, various parameters were identified as having a large influence on mission score. These variables were time on the ground (pit time), wind velocity, flaps, and batteries used.

- **Pit Time:** Time is a direct multiplier in the mission score. This makes it very important to minimize this number. The only way the team can actively minimize mission time in the actual competition is to prepare well and spend the least amount of time required to load and unload the payload.
- **Wind Velocity:** True wind velocity is never predictable. Wind speed averages for the competition site were researched in order to aid in the preliminary design of the aircraft. An average wind speed of 5 MPH was decided upon for final design analysis. This speed gives conservative numbers while allowing us to operate with winds less than 5 MPH. If the wind is higher than 5 MPH, scores should generally improve. The plane was also designed for takeoff within 150 feet for a zero wind condition.
- **Flaps:** Flaps improve takeoff distance and provide for a slower landing speed. The use of flaps lowers the amount of wing area needed. However, flaps increase the complexity of the wing and hurt the RAC. The plane was thus designed for the use of flaperons to decrease complexity and improve the RAC.
- **Batteries:** Batteries affect the overall score due to their capacity and weight. The batteries must provide the energy needed to complete a mission. If a mission is not completed, no scores will be recorded. However, more capacity means more weight and weight has a direct influence on the RAC. Sensitivity analysis showed that a significant change in the number of battery cells or type of battery resulted in small changes in overall score. This allows more flexibility for changes made in the propulsion system as a result of flight testing.

Propulsion System Model

A propulsion analysis program was utilized to perform a more detailed analysis on the number and types of batteries, propeller diameter and pitch, gear ratio, and motor. It also predicted takeoff distance,

thrust, and endurance time under calculated cruise conditions. The program flow is illustrated above in figure 4.1.

- **Battery Study:** Manufacturer's data for different types of NiCad and NiMH batteries were used to predict performance. The type of batteries, the number used, and the capacity of each cell were modeled to predict efficiency and endurance over a range of different loadings.
- **Propeller Study:** Propeller data from wind tunnel tests was used to create both thrust and propulsive coefficient curves. Using the coefficients of the regressions through the data points, the propellers could be modeled. Various dimensions were tested and then used with the propulsion analysis program to predict thrust, torque, and RPM under specific conditions.
- **Gear Ratio Study:** Different gear ratios were also examined through the propulsion analysis program. The tradeoffs between thrust and motor loading were analyzed accordingly. For the Kontronik motor, there are only three available gear ratios. These tests were performed within the 40 amp constraint as to not blow the fuse.

4.3 Aircraft Optimization

After the technical groups had gathered sufficient data to support design selection and sizing, the groups compiled their generated data in order to assess critical aircraft operating parameters and design integration.

4.3.1 Aerodynamic and Mission Profile Analysis Results

Once the Aerodynamics group had clearly identified the mission profile trends with respect to aircraft design, the group began making design decisions and verifying these selections with the other technical groups. The Aerodynamics design responsibilities included wing airfoil selection, wing sizing determination, and selection of the optimum aircraft cruise velocity.

Wing Airfoil

Selection of an appropriate airfoil required extensive use of the numerical optimization program. Initial research into airfoils was focused on high-lift designs, as the aircraft would be lifting nearly its own weight in payload. The program *Profili* was used for research and production of Lift and Drag polars and curves. Extremely exotic, high-cambered airfoils were immediately eliminated due to design complexity and the lack of room inside the wing cross-section for system components. Several moderately cambered airfoils were taken into consideration. The final lineup of airfoils produced for detailed analysis included the Selig/Giguerre 6043, Eppler 423, Selig/Donovan 7062, and the Selig/Donovan 7032. The Eppler was the highly cambered airfoil considered while the two SD airfoils were the more conservative considerations. The SG 6043 airfoil was considered as a compromise between the two extremes and was selected for analysis to provide a "middle-of-the-road" comparison.

All airfoils were initially compared with a 10 MPH wind utilizing the same aerodynamic and propulsion setups. It was felt that this would provide a balanced comparison between the performances of each airfoil. Initial optimization runs concluded that the E 423 and the SD 7062 airfoils routinely produced higher scores than the SD 7032 and the SG 6043. Figure 4.2 illustrates the "shotgun" optimization approach, where the highest scoring wingspan clusters for multiple airfoils are highlighted with a red circle. The scatter in the data is due to the existence of many local maxima; therefore, trends must be observed and applied to the design.

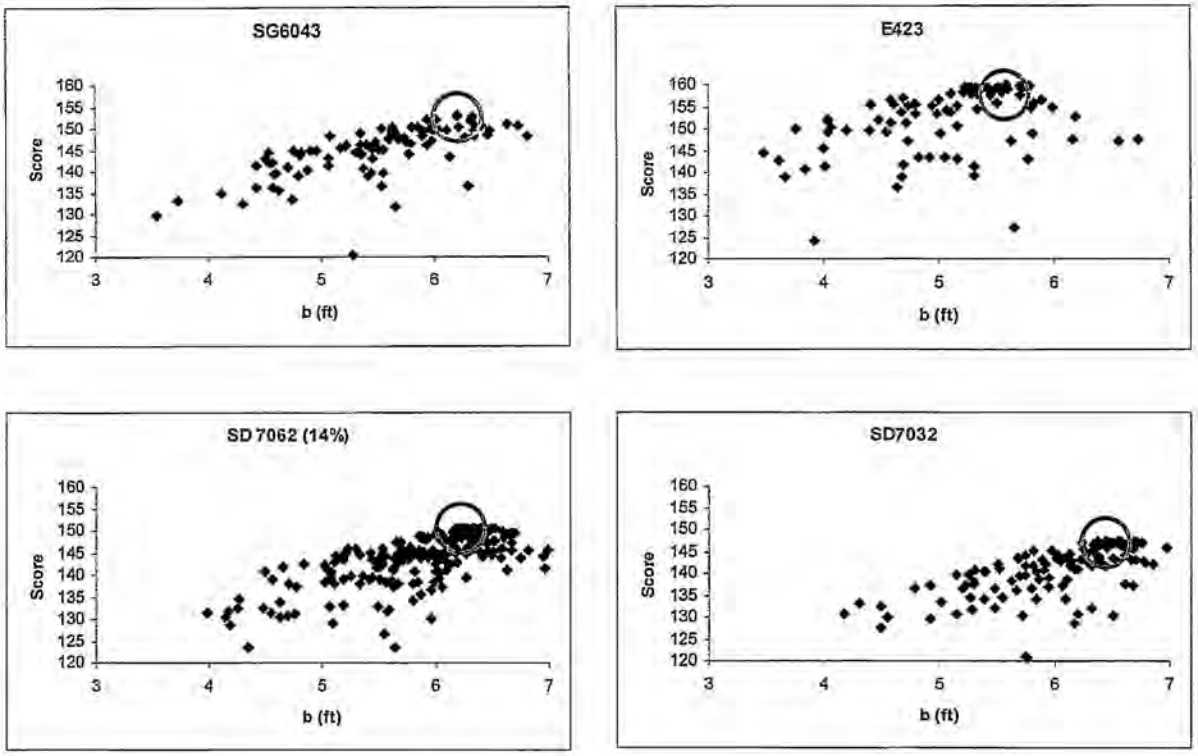

Figure 4.2 – Preliminary Score Comparison between Considered Airfoils – Wind = 10 MPH

With a choice between the SD 7062 and the E 423, the pros and cons of each airfoil were considered. The E 423 produced slightly higher scores than the SD 7062 but was very highly cambered. This high camber would be more difficult to produce and would not provide as much room for internal components as the SD 7062. It also had a higher Drag Coefficient at cruise than the SD 7062. The SD 7062 produced just slightly lower scores but provided more internal room for components and provided better cruise performance. The SD 7062 also seemed less sensitive to condition changes and was thus selected as the wing airfoil.

4.3.2 Wing Sizing

Wing Area

Wing Area was an output parameter returned by the Mission Analysis Program. Given wing area and our previously selected wingspan, wing chord could be determined. Analysis runs were made with 5 MPH wind conditions in order to determine optimum wing area, which was determined to be 4.125 ft^2. With a wingspan of 5.5 feet, the corresponding chord required for an area of 4.125 ft^2 was nine inches. This results in an aspect ratio of 7.333, which falls below the controllability limit of 8. This wing size includes a small margin of safety to allow for zero wind takeoff conditions.

Wingspan and Flap Integration

The next task was to determine both wingspan and flap deflection, if any, would be required. During the preliminary airfoil design phase, the airfoils were all compared at a wind speed of 10 MPH. In the final design phase, the SD 7062 airfoil was analyzed with no wind for takeoff. Looking at the historical weather data for the competition site, the average wind speed ranged between about 5 to 10 MPH. A wing span of 5.5 feet was selected to provide for the best performance over all wind conditions. In the case of zero wind, the propulsion system can compensate for this wing area to allow a takeoff distance less than the 150 feet contest stipulation.

Optimization runs were then made with a 5 MPH wind condition with the SD 7062 airfoil using a 15% wing area flap with 0, 5, 10, and 15 degrees of deflection. The highest scores were consistently generated using 10 degree flaps. Instead of dedicated flaps, flaperons were chosen to simplify wing design and construction. With airfoil, wingspan, and flap conditions now known, further comparisons and sensitivity analysis could be conducted for the design condition of 5 MPH winds.

Cruise Velocity

Analysis of cruise velocity returned somewhat counterintuitive results. As the analysis showed, the optimum cruise velocity for both the payload loaded and unloaded condition is approximately the same. The aircraft will therefore be designed to maintain the same velocity at cruise no matter the loading configuration.

4.3.3 Propulsion Analysis Results

Before any actual propulsion testing took place, the propulsion team ran preliminary tests with a computer program that optimized the motor, gearbox, batteries, and propeller. The program contained an array of variables and modeled the entire propulsion system throughout the mission profile, which established a relatively precise expectation for thrust, power, efficiencies and endurance.

Motor

The propulsion team had three motor choices: the Kontronik, the Graupner, and the Maxcim models. During the preliminary design phase it was determined the Kontronik 600-18 motors would be used due to superior performance results in both efficiency and power at the desired amperage. During the motor

optimization process the propeller, battery and gearbox ratios were held constant while the motor type was varied. Figure 4.3 shows the motor comparisons.

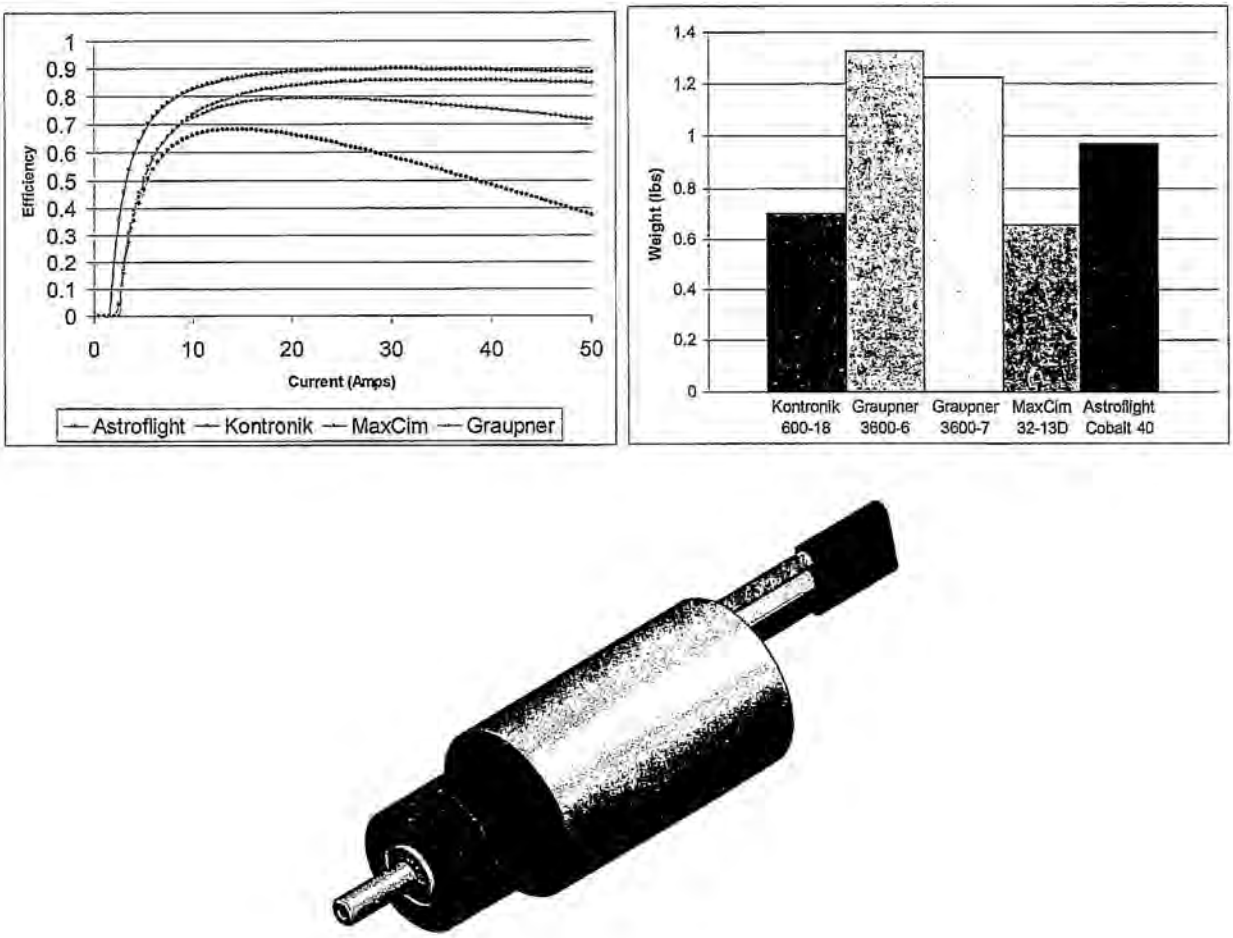

Figure 4.3 – Motor Efficiency vs. Current and Various Motor Weights

Batteries

One of the most important optimizations for the propulsion system is the batteries. For battery selection, the largest consideration is the weight, because any extra weight greatly penalizes the RAC. During the battery type and cell number optimization, the propeller, the motor, and the gear ratio were held constant. Using battery information such as internal resistance, weight, and capacity, a battery type was selected. NiMh provides a high charge density; therefore, the three styles investigated with the program were the KAN 1800, Sanyo 1950, GP-2000 and the GP- 2200. The style and number of battery cells were varied until the thrust and power requirements for the mission profile were met. Due to voltage requirements, 13-15 cells became the working range. Weight issues eliminated the Sanyo 1950 and GP 2200, while high current draws eliminated the KAN 1800. Therefore, the GP-2000 became the battery of choice. Table 4.1 below shows some of the information used to evaluate the optimum battery type.

Battery Selection			
Battery Type	*Capacity*	*Resistance*	*Capacity / Weight*
KAN 1800	1800	0.006*	24000
Sanyo 1950	1950	0.005	22774
GP 2200	2200	0.005	21728
GP 2000	2000	0.005	26016

Table 4.1 – Battery comparison *(*assumed value)*

Motor Gearing Issues

For gear ratio optimization, the propeller, battery, and motor were all held constant in the program. Gear ratios were then varied and thrust, power required, current drawn, efficiency, and endurance were all recorded. Because there were only three gear ratios to choose from for the Kontronik, it was not logical to establish a range; the test resulted in a planetary gear ratio of 4.2 primarily because of takeoff distance and the current drawn from the batteries.

Initial Propeller Selection

After optimization tests, it was found that a low pitch-to-diameter (p/d) ratio has the greatest efficiency at low airspeeds and a high p/d ratio has the greatest efficiencies at high airspeeds; therefore, to compromise, a p/d ratio range of .65 to .68 was chosen. Since all missions require flight with payloads at some point, it must be the design focus, which leads to an optimum propeller size between 17 and 19 inches.

4.4 Aircraft Sizing

4.4.1 Fuselage

The primary factor limiting fuselage size is the internal dimensions of the box. In order to fit the fuselage into the box without removing any tail surfaces, the length of the fuselage is limited by the diagonal of one side of the box (approximately 49 inches). The fuselage length was designed to be 47 inches, which should allow for the propeller to remain affixed to the plane when the aircraft is returned to the box at the end of each mission. The fuselage was structurally designed to fit all of the internal components including servos, batteries, and the motor. The resulting cross-sectional area that also allows for internal storage of the payload and wing box structure was determined to be 38 square inches. The shape of the fuselage then evolved from functionality and aesthetic value.

4.4.2 Empennage

Horizontal Stabilizer

The horizontal stabilizer was mainly analyzed in terms of the size and airfoil. The sizing geometry was performed first, and then the airfoil was selected to fit the pitching moment configuration with

minimum drag. The rules state that tail span must not exceed 25% of the main wing area or it will be considered as a second wing, which limits the tail span to 16.5 inches. Designing for a horizontal tail volume ratio of approximately 0.7 based on historical data, the chosen area of the horizontal tail became 132 in^2, which results in a tail volume ratio of 0.6543. The taper ratio of the tail was decided by the influence of the Reynolds number and the aesthetics of the entire airplane. The root chord was set as 8.5 inches and the tip chord was set as 7.5 inches.

The horizontal tail airfoil was chosen so that the designed airplane became statically stable with respect to the pitch direction. The incidence angle of the tail was also adjusted to allow for downwash created by the wing. The downwash angle with respect to the main wing was 2.20 degrees for the cruise condition (without flaps) and 4.37 degrees for the high lift condition (with flaps). The drag on the tail was minimized by decreasing the angle of attack seen by the tail; hence, its incidence angle was adjusted to be as close to the downwash angle as possible for minimum drag at cruise.

Downwash and stability were the main factors for determining a suitable airfoil. Through an analysis using incidence angles from 1.6 to 2.4 degrees for several airfoils, the inverted NACA 1112 airfoil with an incidence angle of 1.6 degrees was chosen for the horizontal tail. Figure 4.4 shows the moment coefficient versus the angle of attack for each component and the entire airplane. The cruise condition is tailored to have a moment coefficient of 0 at zero angle of attack in order to require less trim in order to reduce the drag.

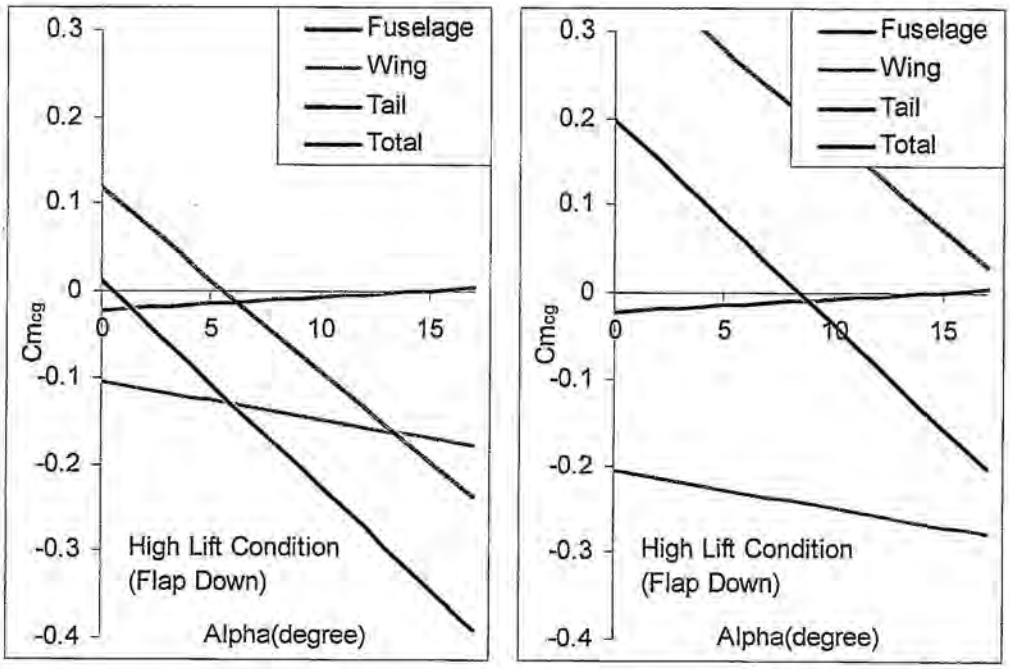

Figure 4.4 – Moment Coefficient versus Angle of Attack for Cruise and High Lift conditions

Vertical Stabilizer

The vertical tail was initially designed to have a volume ratio of 0.07 based on historical data. This was done in hopes of improving the yaw damping and dutch roll mode for an aircraft with a very large moment of inertia about its z-axis. The size was ultimately limited by the constraint of fitting within the box at the end of each mission. Preliminary sizing resulted in a vertical tail surface of 75 in^2. This was accomplished with a root chord of 15 inches, a tip chord of 5 inches, and a semi-span of 7.5 inches from the top of the fuselage. The symmetric NACA 0009 airfoil was selected to allow sufficient structural support and manufacturability. The airfoil of the vertical tail was then projected down to form the aft section of the empennage to increase directional stability. The vertical tail volume ratio then became 0.066.

4.4.3 Aircraft Control Surfaces

Control surfaces were sized to allow for flight control under various conditions. Due to the implementation of flaperons, aileron size was determined by flap and structural requirements to have a hinge line at 15% of the wing chord. Pitch and yaw controls were sized for landing conditions as subsequently described. For the analysis of each control surface, a chart of flap effectiveness was generated using the *Profili* airfoil program for every airfoil (as shown in Figure 4.5). The chart shows the effect of low Reynolds number and viscosity on flap effectiveness versus a theoretical trend.

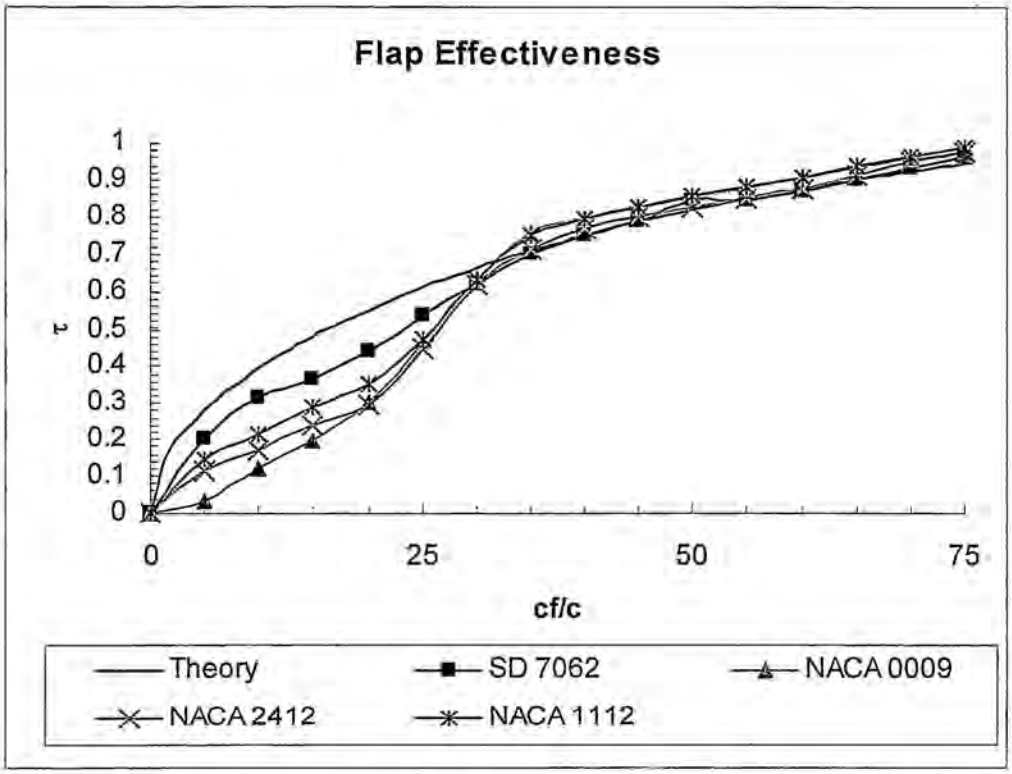

Figure 4.5 – Flap effectiveness parameter versus control surface area ratio.

Wing Control Surfaces

In order to minimize the RAC and maximize lift for the payload sorties, flaperons were employed for use as roll control. Data from *Profili* was used to size the flaperons at 15% of the wing's chord as discussed in the mission profile analysis section. The flaperons were then analyzed as ailerons to determine if they were performance grade. Analysis showed that having flaperons that span 80% of the wing span and make up 15% of the chord performed well even with payloads at the wingtips.

Elevator

The elevator sizing was performed for a high-lift flaps-down landing condition, which requires the most trim. The elevator area required to trim the aircraft at a landing approach angle of 10 degrees for several deflection angles was determined. The deflection angle required for trim is inversely proportional to the elevator size; hence, a reasonable size and deflection was determined. A deflection angle of approximately 10 degrees was chosen for a control surface size of 25% of the horizontal tail surface. This elevator size could also create enough moment to rotate the craft about the landing gear for takeoff.

Rudder

The rudder was sized to trim for a crosswind landing with a crosswind that is 20% of the landing speed. This creates a sideslip angle of 11.5°. The rudder should be able to trim this condition with no more than 20° of deflection according to Raymer (1999). Analysis showed that, with a rudder using 25% of the vertical tail area, a 20° deflection allows for trim at approximately 12° of sideslip. The rudder was then sized accordingly but will be allowed a greater freedom of deflection of 30° to provide a safety margin for higher crosswinds.

4.5 Propulsion System Testing

In order to verify the predictions made by the propulsion optimization program, actual tests were performed on the different propellers and batteries. Real-time tests are the only reliable source when making final decisions; therefore, much time and consideration was placed on the testing procedure and analysis of each major propulsion component.

4.5.1 Dynamic Propeller Tests

Using an in-house dynamometer and wind tunnel, propeller performance was measured across various advance ratios. Using static conditions as the starting point, tunnel velocities were stepped up in pre-determined increments in order to obtain at least ten data points between an advance ratio of 0 and 0.9. For each propeller, the thrust, RPM, voltage, current, and torque were collected from a sensor readout at each velocity and applied to dynamic propeller equations in order to develop regression models of performance coefficients. Each run was done twice to ensure the repeatability of results and compared with the previous years' data to check validity. The graphs on Figure 4.6 show the thrust coefficient, power coefficient, and efficiency against advance ratio for various propellers.

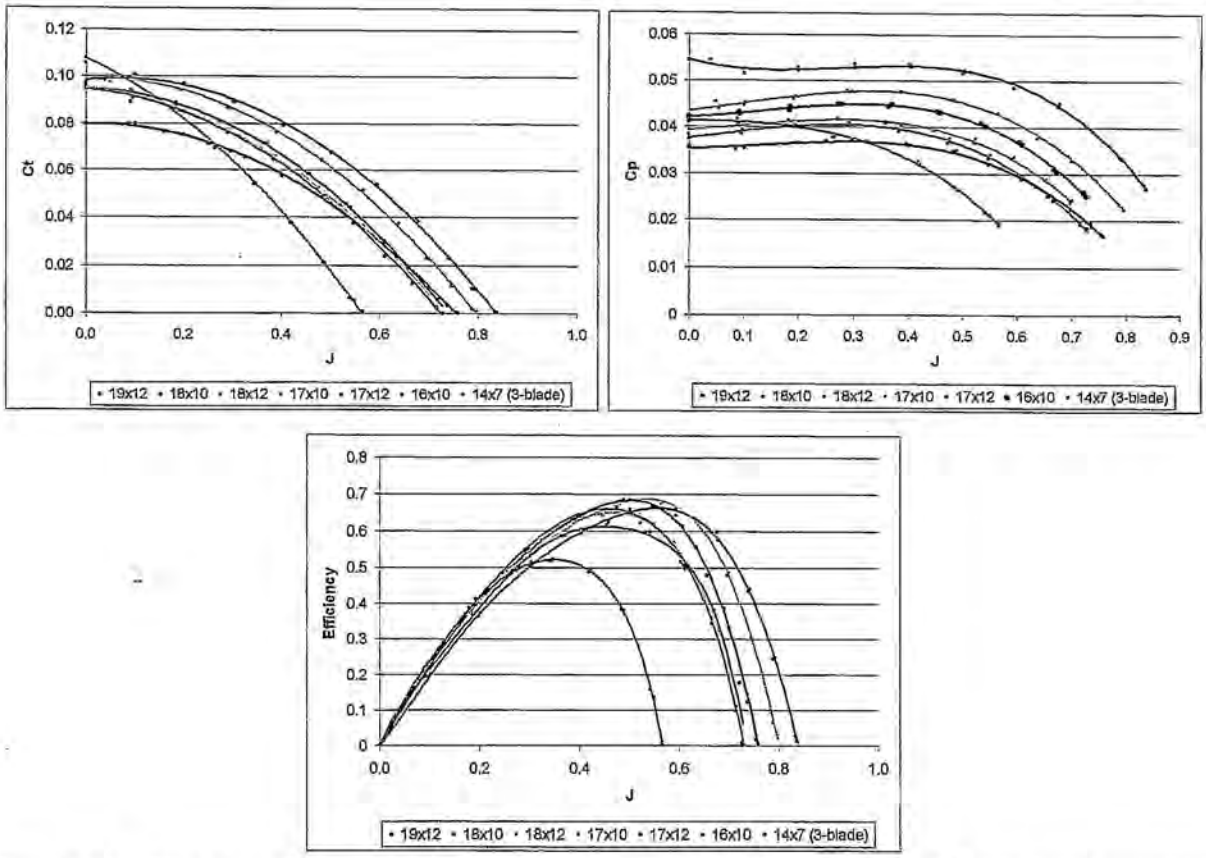

Figure 4.6 – Clockwise from top left: Thrust, Power, and Efficiency Trends for Multiple Propellers

The propeller testing results showed that props with larger pitch-to-diameter (p/d) ratios had slightly higher thrust and power coefficients while exhibiting greater efficiencies at high advance ratios. Low p/d ratio props performed better at lower advance ratios, and are therefore considered due to takeoff concerns. Inputting the regression data into the propulsion optimization program allowed new performance predictions although real-time dyno tests remained the determining factor.

4.6 Structural Preliminary Design

In order to ensure that the aircraft is capable of performing well for all mission profiles, several structural aspects were studied during the Preliminary Design phase. Critical mission performance design areas include the aircraft landing gear, payload systems, and wing structural design.

4.6.1 Landing Gear System

Due to the complicated ground handling requirements of the contest, the gear must be functional, lightweight, and easy to remove. Landing gear design issues involve the selection of the main and wingtip gear, braking system selection, and design of the nose-wheel steering system.

Since the main fuselage gear will take most of the impact during landing, it was determined that a sturdy shock-absorbing strut was needed. A commercially available unit was found that utilizes a heavy gage-spring system for shock absorption and has an extended length that can be adapted to fit the plane.

Once the preliminary choice for the main gear strut was made, the nose gear was examined. Several different types of nose wheel struts were examined in an effort to select the optimal nose gear setup. The key parameters involved in the nose wheel strut decision include steering effectiveness, landing performance, and weight. With a prototype aircraft available for testing, several options were tested to determine the most efficient alternative.

From preliminary tests, and the previously stated parameters, it was determined that the wing-tip gear should be shorter than both the main and nose gear and made from a sturdy support capable of absorbing some of the landing impact force. The first strut attempted was made of a 0.126 inch diameter wire. This gear allowed the wing of the plane to bounce and sag uncontrollably and was therefore too unstable and weak for the needs of the aircraft. This led to the use of a heavier gauge wire with a diameter of 0.188 inches. This proved sturdy enough to support the weight on the wings and still allowed enough weight to rest on the fuselage and nose gear to allow steering during taxiing operations.

The wheels chosen were products of the brake type selected and the main wheel strut. A quality braking system was selected that utilizes compressed air to activate a rubber O-ring that expands and exerts a braking force on the inner surface of the wheel rim. This system comes with a complete brake set and wheels to match. Furthermore, since the aforementioned Robart strut fits a wheel diameter of 2.75 to 3 inches and a 3 inch wheel would be excess weight, the BVM Sport main and nose gear 2 5/8" wheel was chosen.

The final component of the braking system to determine was the air brake supply tank. All the tanks examined were extremely light in weight, so the size defaulted to the number of actuations of the brakes needed per contest run. It was calculated that the maximum number of actuations needed per run was approximately 16 (this does not include the amount of bled air lost or extra actuations from pilot error). A tank rated for 25-30 actuations was selected to provide a sufficient storage of air. The preliminary design of the landing gear can only be truly evaluated by flight testing the aircraft.

4.6.2 Payload System

4.6.2a Payload Fairing Design

Fairings are needed at the nose and tail of the 12 inch PVC tube in order to reduce drag on the payload during the sensor-reposition mission. For the nose cone, minimizing the wetted area is the best approach to minimizing drag for subsonic airflow. An elliptical nose cone was chosen to fit best within the fuselage. The drag characteristics of the trailing edge can be improved by producing a smooth transition of the flow from the sides of the PVC tube to the air stream. This was achieved with an extended ogive cone. The dimensions of the payload fairings are shown in Figure 4.7. The payloads were constructed

using the same method as the fuselage and wing elements. A plug was fashioned using a CNC lathe and then molds were created to produce multiple fairings.

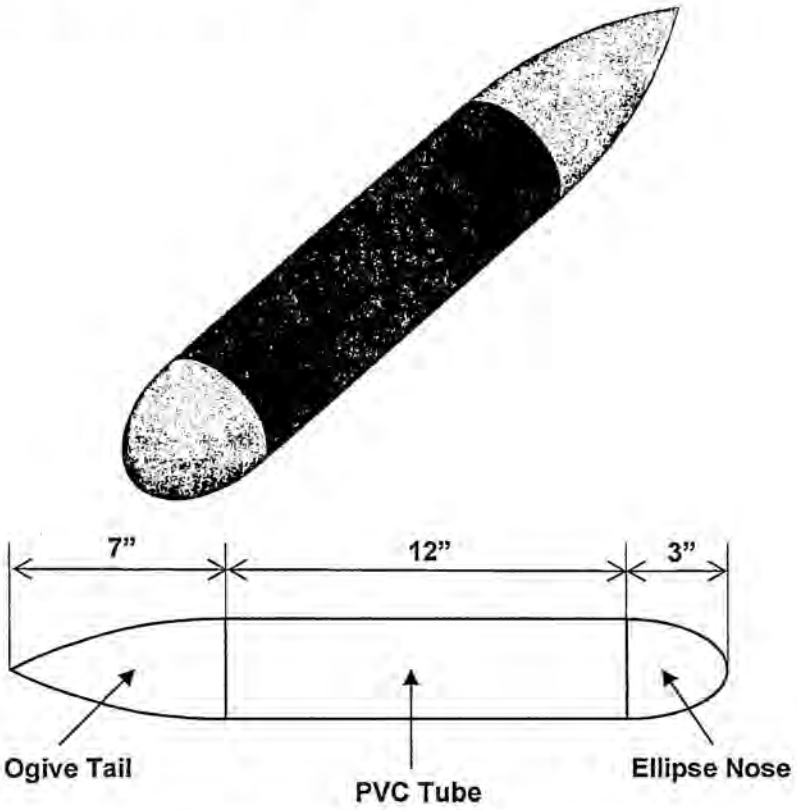

Figure 4.7 – Payload Fairing Design

4.6.2b External Payload Release Mechanism

Two main design avenues were explored in reference to the external payload release: one using rare earth magnets to provide the force to secure the payload; and, the other using a mechanical kick-out latch device to secure and deploy the payload. Prototypes were developed for each alternative to provide ample comparisons based on simplicity, reliability, and weight.

For the rare-earth magnet system, a magnet was mounted to the side of the payload. Two magnets with opposite pole orientation were then affixed to a sliding device that allowed the magnets to shear the payload and eject it. However, the torque produced by a servo was insufficient to shear the magnetic attraction. Attempts to correct the shearing problems resulted in complex and cumbersome mechanism designs.

A prototype of the mechanical kick-out latch design was fashioned out of balsa wood. This design is very reliable and is simple enough to eliminate unnecessary weight. The kick-out latch design outperformed the rare-earth magnets in terms of simplicity, reliability, and weight. These factors led to the elimination of the rare-earth magnet system and the decision to develop the kick-out latch for the final plane.

4.6.2c Internal Payload Storage and Retrieval

The design for internal payload loading and unloading involves a hatch on top of the fuselage. Rare-earth magnets can be used to attach the hatch and fuselage together by attaching each corner with magnets. The magnets must be strong enough to hold the hatch door shut for a negative gravity flight maneuver. The design is reliable and simple to manufacture, and the magnets are able to hold both parts rigidly. This will help save weight on the aircraft and save time for releasing the internal payloads. Integrating the magnets can be done by laying the magnets in the mold during skin lay-up or by building small magnet stands in the fuselage wall to hold the magnets.

4.6.3 Wing Structure

A spar tube fixture was created to investigate spar tube deflection under a static wing-tip load and to provide a visualization of a 5° dihedral. This fixture was constructed of wood and was built to hold a 5/8 inch diameter carbon fiber spar tube. The spar tube was inserted 2.25 inches deep and the entire fixture was mounted to a table using C clamps. A three pound static load was applied on the spar tube at 33 inches from the fixture, which, when measured, showed a one inch deflection of the wing tip. The load was then increased to five pounds which resulted in a deflection of 2.5 inches. With this data, structural analysis was conducted and it was estimated that the deflection of the spar tube could be reduced by approximately 65% if a 7/8 inch diameter spar tube is used.

A test fixture was also created to test the application of rare-earth magnets to bond the spar tubes to the fuselage. The spar tube in the wing slides into a carbon fiber sleeve that extends from the fuselage. The magnets were recessed in the fuselage sleeve and mounted to the wing spar tube tip, providing a flush mount fit of the wing. This system provides for rapid disassembly of the wings as well as a strong anchor point during flight with external payloads. A magnet with a maximum pull force of 6.2 pounds was tested to assess the efficacy of a magnetic wing attachment mechanism. The published maximum pull force was verified through testing, during which the magnet proved to withstand separation while under a 7 lb load. This, in conjunction with the spar tube sleeve arrangement, should be sufficient to maintain wing attachment during flight maneuvers.

4.6.4 Structural Load Simulation

In order to preserve weight, the monocoque skin must handle the majority of structural loads put on the aircraft during its mission. A *Pro/Mechanica* finite element analysis was used to assist in determining the reinforcement requirements of the skin structure for the fuselage and wings. For the computational stress analysis, the loading scenario was assumed to be a hard landing resulting in loads equivalent to four times the pull of gravity with the payloads loaded at the wing tips. The composite skin structure could then be tailored to withstand these conditions. By designing for the worst case scenario, normal operating loads are assumed to be within the bounds of the design.

The monocoque wing was statically analyzed as a cantilever beam of isotropic material fixed to the fuselage. The weight of the payload was assumed to be evenly distributed along the tip of the wing through a rib structure. Figure 4.8 shows the Von Mises stress distribution along the top and bottom of the wing for a 4-g landing. The analysis used a multi-pass adaptive method with the maximum polynomial order constrained to 6. The wing analysis achieved 10% convergence to local displacement, local strain energy, and global root-mean-squared stress within the fourth series. As can be seen in the figure, additional reinforcement in the monocoque structure is necessary at both the root and tip of the wing to account for the wing-tip payload arrangement.

The monocoque fuselage structure was simplified somewhat to ease the computational analysis. The empennage was greatly simplified and all flight surfaces were removed. Isotropic material assumptions were applied to the structure and the fuselage was constrained by fixing a simplified nose and main landing gear support structure in all dimensions and rotations. A 4-g gravitational load was then applied to the entire skin to simulate the weight of internal components. A bearing load was applied to spar holes in each side of the fuselage to simulate the downward force of the wings and payload for a 4-g landing.

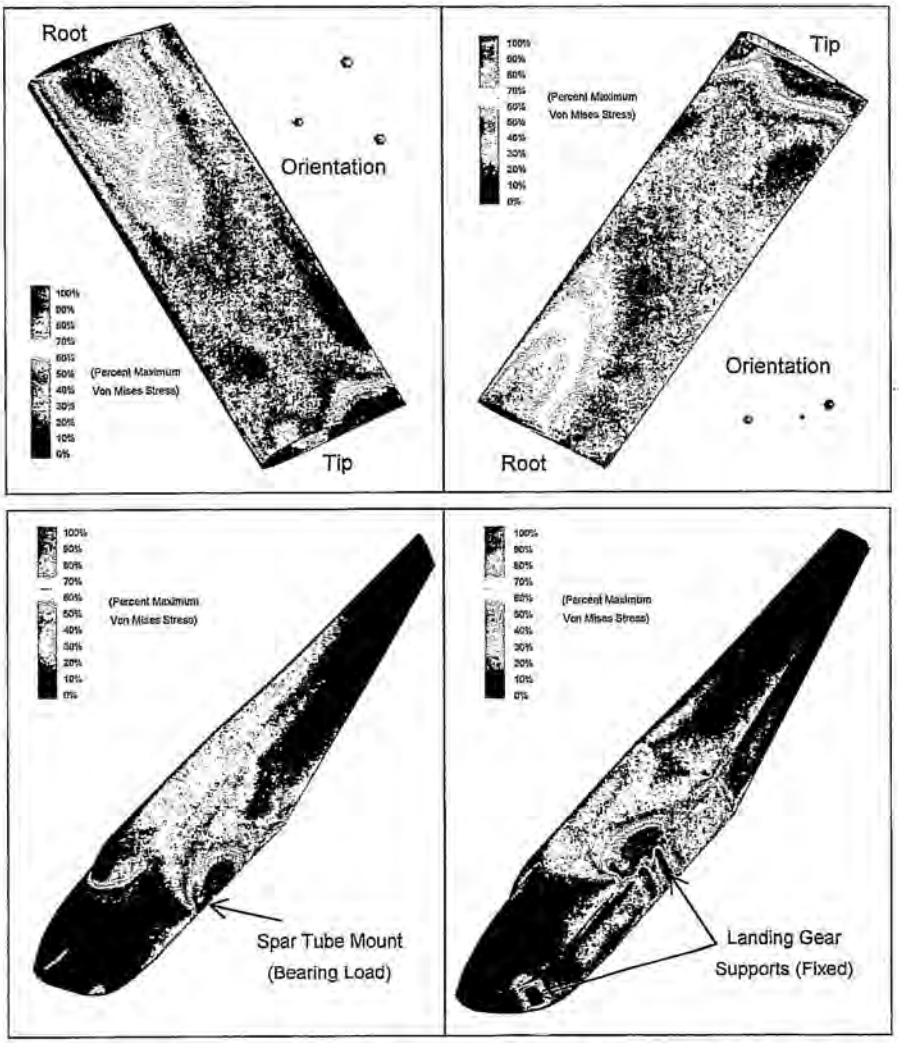

Figure 4.8 – Simulated Von Mises Stress Distribution for a 4-g Landing.

Figure 4.8 also shows the computational results of the Von Mises stress distribution for the fuselage. The same analytical method used for the wing analysis was applied to the fuselage analysis; however, the fuselage required a 6th order pass in order to achieve 10% convergence to local displacement, local strain energy, and global root-mean-squared stress. As expected, the resulting loads were symmetric about the mid-plane of the fuselage. As can be seen in the illustration, the greatest concentration of loading is associated with the main landing gear support and the wing spar mounting location. This shows that significant reinforcement will be required around the payload bay area of the fuselage and the main landing gear support.

4.7 Final Aircraft and Predicted Performance

The technical group efforts during the Preliminary Design phase resulted in aircraft sizing and component selection. The groups worked together to integrate necessary components and ensure that the final design supports the findings of the optimization procedure. The following sections summarize the aircraft design and predicted aerodynamic performance.

4.7.1 Aircraft Configuration

The overall configuration is a low-wing conventional aircraft with an upswept tail. The nose of the fuselage allows for the storage of flight systems in order to keep the center of gravity of the plane slightly forward of the quarter-chord of the wing and to maximize the length of the tail for controllability. The "canopy" allows the payload to be stowed internally and as far forward as possible to allow for a longer tail. The vertical orientation of the internal payload provides directional stability to the plane and also allows for maximum propeller clearance and a stabilizing line of thrust.

The tip-to-tip wingspan of the airplane is 5.5 feet. The flaperons occupy 15% of the wing chord and occupy 80% of the wingspan to allow room at the root for structural support and room at the tip for payload release mechanisms. The span of the horizontal stabilizer is approximately 16.5 inches and the elevator uses 25% of the tail chord across the entire span. The vertical stabilizer airfoil extends into the fuselage and the rudder surface area is 25% that of the entire tail surface. The propulsion system will employ a Kontronik 600-18 motor with a Planetary 4.2:1 gear. Power will be supplied by 13 to 15 GP-2000 battery cells. The propeller will be an APC 18x10.

4.7.2 Aircraft Performance Predictions

Using the Mission Profile Analysis Program, performance estimations were made for a loaded lap in the Re-Supply Mission. These estimations are shown in Table 4.2.

Internally Loaded Condition			
Mission Component	Time (seconds)	Distance (ft.)	Velocity (ft/sec)
Takeoff	5.41	134.47	52.82
Climb	5.97	365.53	56.46
First Turn	10	562.21	Acceleration
Acceleration Leg	8.88	641.77	Acceleration
360 Turn	4.2	0	82.5
Cruise Leg	1.45	358.23	82.5
Final Turn	10.97	348.33	Deceleration
Deceleration and Landing	5.9	744.16	Decelerate to 39.76
Payload Unload/Load Time	15	-	-
	67.78	-	-

Table 4.2 – Performance estimation for one lap of the Re-Supply mission

Takeoff time and distance is 5.4 seconds and 134.5 feet, respectively. The aircraft must accelerate during the transition from takeoff to climb to the optimum climb speed of 56.5 feet per second. The aircraft spends considerable time accelerating to cruise speed before entering the 360° turn. Given an estimated time of 15 seconds to remove the internal payload, the total lap time for an internally loaded aircraft is approximately 68 seconds. Once the payload is unloaded, the aircraft takes off for an unloaded lap. Unloaded lap times will be significantly faster.

4.7.3 Estimated Aircraft Lift and Drag

The maximum lift coefficient of the aircraft was estimated by using the lift coefficient of the SD 7062 wing airfoil corrected for aspect ratio. This resulted in a maximum lift coefficient of 1.15. Drag was estimated within the analysis program using a build-up method, and was based mainly on the maximum cross-sectional area of the fuselage and the drag polar of the SD 7062 wing airfoil. The lift-to-drag ratio for the entire aircraft was plotted and the maximum lift-to-drag ratio was observed to be approximately 10.3. These estimates are not far from those of past Oklahoma State University competition planes that faired well during flight, and therefore reinforce the airfoil selection and fuselage design.

4.7.4 Aerodynamics & Stability and Control Analysis Summary

The pitch static stability was measured by the moment acting on the center of gravity of the airplane. The moment was produced by the main wing, the horizontal tail, and the fuselage. The major concerns of the pitch stability were the slope of the moment coefficient versus the angle of attack and the moment

coefficient at an angle of attack of zero degrees. These were computed from the summation of moment coefficients for each component, and show that the designed airplane is balanced and stable in the pitch direction. The directional stability is provided by the fuselage and the vertical tail. A positive number for the directional stability coefficient shows the designed airplane to be directionally stable. The roll stability was mainly given by the dihedral of the main wing and is negative which indicates stability.

The dynamic stability analysis was separated into two motions of the airplane. The longitudinal motion, controlled by forces in the x and z-directions and by the pitching moment, contains the phugoid and short period modes. The lateral motion was governed by forces in the y-direction and yaw and roll moments. The lateral motion includes the roll, spiral, and Dutch roll modes. These motions were predicted by evaluating stability derivatives, which are the function of stability coefficients and atmospheric and flight conditions. Table 4.3 shows the list of the stability coefficients calculated for the plane design.

Aircraft Stability Derivatives							
C_{L_0}	-0.3417	C_{L_α}	0	C_{L_q}	0.0836		
C_{m_0}	-0.1113	C_{m_α}	0	$C_{m_{\dot{\alpha}}}$	0.3248	C_{m_q}	-0.0487
C_{D_0}	0.1051	C_{D_α}	-1.3516	$C_{D_{\dot{\alpha}}}$	0	C_{D_q}	-0.0645
C_{Y_0}	-0.8866	C_{Y_α}	-5.2678	$C_{Y_{\dot{\alpha}}}$	0.1396	C_{Y_q}	-0.8228
C_{l_0}	-4.9865	C_{l_α}	-12.2915	$C_{l_{\dot{\alpha}}}$	0.0836	C_{l_q}	0.0814
C_{n_0}	-1.7891	C_{n_α}	-0.9393	$C_{n_{\dot{\alpha}}}$	-0.0272	C_{n_q}	-0.0645
C_{l_0}	-4.1745	C_{l_α}	-0.466	$C_{l_{\dot{\alpha}}}$	-0.0848	C_{l_q}	0.0116

Table 4.3 – Stability Coefficients

Assuming the atmospheric conditions at sea level and estimating the weight and moments of inertia for the craft, the eigenvalues for the longitudinal and lateral motion were tabulated and can be seen in the upper left of Figure 4.9. They show the dynamic motion of the airplane in terms of the natural frequency and the damping ratio. The short period mode and spiral mode for all loading conditions were relatively the same; however, the payloads dramatically increase the moments of inertia of the yaw and roll axis in such a way that the yaw mode is drastically affected.

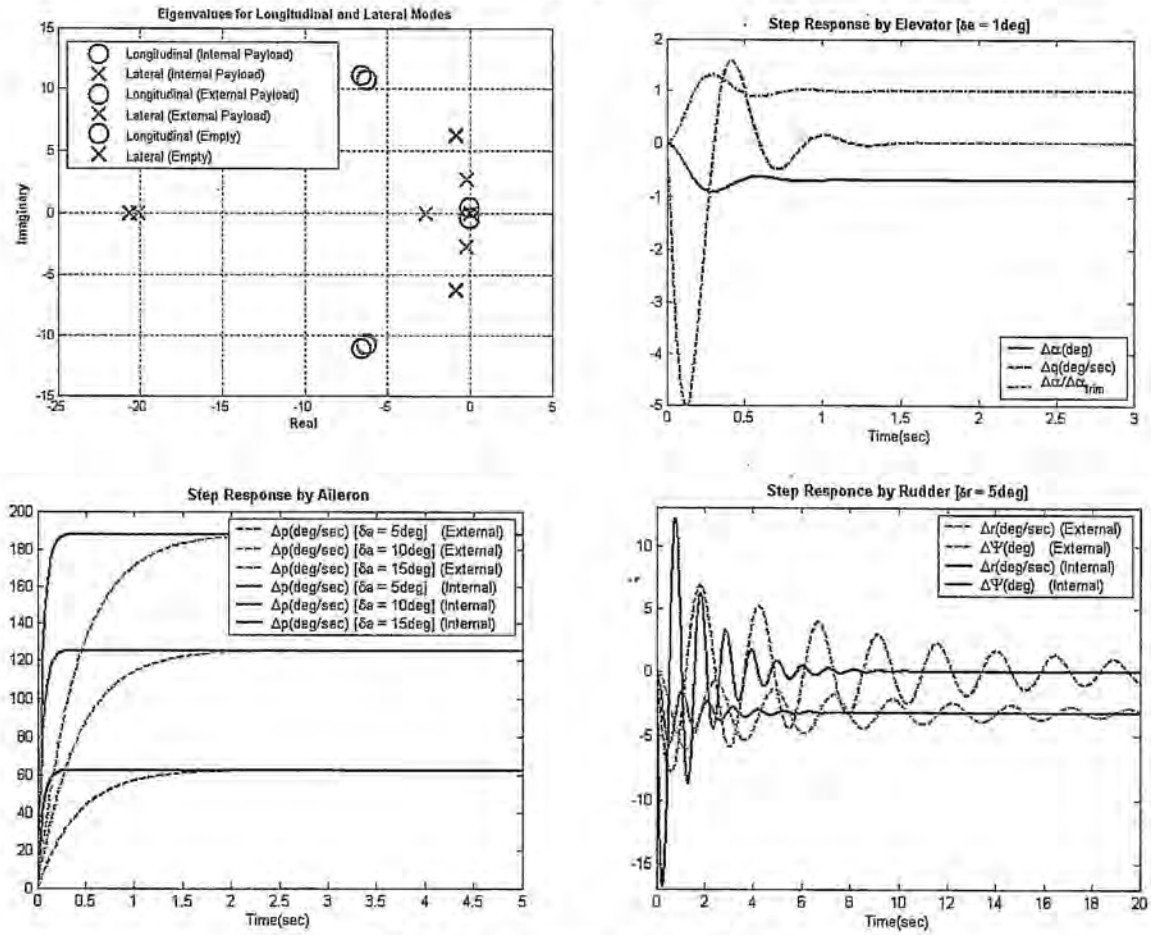

Figure 4.9 – Dynamic Stability Illustrations

Based on the eigenvalues above, several response and parameter relationships were computed and plotted for observation. The upper right chart in Figure 4.9 shows the pure pitching motion of the airplane with external payloads. The figure contains the ratio between the change in angle of attack and the change in trim angle of attack, the step response of the change in angle of attack, and the step response of the change in the pitch rate by the step input of 1 degree of the elevator deflection. This is essentially the analysis of the short period mode. All curves have a time constant of 0.253 seconds. The step response for the empty condition and the internal payload condition were almost identical to the external payload condition. This is because the moment of inertia about the y-axis does not change significantly as the payload is aligned to the longitudinal CG of the aircraft for all loading conditions.

The lower left chart in Figure 4.9 shows the step response of the roll rate (in degrees/second) of the aircraft for a 5, 10, and 15 degree flaperon deflection. As can be seen, the time constant is considerably different for the external and internal payload loading conditions due to the large increase in the moment of inertia about the rolling axis of the airplane.

The lower right graph of Figure 4.9 shows the step response of the yaw rate and the yaw angle for a 5 degree step deflection of the rudder. As can be seen from the figure, the time constant for the external

payload condition is almost six times that of the internal and empty payload conditions. This drastic difference in directional dynamic response may require the use of a yaw-damping control system for flight with external payloads.

5.0 Detail Design

In the detail design phase, the aircraft characteristics were fine-tuned and all propulsion decisions from the preliminary phase were finalized. It is during this phase that all system integrations are fully optimized and weight is reduced, resulting in the competition-ready aircraft.

5.1 Component Selection and Systems Architecture

Table 5.1 below shows the final aircraft specifications and performance data for the optimized aircraft.

General Aircraft Specifications			
Primary Function	Payload Transport	C_L max	1.15
Fuselage		L/D max	10.3
Length, (in)	47	***Gross Weight***	
Width, (in)	4.5	Maximum Climb Rate, (fps)	9.51
Height (in)	9	Stall Speed, (fps)	48.8
Wing		Maximum Speed, (fps)	87.1
Airfoil	SD 7062	Take-off Distance (ft)	130
Span, (in)	66	***Empty Weight***	
Area, (ft^2)	4.125	Maximum Climb Rate, (fps)	18.55
Aspect Ratio	7.33	Stall Speed, (fps)	35.8
Incidence Angle, (deg.)	0	Maximum Speed, (fps)	87.9
Flaperon Area Per Wing, (in^2)	60.4	Take-off Distance (ft)	36
Horizontal Stabilizer		***Aircraft Weight & Balance***	
Airfoil	NACA 1112	Payload, (lb)	6
Span, (in)	16.5	Manufacturer's Empty Weight (MEW), (lb)	8
Chord at root, (in)	8.5 in	Gross Weight, (lb)	14
Chord at tip, (in)	7.5 in	Center of Gravity Location (in)	14
Volume Ratio	0.65	***Aircraft Systems***	
Incidence Angle, (deg.)	1.6	Power Plant	Kontronik 600-18
Elevator Area, (in^2)	33	Battery Configuration	14 GP-2000
Vertical Stabilizer		Gear Box	Planetary
Airfoil	NACA 0009	Gear Ratio	4.2:1
Span, (in)	7.5	Speed Controller	J922 55
Chord at root, (in)	15	Propeller	APC 18x10
Chord at tip, (in)	5	Radio	Futaba 9Z
Volume Ratio	0.066	Receiver	Futaba R138DP
Rudder Area, (in^2)	27	Servos	Futaba S3002

Table 5.1 – General Aircraft Specifications

5.1.1 Propulsion System

The final propulsion system requires a static thrust of 7 lbs and therefore approximately 600 watts of power to the motor. Using the predicted flight characteristics from the aerodynamics optimization program, mission profiles were simulated to guarantee sufficient battery life. Testing the batteries for the more demanding re-supply mission ensures that the aircraft can complete both missions. Flight profile data for the first two laps of the Sensor Reposition and Re-Supply missions is shown below.

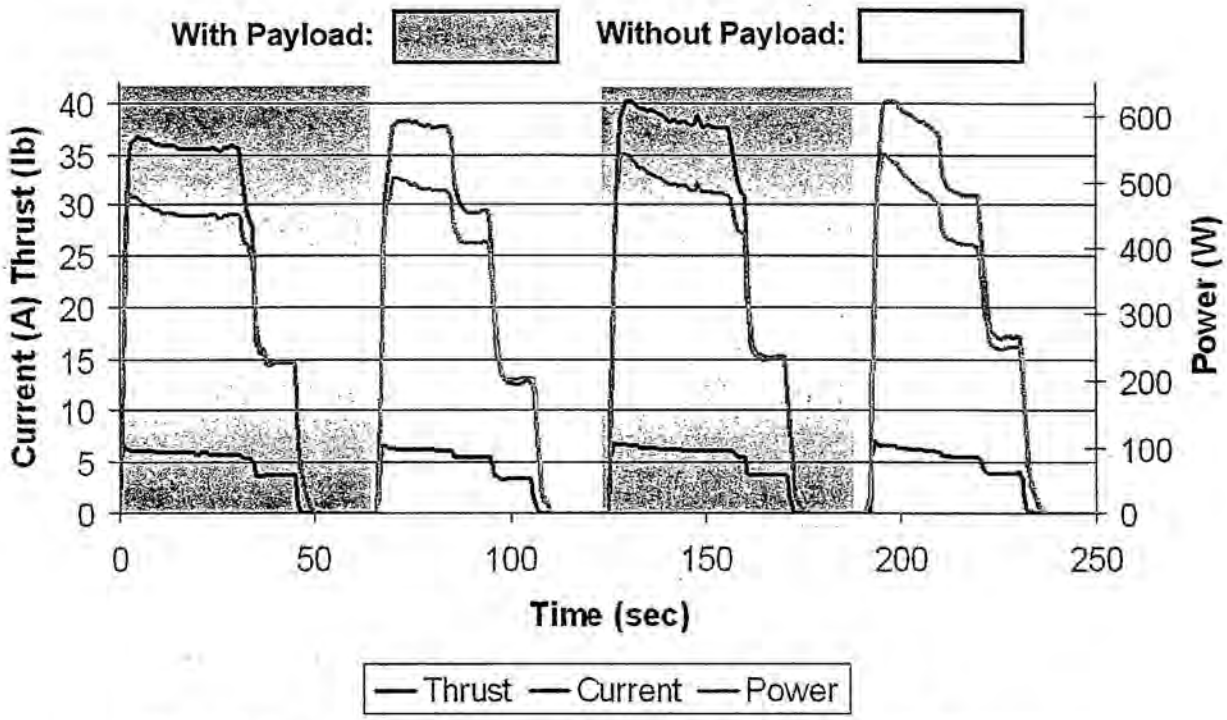

Figure 5.1 – Power, Current, and Thrust vs. Time in Resupply flight profile

Wind tunnel testing of all considered arrangements proved to be invaluable in the final selection of the propulsion system. The 14-cell GP-2000 pack provided ample power for takeoff throughout the Re-Supply mission profile, giving approximately 6.5 lbs of thrust with the 18x10 propeller. Other batteries were tested, but, due to weight concerns and the verification of success with the GP 2000, its selection was finalized. Although the optimization programs were extremely helpful in predicting performance, actual dynamic tests added confidence to design decisions. Flight test data became the next step in determining the real performance capabilities of the aircraft.

5.1.2 Aircraft Structural Systems

Early in the conceptual design phase of the project, the aircraft was divided into key categories to allocate personnel to all design issues. These categories included fuselage structure, empennage structure, main wing structure, landing gear and steering, and external and internal payload systems.

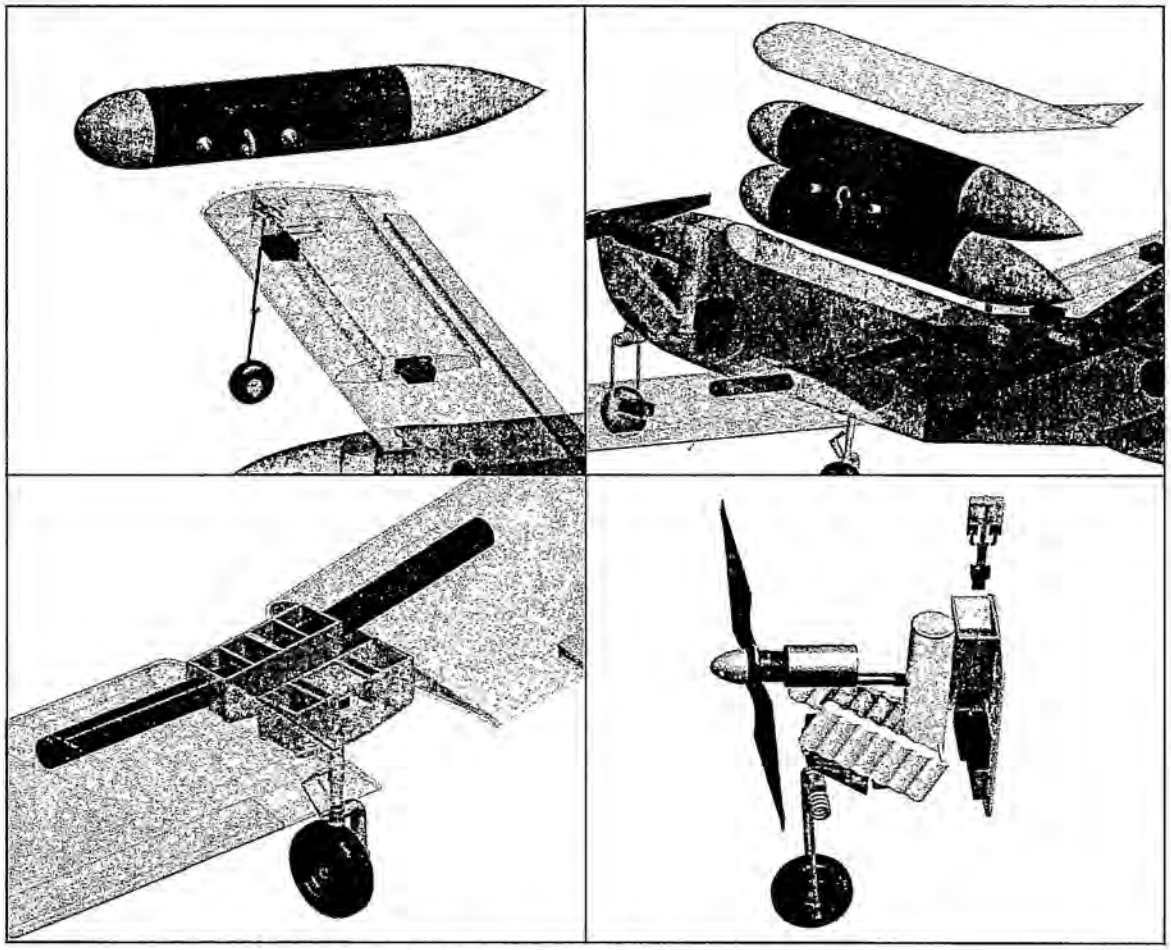

Figure 5.2 – Structural Design Elements

5.1.2a External Payload Release

The final design for the external payload release mechanism essential to the Sensor-Reposition Mission is illustrated in the top left of figure 5.2. A U-bolt affixed to the payload is held to the wing-tip by means of a remotely operated mechanical latch. Two guide pins are attached to the payload on either side of the U-bolt to prevent the payload from rotating about the latch mechanism and to align the payload to the camber line of the wing airfoil. In order to deploy the payload, a servo must release the latch; however, when the servo arm returns to the closed position, the payload may be loaded to the wing-tip without servo actuation. This system provides for an efficient and reliable approach to reducing pit time during the Sensor Reposition Mission.

5.1.2b Internal Payload System

Internal payload storage was a major design criterion for all aspects of the fuselage design. The top right figure of Figure 5.3 illustrates the method for insertion and removal of the internal payload via a hatch that extends along the top of the fuselage for the total length of the payload. The "canopy" at the

nose of the hatch will employ a hook to secure the front end of the hatch to the fuselage. Rare-earth magnets will be used to secure the aft end of the hatch to the fuselage. The dorsal fin connected to the upper surface of the hatch serves as a grip point for shearing the magnetic bond for rapid hatch removal. This design promotes speed and efficiency for reducing pit time for the Re-Supply Mission.

5.1.2c Fuselage-wing Bulkhead

The method for transferring loads between the fuselage and the wings is illustrated in the lower left image of Figure 5.3. Carbon fiber "sleeves" are mounted to a bulkhead assembly within the fuselage. Carbon fiber spar tubes from the wing are inserted into these sleeves to secure the wings to the fuselage and transfer weight loads during flight. Rare-earth magnets attached to the tips of these spar tubes are attracted to magnets within the fuselage sleeves to provide additional strength for the system. The magnets allow the wings to be pulled from the sleeves by hand for disassembly of the aircraft at the end of each mission, but provide reinforcement for the load conditions experienced by the wings with the external payload configuration. An anti-rotation pin (not shown) protrudes from the inner rib of the wing into a receptacle in the fuselage to prevent wing root twist during flight.

5.1.2d Main Landing Gear

The bottom left image of Figure 5.3 also illustrates the support structure for the main bicycle landing gear. The main gear employs a linear shock-absorbing strut that is mounted to a collar which allows for installation and removal of the gear for disassembly of the plane at the end of each mission. The apparatus also provides for rear gear counter-steer by a control arm at the tip of the collar. The area around the wing spar and main gear supports requires extensive reinforcement, as computer simulations showed the highest concentration of stresses occurring in this area during ground maneuvering, flight, and landing.

5.1.2e Nose Layout

The structural layout of the nose is shown in the bottom right of Figure 5.3. This includes the nose gear and steering servo. The nose gear will have a spring structure that allows for lateral deflection to absorb shocks during taxiing maneuvers. The nose steering may also be linked to the main gear to increase maneuverability. The nose structure also includes the forward bulkhead that provides an attach point for the fuse box and gear brake air supply. A servo will serve as a brake actuator and will be located near the air tank.

5.2 Final RAC Calculation

A key requirement of a competitive aircraft design for the competition was the minimization of the Rated Aircraft Cost which results in a maximized potential total contest score. Therefore, a conscious effort was made by the team to continually screen the aircraft RAC value and search for ways to bring further reductions. The final RAC model is shown in Table 5.2 below.

Rated Aircraft Cost Model	RAC Multiplier	RAC Computation	Value	Manufacturing Man Hours	Cost
(MEW) Manufacturer's Empty Weight	$500.00	Aircraft Weight * ($500.00)			
Aircraft Weight			7.7 lbs		***$3,850.00***
(REP) Rated Engine Power	$1,000.00	(1+.25*(# engines-1))*Total Battery Weight * $1000			
Battery Weight			1.076		***$1,076.00***
(MFHR) Manufacturing Man Hours	$20 / hr	($20 * MFHR)			
Fuselage		20hr/ft3	1.11ft3	22.2	
Wings		10hr/ft2	4.125ft2	41.25	
Vertical Stabilizer		10hrs / surface	1	10	
Horizontal Stabilizer		10hr / surface	1	10	
Flaperons		5hrs	1.5	7.5	
Flight Servos		5hrs / servo	8	40	
Total MFHR				130.95	***$2,619.00***
Total Cost					***$7,545.00***
(RAC) Rated Aircraft Cost		[$500*(MEW) +1000*(REP) + $20*(MFHR)] / 1000			***7.55***

Table 5.2 – Rated Aircraft Cost Model

5.3 Drawing Package

The aircraft was modeled in its entirety during the preliminary and detailed design phase using the computer aided design package *Pro/Engineer* in an effort to finalize the conceptual aircraft design and enable efficient communication of design intentions. The drawings on the following pages comprise the drawing package of the aircraft, and include the following aircraft views: three-view overall aircraft, payload system, stowed configuration, exploded view, and control systems configuration.

6.0 Manufacturing Plan

The manufacturing phase of the project resulted in the culmination of the aircraft design as the individual aircraft components began to materialize. It was apparent early in the design process that a detailed manufacturing plan would need to be implemented in order to ensure that the produced aircraft closely matched the quality of the aircraft that had been designed. Topics of interest with respect to the manufacturing phase included the investigation of manufacturing processes, component manufacturing techniques, and analytic methods used to evaluate the teams ability to develop the aircraft within the allotted time.

6.1 Processes Investigated and FOM Screening Process

The investigation of the optimal manufacturing process began early in the conceptual design phase once the overall geometry of the aircraft and components were defined. From the study of alternate manufacturing processes, monocoque construction techniques were chosen for the major structural components. Once this method was chosen, it was possible to develop FOMs and mold method alternatives for the monocoque technique.

Figures of Merit

The following FOMs were developed to help in the mold method decision-making process. The FOMs are implemented with the mold method alternatives in Table 6.1.

- **Build Time:** Time is a crucial factor in any project. A fast construction time will allow for more testing time and any replacement parts needed.
- **Repeatability:** In the event that an aircraft malfunctions or is damaged, it will be necessary to either rebuild or repair, so each method is evaluated on how easily the plane can be fixed or reproduced.
- **Cost:** The method must be affordable for the team to produce a prototype and final aircraft.
- **Weight:** A process that allows for lightweight aircraft components is critical. The lighter the aircraft, the better the RAC, which translates to a higher overall score.
- **Strength:** The construction method must provide the needed strength and structural integrity for the plane to perform all of the desired functions.

Mold Method Alternatives

The following mold method alternatives were investigated for the monocoque construction process for the Black Team aircraft.

- **Male Mold:** Constructing the aircraft using a series of male molds was considered. To accomplish this, an accurate outer image of each part must be constructed and finished to be used as tooling. This requires either skill in woodworking or a reliable way to harden the outer surface of a foam mold that was cut with a CNC foam cutter. The next step would be to lay up the monocoque skins on each side of the mold in either a dry or wet lay-up, cure as necessary, and bond them together. This would

provide sufficient strength, but the best surface of the pieces would be on the inside of the structure, requiring finish work on the outside of the aircraft.

- **Female Mold:** Building based off of female molds is the most labor-intensive method. This method often frontloads the construction schedule with both of the tasks required for foam-filled construction. However, the female mold method provides the strength of the monocoque method while significantly reducing the time to make a second aircraft.
- **Lost Foam:** The lost foam method is the easiest of the monocoque methods, because it does not require extensive tooling construction. Once a foam cutout was constructed of each piece, it would be covered in fiberglass, allowed to cure, and then much of the internal foam would be removed. The foam would be removed by cutting tools or by cleaning agents which break down the foam structure, but do not harm the fiberglass. This provides an extremely lightweight structure, but generally lacks the required structural strength unless a significant amount of the foam is left undisturbed.

Mold Methods				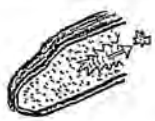
		Monocoque Mold Alternatives		
Figure of Merit	*Weight Factor*	Male Mold	Female Mold	Lost Foam
Build Time	0.1	-1	0	-1
Repeatability	0.2	1	1	1
Cost	0.1	-1	-1	-1
Weight	0.3	1	1	1
Strength	0.3	1	1	1
Total:	**1.0**	**0.6**	**0.7**	**0.6**

Table 6.1 – Monocoque Molding Methods

6.2 Component Manufacturing

The construction of the wings, fuselage, empennage, and external payload release are described in the following section.

6.2.1 Fuselage and Empennage

First, a foam plug of the fuselage was made. The basic shape was cut out of foam using a CNC machine then sanded to fit the desired shape and dimensions. Next, the foam is covered with fiberglass and filler to provide structure to the plug. After the plug is finished, it is mounted into parting boards cut

from coated particle board then covered with a thick gel coating that provides a smooth mold surface. Once dried, the gel coat is reinforced with several layers of fiberglass that also work as a parting board for the second half of the mold. When the second mold is complete, the molds are then pulled apart and checked for any imperfections or dimensional errors.

After the molds are finished, the plug and the parting boards are covered with wax and liquid release for easy part removal. To make the parts, an outer layer of fiberglass is placed in each mold, and then balsa wood is laid down to provide stiffness and strength followed by an inner layer of fiberglass. Any internal structures such as ribs, spars, and bulkheads are then placed in one of the molds using epoxy, and then the two molds are joined together after a bead of epoxy is placed in the open part. Once sufficient time has been allowed for the epoxy to set, the molds are separated and the part is removed. To seal up the edges, a strip of fiberglass is placed on the inside with resin, which secures the two part halves together.

6.2.2 Wing

The method for wing mold construction is the same as that for the fuselage. To lay up the wings, a layer of two ounce fiberglass was used for the outer portion of the wing skins. Next, 1/16" balsa core was put down, and a layer of one ounce was used for the inner portion of the skins. This was done to reduce weight and increase stiffness by increasing the moment of inertia. Two 7/8" outer diameter spar tubes are used to carry the loads for the wings. The tubes are bonded inside the fuselage on both sides and the wings slide off the spar tube for disassembly. A pin was placed near the trailing edge of each wing to prevent wing rotation. Balsa shear webs were used to prevent deformation in the span direction. Five ribs are placed inside the wing, one at each end and three in the middle. Two servos are used inside the wing, one at half-span for the flaperon and one at the end for the external payload release mechanism.

6.3 Analytic Methods

Several analytic methods were used to ensure the team followed an efficient and productive construction process. The methods identified as key issues with the construction process include the aircraft cost, team construction skills, and the detailed construction schedule.

6.3.1 Aircraft Cost

The cost of the aircraft and construction material components was continuously monitored throughout the project to ensure that funding was not exceeded. The primary categories for project cost included aircraft structure, flight controls, propulsion system, and payload systems. A breakdown of the aircraft cost can be seen in Table 6.2 on the following page.

Aircraft Construction			
Item	*Amount*	*Unit Cost*	*Total Cost*
Structure			
Tooling	1	$1,500.00	$1,500.00
Misc.	1	$100.00	$100.00
Gear	1	$300.00	$300.00
Flight Control			
Servos	8	$55.00	$440.00
Receiver	1	$125.00	$125.00
Battery	1	$20.00	$20.00
Gyro	1	$150.00	$150.00
Propulsion System			
Motor System	1	$425.00	$425.00
Batteries	2	$50.00	$100.00
Propeller	1	$15.00	$15.00
Payload System			
PVC	1	$10.00	$10.00
Misc.	1	$20.00	$20.00
		TOTAL:	***$3,205.00***

Table 6.2 – Aircraft Construction Cost

6.3.2 Construction Skills

Another important analytic method used during the manufacturing planning period was to survey the skill level of the team and develop a construction skills matrix. This survey allowed for the architecture of the team and personnel assignments to be made with respect to the most efficient and productive manner possible. Also, this process allowed for the identification of potential weaknesses or areas for improvement in the team skill levels. A list of likely construction and design skills was generated and tabulated against the major aircraft components. For each skill, the number of team members with experience and proficiency was first determined. The skills were then assigned values under each aircraft category to assess their importance in the manufacturing process. Tasks requiring little or no skill level were assigned values of zero. Tasks identified as requiring a moderate level of skill were given values of one, while tasks requiring high levels of skill were assigned values of two. The construction skills matrix can be seen in Table 6.3 on the following page.

Project Required Skills	# of Team Members Proficient	Wing	Fuselage	Payload System	Landing Gear System	Empennage
Composite Lay-up	6	2	2	1	0	2
CNC Foam Cutting	1	2	2	1	0	2
Metal Working	1	1	2	2	2	0
Wood Working	3	2	2	2	2	2
Technical Writing	4	2	2	2	2	2
Aircraft Assembly	5	2	2	2	2	2
Graphic Design	1	1	2	2	2	1
Propulsion System Integration	4	2	2	1	0	1
Structural Design	3	2	2	2	2	2
Computer Aided Design	4	2	2	2	2	2

Table 6.3 – Construction Skills

6.3.3 Construction Schedule

A detailed construction schedule was defined and implemented early in the design process to ensure that a competitive aircraft was produced on schedule. The schedule for the Black Team construction effort can be seen in Figure 6.1 below. The baseline plans for the construction effort were generated early in the design phase and were continually compared to the actual progress of the team.

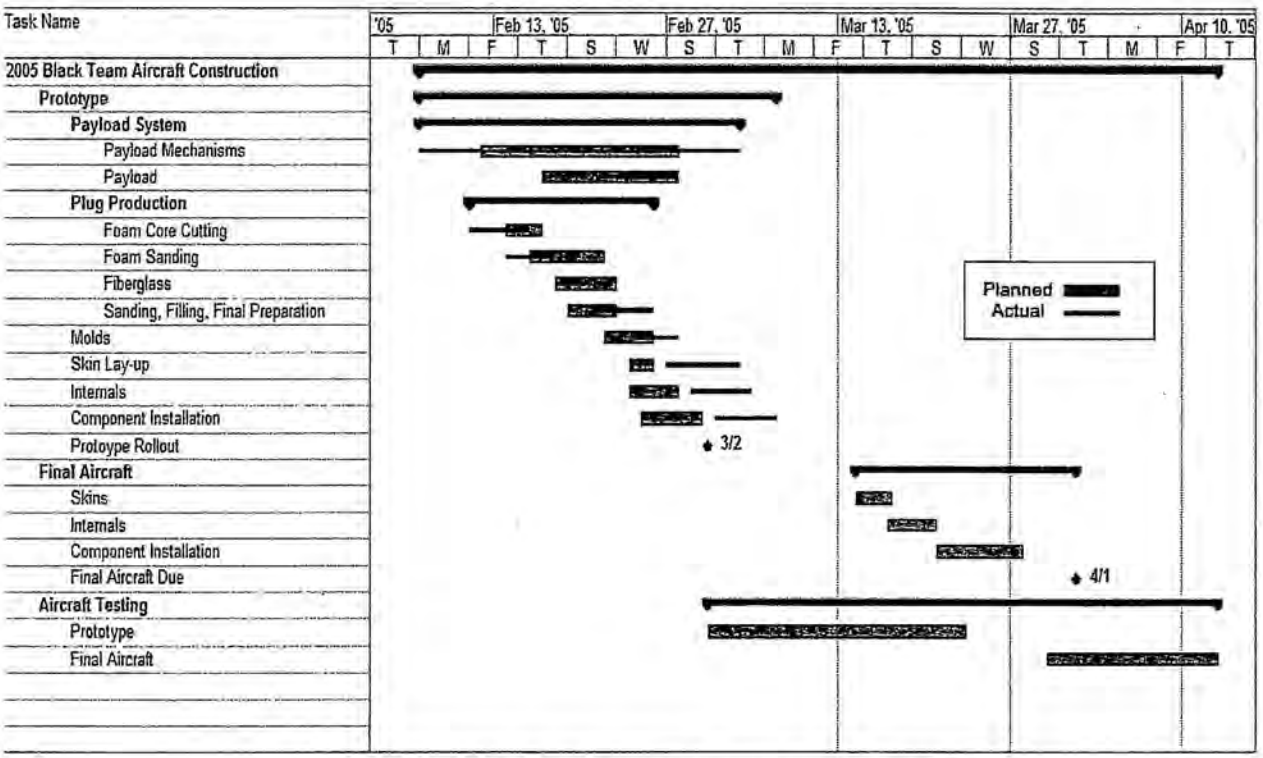

Figure 6.1 – 2005 Black Team Construction Schedule

7.0 Testing Plan

Following conceptual and preliminary designs, testing was scheduled in order to justify the conclusions of the optimization programs. Without a complete and thorough testing schedule, final design decisions could not be made with confidence. As a result, careful testing schedules and procedures were developed for each individual group.

7.1 Test Objectives and Schedule

Each group specified testing goals and estimated times to reach them. In order to ensure testing efficiency, group collaboration produced the schedule shown below in Table 7.1. Scheduling in this manner allows necessary changes to be discovered and implemented as quickly as possible.

Test Focus	Goals	Dates
Propulsion System	Collect motor, propeller, and battery performance data	2/11 - 2/18
Payload Release	Examine release efficiency, reliability, and durability	2/25 – 3/5
Landing Gear System	Test the taxiing ability of the landing gear	2/10 – 3/10
Wing-tip Test	Check to see that the wings can pass wingtip test	3/2 – 3/16
Molding procedure	Prove procedure is most effective	1/26 – 2/16
Final Propulsion Check	Finalize and optimize all propulsion decisions	2/23 - 3/10
Ground Crew	Practice all payload loading and fuse removal	3/5 – 4/15
Flight Tests	Validate stabilization predictions and fine tune aircraft	3/5 – 4/15

Table 7.1 – Testing Schedule

7.2 Flight Test Checklists

Component theory and programs cannot accurately predict every aspect of a real flight. Therefore, flight testing provides the most useful information for the refinement of the aircraft. In order for each flight test to yield as much information as possible, it is imperative that a flight checklist be constructed. This ensures that each component of the aircraft is inspected and examined before, during, and after each flight. The recorded observations can then be used to detect fatigue problems, reliability issues, or overall optimization shortcomings. The aircraft checklists which are shown in Tables 7.2 and 7.3 address every aspect of an actual mission attempt.

Due to the mission specifications, ground testing and optimization is essential to the success of the aircraft. As a result, taxiing, payload release, takeoff, and landing were examined carefully. Propeller and battery selections must be tested to ensure necessary performance while minimizing RAC.

Flight testing is for both possible scenarios: with or without payload. Each flight test will begin with gentle flight maneuvers before progressing to more aggressive turns and stall testing. Flight test observations validate stability and control predictions, while providing the pilot with much needed practice.

Pre-Flight Checklist		
Item	**Comments**	**Complete**
Weight and Balance (CG)	CG within operating range	
Motor Mount	Mounting screws tightened, firewall secure	
Control Surfaces		
Linkages Secure	No endplay	
Proper Deflection	Check trim points and throw distance	
Hinge Integrity	Pull on hinge, check for tears	
Landing Gear	Bolts and wheels secure, no de-laminations on bow	
Payload System		
Release mechanism	Operational, unobstructed, secure attachment	
PVC's	Securely attached, fairings connected	
Structural Rigidity	Wing tip test done at full gross weight	
Radio Range Test (Including Fail Safe)	Collapsed antennae, motor on and off	

Table 7.2 – Aircraft Preflight Checklist

In-Flight Checklist		
Taxi/Ground Handling	**Comments**	**Complete**
Aircraft Tracks Straight		
Sufficient Maneuvering Control		
First Flight (No Payload)		
Sufficient Control in all axes		
Aircraft in control through all flight maneuvers		
Stall Characteristics Verified		
Adequate Control at takeoff and landing		
Payload Release operational		
Second Flight (Full Payload)		
Sufficient Control in all axes		
Aircraft in control through all flight maneuvers		
Stall Characteristics Verified		
Adequate Control at takeoff and landing		
Payload connection stability		
Mission Profile Practice		
Takeoff in less than 150 feet		
Lap Time less than 1 minute		
Landing Distance		
Payload Release operational		
Taxiing time		
Pit times		
Complete mission time		
Overall control		

Table 7.3 – Aircraft In-flight Checklist

All aspects of an actual mission profile will be approximated throughout aircraft performance testing. It is during these tests that flight velocity, flight time, takeoff and landing distances, and turning radius will be determined. In addition to flight performance, payload release mechanisms will be checked for reliability and adjusted where needed. Following the complete testing of the aircraft, final ground crew and pilot practice can begin for each mission sortie.

7.3 Testing Results and Lessons Learned

Testing the actual aircraft configuration in the air gave precise performance characteristics and located problems the programs overlooked. The information gathered during flight tests provided invaluable refinement to the overall design. Every test returned specific information to each group as shown in the following table.

Test	Results and Lessons Learned
Propulsion System	14 GP 2000 cells provide ample power throughout the mission. Also, the Kontronik motor and ESC maintain high efficiency throughout mission. 18x10 prop necessary to get necessary static thrust.
Payload Release	Extremely reliable and quick. No changes necessary.
Landing Gear	Satisfactory taxiing ability. Exceeded expectations. No changes necessary.
Wingtip test	Original spar tube allows too much wing tip deflection; therefore, larger diameter and thickness were used.
Molding Process	Test molds led to more precise construction, therefore, reducing weight. Procedure is optimized.
Final Propulsion	Not yet completed.
Ground Crew	Initial testing begun and estimated pit time around 15 seconds
Flight Tests	Not yet completed.

Table 7.1 – Testing Results and Lessons Learned

References

Allen, D.H. and W.E. Haisler, *Introduction to Aerospace Structural Analysis*, John Wiley and Sons, New York, 1985.

Bertin, J.J. and M.L. Smith, *Aerodynamics for Engineers*, 3rd Edition, Prentice Hall, Upper Saddle River, New Jersey, 1998.

Donald, D. *The Complete Encyclopedia of World Aircraft*, Barnes and Noble Books, New York, 1997.

Nelson, R.C., *Flight Stability and Automatic Control*, 2nd Edition, McGraw-Hill, Boston, 1998.

Raymer, D.P., *Aircraft Design: A Conceptual Approach*, 3rd Edition, AIAA, Reston, VA, 1999.

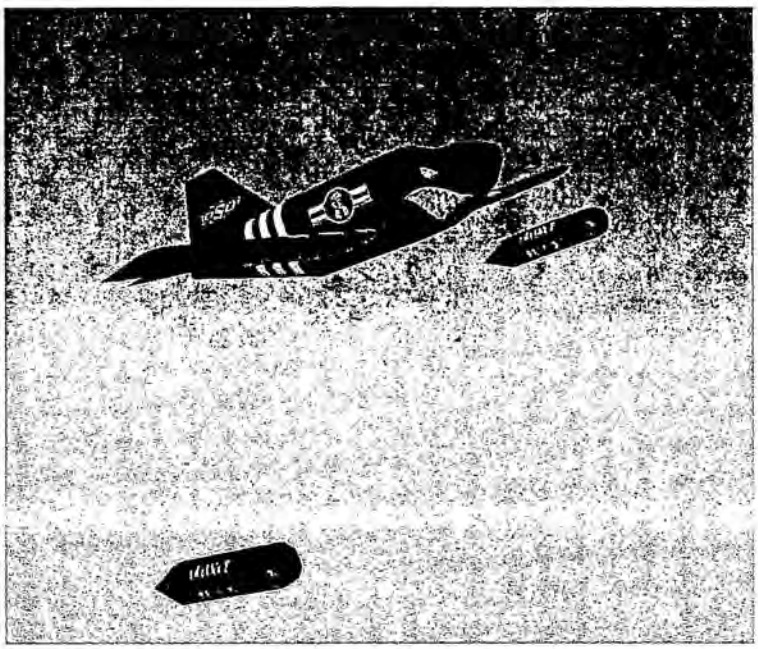

Cessna/ONR AIAA
Design Build Fly 2005

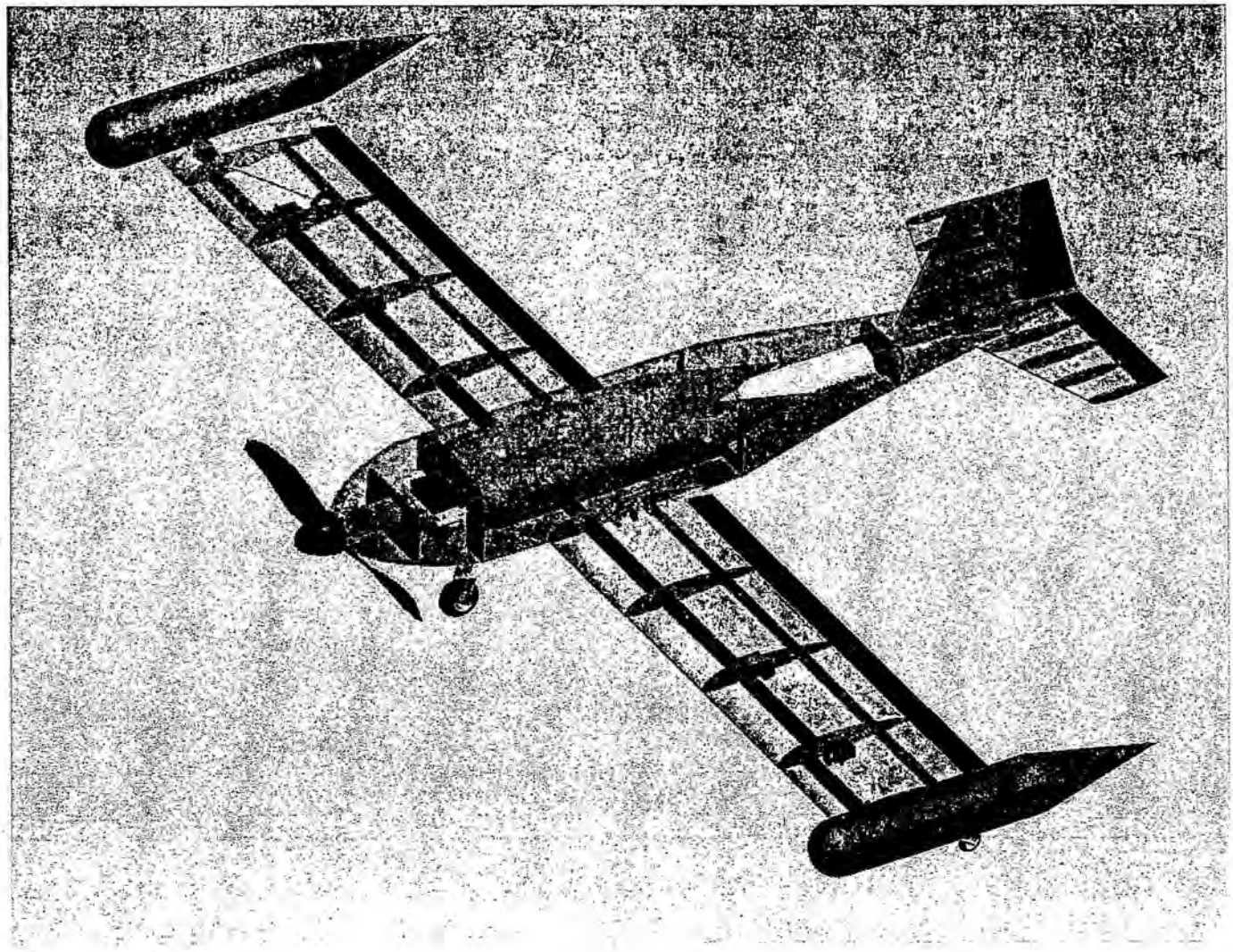

Oklahoma State University
Orange Team

March 5, 2005

Table of Contents

1.0 Executive Summary

This report details the design and construction development of a remotely piloted aircraft built for the 2005 Cessna/ONR AIAA Design/Build/Fly competition. The aircraft was optimized for two of three specified missions which included carrying, removing, and reloading internal and external 3-pound PVC pipe. The total score for the contest is a function of the report score, flight score, and rated aircraft cost.

1.1 Design Development

During the conceptual design phase, many different ideas were analyzed concerning the configurations necessary to complete the Sensor Reposition and Re-Supply missions with the optimal score. These ideas were studied by the Aerodynamic, Structures, and Propulsion Teams to determine the advantages and/or disadvantages for the respective group. Figures of merit (FOM's) were developed to determine the affect each of the parameters had on the overall completion and score of the missions.

The preliminary design phase consisted of detailed analysis of the conceptual configuration. The optimization code was set up to model the conceptual aircrafts mission profiles to determine the airfoil, wing area, wing span, and propulsion configurations. These models determined which criteria had the largest affect on the mission scores. Through iterations, the trade-offs between mission score and rated aircraft cost were analyzed to optimize the overall score.

The detailed design phase finalized all aircraft dimensions including structures, control surfaces, and propulsion systems. Wind tunnel tests were ran for a variety of propulsion configurations to optimize the mission profile. Finite element analysis was evaluated for the structures to determine the stress distributions for further refinement. Stability and control code was used to determine the optimal control surface sizes and study the dynamics of the aircraft throughout the missions.

1.2 Design Alternatives

Bearing in mind all aspects of the aircraft, many alternatives were considered for the basic design. The considerations for the body were conventional, flying wing, blended body, bi-wing, canard, and dual fuselage. Flying wing and blended body were quickly eliminated due to penalties in the RAC. The conventional body was chosen for easy payload incorporation and low RAC factors. Between high, middle and low wing placement, the low wing was chosen because of payload and center of gravity considerations. The traditional empennage was determined best due to manufacturing benefits and simplified servo installation. External and internal payload configurations were vital to this year's missions. A commercial bow release was chosen for the external payload attachment for its simplicity and weight. The internal payload arrangement will be a door/hatch with foam support. The plane disassembly will include wing release using a single spar and pin method. The landing gear configuration is a monocycle with outriggers setup, so that no further disassembly would be needed at the end of a mission. Pneumatic

brakes were chosen because they are more efficient than electric. The monocoque construction method was chosen for its high strength to weight ratio. The motor chosen was the Kontronic for its high efficiency.

1.3 Highlights

The first main stage in the design development was the conceptual ideas. These ideas were then compared using the FOM determined by the mission analysis. Once the conceptual design was narrowed, the Aerodynamics and Propulsion Groups used their optimization programs to investigate combinations within the conceptual design. This involved processing battery, motor, and propeller combinations at specific aerodynamic parameters, then handing aerodynamics back a series of more detailed inputs for their program. This iteration process brought the team to its preliminary design.

During the preliminary design stage Aerodynamics continued running various aircraft configurations to determine the optimal airfoil, wing span, wing area, and cruise velocities. The data collected allowed the team to select sizes for the aircraft which would optimize the score. The missions were also broken down and studied in segments to determine the battery usage, speed, flight times, and turning angles that would produce the highest score. This information was used in conjunction with tests conducted by the Propulsion Team to optimize the mission profiles. Using this information, static and dynamic tests were performed to predict the behavior of the aircraft throughout the missions. These tests ensured that the plane would be stable and easily controllable in all aspects of the missions.

Structures constructed a scaled down version of the fuselage to test the construction method. It was determined that the construction method would start with a foam core. From the foam core plugs would be created that could then be formed to molds. In the molds the skins of the aircraft would be constructed using fiberglass and balsa wood. Structures also determined the weight and location of all the components in the aircraft. The center of gravity and empty weight of the aircraft was estimated from these findings. The landing gear was better defined by setting the placement. The external payload release system was tested for reliability and the internal payload placement was determined.

A prototype was built to test the detailed design configuration. The major concerns for the prototype were battery life, landing gear configuration and external payload release reliability.

2.0 Management Summary

A project of this magnitude requires efficient planning. To organize the project tasks, each team member was put into a technical group and a detailed schedule was developed to track the progress of the project. The following describes the organization of the Orange Team and lists the responsibility of the personnel, describes the responsibilities of each technical group, and outlines the schedule that was developed.

2.1 Technical Groups Architecture

The design team was split into three technical groups: Aerodynamics/Stability and Control, Structures, and Propulsion. The project was assigned a Chief Engineer who managed responsibilities for the project. Additionally, each group was assigned a Lead Engineer to facilitate operations in their group and maintain communication between the other groups and the Chief Engineer. Figure 2.1 below shows the organization of the Orange Team and lists each team member and their responsibilities.

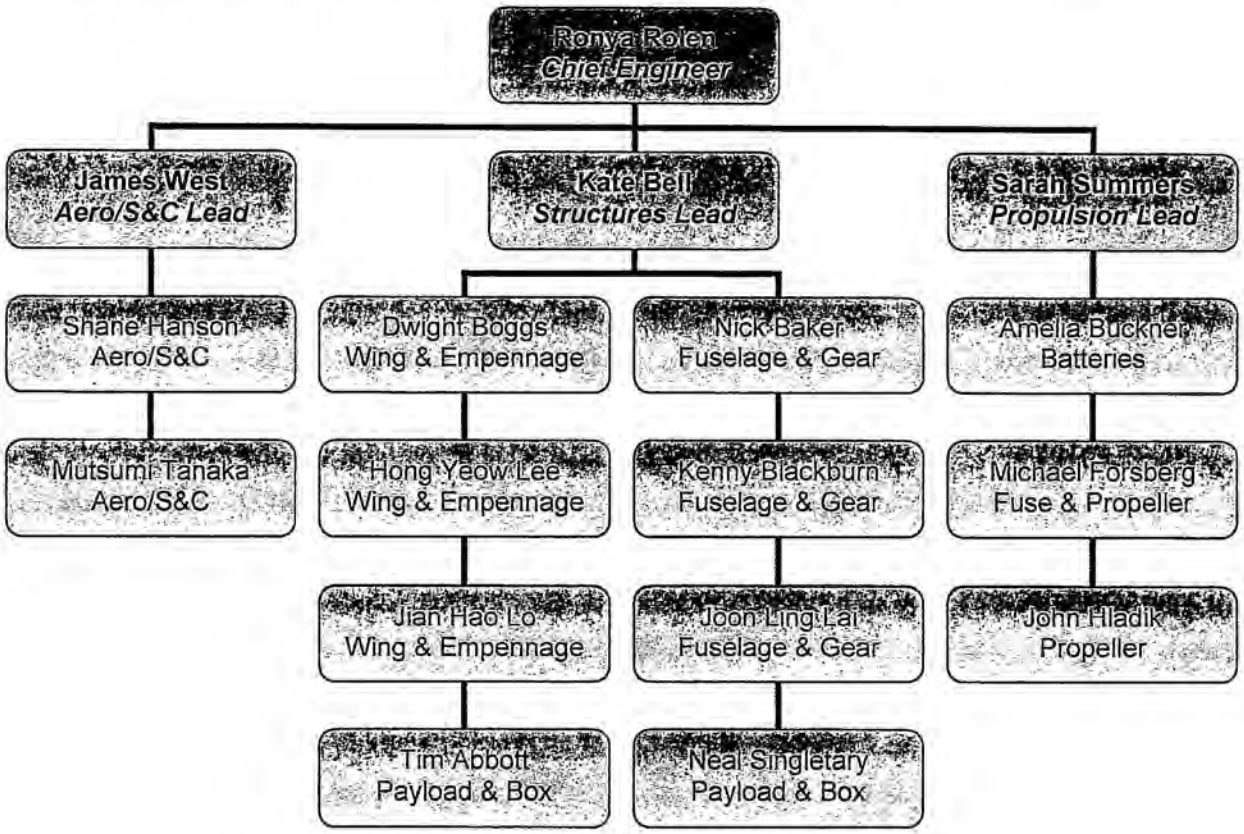

Figure 2.1: Orange Team Organizational Structure

2.2 Technical Groups

The Aerodynamics Group was responsible for all aerodynamic and stability and control design and analysis. For the conceptual design phase, ideas were sketched and considered with respect to the mission tasks. Tables were developed to examine figures of merit for important conceptual ideas such as aircraft design, wing placement, tail configuration, and landing gear setup. They also performed program analysis and sizing parameters for the final aircraft design.

The Structures Group was responsible for developing concepts pertaining to the payloads, construction methods, brakes, and the box design. In addition to sketches and figure of merit tables for the payloads

and box, they also researched construction methods and brake systems. They determined the final construction method and produced all of the 3-D drawings. This group also constructed the aircraft and tested all important structural components.

The Propulsion Group was responsible for researching motor, battery, propeller and gearbox configurations. They also decided the location of the motor and batteries, in conjunction with the Aerodynamics Group for center of gravity (cg) concerns. They performed propulsion tests and ran optimization code to choose the best propeller, motor, gearbox, and battery configurations possible.

2.3 Scheduling

This is an intense project with a rapid deadline for completion. To ensure the project completion meets the required deadline, a detailed schedule was developed. A Gantt chart was created to outline tasks pertaining to the design and manufacture of the airplane and the report writing. The following chart shows the key project tasks and their projected and actual time frames.

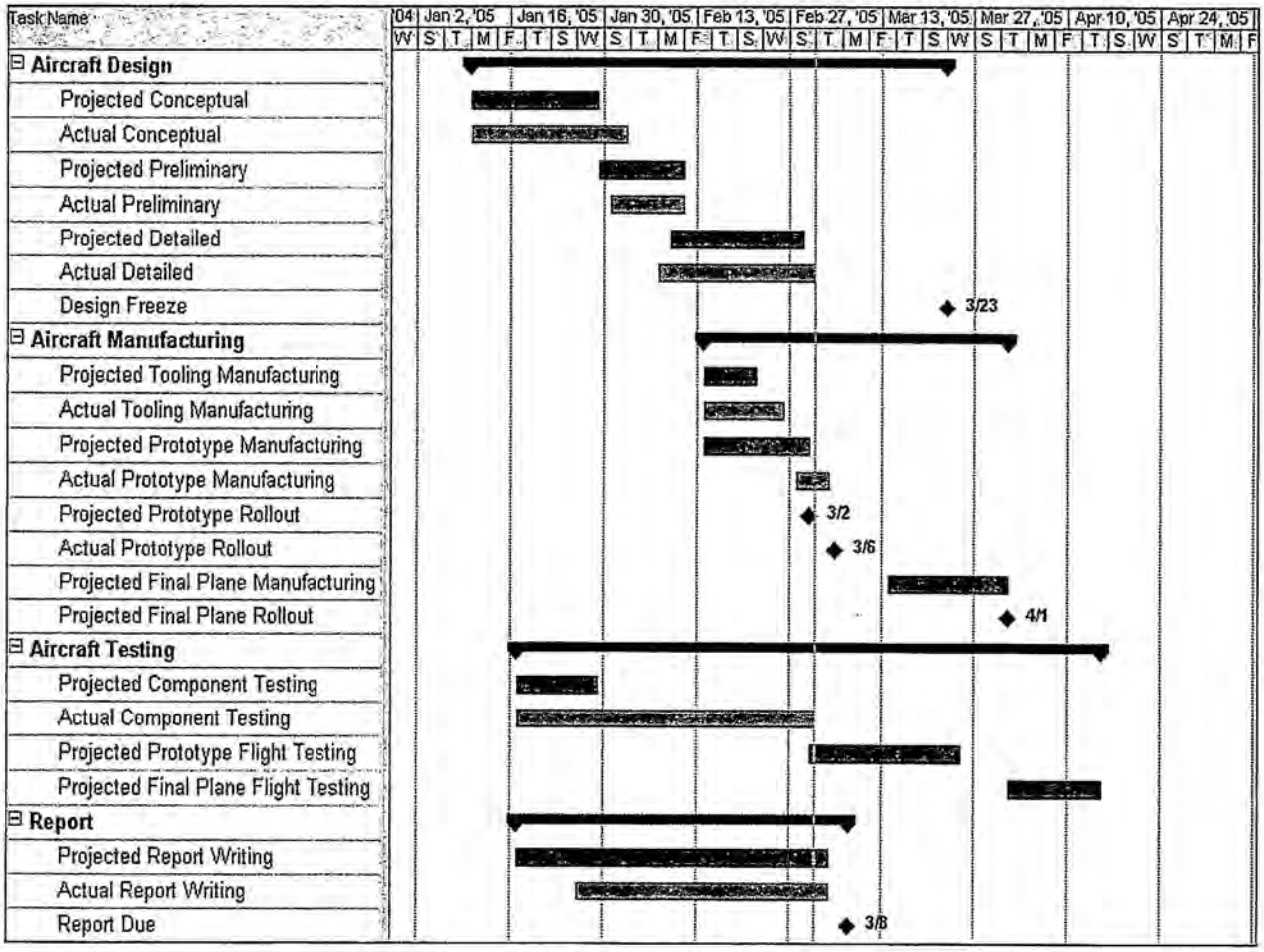

Figure 2.2: Projected Schedule

3.0 Conceptual Design

Once technical groups were assigned and a proposed project timeline was developed, the aircraft design began. The conceptual design phase provided many options for choosing an aircraft configuration as well as gear, wing, tail, and payload configurations. Each concept was examined using figures of merit, which were determined as the factors that most influenced optimal mission performance. To better understand how the figures of merit were chosen, the three missions are outlined below. All of the concepts described in this section were compared using figures of merit.

3.1 Mission Requirements

To win this competition the overall score must be maximized, which means that the RAC (Rated Aircraft Cost) must be minimized and the flight score must be maximized. The total weight of the aircraft cannot exceed 55 pounds, and the propulsion battery weight cannot exceed 3 pounds. Figuring into the RAC are the manufacturers empty weight, the rated engine power, and the manufacturing man-hours. The project goal is to design an aircraft capable of accomplishing two of three specified flight missions while optimizing each of the RAC factors and staying within the constraints. Each mission is described below.

- Sensor Reposition: Requires the aircraft to take-off and fly with the two external payloads, land, and then taxi to two release locations and deploy one sensor package at each location. The aircraft will then take-off and fly one more lap, taxi to a location near the first release location, and the ground crew will re-load the payloads. The aircraft will take-off and fly one more lap, land, and then be stored in the box. *The flight score is 2*(12 – mission time).*
- Maximum Utilization: The aircraft will contain the two internal payloads for this mission. The aircraft will take-off, fly as many laps as possible, land, and then be stored in the box in less than 6 minutes. *The flight score is 1* number of laps completed.*
- Re-Supply: The aircraft will initially contain the two internal payloads. The aircraft will take-off and fly one lap, and then the payloads will be removed. The aircraft will take-off and fly a second lap, and then the payloads will be re-installed. The aircraft will take-off and fly a third lap. Finally, the payloads are removed again and a fourth lap will be flown. Upon landing, the aircraft will be stored in the box. *The flight score is 1.5*(12 – mission time) for 4 laps completed, 1.5*(6 – mission time) for 3 laps completed, and 1.5*(3 – mission time) for 2 laps completed.*

It was determined that the aircraft would be optimized for the Sensor Reposition mission and the Re-Supply mission. Performing sample flight tests under certain aircraft conditions verified that the greatest flight score could be attained from these missions. As described in each mission statement, the mission does not end until the aircraft is securely shut inside a 4 by 2 by 1 foot box. This was heavily considered

during the design development of the aircraft since it is desired to complete the mission as quickly as possible.

3.2 Alternative Configurations and Figures of Merit

Each part of the aircraft had many possible configurations. For each section ideas are discussed and then compared using mission determined figures of merit. To compare the criteria, a numbering system was created. A notation of 1 is below average, 2 is average, and 3 is above average.

3.2.1 Aircraft Configurations

The first consideration was the basic body type of the aircraft. Various aircraft configurations were examined for the mission. To compare each concept, it was determined that the mission could be performed with external and internal payloads under the same operating conditions. Each alternative is listed below along with a description of benefits and/or disadvantages.

- Flying Wing: Due to the complication of the design and the way the RAC is calculated for flying wings, the team decided that this configuration would not be a good choice. This design could have been disassembled quickly for storage in the box; however, the complexity of the molds needed to construct this design and the stability and control problems that would be inherent with this type of aircraft outweighed the benefits.
- Blended Wing Body: The need to disassemble the aircraft very rapidly was a major factor when evaluating this design. In order to receive the benefits of a blended wing body, the complexity of construction would have been enormous. The penalty received in the RAC for the fuselage width was also a discouraging factor.
- Bi-plane: A bi-plane was considered to reduce the span required to produce the necessary lift to carry the payloads. The major deciding factors were the excess drag of the design, the time it would take to disassemble the extra components, and the inaccessibility to the internal payload. The bi-plane would also increase the RAC.
- Canard: Since the internal payloads had to be placed in close proximity to the external payloads to avoid center of gravity problems, the canard design did not seem very feasible.
- Dual Fuselage: The ability to slide the payloads into the "tube" structures of each fuselage was an appealing idea. However, the complexity of the structure and the number of components to disassemble and fit into the box was a major downside to the design.
- Conventional: This configuration can be easily manipulated to allow payload placement without sacrificing drag or RAC score. The design is proven to be effective based on past competitions.

The overall aircraft configuration was determined using a FOM (Figure of Merit) table as shown in Table 3.1 below. The FOM's are defined as:

- Rated Aircraft Cost: The aircraft configuration has a great effect on the RAC in both the Manufactures Empty Weight as well as the Manufacturing Man Hours.
- Takeoff Distance: Aircraft must be able to take off within 150 feet. The shorter the takeoff the distance the better the flight score.
- Handling Qualities: To reach the best score possible the aircraft must handle well for the pilot on the ground and in the air.
- Drag Efficiencies: The drag should be at a minimum for maximum efficiency and endurance.

							
Figure of Merit	Weighting Factor	Conventional	Flying Wing	Blended Wing Body	Bi-Plane	Canard	Dual Fuselage
RAC	0.33	2	3	1	1	2	1
Takeoff Distance	0.26	2	2	2	3	1	1
Handling Qualities	0.26	3	1	3	2	2	1
Drag Efficiencies	0.15	2	3	3	1	2	1
Total	1	2.26	2.22	2.08	1.78	1.74	1

Table 3.1: Aircraft Configuration Figures of Merit

3.2.2 Wing Configurations

Once a conventional aircraft configuration was chosen, wing placement was examined. Each consideration is detailed below.

- High Wing: A high wing placement was first looked at as an easy way to gain roll stability without sacrificing ease of construction. The disadvantage to the high wing placement is that the internal payload would be forced to sit under the wing, making it difficult to access. For any mounting position the wing spars would have to travel the entire width of the fuselage to give the wing the strength needed. This means that the internal payload would have to sit under the spars and removed either through the side of the fuselage or behind the wing.
- Middle Wing: This wing placement is more neutral in regards to roll stability. While this is not necessarily a bad thing, the spar placement through the middle of the fuselage makes the internal payload placement very difficult. This is a result of the variation of center of gravity placement of the unloaded airplane and the airplane with added payload. The center of gravity needs to be the same with and without the payload so that when the payload is removed it

does not shift forward or aft. Therefore, the wing spars will travel directly through the location needed for the payload, which is not acceptable.

- Low wing: While the low wing placement is much worse than the high wing in terms of roll stability, payload access and placement is much easier. The internal payload is allowed to sit above the wing structure making it more accessible in removal. This is much easier than having to go around the wing or behind the wing as is necessary with the high wing placement. Also, the center of gravity can be set lower on the plane because of the wing's weight being lower. Because of this ease and the ability to get roll stability by other means if necessary the low wing placement was chosen.

By examination of the figures of merit shown in Table 3.2, the low wing configuration greatly outweighs the high or mid wing. The low wing is best for this mission because of its superior ground handling and its lack of interference with the payloads—both external and internal.

The wing placement was determined using a figure of merit table as shown in Table 3.2 below. The FOM's are defined as:

- Payload Interference: For the Maximum Utilization and Re-Supply Missions the internal payloads are installed and need to be accessed. Any interference between the payloads and the wings would increase the time needed to remove the payloads.
- Flight Stability: The 360 degree turns and multiple take off and landing procedures cause a need for good flight stability. The aircraft must be as efficient in the air as it is on the ground to quickly and efficiently complete the missions.
- Ground Stability: A large amount of time will be spent on ground handling maneuvers; therefore the ground stability of the aircraft must be high and reliable.
- Ease of Construction: Although not as important as the others, construction will take time and skill from the Structures team. A design that is both stable and simple will be best.

Figure of Merit	Weighting Factor	High Wing	Mid Wing	Low Wing
Payload Interference	0.3	2	1	3
Flight Stability	0.2	3	2	1
Ground Stability	0.4	1	2	3
Ease of Construction	0.1	2	1	2
Total	1	1.8	1.6	2.5

Table 3.2: Wing Placement Figures of Merit

3.2.3 Empennage Configurations

After choosing the wing placement, the next step in deciding the basic configuration of the plane was to look into different empennage setups.

- V-Tail: By looking at the RAC calculations for the empennage, one can see that the number of control surfaces adds to the cost of the plane. Therefore the V-Tail configuration was looked at as a means of reducing the control surfaces and ultimately cost. This configuration creates problems in control; by not having a committed vertical stabilizer, a servo won't be available to drive a tail dragger if that landing gear is chosen. In this setup neither stabilizer can be added to the fuselage mold, meaning that instead of having to add one control surface to the fuselage both would have to be added. While there may be slightly less drag off of a V-Tail setup and a very small reduction in RAC, the reduced effectiveness, addition of a designated servo for landing gear control, and construction difficulties over-shadowed those advantages.
- T-Tail: The T-tail setup allowed for an increase in effectiveness of the horizontal stabilizer by getting it out of the wake of the low mounted wing. The drawback of this placement is the increase in construction difficulty by mounting the control surface so far away from the fuselage, in that the vertical stabilizer would have to be part of the mold or both would have to be added to the fuselage after it has been built, similar to the V-Tail construction problem. This also slightly raises the center of gravity by adding weight high on the plane.
- Cruciform: This tail configuration is a slightly less effective version of a T-Tail. The horizontal stabilizer is mounted approximately half-way up the vertical, keeping it slightly above the wing, but not as far from the wing as the T-Tail, meaning it is still more effective than a traditional placement but not as much as a T-Tail. The construction of the empennage would be the same for the Cruciform configuration as it would be for the T-Tail. Because the horizontal surface goes through the middle of the vertical stabilizer the vertical would be made as part of the fuselage while the horizontal would be an added on surface.
- Traditional: The traditional placement was chosen to allow for a servo strictly driving the rudder in case a tail dragger landing gear was used. This allows for the same servo to control the tail wheel and the rudder. The construction is also easier for a traditional setup, because the mold for the fuselage can also include either the vertical or horizontal stabilizers depending on how the width and height compare. While the effectiveness of the horizontal stabilizer is slightly reduced, it has been decided that this will be only a slight reduction and will not be significant enough to warrant the more difficult construction needed for a higher mounted horizontal surface.

The tail configuration was determined using a figure of merit table as shown in Table 3.3 below. The FOM's are defined as:

- RAC: The tail configuration also has an effect on the Manufactures Empty Weight and the Manufacturing Man Hours. A tail that can be very light will be best.
- Drag Efficiencies: Minimal drag is needed to keep the endurance at a maximum and the take off distance at a minimum.
- Construction: It needs to be simple and quick to produce to keep on schedule.
- Effectiveness: The tail must be able to provide the control needed both in flight and on the ground.

Figure of Merit	Weighting Factor	Conventional	T Tail	Cruciform	V Tail
RAC	0.3	2	2	2	3
Drag Efficiencies	0.3	3	2	2	2
Construction	0.2	3	2	2	2
Effectiveness	0.2	2	3	2	1
Total	1	2.5	2.2	2.0	2.1

Table 3.3: Tail Configuration Figures of Merit

3.2.4 Payload and Payload Release Configurations

For the payloads the placing of the weight was an issue. If the weight was completely centered, the payload could end up rolling out of the 10 by 10 foot box. An idea to place the center of gravity near the front or on the bottom of the payloads was considered to keep the payloads from rolling out of the box and to keep the weight closer to the center of gravity of the whole plane.

External Payloads

For the external payloads there were a few designs that dealt with having the payload drop from the bottom of the wing. Having the payload under the wings meant they could drag on the ground with a tail dragger configuration and would cause the vertical center of gravity to change. The external payload releases for the plane should be very easy to install so that the time building the plane is kept to a minimum. It should also work quickly and reliably for 100 percent of the time so that the mission time is reduced and the score is maximized. The release should be light weight but very strong so that the payloads do not fall off the plane in mid-flight.

- Claw Release: The claw release mechanism was a good idea because of its reliability. However, a claw would be heavy and complicated to get the claw fingers to work in unison. Also, when not flying the external payload mission, the claw would be jutting out into the airflow causing unnecessary drag.

- Bow Release: The bow releasing mechanism seemed to be the best pick for releasing the payload on the side and top of the wing. The bow release works reliably and has a very good strength to weight ratio. One problem with the bow release is that it must have pressure on it in order to release. Also, it only attaches to the payload at one point, which means it would wobble in flight. Two ideas were formed to counteract this. First, springs could be used to secure the payload by providing constant pressure, acting through holes inside the wings. Rods attached to the payload would slide into these springs. Another idea was to use compression foam. This would be much easier to attach than the springs and would securely hold the payload in place.
- Cabinet Release: The cabinet release for the external payloads uses a simple device that most cabinets have to keep them closed. The device has a male and female end. The female end has rollers that roll around the male end and secure the payloads. The male end is on the payload and the female is inside the plane. A servo would need to push the payloads away from the plane and the payloads would fall away.
- Ice Cream Cone Release: The ice cream cone release works just like a kid's toy. It has a clamping system where a circular rod has a lip on it which clamps with another lip. The lips latch together by frictional forces due to an induced load. The simplicity of the clipping mechanism is an advantage; however, it would have to be manufactured and its holding strength may not be sufficient for 6 pounds.

The external payload release was determined using a figure of merit table as shown in Table 3.4 below. The FOM's are defined as:

- Reliability: This release will be used extensively in flight testing and during the competition. It must stand up to repeated usage without failure.
- Simplicity: Needs to be easy to install and replace if necessary. Also, a simple release mechanism will allow for quick release and re-attachment, thus reducing overall mission time.
- Weight: The weight goes into the RAC and must be kept to a minimum to optimize the overall score.
- Holding Strength: Must keep the payloads in place on the wing tips until it is time to release them.

		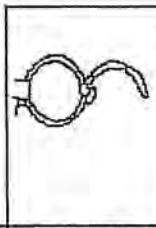	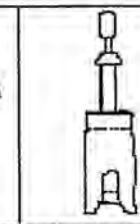	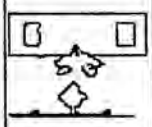		
Figure of Merit	**Weighting Factor**	**Claw**	**Bow Release (with springs)**	**Cabinet**	**Ice Cream Cone**	**Bow Release (with compression foam)**
Reliability	0.4	3	2	1	2	2
Simplicity	0.2	1	3	3	2	3
Weight	0.3	1	3	3	2	3
Holding Strength	0.1	2	3	1	1	3
Total	1	1.9	2.6	2	1.9	2.6

Table 3.4: External Payloads Figures of Merit

Internal Payloads

It is desirable for the internal payloads to be as far forward inside the fuselage as possible and be quickly removable during the competition. The payloads need to be connected together so they can be removed in one fast motion. The ideas considered ranged from a side or top door entrance to a fully removable box. The internal payloads need to be secured inside the plane so that the weight does not shift around. The system holding the payloads needs to be light weight, strong, and simple to build.

- Removable Box: This idea involved the two payloads being inside a single box to ease removal. A removable box is beneficial in that it is reliable and simple to move the payloads in and out. The only problems come about for these reasons. The problems are that it will need a lot of structural support which equals a lot of weight and pulling the box out and putting it back in takes a lot of time. One addition to the removable box is a VCR door. Instead of having a whole section come off of the plane, the payloads would be loaded through a door that would move like a VCR door. The door would move out of the way of the box and the door would fall down when the box is removed. However, this would not be easy to construct and would have added weight due to the box and the VCR-type doors.
- Dual Fuselage: This was a concept to have a fuselage for each of the payloads. This idea seemed good at first but having two different fuselages increases the difficulty in building the aircraft. The RAC would be maximized and two people would have to remove the internal payloads instead of one, thus increasing the total mission time.
- Removable Payloads with Clips: The removable payloads with the clips was a system related to a fuse box where a clip secures a fuse, but in this case a clip secures the payloads and can be removed quickly when a door is removed. The clips are very reliable for holding the

payloads secure and are very light weight. The disadvantage is that the clips would be difficult to manufacture and install.

- Removable Payloads with Door/Hatch: The removable payloads with a door/hatch would have the bottom of the internal device formed to the shape of the payloads. The top of the payloads will have a rib of foam between them. The door with a hinge will be opened from the back to the front so that the RAC will be less than the removable box idea. The cabinet release idea for the external loads will be the latch used for the door. The reliability of the system is very good because nothing inside the plane has to be removed or disengaged to release the payloads.

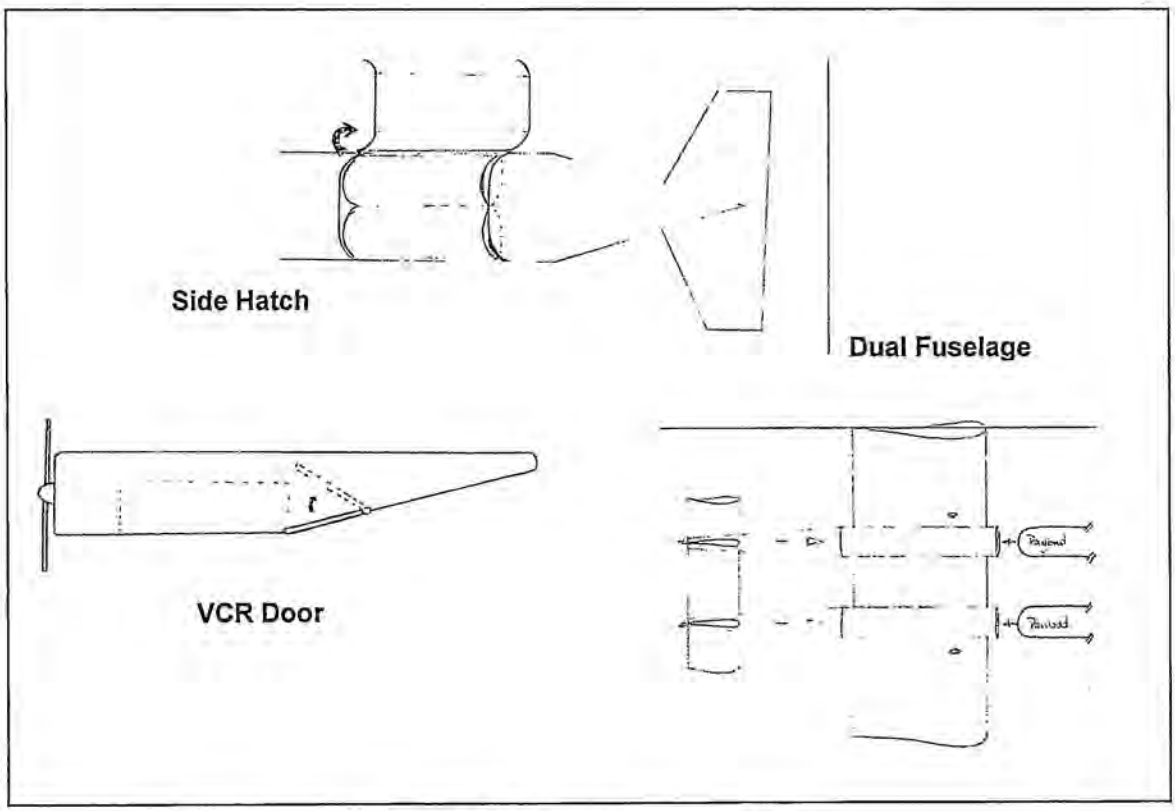

Figure 3.1: Internal Payload Ideas

The internal payload release was determined using a figure of merit table as shown in Table 3.5 below. The FOM's are defined as:

- Reliability: Similar to the external payloads, this release will be used very often and cannot fail. The hinge for the hatch must be strong and be able to withstand multiple openings and closings.
- Simplicity: For ease in construction and quickness the latch needs to be simple; every second counts in the flight missions, so simplicity can greatly increase the overall score.

- Quickness: The payloads need to be removed in the least amount of time possible for efficient missions.
- Weight: Every ounce increases the RAC, so the weight needs to be at a minimum.

Figure of Merit	Weighting Factor	Removable Box (with removable door/hatch)	Removable Box (with VCR door)	Dual Fuselage	Clips	Door/Hatch with Foam Support
Reliability	0.4	3	2	1	3	3
Simplicity	0.1	3	1	1	1	2
Quickness	0.3	1	3	2	2	2
Weight	0.2	1	1	3	2	2
Total	1	2	2	1.7	2.3	2.4

Table 3.5: Figures of Merit for Internal Payloads

3.2.5 Plane Disassembly Configurations

Wing attachment is crucial for this competition because of the time constraint. The aircraft must be disassembled and placed in the box in the shortest amount of time necessary. It was determined that the wings must be removed for the aircraft to fit into the box. There were four concepts evaluated for the wing attachment.

- Dual Spars: The first idea was using dual spars that would extend out of the wing into the fuselage. The main problem with this attachment would be payload interference. However, the reliability, weight, and aerodynamics would be great for this idea.
- Forks: Another consideration was using a fork to hold the wings in place. The wings would be fitted into the fuselage slightly and a fork inserted from the top to hold the wings on. The disadvantages include manufacturing complications, decreased reliability, and increased weight.
- Folding Wings: One more idea was for the wings to not detach at all, but instead would fold up. This would be great for payload interference, but the reliability, weight, and aerodynamics would be poor. Also, the construction for this type of wing would not be easy.
- Single Spar: An alternative to the dual spars would be to use only one spar. A pin could be used in conjunction with the spar to stop rotation. A single spar would eliminate interference with the payload given that a low wing placement was chosen. Since a single spar would also make disassembly much easier and quicker, it was evaluated to be the best design.

The wing attachment was determined using a figure of merit table as shown in Table 3.6 below. The FOM's are defined as:

- Payload Interference: Release of the payloads, both internal and external, is imperative to the missions; therefore there should not be any interference between the wing attachments and the payloads.
- Reliability: The wings must be detached multiple times from the aircraft. Keeping the method simple and using strong material will increase reliability, thus increasing the overall score.
- Weight: Figures into the RAC and needs to be a minimum. Choosing a wing attachment that is light weight will increase the overall score.

		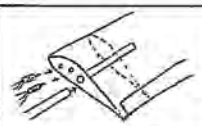			
Figure of Merit	**Weighting Factor**	**Single Spar with pin**	**Dual Spars**	**Fork**	**No Detachment Folding Wings**
Payload Interference	0.3	1	1	1	3
Reliability	0.4	3	2	2	1
Weight	0.3	3	3	2	1
Total	1	2.4	2	1.7	1.6

Table 3.6: Wing Attachment Figures of Merit

3.2.6 Landing Gear Configurations

Choosing the right landing gear for this mission required investigation of many concepts. Carrying a 3 pound load within 3 inches of each wing tip is not an easy task. Stability of the aircraft had to be examined closely. The concepts that were considered are described below.

- Tricycle gear: This type of landing gear has good stability and landing performance, but weighs more than desired. Another disadvantage of this landing gear type is that it makes the task of fitting the aircraft in the box very difficult. Due to the spacing that the main gears would require to avoid tipping, ground stability would suffer.
- Tail Dragger: This configuration is not very stable on the ground, with the two-wheel setup towards the front of the fuselage. Due to the wide wheel spacing, his type of landing gear also has the disadvantage of increasing the difficulty to fit the aircraft in the box.

The next concept was to add outriggers to the aircraft. This idea increases the ground stability and helps offset the unstable wing load. With this idea, two configurations were analyzed: a monocycle and a bicycle.

- Monocycle with Outriggers: This setup is similar to a tail dragger, with only one large wheel near the front/center of the fuselage. This landing gear configuration is light weight and has

good predicted stability. This configuration is also the best choice for fitting the aircraft in the box, as no modifications will be needed.

- Bicycle with Outriggers: This landing gear setup is another option to improve aircraft stability. This landing gear consists of a bicycle-type gear, equipped with outriggers. Similar to the mono with outriggers, the bicycle has good stability and landing performance. However, this configuration makes it harder for the aircraft to fit in the box. Depending on the propeller size, no modifications may be needed. In the event that the propeller size causes the front gear to be too long, a wheel can be found that will disconnect from the gear shaft, giving extra clearance.

The landing gear configuration was determined using a figure of merit table as shown in Table 3.7 below. The FOM's are defined as:

- Stability: With all of the ground maneuvers needed, the gear needs to be stable while moving at slow speeds with an unstable wing loading as well as take off and landing speeds.
- Landing Performance: The gear needs to keep the aircraft straight during landing and be able to withstand heavy loading on impact.
- Weight: Needs to be as light as possible without changing the center of gravity.

Figure of Merit	Weighting Factor	Mono with Outriggers	Bicycle with Outriggers	Tail Dragger	Tricycle
Stability	0.4	3	3	1	2
Landing Performance	0.3	2	3	2	3
Weight	0.3	3	2	2	1
Total	1	2.7	2.7	1.6	2

Table 3.7: Landing Gear Figures of Merit

Based on the figures of merit alone, a gear setup with outriggers was chosen. The mono with outriggers was chosen because of the reduced drag effect and ability to fit the aircraft in the box easier than the bicycle configuration.

3.2.7 Brakes

Brakes are very important to this mission because a large amount of time will be spent on the ground. From electric to disc, brakes come in many different forms and therefore were scrutinized to attain the best choice. Research of current brake systems available—detailed below—proved valuable in findings.

- Electric: About 1.5" in diameter, this brake appears to have a simplicity factor as well as a reasonable price. The stopping speed of this break is known to perform well at low speeds,

but at higher speeds the brake would need to be tested. Also, the stopping speed will be determined by the number of wheels that have brakes. The price of these brakes is much cheaper than most other types.

- Pneumatic: Another option would be to use pneumatic brakes. These brakes use compressed air that swells a bladder between the tire and wheel. One advantage of pneumatic brakes is the braking speed. The disadvantage is the amount of room the air tank and equipment consume in the fuselage.

Pneumatic brakes were chosen because of their reliability and proven effectiveness. The setup is not complicated and their operation is simple.

3.2.9 Propulsion System

The propulsion system configuration was examined to determine the best motor and propeller selection. The following combinations were considered:

- Dual Motor and Propeller: This configuration would be useful for a dual fuselage configuration, but otherwise is not necessary as this much power would be excessive for the chosen flight missions, which would increase the RAC.
- Single Motor and Dual Propeller: Produces a lot of thrust, but will increase RAC.
- Single Motor and Propeller: This configuration is the best solution for a low RAC and required thrust.

The propulsion system was selected based on the criterion below.

- RAC: The RAC is partially a function of the propulsion system and should be minimized.
- Weight: As on all aircraft, weight is an important factor for aircraft performance and should be minimized as well.
- Efficiency: The efficiency should be as high as possible in order to maximize the battery life and obtain the maximum performance.

Figure of Merit	Weighting Factor	Dual Motors/Propellers	Single Motor, Dual Propeller	Single Motor/Propeller
RAC	0.4	2	3	3
Weight	0.3	1	2	2
Efficiency	0.3	1	1	2
Total	1	1.4	2.1	2.4

Table 3.8: Propulsion System Figures of Merit

From this selection the Propulsion Group researched motors, batteries, and speed controllers to fit the conceptual design. Conceptual ideas for disarming the propulsion system were also developed.

- Motor and Speed Controller: Three motors were investigated: Kontronic Fun 600-18, Graupner Ultra 3300-7, and MaxCim N32-13D. Once a motor is chosen, the various gearing ratios for that motor are investigated. The speed controller matches the motor chosen.
- Batteries: Research was performed to examine the difference between NiCad and NiMH batteries. Next, it had to be determined what battery sizes are required.
- Component Placement: The motor will be located in the nose of the aircraft with the propulsion system batteries close behind it. It is desired to keep the center of gravity forward, so the batteries will be as far forward as possible to accommodate the airplane aerodynamics.
- Fuse Design: The fuse will be placed in the nose of the aircraft near the batteries and motor. This allows for a simple wiring system and thus fewer losses.

3.3 Conceptual Summary

The overall airplane design was determined during the conceptual design phase by considering the mission characteristics and the size limitation of the box, 4x2x1 foot, as shown in Figure 3.2. The fuselage size was decided based on the size of the payloads and other components essential to the configuration used.

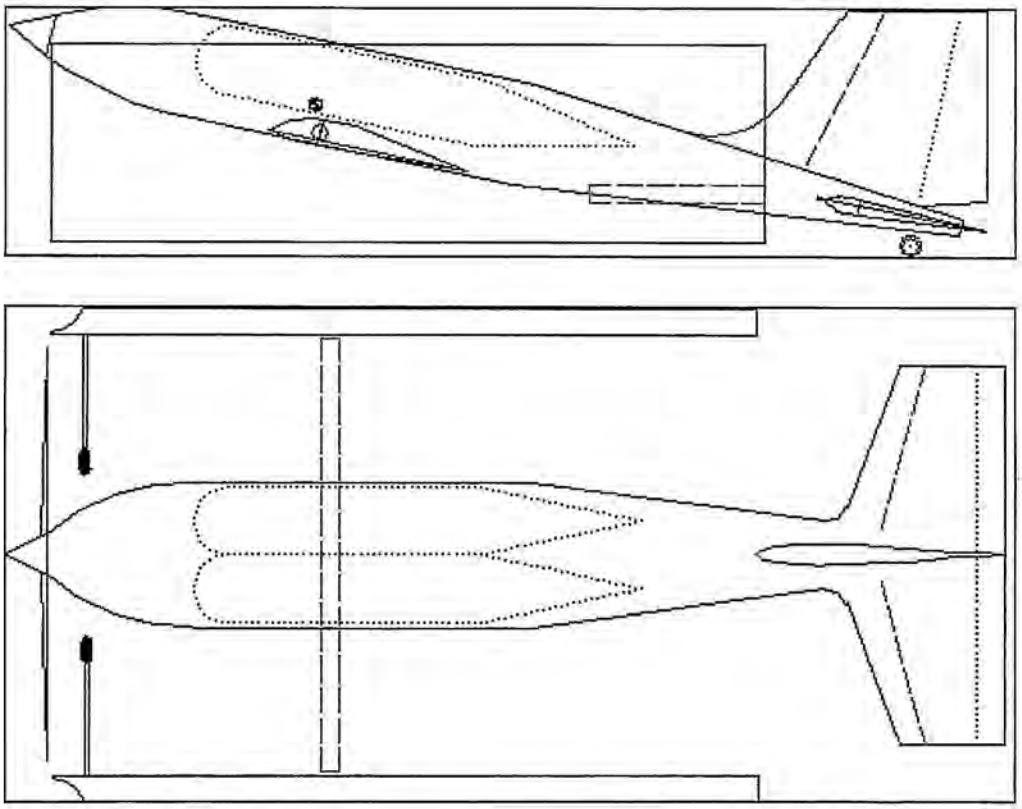

Figure 3.2: The Airplane from the Conceptual Design

The final concept design of our aircraft is a conventional body with low wing and a conventional tail. The landing gear will be the mono with outriggers, due to ease of manufacturing, and include pneumatic brakes. The external payloads will be released using a bow release with compression foam and the internal payloads will be removed using a door/hatch with foam support. The plane disassembly will include a single spar with pin set up. Figure 3.3 shows the final conceptual design.

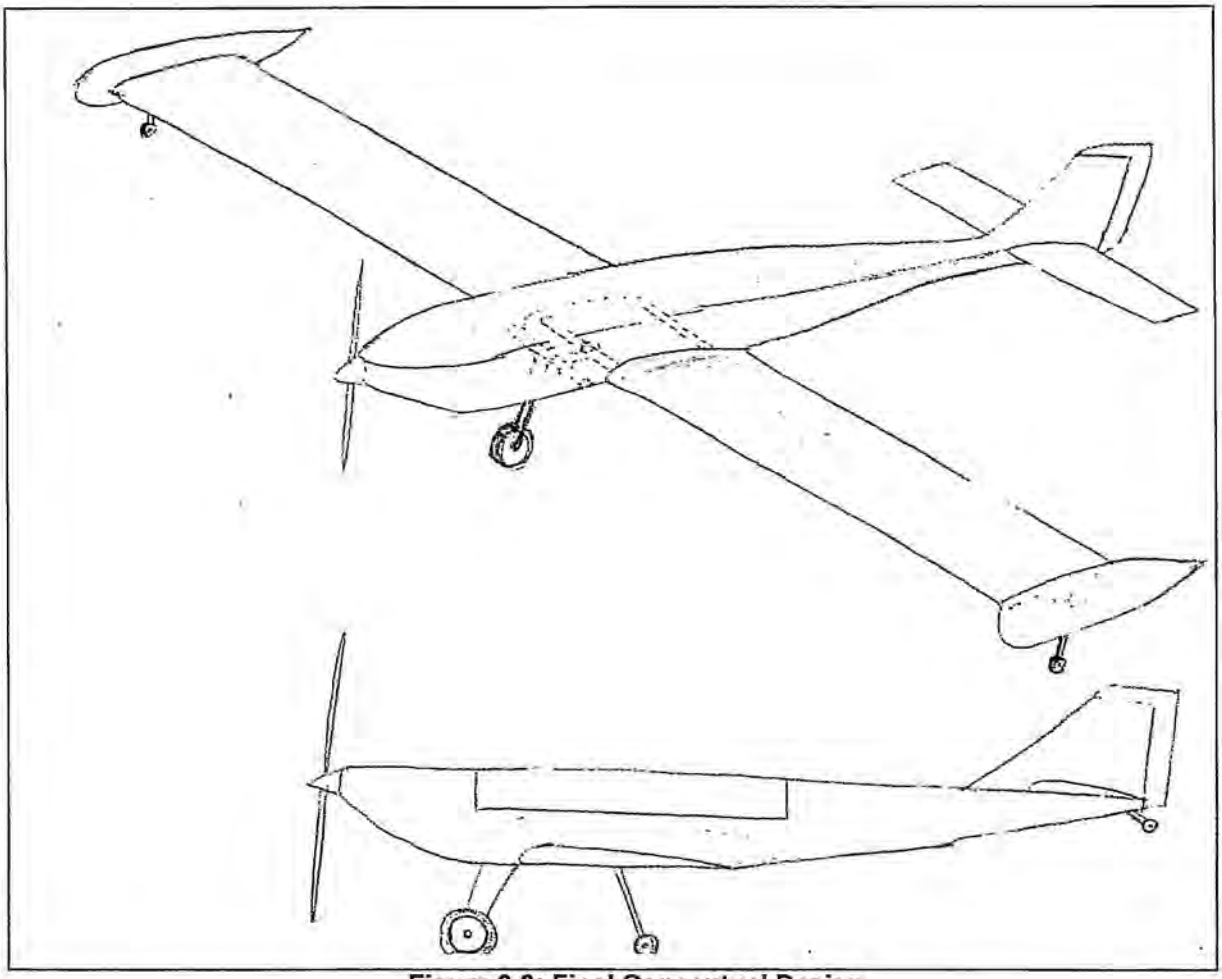

Figure 3.3: Final Conceptual Design

4.0 Preliminary Design

After the conceptual ideas were compared using the figures of merit and designs were chosen, the aircraft and all components had to be optimized for the Sensor Reposition and Re-Supply missions. The parameters with the greatest influence on score were examined and trade studies were performed to arrive at the optimal design.

4.1 Parameters and Sizing Trades

The most important aspects of the design were each separated between the technical groups in charge of the overall airplane design. The Aerodynamics Group investigated the fuselage length and empennage sizing, the wingspan and area of the specific airfoil. The goal was to have as small an aircraft as possible to accommodate the internal components, but be stable enough to successfully complete the missions as quickly as possible.

As a result, the Aerodynamics Group investigated the effects of the following parameters:

- Fuselage Length: The fuselage length could be determined by the requirements of the internal components and structure.
- Wing Span/Area: The optimum wing area needed to be found to ensure payload carrying capability. The minimum lifting surface required to meet the takeoff distance requirement could be used so long as it meets propulsion capabilities.
- Battery Selection and Quantity: A low number of batteries would decrease RAC. However, depending on the capacity, a low battery cell count may not complete the mission. Batteries of different capacity and cell count need to be tested to determine the best trade-off.
- Propeller Size and Pitch: The propeller size affects the ability of the aircraft to fit in the box, in addition to the more important factor of required thrust. The propeller selection will have to be tested to determine trade-off between takeoff and flight performance.

4.2 Refined Mission Modeling and Optimization

Once the trade-off factors were determined, analysis and optimization began. Two computer programs were written to optimize most important parameters to the design. The following sections describe the aerodynamic and propulsion programs.

4.2.1 Mission Profile Optimization Analysis Program

An optimization code was used to analyze the most difficult mission, the Sensor Reposition, which is also the mission that is potentially worth the most in the competition. Due to the similarity between the Re-Supply and the Sensor Reposition mission, it was determined that if the airplane was optimized for the mission with the higher number of laps, then the plane will be very close to the optimal design for the simpler mission as well. With the two missions so similar and the Maximum Utilization, the second mission, being completely different, it was decided that the first and third missions would be the ones primarily designed for with the second mission not being relied on for a high score.

The optimization code was used to predict the highest score possible and the trends for obtaining high scores by varying parameters such as airfoils, efficiencies, drag models, and wind conditions. The program would only give scores if the plane was able to finish the mission profile being run. From the aircraft details given by the optimization program the Aerodynamics and Propulsion Teams worked in unison to make sure that all of the results were obtainable from a propulsion aspect. The initial runs were done using rough approximates for different propulsion efficiencies, providing the plane design in terms of needed power, wing dimensions, and cruise velocities. These numbers were then given to the propulsion team to find more accurate efficiencies, which were then used to update the airplane's design.

A few of the aspects that the program included are as follows:

- Time and power needed for 150-foot takeoff distance
- Time and power used in cruise, both with and without the payload
- Elevation at the first pylon
- Percent of battery power used for the mission
- Sensitivity to wind and weight for takeoff
- Time and distance to stop upon landing
- Climb rate and turning distances

The optimization program would "guess" an initial condition and then from the guess it would find a local maximum score and output the conditions that provided that score. Historical data and rules limits were set to limit the range that the program would output in its search for the maximum score for each run. For the program to calculate all of the needed information about the aircraft it had to estimate values for weight, drag, propulsion factors, and RAC.

- Weight Model: This model took historical data for the construction method used and set the total empty weight as a function of wing area. This helps account for changes in aircraft weight from changes to the wing size.
- Drag Model: The drag model allows for an overall parasite drag value to be input, and calculates the induced drag from the chosen airfoil and aspect ratio. To make the model more accurate the program also calculates the Reynolds number at takeoff and in cruise.
- Propulsion Model: The propulsion team has a much more accurate model, but the aerodynamics optimization and analysis programs also had a propulsion model that was a simplified version. This model would calculate the takeoff thrust and the power required for cruise and takeoff.
- Rated Aircraft Cost Model: The program calculates the RAC using an assumed number of servos, and control surfaces, as well the given wing sizes and battery weight as information from the weight model.

4.2.2 Propulsion Program Analysis

A program was used to do preliminary analysis and selection for the propulsion system. This program uses previously input experimental propeller information along with user supplied information on propeller diameter, motor characteristics, battery characteristics, and flight speed. From this data the program outputs efficiencies, thrust, takeoff distance, current and voltage used, as well as several other useful values. For optimization, the aerodynamics group provided a list of likely airfoil types, wing spans, wing areas, and speed ranges. From this information tables were compiled of data required by the

Aerodynamics Group such as efficiencies, thrust, and batteries required. With this information the Aerodynamics Group sized the wing and selected the flying speed based on optimizing the possible score.

Using the complete aerodynamic data, the Propulsion Group optimized the propeller, gearbox, and battery combinations for the desired range. With this information it was determined that the propulsion system must develop approximately 4.6 pounds of thrust to take off in the required distance. To meet this requirement, fourteen to sixteen inch propellers with the Kontronic 600-18 motor and twelve to fourteen batteries were examined with the propulsion program.

- Battery Model: Using manufacturer's data for multiple styles of NiCad and NiMH batteries, trends were found from the propulsion model program. The type of battery and number of cells were varied within the program to produce realistic performance characteristics.
- Propeller Model: Data runs were performed with a range of propellers with diameters from fifteen to twenty inches with varying gear ratio and number of battery cells to create the necessary thrust required for takeoff while maintaining the maximum current allowed. The parameters the propulsion system designed for are a flight speed of 80 feet per second, power of 400 watts, and propeller efficiency of 65 percent.

The propulsion model program was used for initial decisions concerning the propulsion system. The aerodynamics program was used in conjunction with the propulsion program to determine an optimal range of values for airplane sizing parameters as well as propulsion components.

4.3 Optimization

Using an optimization code, the mission profiles were evaluated to determine the aircraft components which would maximize the score. The following sections discuss the airfoil selection and wing sizing results of the code.

4.3.1 Mission Profile Program Results

Several graphs for each airfoil were created after the data was collected comparing the five parameters with the score that was found for each potential airplane design. The airfoils that were chosen for further evaluation included:

- Eppler 423
- Selig Donnovan 7032
- FX63137b
- Selig Donnovan 7062
- Selig 1210

Figure 4.1 show the plots of the most important airfoil possibilities, the SD 7062 with and without a flap, the SD 7032 also with and without a flap, the Eppler 423, and the FX63137b. These plots were used to

help make the decision on which airfoil to use in the final design. All the data was found for a low wind condition to compare all of the airfoils and their tendencies in size required to fulfill the takeoff requirements as well as optimum cruise conditions.

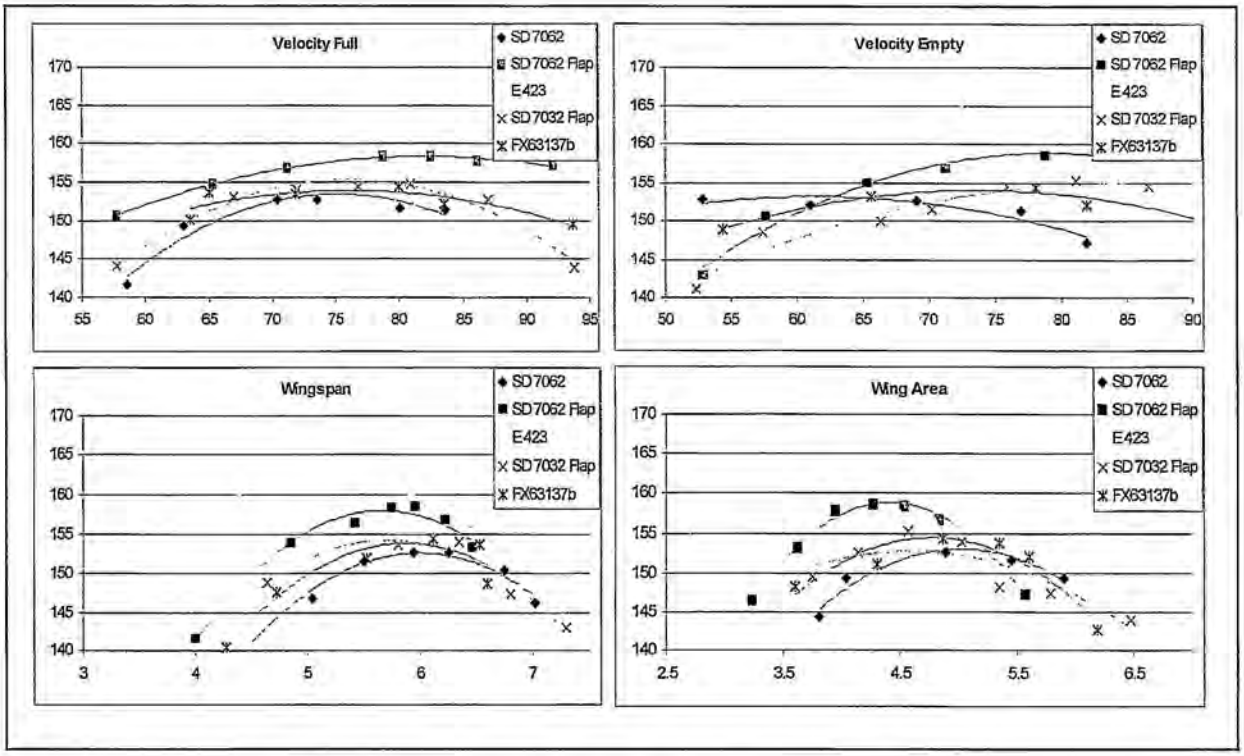

Figure 4.1: Graphs of Score vs. Each Parameter Evaluated

Looking at Figure 4.1, the top plots show the velocity (in ft/s^2) versus score plot for each airfoil investigated with and without the payloads. As shown above, the velocity plots show a gradual curve that peaks in the middle and trails off to each end. This guided the decision as to what speed the mission should be flown both with and without the payloads. The wing sizes are plotted with respect to score to show the optimum size that should be chosen for the final design. Because the wing dimensions are difficult to change after testing has begun it was very important to find the most advantageous wing dimensions so that changes would not be needed. Therefore the plots were closely scrutinized to find the maximum score on each plot while staying away from any rapid score changes. The wing dimension plots show a stronger relationship between both span (ft) and area (ft^2) to the resultant score. While the velocity plots show a weak relationship and therefore gradual slopes of the trends, the wing dimension plots show more drastic changes in score as the parameter changes. For all of the plots the values used corresponded to local maxima. The plots shown are the top scores from "shotgun" plots showing a large number of these local maxima points.

The above plots show how each airfoil compares to the others and while the Eppler 423 produced the highest score, the difficulty in construction and the high drag at high speeds reduced its appeal. The Selig

1210 produced very nice plots with high scores but because of the near impossibility to build it with the preferred construction method it was also removed from the list of possible choices. The Selig Donnovan 7032 was a very good high-speed airfoil but takeoff distance became a problem even with a flap unless a larger wing or more battery cells were used. The Selig Donnovan 7062 showed to be a very good all-around airfoil. The takeoff distance required is much easier to obtain while still allowing high speed cruise.

The optimization code was run with no wind present so that the design would not be dependant on wind to get off the ground in the required 150 feet. It was found that by adding a flap to the wing the takeoff distance could easily be held low for a zero wind condition, while the same wing with no flap used would only require a four to five mile per hour wind to get the same takeoff distance. The following figure, Figure 4.2 shows similar data to what is in Figure 4.1, but only shows the selected airfoil, the SD 7062 with a 15 percent flap. The optimization for the selected airfoil was done in a no wind condition by further refining the low wind condition data that was collected along with the other airfoils. The initial investigation was done using the same conditions for each airfoil then the condition was changed for the final optimization.

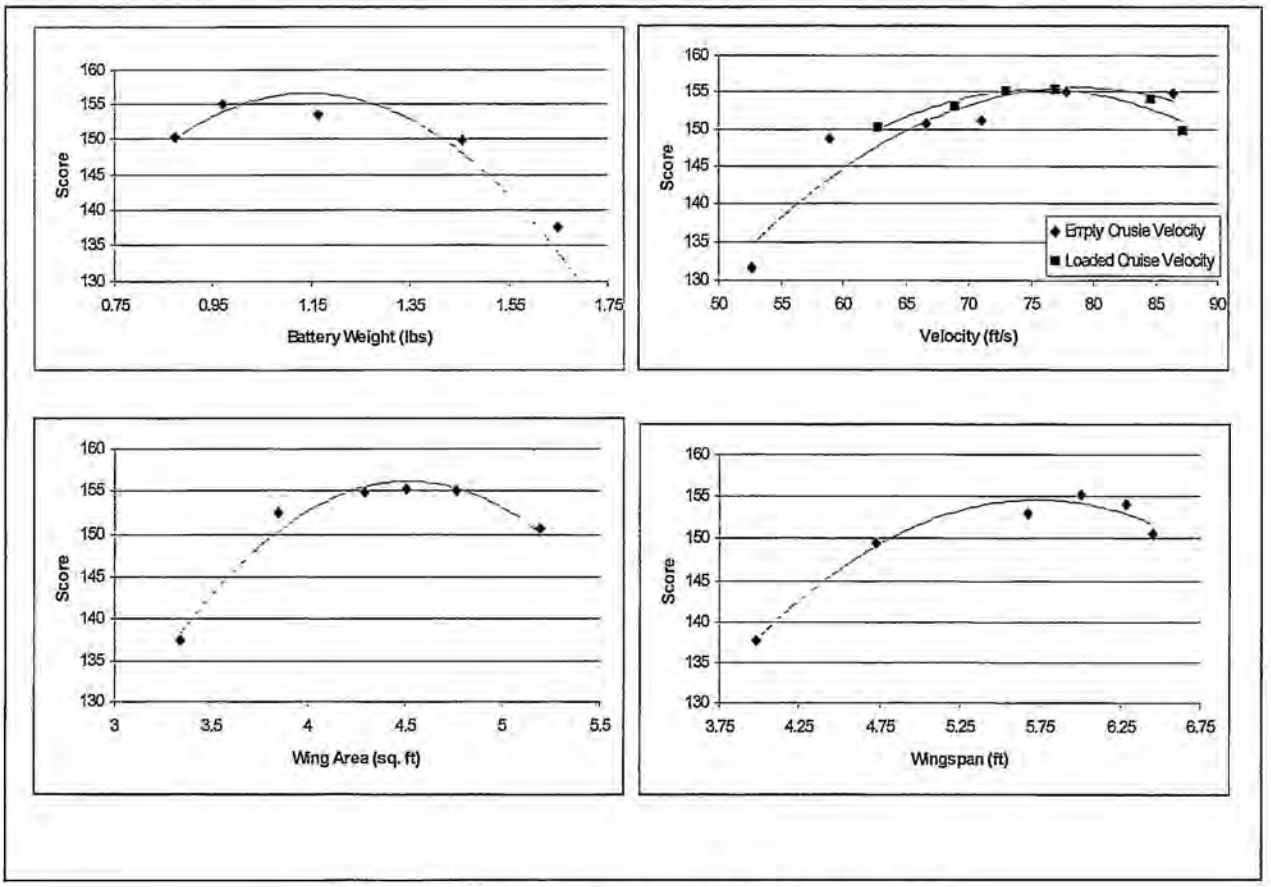

Figure 4.2: Optimization Curves for SD 7062 Airfoil

From Figure 4.2, it was determined that as long as the battery weight stayed from approximately 0.95 to 1.2 pounds the score stayed in a peak range. The score started to reduce after approximately 1.2 pounds.

The optimal battery weight range corresponds to a cell count of 10 to 14 cells with the battery weight per cell of the battery type that was suggested by the propulsion team. By looking at the score versus empty-cruise-velocity graph, it can be seen that the score increases with velocity up to the maximum at approximately 80 feet per second. This appears to be a very linear relationship up to that point, with the score leveling off and then slightly lowering after the 80 feet per second value is passed. The maximum score is covered by a broad range of velocities, from approximately 75 to 85 feet per second. The maximum score for cruise velocity, while carrying the payloads is slightly lower than that of the empty speed value. The peak score shifted over to around 75 feet per second, but the same wide range of maximum scores can be seen. The ranges of velocities that are most desirable are from 70 to 82 feet per second. The wing area trend shows a slightly more defined peak area for score, and more of a drop-off at either end of the range. The optimal range for wing area was found to be from 4.2 to 4.9 square feet. At either end of this range and especially at the high end the score drops fairly quickly. There is a very definite rise and fall in score based on wingspan. This strong relationship between span and score shows that this is one of the most important parameters in the design. The peak range here is very narrow, at only 5.7 to 6.2 feet, and on either side of this peak the score reduces quickly.

4.3.2 Propulsion Program Results

Batteries

Finding the right combination of propulsion components is vital to the success of the missions. This year a choice between two types of batteries had to be made. Initially the choice was made to use NiMH batteries; however to get a good comparison, two of the five batteries in the FOM matrix are NiCad batteries. The range of capacitance investigated was determined by running sample numbers though the propulsion program. The final comparison was between the Sanyo 4/5AUP 1700 (NiMH), Sanyo CP-1300SCR (NiCad), Sanyo 4/5AUP 1950 (NiMH), Sanyo CP-1700SCR (NiCad), and GP2200 (NiMH).

Battery	Resistance (ohms)	Weight (lb)	Capacity (mAh)	Capacity/Weight
Sanyo 4/5AUP 1700	0.006	0.075	1445	19266.66667
Sanyo CP-1300SCR	0.0065	0.076875	1105	14373.98374
Sanyo 4/5AUP 1950	0.005	0.085625	1657.5	19357.66423
Sanyo CP-1700SCR	0.006	0.10125	1445	14271.60494
GP2200	0.004	0.10125	1870	18469.1358

Table 4.1: Battery Capacity Comparisons

From the data table it can be seen that the capacity to weight ratio is highest for the Sanyo 4/5AUP 1950. However, the ratio does not take into account the internal resistance. Therefore, the following figures of merit were used to further investigate battery options. The FOM's are defined as:

- Weight: Keeping the total weight at a minimum will decrease the RAC. Therefore the lighter the cells the better.
- Capacity: As the capacity increases the endurance also increases.
- Internal Resistance: The internal resistance of the cells decreases the available output and thus lower resistances are desirable.

Factor of Merit	Weighting Factor	Sanyo 4/5AUP 1950	Sanyo 4/5AUP 1700	SanyoCP 1300SCR	SanyoCP 1700SCR	GP2200
Weight	0.3	2	3	3	1	1
Capacity	0.5	3	2	1	2	3
Internal Resistance	0.2	2	1	1	2	3
Total	1	2.5	2.1	1.6	1.7	2.4

Table 4.2: Battery Figure of Merit

The two top batteries from the matrix are the Sanyo 4/5AUP 1950 and the GP2200. When combined with the result from the capacity to weight ratio it can be seen that the Sanyo 4/5AUP 1950 is the best choice.

Propeller Model

Propeller selection is extremely important based on the mission profiles and requirements for each leg. Some of the most important details that were calculated involved the propulsive efficiency η_p, power required for each mission leg, cruise velocity, and thrust for takeoff while maintaining the 40 amp limit. From this a Pitch/Diameter ratio ranging from 0.58 to 0.75 would produce sufficient results for blades ranging from 15 to 20 inches in diameter.

With the varying characteristics of the motor, battery packs and propeller sizing, many runs were performed to determine the best combination to achieve the desired flight profile from a wide range of diameters and pitch settings.

Gear Ratio

The Kontronic Fun 600-18 that has been chosen only has three gear ratios available: 3.7:1, 4.2:1, and 5.2:1. Increasing the gear ratios increases overall efficiency, decreases propeller efficiency, increases the take-off distance, and decreases the current draw.

Using the information gathered it was determined that the 5.2:1 gearbox was impractical due to the takeoff requirement. It was also determined that for smaller diameter propellers that the 3.7:1 gearbox is necessary for the takeoff requirements while the 4.2:1 is adequate for mid to large diameters.

Motor/Speed Controller

Using the propulsion program, it was determined that Kontronic Fun 600-18 is the best motor. It is the most efficient; it weighs the least and has the smallest overall size. Each FOM is described below.

- Weight: As always the weight needs to be minimized for RAC.
- Efficiency: For optimum performance the efficiency should be high so that the battery pack required is as small as possible.
- RPM: The RPM is an indication of the power out of the system and needs to be optimized for the best performance.

Figure of Merit	Weighting Factor	Kontronic	Graupner	MaxCim
Weight	0.3	3	1	2
Efficiency	0.4	3	1	2
RPM	0.3	2	2	3
Total	1	2.7	1.3	2.3

Table 4.3: Motor Figures of Merit

4.4 Analysis Methods and Sizing

The sizing and analysis of the aircraft was done by splitting the task between the three teams, with each team working in their area of specialty. The following sections describe the analysis methods

4.4.1 Aerodynamics Group

Each individual aspect of the aircraft was designed in a way to optimize score either through performance or through RAC. The following sections will explain the methodology used for each major part of the aircraft.

Geometry Sizing

As was stated in the conceptual design discussion great care was taken to make sure that the fuselage was as small as possible to reduce RAC and to aid in the aircraft's ability to fit into the 4x2x1 foot box at the end of each mission. It had been decided that as few parts of the plane that had to come off to accomplish this task the better. Therefore the fuselage was shaped so that the only thing required to take off would be the wings. To make sure of this the entire plane was drawn in Pro-E to ensure that no components interfered with each other. This was extremely important since the minimum fuselage area required would be used.

Wing Sizing Analysis

Since the area of the wing is such a large portion of the RAC, the dimensions were optimized to obtain the smallest wing necessary to complete the mission while allowing room for unforeseen problems. The rectangular wing chosen has a lower efficiency than an elliptical wing; however, the payload-deployment system and the construction method favored this design. For ease of construction, the wing was designed with zero angle of incidence and zero dihedral, which was not necessary due to the low vertical center of gravity. After optimizing and evaluating the best score for each mission, the wing area and the wing span were obtained as 4.97 square feet and 6.23 feet respectively.

Entire Airplane

By approximating the location and weight of all parts, and the empty weight of 7 pounds the center gravity and the moment of inertia of the airplane were calculated as follows:

$$cg = \begin{bmatrix} 13 \\ 0 \\ 9 \end{bmatrix} \text{ in.}$$

The center of gravity was measured from the fuselage nose, and from the ground.

$$I_{empty} = \begin{bmatrix} 1.038069 & -.161133 & -.027706 \\ -.161133 & .264759 & -.244883 \\ -.027706 & -.244883 & .556132 \end{bmatrix} \text{ slug ft}^2$$

$$I_{internal} = \begin{bmatrix} 1.051 & -0.060532 & -0.153534 \\ -0.060532 & 0.302381 & -0.238575 \\ -0.153534 & -0.238575 & 0.588506 \end{bmatrix} \text{ slug ft}^2$$

$$I_{external} = \begin{bmatrix} 3.020371 & -2.122904 & -0.153534 \\ -2.122904 & 0.302381 & -0.238575 \\ -0.153534 & -0.238575 & 2.557876 \end{bmatrix} \text{ slug ft}^2$$

I_{empty} is the moment of inertia with no payloads, $I_{internal}$ is with internal payloads, and $I_{external}$ is that with external payloads. These were found by using the mass and shape of each component along with its location relative to the center of gravity. As can be seen there is a very significant change in yaw, I_{zz}, and roll, I_{xx}, moments of inertia depending on the whether the payload was being carried and where it was being carried. These values determined the response characteristics of the aircraft for each configuration.

Horizontal Tail Sizing Analysis

It was important to have a relatively small tail, a span less than a quarter of the wing in order to avoid being considered a second wing for the RAC analysis. The historical approach was utilized for the estimation of the horizontal tail size. According to "Aircraft Design: A Conceptual Approach" p.123, the tail sizes can be determined by the following equation

$$S_t = \frac{C_t C_m S_w}{L_t}$$

where C_t and L_t are the tail volume coefficients and the distance from the wing ¼ chord to the horizontal tail ¼ chord respectively. Using the tail volume coefficients for the homebuilt aircraft, the calculated size of the horizontal tail was 0.848 square feet. Using the 25% of the wing span, the horizontal tail chord was found to be 6.6 inches. From the historical data, the designed horizontal tail had a sweep angle of 15%. In order to make the airplane pitching moment at the zero angle of attack negligible, a horizontal stabilizer with the correct lift had to be designed. Since the horizontal tail would be molded directly into the fuselage, an incidence angle could not be used for the stabilizer. Therefore, and inverted cambered airfoil was needed. Lift coefficient versus angle of attack graphs of different airfoils were reviewed using the Profili program to obtain the appropriate airfoil for the horizontal tail. The optimum airfoil was a NACA 1212. The airfoil's graph showed the needed lift coefficient located around zero degrees (after taking into account the downwash effect from the wings).

Vertical Tail Sizing Analysis

Similar to the horizontal tail, the historical approach was utilized for the estimation of the vertical tail size. The vertical tail sizes can be determined by the following equation

$$S_v = \frac{C_v b_w S_w}{L_v}$$

where C_v and L_v are the vertical tail volume coefficients and the distance from the wing ¼ chord to the vertical tail ¼ chord. Using the tail volume coefficients for the homebuilt aircraft, the calculated size of the vertical tail was 0.555 square feet. Taking into account the sweep angles for the vertical tail, the tip and root chord were calculated as 6 inches and 11.8 inches respectively. Reviewing airfoils found in the airfoil analysis program lead to the decision of using an airfoil that was fairly thin and symmetrical. The optimal airfoil was found to be the NACA 0009. This would allow for the needed static conditions for stability as well as provide a feasible thickness for ease of construction.

Control Surface Sizing

The control surfaces were analyzed at landing with a crosswind condition, the worst case possible during the missions. The results are as follows:

- Aileron: The flaps were applied to the wing in order to generate the lift needed for landing. From the historical data, the aileron was found to be 90 percent of the span since the extra ten percent can provide little control effectiveness due to the vortex flow at the wingtips. Calculated size of the aileron was 0.665 square feet at 15 percent of the chord.
- Rudder: Taking account for the worst condition of the crosswind at the landing, the rudder size was calculated. According to the weather history, the strongest wind in March in St. Indigoes was 24 miles per hour. Assuming the rudder deflection angle of 15°, the calculated rudder area was 0.139 square feet which satisfied the historical range of 25 – 50 % of the vertical tail chord.
- Elevator: Assuming the deflection angle of 20° and the angle of attack of 11°, which was the predicted angle of attack at the landing, the elevator area was determined so that the airplane can trim at the landing. Using the obtained pitching moment coefficient of the airplane, the size of the elevator was found to be 0.193 square feet.

4.4.2 Propulsion Group

Along with the provided program, wind tunnel testing was performed on a wide range of propellers to compare actual performance along with predicted calculations and performance. Overall, thirteen propellers were tested, including several two blade propellers, two three blade propellers, and two pairs of two blade propellers modified to be four blade propellers. Several of the considered propeller's efficiency curves were plotted and it was determined that larger diameter propellers have superior efficiencies. This must be balanced with sizing considerations for the landing gear and the box size. Also compared in the wind tunnel were the MaxCim and Kontronic motor efficiencies. Data for the motors at various voltages are shown in Figure 4.3.

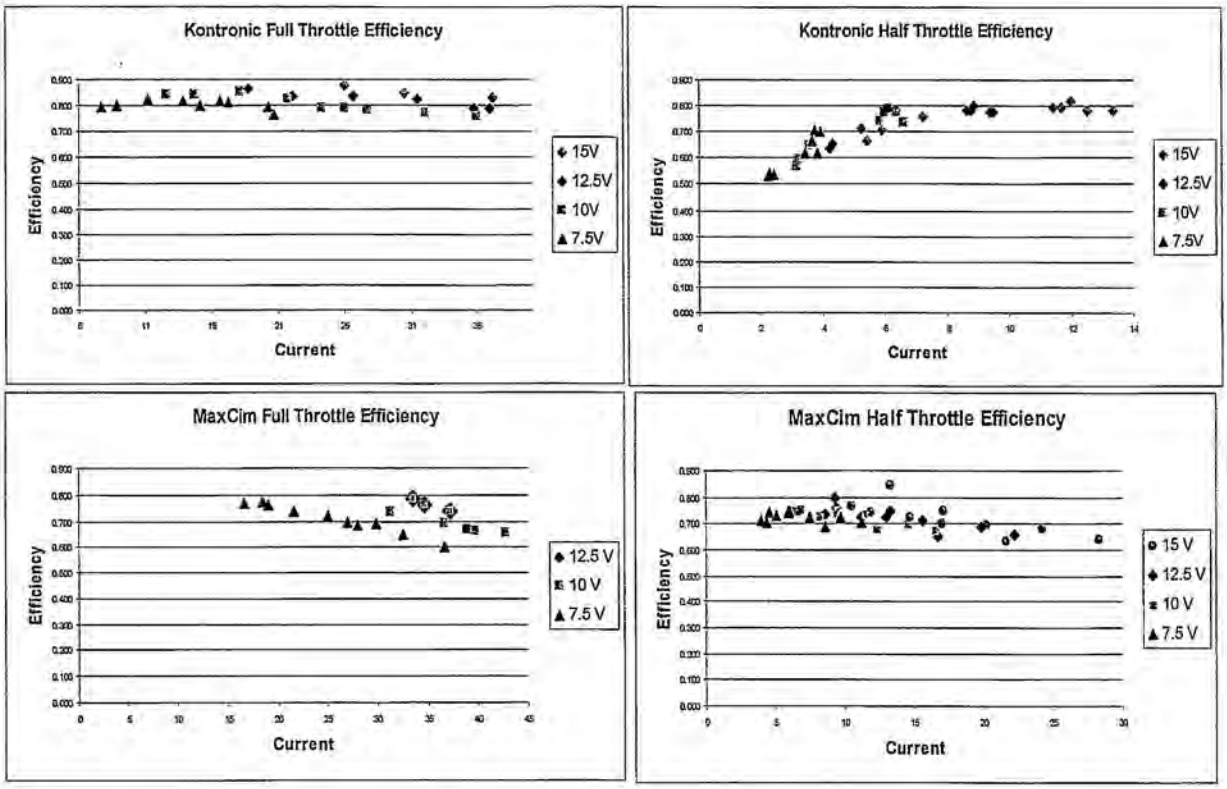

Figure 4.3: Experimental Efficiency Data

During the conceptual design phase it was determined that the Kontronic and MaxCim motors were the better choices. Using test data for both motors efficiency graphs were made. These graphs compare the current draw to the efficiency of the motor at various voltage settings. From the graphs it can be seen that at full throttle the Kontronic is more efficient. Although the MaxCim's lowest efficiency is not as low as the Kontronic's in the range tested, the MaxCim reaches its peak efficiencies at lower currents. For the final design the Kontronic was selected because the motor will mainly be operated at full throttle and high current.

4.4.3 Structures Group

For the Tail Dragger fuselage, the stress is concentrated in 3 major sections. The first high stress section will be at the location in front of the fuselage where the propulsion motor is attached. In addition to creating thrust and drag forces, the motor will produce a twisting force when the propeller rotates. The second high stress section will be at the left and right sides of the fuselage where the wings will be attached. With the external payload of 3 pounds on the tip of both wings, there will be a moment and a shear force at the wall of the fuselage. The third section will be at the base of the fuselage where the landing gear, internal payloads, and batteries are located. The load will be high in this area. The single area of stress concentration can be analyzed as a single wall with stress imposed to it.

The wing is designed to connect to both sides of the fuselage. Since there is a 3 pound load at each wing tip, the stress will be concentrated at that particular location. In order to balance the stress, the length of the spar that fits into the wing has to be decided. The number of ribs that are built into the wing also has to be taken into account. The functions of the ribs are to prevent twisting due to the torsion and strengthen the wing during flight. Building unnecessary parts into the wing will add additional weight onto the wing. Testing has to be carried out in order to have an ideal performance wing.

Analysis regarding to the horizontal tail and vertical stabilizer can be performed like the wing analysis. Rudder of the vertical tail is mainly responsible for yawing. The horizontal tail is used for landing and departing of the airplane, but it is not required to handle any external loads. The skin of the tail will carry most of the load. Figure 4.4 below shows the complete internal structure of the aircraft with ribs, bulkheads, etc.

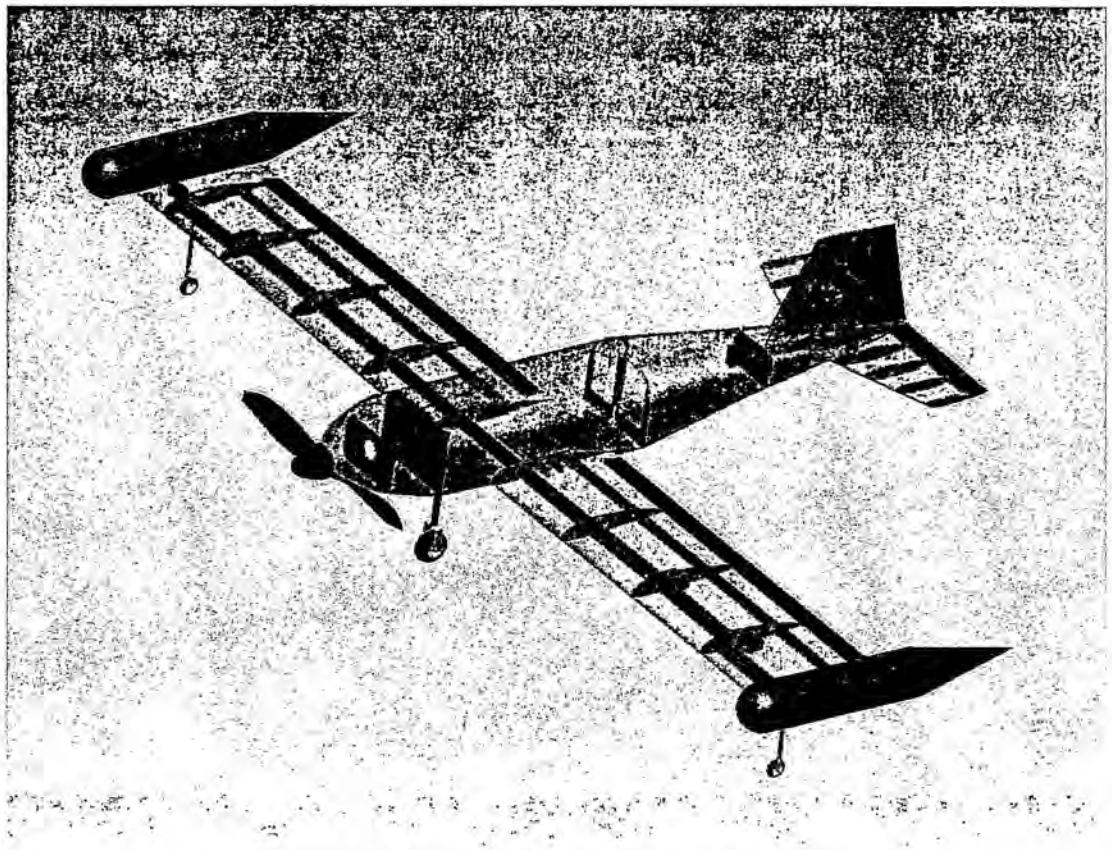

Figure 4.4: Complete Aircraft Internal Structure

Finite Element Analysis

Finite Element Analysis, or FEA, models were created for several critical aircraft components. A polynomial based FEA solver was used to analyze the maximum stress and displacement of a component under certain loading conditions. The analysis was based on convergence of three variables: local displacement, strain energy, and root mean squared stress. The limit was 10% convergence for

each variable. If any of the three variables were not within 10% convergence the order of polynomial equations increased at every point on the grid. The maximum polynomial order was nine, although all components converged at six or below.

As shown below, the wing and fuselage were modeled with the 3 pound payload at each wing tip during flight. Red is a high stress concentration point, while green is 30-50 percent stress, and blue has no stress concentration. The greatest stress point on the wing is at the tip where the payload is located. This area will have two light plywood ribs and extra fiberglass skins applied for strength.

Figure 4.5(b) shows the fuselage in flight with the external payloads loaded. It can be seen that the stress concentration is high at the location where the wings join to the fuselage. From this, it was determined that extra fiberglass would be used to bulk up those areas.

Similar analysis was performed on the wing and fuselage while landing at four times gravity. This stress distribution showed high loading concentration at the location of the main landing gear, wing tips, and fuselage nose. This was expected and the fuselage skins were laid up accordingly. Additionally, it was determined that the root of the wing experiences a high stress load at this landing in addition to the tip load. Supplementary composite will be laid in this region as well to prevent wing failure.

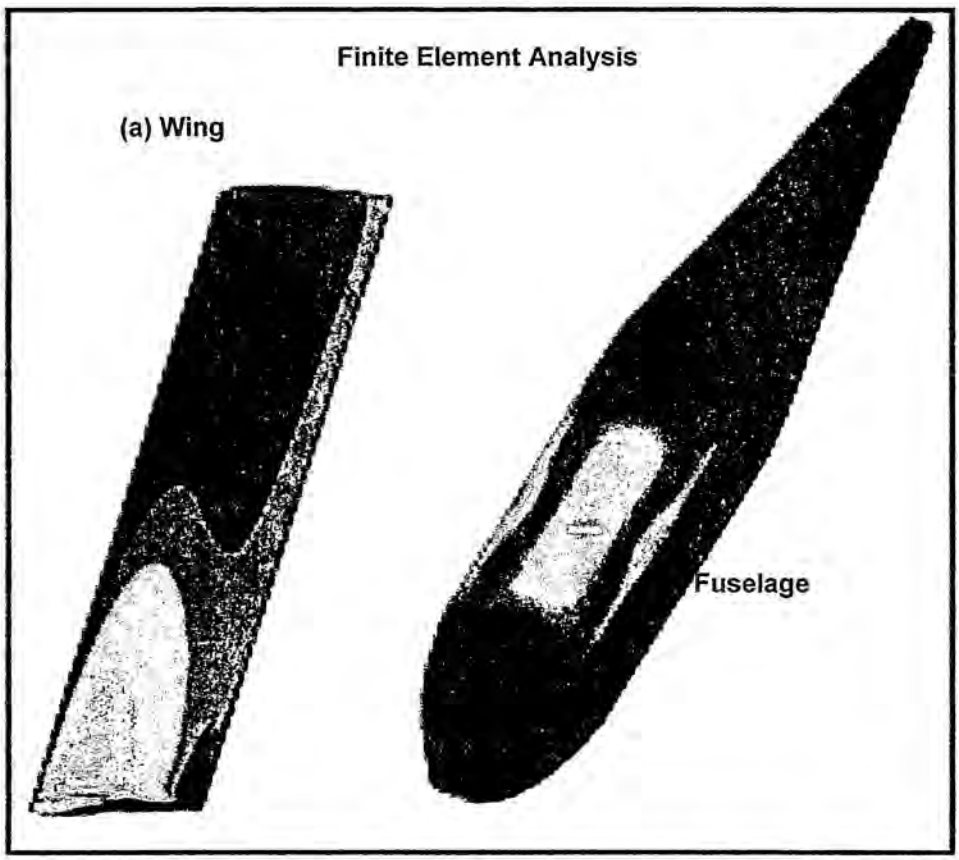

Figure 4.5: Root Mean Squared Stress Distribution During Flight

4.5 Final Aircraft and Predicted Performance

After finding the optimal ranges of each component and combining them together to define the final aircraft design it was possible to make certain predictions. By running a mission simulation the times for each lap could be predicted. Similarly, by running a stability and control analysis the static and dynamic stability and response characteristics could be calculated.

4.5.1 Aircraft Configuration

The final aircraft configuration consists of a streamlined fuselage contoured to fit the payloads and flight equipment. The low-mounted wing has a span of 6.23 feet. The wing area of 4.965 feet squared gives a wing loading of .331 ounces per square inch. A conventional configuration was used for the tail. The vertical tail area is .555 square feet with a rudder area of .139 square feet, a ratio of 25 percent. The horizontal tail area is .848 square feet with an elevator area of .193 square feet, a ratio of 23 percent.

4.5.2 Predicted Performance

Using the analysis program the performance of the aircraft could be predicted in nearly all aspects to a lap both with and without the payloads. Table 4.4 shows the values from the analysis program.

Mission Components	Time (sec)	Distance (ft)	Velocity (ft/sec)
Takeoff (loaded)	5.48	145.71	48.2
Takeoff (empty)	2.01	39.03	36.38
Climb (loaded)	5.89	299.46	51.53
Climb (empty)	3.03	106.62	38.89
First Turn (loaded)	9.1	149.05	Accelerating
First Turn (empty)	6.9	84.88	Accelerating
Acceleration (loaded)	7.58	506.07	Accelerating
Acceleration (empty)	5.99	364.84	Accelerating
360 Degree Turn (loaded)	4.4	0	Accelerating
360 Degree Turn (empty)	2.2	0	Accelerating
Cruise Leg (loaded)	4.76	346.68	77
Cruise Leg (empty)	10.08	635.16	80
Deceleration and Landing (loaded)	10.52	647.85	Decelerate to 36.38
Deceleration and Landing (empty)	10.39	586.37	Decelerate to 36.38
Stop (loaded)	6.08	166	-
Stop (empty)	4.59	94.54	-
Total per lap(loaded)	**66.3**		
Total per lap (empty)	**53.16**		

Table 4.4: Times and Distances for One Lap with No Headwind

These values were found using the SD 7062 with a 15 degree flap deflection that is 15 percent of the chord. With a slight head wind the flap becomes unnecessary for takeoff within the 150 foot distance.

4.5.3 Aerodynamics Coefficients and Stability and Control Derivatives

Static Stability

Figure 4.6 indicates the plot of the component contributions to pitching moment vs. the angle of attack. It shows that the designed aircraft is trimmed at approximately zero angle of attack and is stable.

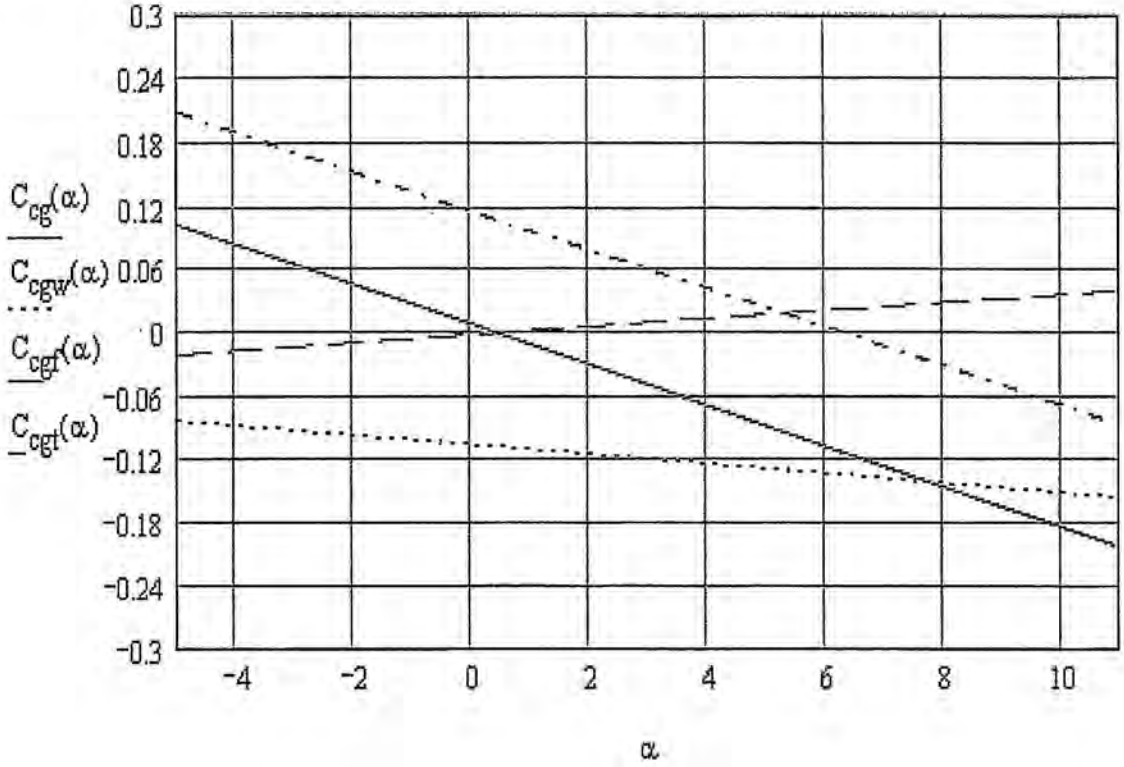

Figure 4.6: Component contributions to Pitching Moment

Longitudinal Stability

In order for the designed aircraft to have static longitudinal stability, the pitching moment curve must be a negative slope. In addition, it has to be trimmed at a positive angle of attack. Figure 4.7 indicates the plot of the pitching moment coefficient vs. the angle of attack of the designed airplane. From the detailed calculation, the airplane trimmed at an angle of attack of 0 degrees with an elevator deflection of 1 degree.

The pitching moment of the zero angle of attack, C_{m_0}, consisted of the summation of the contributions of the wing, tail and fuselage. When C_{m_0} is positive value, it can be said that the system is balanced. C_{m_0} of the designed airplane was found to be 6.857E-3. The pitching moment with respect to the angle of

attack, C_{m_α}, was also calculated by adding the contributions of the wing, tail and fuselage; however, it must be negative for the pitching moment stability. The calculated value was -1.094. In addition, in order to investigate the static stability, the control power due to the elevator calculated as -0.796.

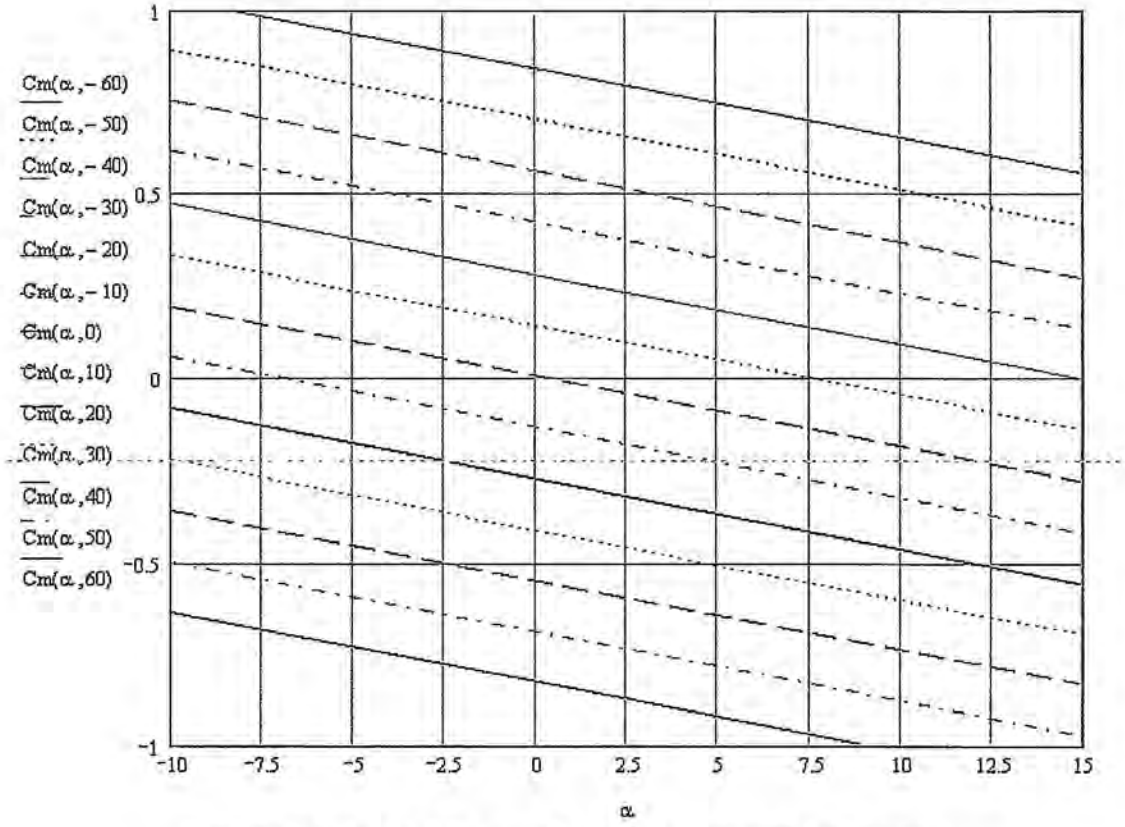

Figure 4.7: Pitching Moment Coefficient vs. Angle of Attack

Lateral Stability

For the lateral static stability, the directional stability coefficient, C_{n_β}, was computed to 0.098. The positive value represented that the system was statically stable. Furthermore, in order to investigate the static stability, the control power for the rudder was calculated as -0.044.

Roll Stability

For the roll static stability, the roll moment curve must be a negative slope. The major contributor to the roll coefficient is the wing dihedral angle. The roll stability coefficient C_{l_β} was computed to 0. Although the negative value for the roll stability coefficient meant the system had roll static stability, it can be said that the designed airplane has roll stability because it does not have the wing dihedral angle and the maximum ordinals on mean surface. Also, in order to investigate the static stability, the control power was calculated in the aileron, which was 0.342.

Dynamic Stability

For all stability calculations a five degree disturbance was used and the responses were calculated assuming that the aircraft was stable at the time of the disturbance. All of the responses can be found plotted for a five degree disturbance in Figure 4.8. As can be seen in the figure, for all lateral modes the wing tip payloads have a lower frequency but damp out slower, while the no payload situation has the highest and most quickly damped response.

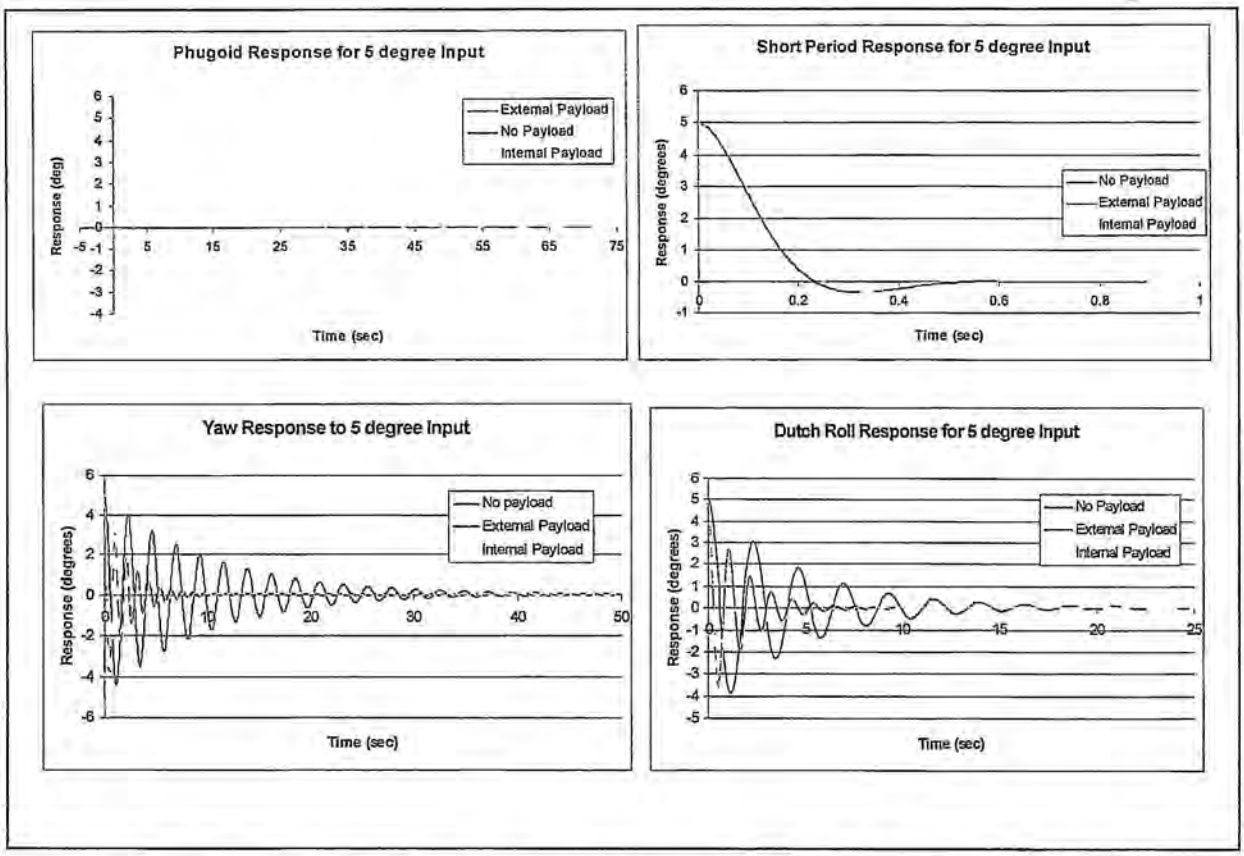

Figure 4.8: Response Curves for Five Degree Disturbance from top left Phugoid, Short Period, Pure Yaw and Dutch Roll

- Longitudinal Stability: In order to analyze the dynamic stability of the designed plane such as the short longitudinal mode and lateral mode, it is necessary to calculate the characteristic roots or eigenvalues for both longitudinal and lateral set of the state-space equations. The state-space equations need the longitudinal and lateral stability derivatives as well as the stability coefficients. Following the required assumption, the low-speed drag coefficient or parasite drag coefficient of 0.03 based on the max frontal area must not change during the flight.

For longitudinal analysis, two sets of complex numbers of the eigenvalues are expected for its dynamic stability; indicating the phugoid mode or short period. If both the real and imaginary number are negatively large, it is the short period mode. If both numbers are negatively small, it can be said that these eigenvalues represents the phugoid mode. It was found that because the internal payloads and external payloads are placed in the same location relative to the center of gravity, they have no effect on the phugoid response. The obtained eigenvalues led to a natural frequency of 0.551 radians per second and a damping ratio of 0.133 for the phugoid response.

The short period response does change slightly when the payloads are removed. For a loaded aircraft the short period was found to have a natural frequency of 12.06 radians per second and a damping ratio of 0.651, as compared to the 12.888 radians per second and 0.646 respectively for an unloaded aircraft. This change is due to the increased weight of the aircraft when the payloads are carried.

- Lateral Stability: Similarly for lateral analysis, a pair of complex eigenvalues indicates the Dutch roll mode which has both real and imaginary parts for its dynamic stability. The eigenvalues were studied for each payload configuration giving different natural frequencies and damping ratios for each case. Table 4.5 has the values for all three possible payload configurations.

	[illegible]	[illegible]
internal	5.648	0.099
external	2.709	0.081
empty	5.81	0.101

Table 4.5: Response for Each Payload Configuration for Dutch Roll

Using the stability coefficients found for the designed plane, the response to a purely yawing disturbance and response was found. The following table, Table 4.6 contains these values for each configuration.

	ω_n	ζ
internal	5.649	0.078
external	2.709	0.038
empty	5.811	0.08

Table 4.6: Response Characteristics for Pure Yaw for Each Payload Configuration

The roll rate was calculated by the equation of

$$-\frac{C_{l_{\delta_a}}}{C_{l_p}} \cdot \Delta\delta_a = \frac{P_{ss} b}{2u_0}$$

With the deflection angle of the aileron of ±15 degrees, the roll rate P_{ss} was 96.788 degrees per second.

5.0 Detail Design

The final design consisted of optimization of the preliminary design for the mission based upon limitations due to structural configurations and propulsion systems. The design was then optimized for stability and control while meeting the requirements described above.

5.1 Aircraft Sizing and Component Selection

From the design analysis, the following results were obtained for aircraft sizing and component selection.

Geometry	Value	Performance Data	Value
Center of Gravity Location (in)	13	CL Max	1.69
Fuselage		L/D Max	81.75
Length (in)	48	**Gross Weight Conditions**	
Width (in)	7	Maximum Rate of Climb (ft/sec)	8.49
Height (in)	5	Stall Speed (ft/sec)	36.9
Wing		Maximum Speed (ft/sec)	91.02
Airfoil	SD7062	Take-off Field Length (ft)	123
Span (in)	74.76	**Empty Weight Conditions**	
Area (in^2)	715.68	Maximum Rate of Climb (ft/sec)	16.51
Aspect Ratio	7.81	Stall Speed (ft/sec)	27.4
Incidence Angle	0	Maximum Speed (ft/sec)	91.25
Flaperon Area per Wing (in^2)	43.056	Take-off Field Length (ft)	35
Horizontal Stabilizer		**Weight Statement**	
Airfoil	Inverted NACA 1212	Payload (lbs)	6
Span (in)	18.5	Manufacturer's Empty Weight (MEW), (lbs)	7
Chord at Root (in)	8.25	Gross Weight (lbs)	13
Chord at Tip (in)	4.95	**Systems**	**Details**
Volume Ratio	0.482	Motor	Kontronic Fun 600-18
Incidence Angle	0	Battery Configuration	14 X Sanyo 1950
Elevator Area (in^2)	27.75	Gear Box	Kontronic KPG-27
Vertical Stabilizer		Gear Ratio	3.7:1
Airfoil	NACA 0009	Speed Controller	Jazz 55-10-32
Span (in)	8.5	Propeller	APC 16x12E
Chord at Root (in)	14	Radio	Futaba 9WC2
Chord at Tip (in)	8.5	Receiver	Futaba 9-channel
Volume Ratio	0.043	Servos	Futaba S3002
Rudder Area (in^2)	24.5		

Table 5.1: Final Aircraft Parameters

5.2 Propulsion System

The final propulsion configuration includes using the Kontronic 600-18 electric motor with 14 cells Sanyo 1950 mAh NiMH batteries and the Jazz 55-10-32 speed controller. The propeller will be 16x12E with a gearing ratio of 3.7. The takeoff thrust is 5.76 pounds and the expected power is 601 Watts.

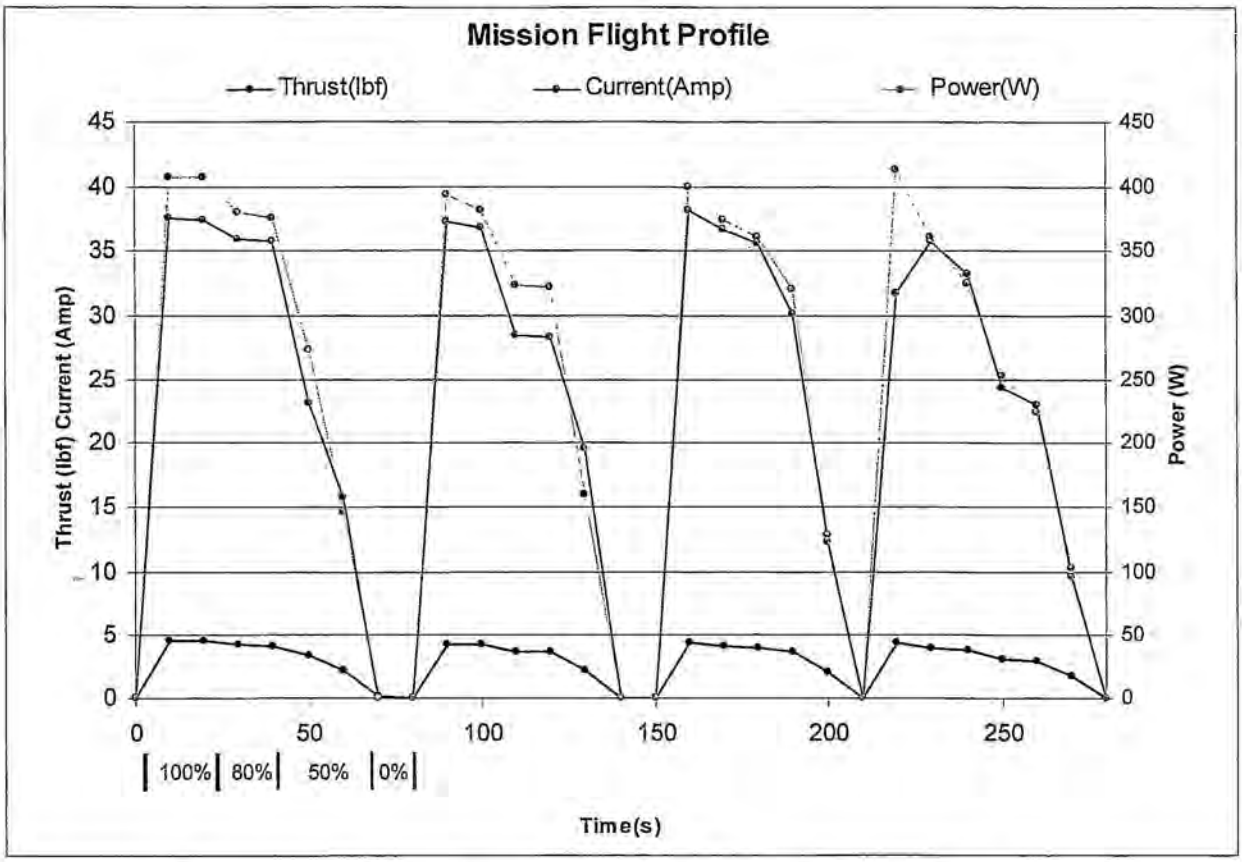

Figure 5.1: Simulated Mission Profile with Thrust, Current, and Power

To ensure that the selected system would perform as predicted a mission profile was run on the dynamometer for the Re-Supply mission. For this test the selected gearing ratio was unavailable for the experiment so the selected package was run with a gearing of 4.2:1 to insure the accuracy of the predictions. This combination performed as predicted from the propulsion analysis program and confirmed that the battery package is adequate for even the longest mission.

5.3 Structures System

Each component of the aircraft was analyzed for structural purposes. The goal for the structural analysis was to make the aircraft strong, but also as light as possible. The landing gear attachment, wing attachment and motor mount were taken into account for the fuselage. The external payload attachments were analyzed for the wing. The internal structure of the horizontal and vertical tails was also evaluated. The landing gear, including the main gear, the outriggers, and the tail dragger, were taken into consideration for heavy landings.

5.3.1 Fuselage

The main areas of stress discussed above must be considered when building the fuselage. Bulkheads will be included in the structure so that twisting of the fuselage does not occur. The first bulkhead will be place in the forward section of the fuselage to mount the motor. Another bulkhead will be placed in front of the internal payload area and one directly behind it. One will also be placed in the tail to decrease twisting and provide a place to secure the servos.

The foam core of the fuselage will be cut in three sections. The forward and aft sections will be cut from the four sides, while the middle section will be cut from the cross section. This will cause the cross section to be exactly sized to the dimensions. The main cross section of the fuselage must be cut exactly so that the payload, wing attachments, and landing gear will fit perfectly.

5.3.2 Wing

The entire wing span is 6.23 feet long with a chord of 9.6 inches. The wings will be cut on a foam cutter using data imported from the airfoil. This will allow for a perfectly shaped wing with the least amount of drag. The structure of the wing will consist of five ribs on each wing including closeout ribs. The external payload system requires an extra rib to mount the release mechanism. Two servos are needed, one for each wing flaperon. They are contained completely inside the wing to eliminate undesirable drag.

Wing Attachment

The wing attachment of the plane offers a unique challenge to this year's competition. This is first year that the wing will be required to support a heavy load. Because of this, special care has been used to design a durable, reliable, and quick-attachment wing.

In previous years, great success was achieved by running one carbon fiber rod through the fuselage in the port and starboard direction. We will also use this feature, but in efforts to increase strength, each wire will run from the two servos mounted in the wing to the fuselage. Each servo has three wires that will need attachments. The total of six wires will attach to very reliable stereo jacks mounted in the fuselage.

5.3.3 Horizontal Tail

The horizontal tail does not require any external loading for our missions. However, the elevator of the horizontal tail is responsible in landing and departing of the airplane. Nine ribs will be placed in the tail to keep the structure from twisting. The horizontal tail will be mounted onto the fuselage after the internal structure of each is completed.

5.3.4 Vertical Tail

The vertical tail is used for yawing, which does not require heavy loads. The internal bracing used will consist of horizontal ribs stiffened with diagonal balsa braces. The skin will be Monokote, a shrinkable

plastic material which will carry the flexing loads. The vertical tail will be fixed through the aft end of the fuselage with attachment points on the lower and upper surfaces.

5.3.5 Landing Gear

The horizontal location of the main gear was determined by the cg location. The main gear for the tail dragger must be placed in front of the cg so that the aircraft does not tip forward. It also must not be placed too far forward or else the gear will not be able to support the weight of the aircraft. After taking this into consideration the main gear wheel was placed in front of the cg. The gear structure was placed in front of the cg but behind the wheel. A shock absorber must also be placed on this gear because it will be carrying the majority of the aircraft weight.

The outriggers (1 inch diameter) are going to be mounted 1.75 inches from the tip of the wings at the quarter chord. These must be stiff enough to support the 3 pound external payloads for takeoff and landing. Therefore, 1/5 inch diameter landing gear struts will be used for the outriggers. They will attach to the rib that also attaches the back end of the external payload release.

The tail dragger wheel (1 inch diameter) must be attached to the rudder for ground control. As the rudder turns the tail dragger must turn in the same direction. This will require only one servo to power both the wheel and rudder.

5.3.6 Payloads

Internal Payload

The internal payloads must be as far forward in the fuselage as possible to be quickly removed during the competition. The payloads should be connected together and removed in one fast motion. The final design uses a hatch that opens from back to front with a foam base for the loads to settle into. The door hatch has a rib that is contoured to the payloads. The payloads will be about 21.125 inches long, including 7.5 inches of faring, 1.625 inches dome, and 12 inches of the original payload.

The internal payloads need to be secure inside the plane so that the weight does not shift around while the airplane is in flight. The system holding the payloads needs to be light weight but strong, therefore simple foam was chosen. The foam that will be used for the inside to contour the payloads is the same foam used for the plugs. The foam will only go up half way on the payloads so that there is air flow through the plane for engine cooling.

The payloads will be taken in and out by a strap that will hold the payloads close together. The loops that are used for the external payload holding system will be placed into the foam toward the center of the plane. The payloads will be kept from moving forward by the bulkheads supporting the fuselage. The motor and batteries will be taking up most of the space in the front of the plane so the payloads will not have room to move forward too much. The backward movement of the payloads should be worried about

more and will be stopped by the foam that is contouring the payload fairings. The bulkheads supporting the fuselage will help to stop the payloads from sliding forward.

The door will be cut into the skin of the plane and will be cut halfway down the plane's side. The hinge for the door will be made of Kevlar while a cabinet release will be the latch used to secure the door. The rib on the door will help keep the door and payloads in place and direct the door to the right position.

External Payload Release System

The extra length needed for the payload system in the wing skins will be added along with two additional ribs. These ribs will provide needed support for the 3 pounds of external payload. In addition to the extra ribs a series of contour pieces will be placed to support the payload on the wing. A birch veneer will then be added over the contour pieces to eliminate some of the drag and to add strength.

The payload release will be mounted to the innermost one of the extra ribs. Attached to the release will be the control servo which will activate the release. The payload itself will connect to the release via a wire loop placed on the outer surface of the payload. Foam tape will then be added to the surface of the birch veneer to keep the payload from moving around while it is fixed to the release. The external payload release prototype can be seen in Figure 5.2.

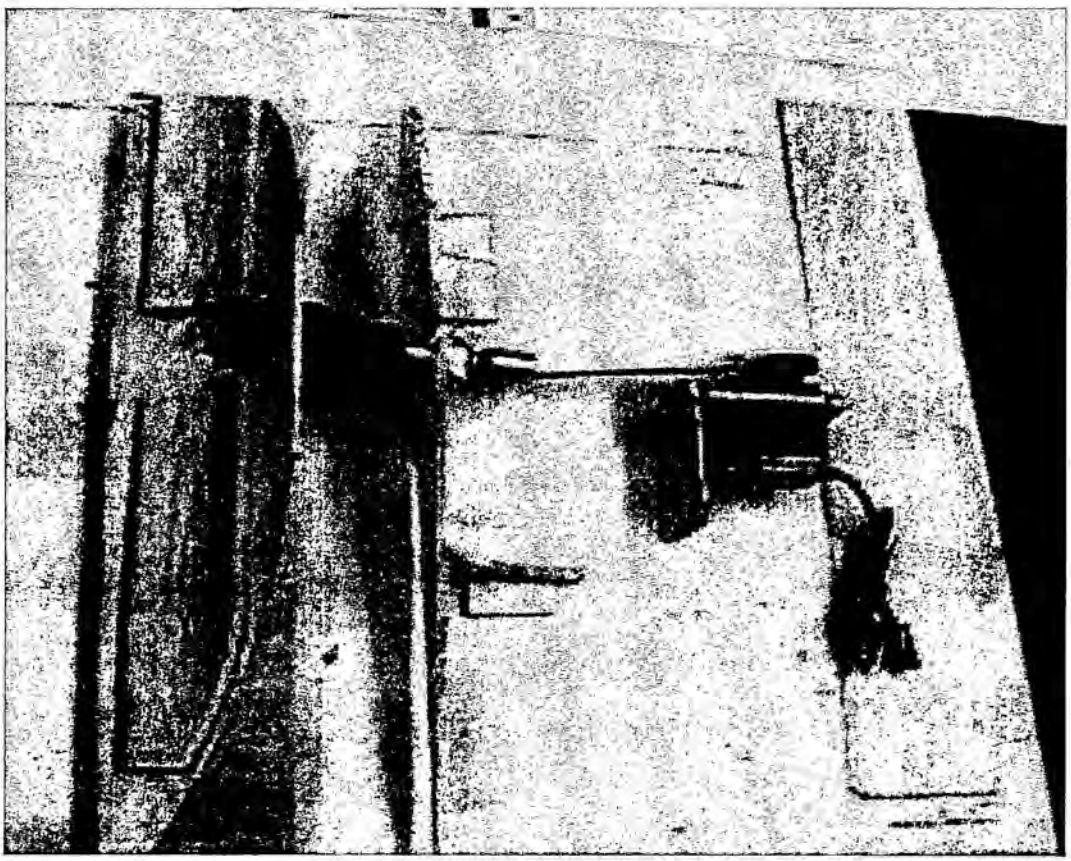

Figure 5.2: External Payload Release Prototype

5.4 Final RAC Calculation

The predicted rated aircraft cost for the final aircraft is shown in the table below. Recall the equation:

$$RAC(\$1{,}000) = (\$500 * MEW + \$1000 * REP + \$20 * MFHR)/1000$$

Item	Multiplier	Man Hours	Value	Hours	Cost (k$)
Manufacturers Empty Weight	$500				
Aircraft Weight			7 lb		3.5
Rated Engine Power	$1,000				
Battery Weight			1 lb		1
Manufacturing Cost	$20				
Wing Area		10 hrs/ft^2	4.965 ft^2	49.65	
Flaperons		5 hrs	1.5	7.5	
Fuselage		20 hrs/ft^3	0.9722 ft^3	19.444	
Vertical Tail		10 hrs/surface	1	10	
Horizontal Tail		10 hrs/surface	1	10	
Servos		5 hrs/servo	8	40	
Total MFHR				136.59	2.73
Total RAC					7.23

Table 5.4: Final Rated Aircraft Cost

5.5 Drawing Package

The next five pages of the report consist of the drawing package. The first drawing is a 3-view representation of the aircraft with dimensions and the next four include an exploded view, the external payload release system, the plane in the box, and structure and control configuration.

6.0 Manufacturing Plan

The manufacturing plan was determine by five figures of merit. These were evaluated closely to determine the best construction method possible. It was found that the vertical tail would be constructed differently from the rest of the aircraft due to time constraints. The fuselage, wing, and horizontal tail will be constructed using a fiberglass and balsa sandwich method for the skins.

6.1 Manufacturing Figures of Merit

- Cost: The cost of each construction method must be considered for budget reasons.
- Strength to Weight: The structure of the aircraft must be light, but also must be structurally sound to hold the required loads.
- Availability: The construction materials must be readily available for the construction to proceed in a timely manner.
- Durability: Repeated takeoff, landings, and payload deployments will need to be handled by the structure of the aircraft.
- Required Skill Level: The structures team must have the skills to perform the chosen construction method.

6.2 Manufacturing Alternatives

There were three methods explored for fabricating the aircraft. The first was balsa wood build-up. The next was the composite foam core method and finally the balsa reinforced composite method was explored. Each of these construction methods are more thoroughly discussed below.

- Balsa Wood Build-up: This method for construction was initially looked at because of how inexpensive it was to manufacture. The make-up for this method involves making the entire aircraft out of balsa wood. To make this type of aircraft full scale drawings are made for the craft and used to cut, fit, and shape the balsa wood into structural frame works, much the same as ships are made. The structural frame is then covered with sheets of balsa to make the skins. The amount of time required for this type of construction is feasible and is the least expensive of the three methods. However, the most limiting factor is the structure's strength to weight ratio. Compared to the other two methods this is the lightest structure, but it is also the weakest.
- Composite Foam Core: The composite foam core method was investigated heavily. This method is the most structurally sound of the three and is next to the quickest construction method. In order to fabricate parts for this method all that needs to be done is to draw the parts in a CAD program and have the parts cut out of foam using the Aero Labs foam cutter.

The foam is then covered with composite material and now the part is complete. The fallbacks to making parts out of foam core are the added weight to the structure and the internal space that the foam takes up. Lightweight is crucial for having a low RAC and internal space in the aircraft is vital to fit all the mechanical components and payloads inside the plane.

- Balsa Reinforced Composite: The final method examined for constructing our aircraft was the balsa reinforced composite. To produce a part with this method drawings are made with a CAD program and used to cut the part out of foam. The foam is then used to make a mold. Next, the mold is used to lay composite material into the exact shape of the part and is reinforced by placing sheets of balsa wood between the composite plies, producing the skins for the aircraft. Finally, the rest of the structural frame is either made with balsa or more composites. This method provides the nearly the same strength as the foam core, but without the added weight and space occupied by the foam. Though this method takes the most amount of time, the benefits far out weigh the disadvantages.

Figure of Merit	Weighting Factor	Balsa	Foam Core	Reinforced Composite
Cost	0.1	3	2	1
Strength to Weight	0.4	1	2	3
Construction Time	0.1	3	2	1
Durability	0.3	1	3	3
Required Skill Level	0.1	1	3	2
Total	1	1.4	2.4	2.5

Table 6.1: Construction Figures of Merit

6.3 Manufacturing Selection

Based on all the methods explored the decision was made to use balsa reinforced composite method. This method provides greater strength than the traditional balsa build-up method and provides nearly the same strength as the foam core method. Using this type of construction allows for the most internal space in the aircraft. The overall weight of the aircraft will be comparable to balsa build-up, which is vital for a low RAC score. Combining all of the advantages for this method and comparing them with the figures of merit, the balsa reinforced composite construction method was found to be the best choice.

The fuselage has different areas of the structure that have various strength requirements depending on the area of stress concentration. The front area consists of twisting, thrust, and drag force; therefore stronger fiberglass with balsa wood configuration is required. This configuration is also required for the wing attachment area and base of the fuselage. Strips of fiberglass at 45 degrees will be laminated with balsa wood in between to help strengthen the wall at the area of stress concentration. It can also help carry shear loads that were imposed in those areas. Other areas of the fuselage such as the upper

structure are not in the areas of high stress concentration. These areas can be constructed with lighter-weight fiberglass to keep the aircraft weight minimal.

The use of fiberglass and balsa wood is introduced for the skins of the wing. Two layers of 2 ounce fiberglass and a layer of 1/16 inch thick competition balsa is used to build the wing. Around the payload release system an extra layer of 2 ounce 45 degrees fiberglass will be placed. This will help stiffen the tip of the wing from twisting due to the payloads. Kevlar will be used along the hinges of the flaperons instead of fiberglass because it is fatigue resistant.

Competition balsa (1/16" thickness) will be covered between layers of 0.7 ounce fiberglass for the horizontal tail. A lighter fiberglass can be used on the tail because it does not experience heavy loads. A Kevlar hinge will be placed along the elevator. The vertical tail will be constructed by a different method. The vertical tail uses a traditional balsa wood build-up. The reason for choosing this method versus the monocoque method is mainly because of time. This technique will allow for easy construction, and will take much less time than making a mold.

6.4 Analytic Methods

Several analytic methods were used for efficient project planning. The following sections describe each of these methods, which were cost analysis, required skills matrix, and construction schedule.

6.4.1 Cost Analysis

This project requires considerable funding to be completed. The initial project cost estimated was $3,000. This includes the cost to build two aircraft, a prototype and a final. The actual project cost is shown in the table below.

ITEM	QUANTITY	UNIT COST	TOTAL COST
Construction			
Foam	5 sheets	$20	$100
Tooling & Mold Parts	Various	$370	$370
Composites	Various	$1,430	$1,430
Gear	1	$60	$60
Brakes & Main Wheel	1	$220	$220
Wheels	4	$10	$40
Flight Control			
Servos	14	$50	$700
Batteries	3	$29	$87
Miscellaneous	N/A	$50	$50
Payload Systems			
PVC	8 feet	$2	$16
Release Mechanism	4	$32	$128
Miscellaneous	N/A	$50	$50
Propulsion System			
Motor Gearbox	1	$65	$65
Batteries	14 cells	$10	$140
Speed Controller	1	$90	$90
TOTAL			$3,546

Table 6.2: Project Cost

6.2.2 Required Skills

It was necessary to identify the skills required for successful completion of the aircraft. Each skill was examined on a scale of 0 to 2, with a 0 requiring little or no skill and a 2 requiring high skill. The matrix below identifies the skills and the skill level for fuselage, empennage, wing, and the payload and propulsion system.

Skill	Fuselage	Empennage	Wing	Payload Systems	Propulsion System
Foam Cutting	2	1	1	1	0
Composite Lay-up	2	2	2	1	0
Mold/Skin Construction	2	2	2	1	0
Wiring	2	2	2	2	2
Aircraft Drawings	2	2	2	1	1

Table 6.3: Required Skills Matrix

6.3.3 Construction Schedule

The manufacturing process that was chosen required careful planning for timely completion of the aircraft. As a result, a construction schedule was developed to keep the project on track. Figure 6.1 below shows the timeline with projected and actual completion dates.

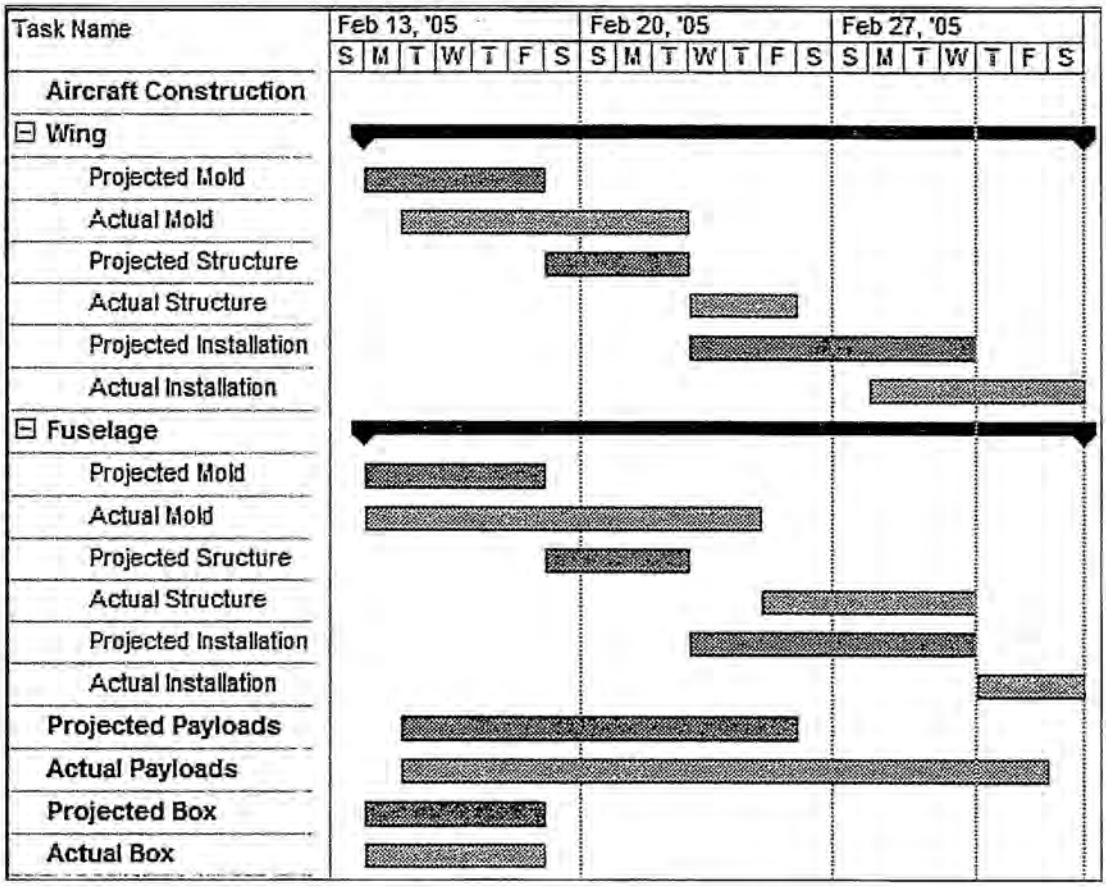

Figure 6.1: Manufacturing Milestone Chart

7.0 Testing Plan

A comprehensive testing plan was developed to verify the aircraft design, component selection, and structure. A schedule was developed for testing, in addition to preflight and flight testing checklists.

7.1 Test Objectives and Schedule

Several tests had to be performed to ensure sound construction of the aircraft. The testing was used to verify analytical data and calculations. Table 7.1 shows the comprehensive testing schedule which outlined the testing objectives.

Test	Objective	Dates
Mold Construction	Practiced construction method and made sample mold and part	1/17-2/11
Payload Release	Made prototype to test repeatability and efficiency of selected release mechanism	2/7-2/11
Tail Dragger Landing Gear with Outriggers	Tested ground control with desired landing gear configuration	1/10-2/20
Wing Structure	Determine weight of fiberglass and thickness of balsa for skins. Also, determine internal structure (ribs, spars, etc.)	1/17-2/20
Propeller	Test propellers and run optimization code for best prop selection	2/10-3/4
Motor/Battery	Test batteries and motor for optimal selection with aerodynamic conditions	2/10-2/26
Ground Crew	Evaluate time it will take to disassemble the airplane and place it in the box	2/28-3/2
Flight	Flight testing to validate expected aircraft configuration and component selection performance	2/19-4/15

Table 7.1: Test Objectives and Schedule

7.2 Flight Testing Checklists

Checklists are an essential part of flight testing. A pre-flight checklist, shown in Table 7.2, will be used before each flight to ensure airworthiness of the aircraft. Ground handling is crucial in this contest, especially for the external payload mission. A test plane will evaluate the external payloads and outriggers so that the pilot can become accustomed to ground handling with 3 pound weights at the tips. The strength of the wings and outriggers are of concern and will be monitored closely.

Preflight Checklist		
Item	**Comments**	**Complete**
Payload System		
-Proper Release	No release interference	
-Secure Attachment	Payload rigidly held in place	
CG location	13 inches from front bulkhead, within operational range	
Wingtip Test	Performed at full gross weight	
Wing Attachment		
-Secure Attachment	Check for sliding on spars	
-Electrical Connections Made	Aileron and payload servos functioning	
Battery		
-Properly Charged	Labeled fully charged	
-Secure Connection	Batteries do not shift in aircraft	
Motor and Propeller		
-Motor Mount Bolts	Tightened	
-Propeller	Prop nut secure	
Control surfaces		
-Attachment	Secure attachment at hinge	
-Deflection	Proper direction and distance of deflection	
-Linkage	Secure connection and no endplay	
Radio Range Test	Fail safe mode	

Table 7.2: Pre-Flight Checklist

Additionally, testing will be done with a prototype before the final plane is built. A flight testing checklist, shown in Table 7.3, lists the important items that should be tested to ensure that the aircraft meets the contest specifications and can successfully accomplish the two chosen missions.

Flight Testing			
Item	**Date**	**Comments**	**Results**
Taxiing and Ground Handling	3/6		
-Single Payload			
-Payload Release			
-Braking			
Empty Flight (First Flight)	3/9		
-Stability & Control in All Axes			
-Investigate Stall Characteristics			
-Investigate Behavior in All Flight Regimes			
-Takeoff and Landing Controllability			
Internal Payload (Second Flight)	3/13		
-Stability & Control in All Axes			
-Investigate Stall Characteristics			
-Investigate Behavior in All Flight Regimes			
-Takeoff and Landing Controllability			
External Payload (Third Flight)	3/15		
-Stability & Control in All Axes			
-Investigate Stall Characteristics			
-Investigate Behavior in All Flight Regimes			
-Takeoff and Landing Controllability			
Mission Profile Flight	3/17 - 4/14		
-Check Takeoff Distance			
-Check Landing and Braking Distance			
-Disassembly and Box Time			
-Lap Flight Time Empty			
-Lap Flight Time Internal Payload			
-Lap Flight Time External Payload			

Table 7.3: Flight Testing Checklist

7.3 Testing Results and Lessons Learned

It was found that the wings would slip off with ½ inch spar tubes connecting it to the fuselage. This meant that a larger spar tube and/or a more secure way of attachment was needed. Also, it was found that the wings flexed a lot even with the outriggers. This reinforced the idea of a larger spar tube and would also include making the outriggers more rigid. A larger diameter for the outrigger struts would help increase rigidity. Also, it was found that with only one payload the aircraft rode on the outrigger with the payload still attached. The other outrigger did not touch the ground. This helped determine which payload should be released first. The tail dragger also proved to perform well in ground steering testing.

The testing device for the external payload determined that dense foam was needed to keep the payload securely attached. Also, the added pressure from the foam helped the payload release easily. The hook that attached the PVC pipe to the wing tip also had to be mounted properly so that it would not catch on the release.

References

Allen, D.H. and W.E. Haisler, *Introduction to Aerospace Structural Analysis*, John Wiley and Sons, New York, 1985.

Bertin, J.J. and M.L. Smith, *Aerodynamics for Engineers*, 3rd Edition, Prentice Hall, Upper Saddle River, New Jersey, 1998.

Nelson, R.C., *Flight Stability and Automatic Control*, 2nd Edition, McGraw-Hill, Boston, 1998.

Raymer, D.P., *Aircraft Design: A Conceptual Approach*, 3rd Edition, AIAA, Reston, VA, 1999.

2004/2005 AIAA

Cessna/ONR Student Design/Build/Fly Competition

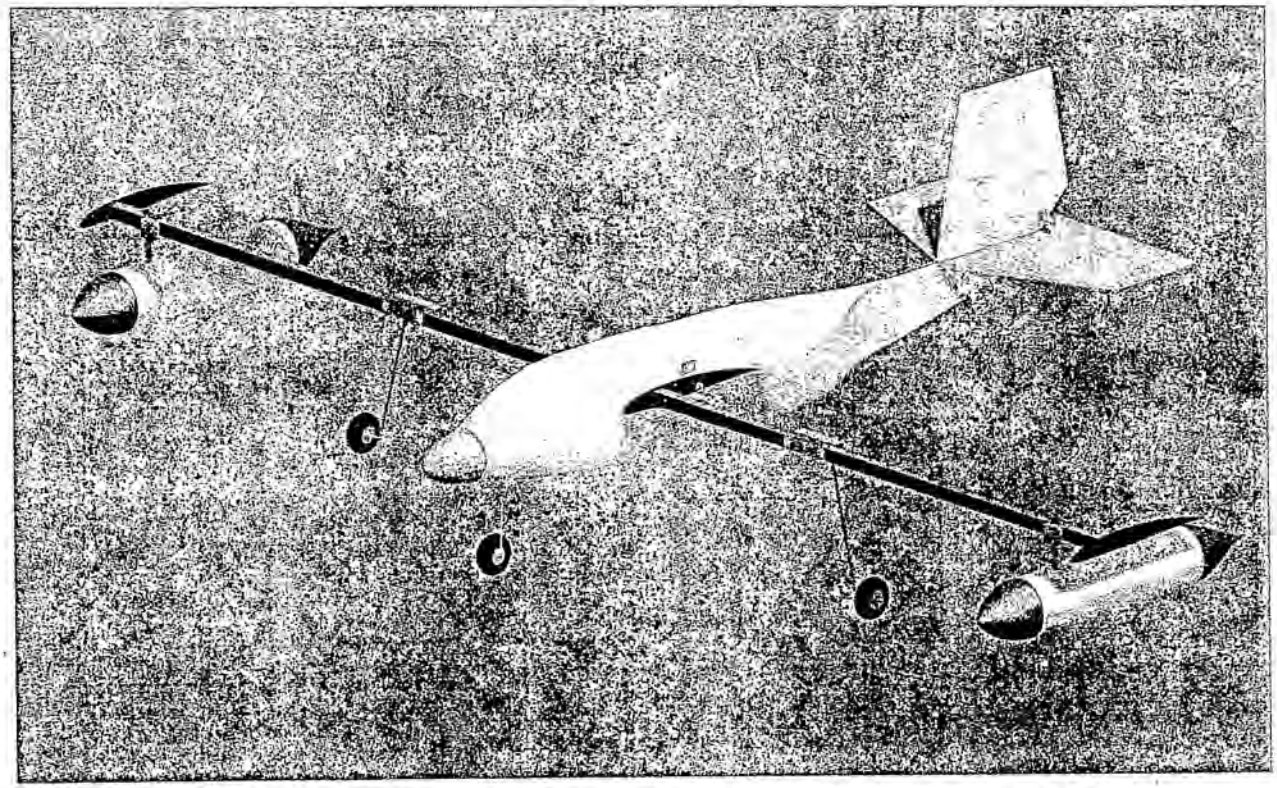

Wazzugar Flieger

Washington State University

Table of Contents

1.0 Executive Summary

The following report summarizes Washington State University's entry, the Wazzugar Flieger, into the 2004-2005 Cessna/ONR Design/Build/Fly competition. The goal of our team was to achieve the maximum score possible. This is accomplished by minimizing the RAC (rated aircraft cost), while maximizing the flight score. The flights consist of choosing two of three types of missions. These missions include a sensor reposition mission (SRM), a re-supply mission (RSM), and a maximum utilization mission (MUM). In addition to minimizing the RAC and maximizing flight scores, the paper score must be maximized to perform well in the competition.

1.1 Overview of Design Development

In the conceptual design phase of the design process, analytic approximations, and figures of merit (FOM) were created from the mission requirements of the SRM, RSM and MUM. Analysis of the three missions showed the combination of flying the SRM and RSM to be the most critical missions, outscoring any combination with the MUM. The SRM was also evaluated to contribute 56% to the total flight score. This early evaluation focused our efforts on the issues relating to the SRM and RSM. FOMs were developed to evaluate numerous aircraft configuration concepts. These FOMs were based on qualities that were determined to be important to the aircraft performing well for the two missions. The results of these FOMs laid a foundation for the design of the Wazzugar Flieger.

In the preliminary design phase, detailed analyses were performed on the selected aircraft configuration. A simulation program was developed to evaluate how small changes in the aircraft configuration affected several parameters, including total score. The simulation program used numerous equations for modeling all aspects of the aircraft's flight from takeoff to landing. It evaluated several combinations of parameters to determine the combination resulting in the best score. Some important observations were made when reviewing the results from the simulation program. The results showed that having a low RAC far outweighed the benefit of having a large, powerful propulsion system designed to make the aircraft fly as fast as possible. It also showed that the smaller and lighter the aircraft, the better the final score would be. In addition to the simulation program, composite test coupons were made and propulsion system tests were performed. This gave the computer model accurate figures for modeling and evaluation. When the simulation program completed all the combinations, a final result was presented as to the particulars of the aircraft's configuration. These results included details on weights, loads, speeds, distances, and sizes.

In the detailed design, calculations were performed to determine exact sizes and loads the aircraft would encounter. Stability analysis and experiments were run to finalize component selection. Final decisions were made concerning the sizes, systems, structures, and weight goals for the aircraft. Throughout the rest of the design process, continued improvements were made to exceed the goals set in the detailed design. Construction drawings were finalized to specify parameters for components to be manufactured quickly and accurately.

In the manufacturing plan, material and construction methods were specified. Processes for manufacture of components were also specified. A manufacturing dependencies table was produced to show which components required other components to be completed first. A skills matrix was produced to ensure personnel were assigned tasks based on their competency.

In the testing plan, materials testing, propulsion system testing, and flight testing were described. Testing of composite coupons produced data that was useful in estimating weight and stiffness of composite components. Propulsion system testing produced data that was critical to modeling the aircrafts performance accurately and selecting the correct propeller, motor, and battery combination. The final result was the combination of many parts working in harmony to minimize weight and RAC, and maximizing scoring potential.

1.2 Design Alternatives Investigated

The conceptual design process effectively narrowed down aspects of the design for the Wazzugar Flieger. FOMs were used to evaluate several alternatives for many components of the airplane.

For the overall airframe configuration, four configurations were considered. These were biplane, canard, flying wing and traditional. The traditional configuration was chosen for simplicity, lightweight, and low RAC. The wing configuration included three positions. These wing positions were high wing, mid wing, and low wing. The high wing was chosen for stability and for payload clearance.

Five types of wing construction were considered. These were stressed skin, built up balsa, foam core, spar & shell, and shell over foam. The foam core method was chosen because of strength to weight and ease of building/rebuilding. The empennage configurations that were considered were many. These included the T-tail, standard tail, V-tail, inverted V-tail, H-tail, and cruciform tail. The standard tail was chosen because of the ability to fit in the aircraft box, the number of servos required, and the durability of such a configuration.

For the payload configuration, four configurations were considered. These were side by side, over and under, vertical staggered end to end, and collapsible nose/tail cone end to end. A side by side configuration was chosen because of ease of aircraft manufacture and removal of the payload. Four types of fuselage construction were considered. These were stressed skin, built up balsa, foam core, and spar & shell. To get the smallest lightest airplane possible, the stressed skin construction was chosen.

The configuration of the landing gear had five different choices. These were tricycle, tail dragger, outrigger, wing mounted tricycle, and quadricycle gear. The wing mounted tricycle gear was selected because of ground handling and speed. Finally, the propulsion configuration choices were tractor propeller, pusher propeller, ducted fan and ducted propeller. The tractor propeller was chosen because of simplicity and thrust potential.

1.3 Design Tools

In the design of the Wazzugar Flieger, computer simulations, CAD and CAM software, and math solvers were used. The geometry of the plane was created primarily with the use of Pro Engineer Wildfire because of the programs ability to draw in 3-Dimensions, analyze volumetric shapes, and the availability of computers with this CAD platform. Matlab was used as a development environment for the simulation program since it has the ability to print charts and parse scripts. This was very useful in coming up with values for the design of the fuselage, wings, stabilizers and spar. Mastercam was used to convert drawings and set tool paths for post processing into NC code.

1.4 Results of Conceptual, Preliminary, and Preliminary Design

The conceptual design stage narrowed the configuration of the Wazzugar Flieger down to some specific choices. The plane was decided to be traditional fuselage configuration with a tractor propeller. The wing was determined to be a high wing, with a foam core construction, and as high an aspect ratio as practical. The fuselage would be a side by side payload configuration with a stressed skin structure. The empennage was determined to be a standard tail, and the landing gear was determined to be a wing mounted tricycle configuration.

The preliminary design involved optimizing individual components and simulating the mission using a Matlab program. The simulation program was written to simulate the most critical mission, the SRM. The speed of the aircraft, mission time, RAC, and SRM flight score are a few of the key unknowns determined by the code. The results of the preliminary design were used to narrow the focus of the detail design.

The detailed design specified the size and geometry for all the aircrafts components. The detailed design also made performance estimations for the aircraft with the size and geometry that was calculated by the simulation program and other calculations.

1.5 Results of Manufacturing and Testing Plan

The manufacturing plan specified the method of manufacture, material, and part selection for all the components of the aircraft. Descriptions were made outlining the manufacturing processes for each component.

The testing plan contains a thorough checklist for all aspects of flight testing of the aircraft. In addition to flight testing, bench testing of the propulsion system was performed. The results were used to help correct errors made in modeling the propulsion system in the simulation program.

2.0 Management Summary

Design work for the Wazzugar Flieger commenced in late August. At the beginning of the fall semester, the branch started with 8 members and gained 8 new members. In December, the WSU student branch's Vice-President graduated and entered the work force. The team consists of a total of 15 members, which can be broken down into two graduate students, six seniors, three juniors, two sophomores, and one freshman.

2.1 Breakdown of Design Team

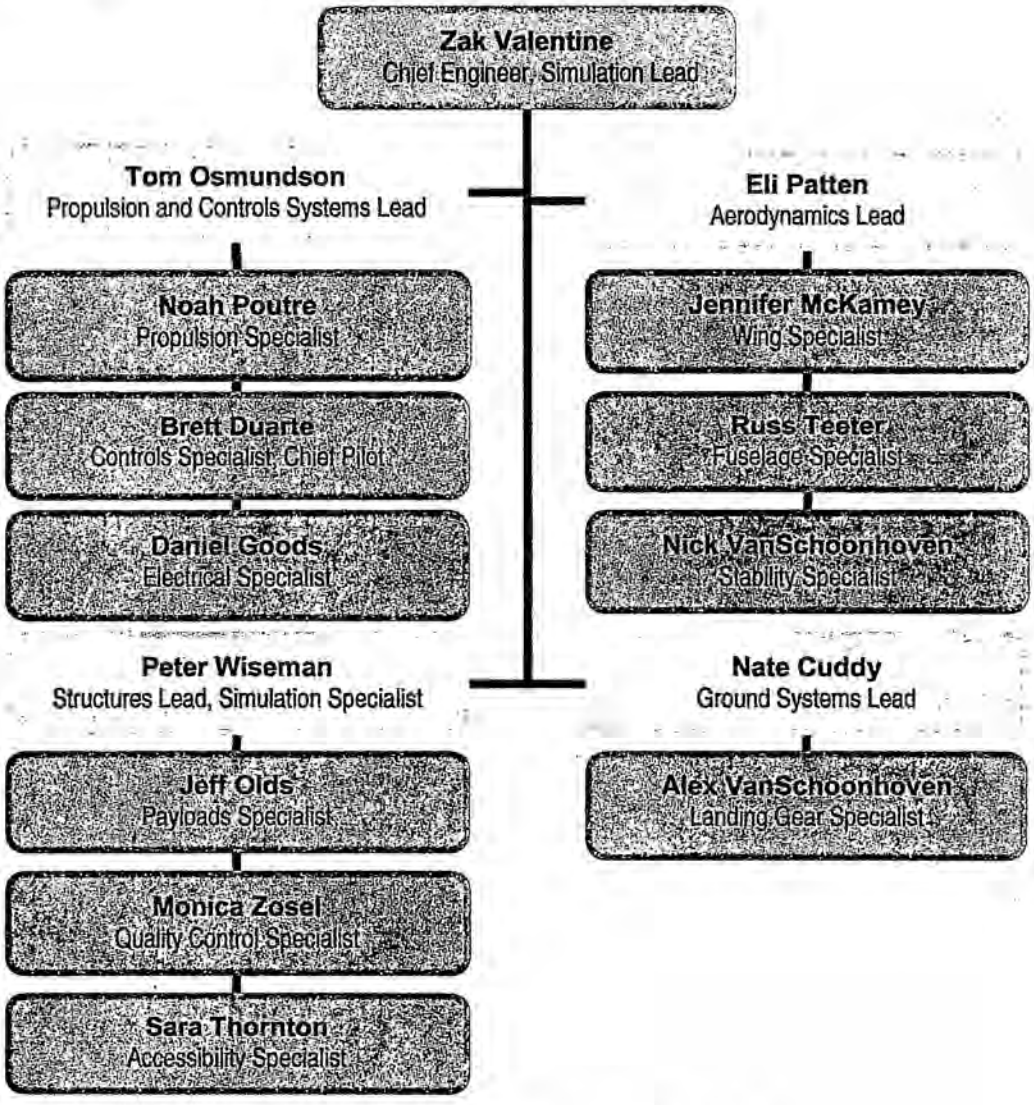

Figure 2.1 Organizational Breakdown

2.2 Organization of Design Groups

The final configuration of the Wazzugar Flieger was the result of the combined efforts of four teams. Each team had the task of developing a system that had to integrate with all other aircraft systems

to result in a functioning aircraft. Under the direction of the lead engineer, the design of systems was integrated, and tasks were delegated and performed.

The propulsion and control systems team had the primary function of testing of propulsion system components. Additional functions were designing the control system and working with the structures team to ensure systems could be integrated into the aircraft. Dozens of propeller and battery combinations were performed with the motor that was selected. The results of this team were specifying the motor and propeller used, specifying servos and linkages used, and specifying and constructing the propulsion and control system battery packs.

The structures team had the primary function of performing stress analysis and designing structural components. The structures team also had to make accommodations for all other systems to be supported in the aircraft and manufacturing components. The testing of composite coupons was performed by the structures team and a weights table was maintained. The result of their work was designing the wing spar and fuselage center plate, determining materials used for the fuselage and wing, designing the payload release mechanism, designing manufacturing tools, and manufacture of aircraft components. The structures group was also responsible for all construction drawings.

The aerodynamics team had the responsibility working with the simulation program to size the aircraft and ensure the stability of the aircraft. The result of their work was defining airfoils used, wing area, horizontal and vertical tail area, control surface sizing, and shaping of the fuselage. The aerodynamics team was also responsible for calculating aerodynamic loads on control surfaces.

The ground systems team had the primary responsibility of designing the landing gear. The landing gear was very important to the success of the aircraft. The ground stability of the aircraft had to be ensured to successfully of perform the SRM and RSM. The result of their work was designing the landing gear, specifying the tires used, and the placement of the gear assemblies.

2.3 Planning and Scheduling

Early in the design process, the team defined major design milestones and the dates by which tasks should be achieved. Changes to the schedule and announcements are made at weekly meetings or announced over the team e-mail list.

2.4 Milestone Chart

Task Name	Start	Finish
Aircraft Design		
Conceptual Design	30-Aug	30-Sep
Actual	30-Aug	11-Oct
Preliminary Design	1-Oct	31-Oct
Actual	12-Oct	25-Oct
Detailed Design	1-Nov	30-Nov
Actual	26-Oct	9-Dec
Design Report Writeup	1-Dec	7-Feb
Actual	24-Jan	1-Mar
Conceptual Design Writeup	1-Dec	10-Jan
Actual	24-Jan	25-Feb
Preliminary Design Writeup	1-Jan	24-Jan
Actual	7-Feb	25-Feb
Detailed Design Writeup	24-Jan	7-Feb
Actual	7-Feb	28-Feb
Manufacturing Plan Writeup	1-Jan	7-Feb
Actual	28-Jan	14-Feb
Testing plan,Exec & Mgmt Summaries	1-Feb	7-Feb
Actual	15-Feb	22-Feb
Drawing Pakage	1-Jan	7-Feb
Actual	22-Nov	25-Feb
Manufacturing	**1-Dec**	**1-Mar**
Actual	10-Dec	
Prototype Construction	1-Dec	31-Jan
Actual	10-Dec	4-Mar
Final construction	1-Feb	28-Feb
Actual	25-Feb	
Flight Testing	**1-Apr**	**20-Apr**
Actual		
Prototype testing	1-Mar	20-Apr
Actual		
Final testing	1-Mar	20-Apr
Actual		
Contest	**23-Apr**	**26-Apr**

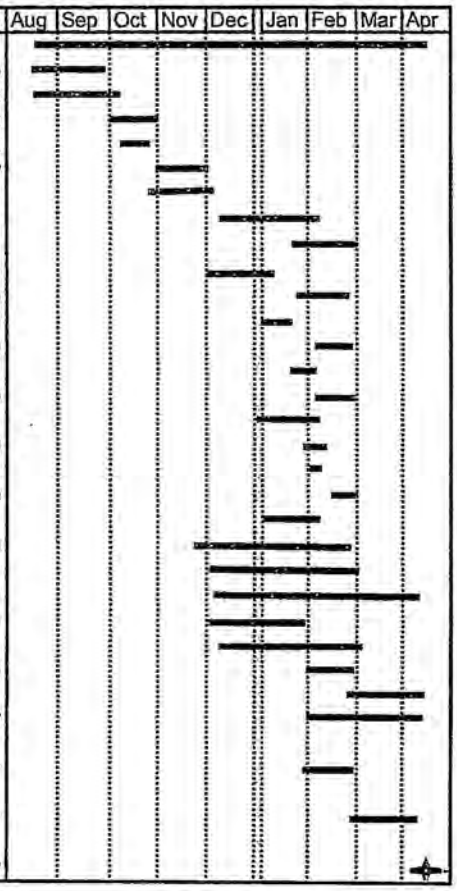

Table 2.4 Milestone Chart

3.0 Conceptual Design

The goal of the conceptual design stage was to investigate general requirements for the competition, the requirements for the three missions, the influence of RAC, and realize how all of these factors influence our design. Different aircraft configurations were considered and evaluated with the use of several decision matrices or FOMs (Figures of Merit). These included the alternatives for aircraft payload configuration, fuselage construction, wing construction, tail configuration, and landing gear type. The result and explanations of these FOMs can be found in section 3.2. These configurations will be further evaluated in the preliminary and detail design stage.

3.1 Mission Requirements

To win the competition, the maximum total score must be achieved. The total score was based on report score, total flight score, and rated aircraft cost (RAC), shown in the equation below.

$$\text{Total Score} = (\text{Total Flight Score} \times \text{Report Score}) / \text{Rated Aircraft Cost}$$

The report score was arbitrarily fixed at 90 to simplify calculations. The two other factors, total flight score and rated aircraft cost would be the main focus during our conceptual design.

3.1.1 General Requirements

General requirements for the aircraft are numerous and those that affected the conceptual design phase are as follows: must be any configuration other than rotary wing or lighter than air, all energy for take-off must come from the plane's propulsion batteries, and must be propeller driven and electric powered with or without gear reduction. A commercially produced propeller or ducted fan must be used. Motors are limited to 40 amps by means of a specific ATO blade type fuse. Batteries must be over the counter NiCd or NiMH. The propulsion batteries must not be more than 3 lb, and cannot be exchanged or charged during a mission. The receiver must be on a separate battery pack. The aircraft and pilot must be AMA legal, and the gross takeoff weight of the plane must be 55 lb or less.

Additionally, the aircraft will be subject to a safety inspection. The inspection will verify all components, and propellers are securely attached. The integrity of the payload system will be inspected. A visual inspection of the electronics, wiring and, connectors will be conducted. A radio range check will be performed, as well as verifying all controls move properly. The fail safe mode will be tested during the radio range check. The payload must not release during fail-safe activation. The wing system will be inspected using a wing tip lift test and an inverted wing tip lift test. The payload will be inside the fuselage at the time of the test so that the maximum payload capacity requirement was met. The aircraft must have a propulsion system fuse to disarm the motor as mentioned earlier. This fuse must be accessible from outside in such a way that one does not have to reach across the plane of the propeller to disarm the plane.

3.1.2 General Mission Requirements

In addition to general rules and safety requirements, there are requirements specific to the flight missions. Each team will be given five flight attempts. At each attempt the team must choose one of three missions. The final flight score was figured from the best score of two different mission types. This means that the plane must be configured to fly at least two different types of missions. The scores will then be added together to obtain the total flight score.

Before the mission was complete the plane must be disassembled quickly and placed into a 2 ft wide by 1 ft high by 4 ft long box. Mission time does not end until the lid on the box is closed and latched.

The payload may be carried either in the fuselage or on the wing tips, but must be capable of carrying the payload in either location. The payload itself is actually 2 separate payloads, constructed out of 12" long 3" diameter PVC pipe. The ends must be closed but with any choice of fairing. The total weight of the payloads must be at least 3 lb each, and the same identical payloads must be used internally and externally. When carried externally, the payloads must be located on a hard point within 3" from the wing tip. They must be capable of remote release. When carried internally the payloads must be fully enclosed inside the fuselage, and symmetric about the fuselage centerline.

The aircraft must take off in 150 ft or less, measured from the start line. In each mission, 360° turns are required. Therefore our plane must be able to turn quickly to be competitive. Landing must begin on the runway to obtain a score for the flight. The general maximum mission time was limited to 10 minutes, but the MUM has a reduced mission time limit of 6 minutes.

3.1.3 Sensor Reposition Mission (SRM)

The sensor reposition mission was given a difficulty factor of two. The aircraft will be loaded with two external payload packages, take off and fly one lap. After landing the aircraft will remotely deploy one sensor package at each of two separate release locations, then take off and fly one lap. After landing, the aircraft will taxi to a specified reload location near the first release location. The ground crew will go out to the aircraft, safe the propulsion system and reload the first payload. Once the ground crew has cleared the area the aircraft will taxi to the second reload position and the ground crew will again safe the propulsion system and reload the second payload. The aircraft will then take off and fly one lap, land past the start line. When the flight line judge gives instructions the ground crew must retrieve the aircraft and disassemble it. When the box is closed and the aircraft is inside the box the timer stops.

SCORE = Difficulty Factor * (12 - Mission Time)

Each lap must include one 360° turn on the downwind leg of the lap, and the turn must be in the opposite direction of the base and final turns.

This mission was weighted as having an importance of about 54% of our final flight score. An explanation of how this number was estimated see is given in section 3.1.6. Therefore our conceptual design will focus mostly on the needs for this mission.

3.1.4 Maximum Utilization Mission (MUM)

The maximum utilization mission has a difficulty factor of 1. The MUM consists of loading the aircraft with 2 internal sensor payload packages, after which the aircraft must take off and fly as many laps as possible before landing past the take-off start line and come to a complete stop. After being instructed by the flight line judge the ground crew will retrieve the aircraft, disassemble the aircraft and place the aircraft into a box. Time stops when the box is closed and the latch is in place. A maximum mission time of 6 minutes is allowed for this mission.

SCORE = Difficulty Factor * Number of Laps

Each lap must include two 360° turns on the downwind leg of the lap, and the turns must be in the opposite direction of the base and final turns. It was decided not to let this mission affect our conceptual design since its weighted importance was the lowest.

3.1.5 Re-Supply Mission (RSM)

The Re-Supply mission has a difficulty factor of 1.5 and consists of loading the aircraft with two internal sensor payload packages, after which the aircraft must take off and fly one lap and land. After landing the ground crew will go out and remove both sensor packages. The aircraft will take off again and fly one lap and land. After landing the ground crew will go out and reinstall the sensor packages. The aircraft will take off again, fly one lap and land. The ground crew will go out and remove the sensor packages. The plane will take off, fly one lap, and after landing the ground crew will retrieve the plane, disassemble the aircraft and place it in a box. The timer stops when the box is closed and latched.

SCORE = Difficulty Factor * (12 - Mission Time)
If only 3 of the 4 sorties are completed
SCORE = Difficulty Factor * (6 - Mission Time)
If only 2 of the 4 sorties are completed
SCORE = Difficulty Factor * (3 - Mission Time)
(Scores less than 0 will be counted as 0)

Each lap must include one 360° turn on the downwind leg of the lap, and the turn must be in the opposite direction of the base and final turns.

This mission was weighted as having an importance of about 31%. An explanation of how this number was estimated is given in section 3.1.6.

3.1.6 Mission Importance Weight

To get a general idea of which missions the airplane should be optimized for, some simple assumptions were made. The lap time for the SRM and RSM missions was assumed to take one minute and 10 sec. The lap time for the MUM mission is assumed to take one min, since the plane does not have

to take-off and land in between laps. Even though the MUM did require two 360° turns in each lap, it was not thought to be as big of a time penalty as taking-off and landing.

Remote deployment during the SRM is assumed to take 20 sec, but the reload process 40 sec. The reload is assumed to take longer since the ground crew will be required to run out to the plane, safe it by pulling the fuse, manually re-load the payload, run back, and repeat the process for the second payload. Both unloading and reloading during the RSM is assumed to take the same amount of time at 30 sec. If disassembling the plane and loading it into the box is assumed to take the same amount of time, 30 sec, for all three missions, then the results are as follows:

Mission Imprt.	Laps	Lap time (sec)	Num. of Unloads	Deploy/unload time (sec)	Num. of Reloads	Reload time (sec)	Box time (sec)	Total time (min)	Mission score	Imprt. factor
SRM	3	70	1	20	1	40	30	5	14	**0.538**
MUM	4	60	0	0	0	0	30	4.5	4	0.154
RSM	4	70	2	30	1	30	30	6.667	8	0.308

Table 3.1.6

Although a total of 5 laps could be accomplished in the MUM if the time to do one lap remained one min. or less, this did not seem likely. By the time the plane is on its last laps, the voltage in the battery pack will have dropped significantly, and so the power to pull the aircraft through the air. Although this problem could be solved by adding more battery capacity, it was thought that the effective increase on the RAC would be too great. The additional battery required for one more lap would not be worth the added weight, and effect on RAC. Therefore the number of laps in the chart above was changed form 5 to 4 for the MUM mission. Even if a value of 5 had been left, this would have only brought the score up by 1 point, and not changed the importance factors significantly.

Each of the mission scores above were divided by the total mission score to get the mission importance factor. With these results it was decided that only the SRM and RSM missions would be considered for our conceptual design.

3.2 Configurations Studied

Different configurations were examined for our design. These included differences in aircraft type, payload configuration, tail configuration, landing gear, propulsion configuration, and wing configurations.

3.2.1 Airframe Configuration

Aircraft Configuations							
Benefit	Low RAC	Low Weight	EZ To Build	High Speed	EZ to Fly	Total	Final Ranking
Weight	0.3	0.2	0.1	0.3	0.1	1	
Traditional	**90**	**90**	**90**	**80**	**80**	**86**	**1**
Canard	90	80	50	70	90	78	2
Flying Wing	30	70	50	90	20	57	3
Biplane	50	50	60	60	70	56	4

Table 3.2.1

Comparisons of four different airframe configurations were performed to conceptualize the layout of the Wazzugar Flieger. Those considered were the biplane, canard, flying wing and traditional. These four choices were selected since the group was not familiar with any other layouts. Five qualities (columns) were created that the team felt would have the most influence on the decision. These were: low weight, simple to build, low RAC, high speed and easy to fly. Each configuration was ranked in terms of how well it met the design criteria. Each score was multiplied by its importance, and the final results determined which design would be used.

Speed and low RAC were given the most weight (30%) since these factors directly influence the final score. Low weight was valued at 20% since a heavier design will influence all of the scoring factors. Simplicity of construction and easy to fly were given the lowest weight (10%), since the teams building and flying skills have matured greatly in the last two contest years.

The biplane was the first possibility considered. It is a much heavier design since two wings need to be supported, is more complicated, would have a high RAC, and would fly slower than a traditional plane. These downsides are reflected in its low score of 56.

The canard faired quite well in every category except simple to build and speed. The canard would be harder for the team to construct because our team has never built or flown a canard aircraft before. The speed was penalized since the more efficient main wing would be in the wake of the less efficient nose wing, possibly creating more total drag than for a conventional layout.

The flying wing was quickly excluded due to a higher RAC. It was found that an increase in width of the fuselage (fixed at 18 inches for Flying Wing) accounted for an 8% increase in the RAC (6.7 to 7.26). This negates the supposed advantage of removing the vertical and horizontal control surfaces. Flying wings are also known for their difficulty to design in stability, so a large flyability penalty was given.

The traditional layout was chosen over all the other designs since it fared well across all categories. This configuration would be lightweight, simple to build, have a low RAC, fly fast and be fairly easy to fly. This conclusion is based on its overall score of 86, which wins over the runner up, the canard, by only 8 points.

3.2.2 Payload Configuration

Payload Configuration						
Benefit	Low RAC	High Speed	EZ to build	EZ rem Payload	Total	
Weight	0.2	0.3	0.1	0.4	1	Rank
Side by Side	**70**	**80**	**100**	**100**	**88**	**1**
Over-under	60	70	90	80	74	2
Staggered end to end	80	90	70	50	70	4
End to end collapsable	90	100	60	60	78	3

Table 3.2.2

Although the aircraft was limited to where the payloads could be placed externally, carrying the payloads internal had a couple of different options. It should be noted that at the time of making Table 3.2.2, the WSU team had interpreted the rules to permit payloads arranged end to end along the centerline of the fuselage. Although this configuration had symmetry about the axis, the payloads are not symmetric to each other about the centerline. Therefore a side by side configuration was chosen.

The end to end collapsible configuration was to have a cone head, and possibly a cone tail, that could be compressed in some way. It would be compressed as if made with foam, or included a spring that would allow the nose cone and tail fit partially inside the PVC tube. The reason for this was so that the space consumed by the payloads could be reduced; yet keep the aerodynamic shape for when the payloads were used externally.

The characteristics determined to be important included low RAC, high speed, easy to build, and ease of payload removal and reload. RAC was only given a weight of 20% since the only effect the payload configuration has on it is slight and indirect. For example the side to side, and over-under arrangement would increase the necessary height or width of the fuselage and therefore increase the RAC slightly. The end to end configuration would likewise increase the necessary length of the fuselage and therefore increase the RAC slightly. However, a collapsible system would decrease this problem and was therefore given the highest score.

The less space the payloads take up decreases the total volume of the fuselage, and therefore the total drag. The side by side and over-under configurations got the lowest scores in this category followed by the end to end configuration. The end to end collapsible configuration had the greatest advantage and was given the highest score.

Ease of manufacture was given a low importance weight since the fuselage is easier to construct than the wings. The collapsible payloads got the lowest score in this category, since they would be difficult to manufacture.

The speed at which the payloads could be removed or removed from the fuselage was given the heaviest weight of 40%. The side by side configuration scores the highest here, followed by the over-under configuration. Using the assumption that the ground crew will have the easiest time unloading and loading a plane with this configuration since both payloads could be pulled out at the same time. With the

end to end configurations, only one payload at a time could be pulled unless a large access door was placed in the side of the fuselage.

3.2.3 Empennage

Empennage						
Benefit	Durability	RAC	Effectiveness	Fit In Box	Total	Final Ranking
Weight	0.3	0.4	0.2	0.1	1	
Std Tail	**100**	**100**	**70**	**90**	**93**	**1**
Reg V	90	90	100	80	91	2
Cruciform	80	100	80	80	88	3
T tail	70	100	90	60	85	4
Inv V	20	95	95	100	73	5
H tail	60	75	60	100	70	6

Table 3.2.3

Six different configurations were considered against 4 characteristics. The characteristic durability, accounts for how sturdy the structure is, and how likely it is to be damaged during landings. The inverted V tail scored the lowest due to the fact that it would have the lowest ground clearance, and could be easily damaged.

The Empennage chosen can have a big impact on RAC, and was thus given the largest weight value of 40%. Empennage choice affected the RAC directly in two ways. The first dealt a multiplying factor applied depending upon the number of vertical and horizontal surfaces, and whether they are considered to have a controllable surface or not. For example a standard tail has a multiplier of 20. (One horizontal surface and one vertical surface with control) A V tail only had a multiplier of 15, and an H tail scored lowest with a multiplier of 30. The other factor that affected the RAC is the number of servos. An H tail required an additional servo for a total of 3 servos instead of the usual 2 servos required, unless some sort of linkage was constructed to move both vertical surfaces at once. The V tail would not require an extra servo but would be more complicated to program due to the fact that the output to the two servos would need to be mixed. The effects of both of these factors were combined before they were added to the RAC category. Weight was also considered since it has a small indirect effect on RAC.

Effectiveness accounts for the ability of the empennage to keep the aircraft stable and provide control, per surface area. The drag produced should also be minimal. The V-tails are assumed to have the highest control effect per surface area. The T-tail is assumed to have an advantage over the standard tail since the horizontal surface is out of the wake of the wind disturbed by the wing. The H-tail scored lowest in this category since it was assumed that more surfaces would be required to provide the same control. This also means that more drag would be produced for the same control.

Little concern was given to the tail surfaces fitting in the box and only given a weight of 10%. The current year's fuselage will be rather short due to the side by side payload configuration chosen above. Due to the configuration, it is assumed that the tail surfaces attached to the fuse would fit in the box. A

concern was that the more tail surface later on would not allow the tail to fit in the box. The H-tail scored highest here since having two vertical surfaces meant that each surface could be shorter and be less likely to extend beyond the dimensions of the box.

The standard tail scored the highest, with a value of 93 and the V-tail a close second.

3.2.4 Landing Gear Configuration

Landing Gear							
Benefit	Low RAC	Simplicity	High Speed	Ground handling	Crash Resist.	Total	Final Ranking
Weight	0.2	0.1	0.1	0.3	0.3	1	
Wing Tri-gear	**85**	**75**	**100**	**90**	**70**	**82.5**	**1**
Quad	30	50	80	100	100	79	2
Tail Dragger	100	100	60	80	60	78	3
Tri-gear	75	75	80	60	70	69.5	4
Outrigger	85	60	40	30	40	48	5

Table 3.2.3

This year 5 different landing systems were considered. The tricycle gear has three wheels such that two are placed slightly behind the center of gravity and the third is placed in the front in the airplane. The tail draggers uses three wheels, with two wheels sitting towards the front of the aircraft, and a third wheel sitting at the rear of the airplane under the tail. This configuration has distinct advantages and disadvantages when it comes to landing and taking off. On the ground the angle of attack is high, which allows the aircraft take off without having to rotate like on a tricycle gear aircraft. During landing with a tail dragger, the pilot must be careful with pitch control to avoid bouncing and a possible ground loop. The advantages of a tail dragger include that the tail wheel is tied into the rudder, which eliminates a servo and the weight of a heavy wheel in the nose.

The tricycle system is the most common landing gear used on modern aircraft. Tricycle gear is popular due most modern airplanes use a low wing configuration and can be easily integrated into the structure of the aircraft saving weight. The take-off and landing for tricycle gear is straight forward when compared to the tail dragger because of the take-off and landing in tricycle gear occur in level situations.

The wing tri-gear is like a normal tricycle system except that the two main wheels are attached to the wings. This configuration was added this year due to ground stability concerns.

For the outrigger gear, there is one main wheel forward of the CG. There is also a tail wheel and two small wheels at each wing tip. The disadvantage is that the plane starts and stops leaning to one side slightly, giving it poor ground control. The advantage is there is only one large wheel producing drag.

Quad-gear consists of four wheels like a car. Quad-gear can provide good stability, but there are four large wheels producing drag.

Retractable tricycle gear and retractable tail dragger gear were also considered. It was decided that the increase in weight, complexity, and effect on RAC, did not outweigh the drag reduction.

Out of the five different characteristics, crash resistance and ground handling were given the highest weight of 30%. The quad-gear is assumed to perform best here due to having the best stability and four wheels and struts to absorb shock.

The 'High speed' characteristic considers both ground and air speed. The wing tri-gear was the winner here since it handles well on the ground and has less wind resistant than the quad gear.

'Simplicity' dealt with how easy the landing gear can be constructed. The tail-dragger received the highest score, and quad gear received the lowest due to having essentially two main gears with one set that must steer.

The only effect landing gear had on RAC was its indirect effect on weight. The exception to this is the retractable gear, which requires some servo mechanism to actuate the gear. The tail dragger was considered to score best since the back wheel can be very small compared to the front wheels and was light when compared to other options. The quad gear was considered the heaviest and was given the lowest score.

The configuration that received the highest overall score was the wing tri-gear.

3.2.5 Propulsion Configuration

Propulsion Configuration						
Benefit	High Eff.	High Thrust	High Speed	EZ Construction	Total	Final Ranking
Weight	0.1	0.3	0.4	0.2	1	
Propeller Tractor	70	90	80	100	**86**	**1**
Propeller Pusher	90	90	80	50	78	2
Ducted Propeller	60	50	90	60	69	3
Ducted Fan	60	20	100	75	67	4

Table 3.2.5

The decision to use only one motor was decided early on and verified to be a good decision with the RAC. This left the decision between four different propulsion systems, each using one motor. The four different basic layouts are: pusher, tractor, ducted fan or ducted propeller. The ducted fan or propeller could be in either pusher or tractor configuration. Efficiency, takeoff thrust, and high top airspeed were the factors most influenced by this decision. Speed was assigned a weight of 40%, while takeoff thrust was assigned a 30% weight. Simple to build was assigned a 20% weight, and efficiency a 10% weight. Speed was assigned the highest weight due to the direct affects on the flight score.

The propeller driven pusher obtained the second highest score. This was due to its tendency to increase efficiency of the airplane by not producing a wake that reduces efficiency of the main wing. However, it was given a low score for simple to build since such a configuration requires either a canard fuselage or two motors.

The propeller driven tractor had a lower efficiency, but was simpler to build, giving it the high score of 86. It had the same speed and thrust as a pusher configuration.

The ducted fan and propeller were determined to provide the highest flight velocity due to their higher rotation speed, but the static thrust from these units would be lower and takeoff performance would suffer. The result was the tractor propeller configuration which earned a score of 86.

3.2.6 Wing Configuration

Wing Configuration						
Benefit	Weight/Strength	Stability	High Efficiency	EZ Construction	Total	Final Ranking
Weight	0.2	0.3	0.2	0.1	0.8	
High wing	70	100	100	70	**71**	**1**
Low wing	90	60	80	90	61	2
Mid wing	50	80	90	60	58	3

Table 3.2.6

For the 2005 DBF, having a high wing was more important to allow clearance for the payloads. The payload could be mounted on the top surface of the wingtips, but this would be considered undesirable due to the instability of having weight above the center of lift.

Stability, was weighted the most important, and was assigned weight of 30%. Strength to weight and high efficiency were equally weighted with at 20%. Easy to build was assigned a weight of 10%.

The high wing configuration was ranked second in the strength to weight, first in Stability, first in efficiency, and second in easy to build. The high wing configuration had the highest aerodynamic efficiency given the average operational speeds the team decided to operate in, which ranges in the slow speed aircraft category given its scale. Additionally, the high wing configuration, through practice, was easiest to control with less risk for spinning or other flight failures from pilot error. During flight, the design has natural stability due to its geometry, and was less affected by ground effect.

The other wing configurations ultimately proved less favorable in the decision matrix. The low wing configuration was the most favorable in the weight to strength category along with its ease of manufacturability, because the landing gear would have easily been incorporated into the low-wing design by placing the gears underneath the wing. However, in terms of flight control, the low wing configuration was less stable. The thrust line would be above the aircraft's CG, and the wing would require considerable dihedral to provide adequate roll stability. While the mid-wing configuration would have decidedly performed in between high wing and low wing configurations in terms of stability and efficiency, the configuration would have fared poorly with strength to weight and easy to build. The mid-wing would have the wing spar through the middle of the fuselage.

3.2.7 RAC – Rated Aircraft Cost

The rated aircraft cost is based on many parameters. These parameters include empty takeoff weight, total battery weight, wing span, wing chord, ailerons and/or flaps and/or spoilers, fuselage length, width, and height, vertical surfaces with or without control, horizontal surfaces, and the number of engines, servos, and motor controllers.

The following RAC table is the same chart available on the DBF web site, but modified to fit in the page. The values filled in are those that were estimated during the conceptual phase.

	RAC	6.70				
Empty Weight	6.00					
	REP	1.16				
# Engines	1					
Battery Weight (lb)	1.2					
	MFHR	127.22				
	Wing Subset	55.00			Fuselage Subset	22.22
Wing #1 Span (in)	72.00			Max Length (in)	48.00	
Wing Max Chord (in)	10.00			Max Width (in)	8.00	
Wing #2 Span (in)	0.00			Max Height (in, w/o landing gear)	5.00	
Wing Max Chord (in)	0.00				Empenage Subset	20
Controls Type, Enter "1" in correct type				# verticals w/ no controls	0	
Ailerons	1			# verticals with controls	1	
Flaperons	0			# horizontals (any)	1	
Ailerons+Flaps	0			V-tail (uncheck all others)	0	
Ailerons+Spoilers	0				Flight Systems	30
Ailerons+Flaps+Spoilers	0			#servos (any function)	5	
				#motor controller(s)	1	

Table 3.2.7

3.3 Conclusions

In summary, the Wazzugar Flieger will have the following basic configuration:

- Tractor prop, traditional fuselage configuration
- High wing
- Side by side payload configuration
- Wing mounted tricycle landing gear
- Standard (Inverted T) empennage

4.0 Preliminary Design

4.1 Design Parameters and Sizing Trades Investigated

4.1.1 Design Parameters Considered

To optimize Wazzugar Flieger for the competition, it was decided to optimize the aircraft for the highest scoring missions, SRM and RSM. The most important variable to minimize was determined to be weight. By choosing to minimize weight, drag, size, power requirements and wing area can be reduced.

This very effectively minimizes RAC and increases flight score. Thus the overall goal was to reduce the Empty Weight/Payload to 1, without reducing the safety factors of any of the components.

4.1.2 Sizing Trades Investigated

In order to reduce the weight of the aircraft, it was necessary to reduce size. We began by choosing our motor. In the past 2 years, WSU used AstroFlight Cobalt 40 brushed motors with no reliability problems at all.

However, the Cobalt 40 is heavy, and the team wanted a motor that did not require timing adjustments, so the team purchased an AstroFlight 825G. This is the smallest motor AstroFlight makes that produces the same or more power output than the Cobalt 40, and weighs half as much as the Cobalt 40. It also used 6-18 cells as opposed to 12-24 cells, which helped reduce the weight of the aircraft.

Once the motor size was chosen, it was possible to use the simulation program to estimate the takeoff distance of the aircraft. The team adjusted the wing area of the simulated aircraft so that the aircraft would climb out at greater than 500 fpm and be able to take off within 150 ft on the third lap of the SRM, which is the most critical takeoff condition. The necessary wing area was found to be 5.5 ft^2. Still assuming an gross weight of 12 lb, the wing loading was roughly 40 oz/ft^2, which historically provides good wind penetration and acceptable handling for the DBF competition.

4.2 Analysis Methods Used For Aircraft Components

4.2.1 Wings

4.2.1.1 Wing Planform Optimization

Wing area was chosen as the primary dimension to alter during the optimization program run. The airfoil was changed to an SG6042 from the Eppler 205 used previously, due to its higher Cl. Aspect ratio was set at 7.25, since this was a good compromise between efficiency, roll rate and strength occurs near this point. Since wing area affects RAC and nearly every other aspect of flight, it was a crucial variable to analyze. Wing area was related to wing span by the fixed aspect ratio. The wing span was varied manually by the user until the aircraft took off in 150 ft on the critical 3rd lap of the SRM. The weight of the wing was estimated to be 5 oz/ft of span, based on the 2004 aircraft. Flaperons were omitted from the simulation code, but would be used as a safety factor should a headwind not be present at the flying site.

4.2.1.2 Wing Spar Design

The spar for the wing had to be able to withstand the greatest forces that were going to be exerted during flight, in addition to landing impact loads, since the gear width needed to be so wide. The wing spar also had to be stiff in torsion to prevent changes in AOA during takeoff and landing due to

bending moments exerted by the landing gear. From the optimization code, it was determined that the weight of the aircraft would be approximately 12 lb. and would undergo a maximum of 4.0 g's while in flight, with a Safety Factor of 1.5. The wing also had to have a span of 33" for one wing, a maximum deflection at the wing tip of 0.5 inches, and weigh less than four ounces per foot. From the design of the airfoil, it was determined that the wing spar could be no taller than 0.875", and would have to be able to slide onto a rod to attach it to the fuselage.

To model the spar, the equation for a cantilever beam with a uniformly distributed load was used. The spar was to be made of competition balsa with vertical grain orientation for the shear web, and Toryaca pre-preg uni-axial carbon fiber for the upper and lower cap strips. The layers were to be held together with Shell epoxy and wrapped with 1mil x 1" Kevlar tape at 45 degrees. By assuming these construction methods, the amount of carbon fiber to generate the required stiffness was found. A carbon tube extending 3" into the wing for the fuselage interface was added to the weight of the spar in the model, as well as the weight of the carbon rod that extends through the fuselage.

Since the landing gear loads could easily destroy the wing spar on a high g landing, a nylon screw anti-rotation pin was sized to fail on a landing load exceeding 6.5 g's, so the low Safety Factor of 1.5 could still be used.

4.2.2 Fuselage

To simplify the simulation code, the fuselage was approximated as an ellipsoid with a circular cross section. The cross sectional diameter was fixed at 7.25". The length of the fuselage was set to make fitting in the box easy. The total length was set at 48", which minimized RAC, had adequate length for reasonably sized control surfaces, and fit in the box. The fuselage weight was modeled upon predicted surface area and assuming a 2 oz/yd^2 fiberglass and 1/16" balsa core sandwich.

4.2.3 Empennage Sizing and Stability Estimate

When designing the empennage, several aspects were considered. To keep sizing of control surfaces simple at this stage of design, calculation of only vertical and horizontal tail volume was performed. A more detailed stability analysis would be performed after analysis of the mission model and completion of a more finalized aircraft design. Since it was decided that the overall aircraft length should be no longer than four feet, the empennage sizing was based on a four foot long plane with a six foot wingspan and five square feet of wing area. The tail arm was roughly calculated at two feet.

To determine the size of our horizontal and vertical stabilizers, the equations from Raymer (1999) were used.

$$S_{vt} = \frac{c_{vt} b_w S_w}{L_{vt}} \qquad S_{ht} = \frac{c_{ht} \overline{C}_w S_w}{L_{ht}}$$

Knowing that there was a limitation in the width of the horizontal stabilizers of 25% of the wingspan, the horizontal stabilizer span was limited to 18". The height of the vertical stabilizer needed to

be such that it could fit in the 1x2x4' box. Estimating the fuselage to be about 3", this left 9" of height for the vertical stabilizer. Next, minimum goals were set for C_{vt} and C_{ht}. Based on typical values for homebuilt aircraft from Raymer (1999), a minimum of 0.50 was set for C_{ht} and 0.04 for C_{vt}. Knowing all the variables, the stabilizer areas were calculated. The results were a vertical stabilizer area of 0.6 ft^2, or 9.0" tall with a 9.6" average chord. The horizontal stabilizer was determined to be 1.04 ft^2, or a span of 18.25" and an average chord of 8.3".

4.2.4 Propulsion System

The propulsion system was broken into four main variables, propeller diameter and pitch, number of battery cells, and cell size. Due to budget constraints, only combinations with the AstroFlight 25 brushless system were performed. Propulsion system tests were performed in parallel with programming the analysis methods used in the simulation program. From propulsion test data, the simulation code focused on using propeller diameters from 12 to 18", and propeller pitch from 8 to 14", each in 2" increments. Test data also suggested on focusing on battery packs with 12 to 20 cells. NiCd's were used throughout the analysis, since NiMH cells that could withstand high current discharge were only available in large capacity cells. Table 4.2.4 was generated to assist the user in selecting NiCd battery combinations that had equivalent weight to test in the simulation program.

Battery Weight Chart (ounces)							
#cells	CP1300SCR	SR1200	CP1700SCR	SR1500	SR2000	CP2400SCR	SR2400
10	11.6	12	15.3	16	19	20.9	21
11	12.76	13.2	16.83	17.6	20.9	22.99	23.1
12	13.92	14.4	18.36	19.2	22.8	25.08	25.2
13	15.08	15.6	19.89	20.8	24.7	27.17	27.3
14	16.24	16.8	21.42	22.4	26.6	29.26	29.4
15	17.4	18	22.95	24	28.5	31.35	31.5
16	18.56	19.2	24.48	25.6	30.4	33.44	33.6
17	19.72	20.4	26.01	27.2	32.3	35.53	35.7
18	20.88	21.6	27.54	28.8	34.2	37.62	37.8
19	22.04	22.8	29.07	30.4	36.1	39.71	39.9
20	23.2	24	30.6	32	38	41.8	42
21	24.36	25.2	32.13	33.6	39.9	43.89	44.1
22	25.52	26.4	33.66	35.2	41.8	45.98	46.2
23	26.68	27.6	35.19	36.8	43.7	48.07	48.3
24	27.84	28.8	36.72	38.4	45.6	50.16	50.4

Table 4.2.4 Battery Pack Weight Table

4.3 Mission Modeling

4.3.1 Aircraft Drag Model

To estimate total aircraft drag, a reference area method was used. Wing area, Sref, was first calculated. For each additional component, a planform area was calculated. The ratio S_{comp}/S_{ref} was used to calculate the percentage that each component contributed to the total drag of the aircraft. Drag coefficients were found by calculating the Reynolds number for each component at an assumed average speed of 50 mph, and using appropriate empirical data. The total of these coefficients make up the C_{Dmin} component of the following formula:

$$C_D = C_{D\min} + \frac{(C_L - C_{L\min})^2}{(\pi AR \cdot 0.90)}$$

The simulation code modeled flight by varying angle of attack of the aircraft for different flight regimes. For the SG6042 used in the simulation, the response between angle of attack and C_L and C_{Lmin} is the lift coefficient at 0 degrees AOA. Thus all components of the equation for C_D were known and the drag was calculated for the aircraft for any given moment during flight simulation.

4.3.2 Aircraft Maximum Lift Coefficient

To keep the Mission Simulator simple, the AOA was not to increase high enough to stall the wing, since stall was not modeled by the program. For the SG6042, this corresponded to a $C_{L,max}$ of 1.2 and a maximum AOA of 10 degrees.

4.3.3 Propulsion System Model

Modeling of the power system was accomplished in the same manner as last year's optimization program. The propeller was modeled using rotating wing theory and an empirically determined power formula. The power for the static condition was approximated as follows:

$$P_{abs} = C_p\, D^4\, P\, RPM^3$$

P_{abs} = power absorbed by propeller

C_p = propeller constant, 1.11 for APC fiberglass propellers

D = diameter of propeller in ft.

P = pitch of propeller in ft.

RPM = speed of propeller in kRPM

An empirical formula was found for static thrust, but was proven to be far too inaccurate during static testing, so an equation based on rotating wing theory was derived. The equation is as follows:

$$Thrust = nb \cdot ch \cdot r \cdot 1/2 \cdot \rho \cdot asv^2 \cdot (C_l \cdot \cos(\tan^{-1}(V_x / V_p)) - C_d \cdot \sin(\tan^{-1}(V_x / V_p))$$

nb = number of blades

ch = chord

r = radius of propeller

ρ = density

asv = accelerated stream velocity

C_l = propeller coefficient of lift, Clark-Y

C_d = propeller coefficient of drag, Clark-Y

V_x = forward velocity

V_p = propeller speed at 75% radius

This thrust relationship allowed modeling of unloading the propeller during flight, as well as during static conditions. Energy consumption could then be modeled with reasonably accuracy, and a suitable battery choice be made.

4.3.4 Gross Weight Model

Gross weight estimations were based on breaking down the aircraft into individual components or systems. Weight estimates were made for components that were required to operate the aircraft. A table was produced for the battery cells. The total weight of the propulsion system was calculated by adding the weight of the 825G motor and speed controller to the number of cells, the weight of a 3" spinner, and a 16x10 APC propeller. The payload of 6 lb was added to the total weight for the 1st and 3rd lap of the SRM, and removed for the 2nd and 4th using a logic statement. The weights of the landing gear and control system were assumed to be the target values from the conceptual design. The weight of the wing was modeled from the 2004 wing, which weighed 5 oz/ft of span. The fuselage weight was modeled upon predicted surface area and assuming a 2 oz/yd^2 fiberglass and 1/16" balsa core sandwich.

4.3.5 Dynamics of Flight Model

The dynamic simulation of the aircraft's flight was key in understand both the flight and structure requirements of the aircraft. The simulation focused on the fundamental dynamic forces to derive the velocity and position. The dynamic elements were then applied to a variety of equations to simulate the many aspects over the entire flight. The derived elements allowed us to begin the structural analysis with both the dimensions and forces known. The model used had three degrees of freedom, a pitching axis, a roll axis and a yaw axis motion.

4.3.6 Take-off and Climb

The simulation code was initialized with the aircraft on the ground. A logic statement is used to specify when the aircraft is on the ground, when it is, ground=1, when it is not, ground=0. This statement allows the application of wheel friction to the model, which is a function of the aircrafts normal force as sensed by the ground. As the vehicle accelerates, the friction decreases due to the decrease in normal force. Drag and lift increases with speed, which are also modeled. Thrust decreases with increasing speed, which is modeled using rotating wing theory. A counter is used to measure the distance the aircraft travels before the aircraft takes off. When it does take off, the counter is reset so that the critical takeoff distance can be found, which occurs during the third lap of the SRM. At take off, ground=0. If the aircraft fails to takeoff in 150 ft, an error is given and the user could change any part of the aircraft to remediate the problem.

Once airborne, another counter measures the time (dt) it takes to climb 30 ft during the steepest part of the ascent. With dY=30 ft and dt known, the rate of climb was calculated. The aircraft is allowed to climb until it reaches an altitude of 100 ft AGL. At this point, the AOA is no longer the maximum value, and the level flight condition is assumed.

4.3.7 Level Flight

The level flight simulation of the aircraft focused on the angle of attack. The key to the level flight portion of the code is maintaining the lift so it equals the weight of the aircraft at any time. The difficultly is the fact that lift changes with speed while the aircraft is accelerating in level. The AOA must change to compensate for the acceleration. By changing this value as opposed to using a constant, the aircraft's performance can be measured more accurately. The AOA is found by using a sub-loop that balances forces in the vertical direction by increasing or decreasing AOA in 0.1 degree increments.

4.3.8 Turning

The turning simulation of the aircraft focused on banking angle and calculating turn radius. The banking angle is important due to the inability of the aircraft to maintain a high angle of attack for level flight. A force balance equation is required to maximize the banking angle for the tightest turn possible. The banking directly effects lift by lowering the vertical lift, which must not go below the weight of the aircraft to complete a level turn. Another important aspect is the radius at which the aircraft makes the turn-in. If the turn radius is too small the velocity is reduced, but if the turn radius is too large time is lost because there is more distance to travel then required. A force balance equation along the fuselage axis was developed to maintain a constant turn velocity. With the radius and velocity known the gravitational loading could be calculated and applied to the structural calculation for flight components.

4.3.9 Descent and Landing

The descent and landing are similar to the takeoff and climb but with no thrust being produced by the aircraft. With the thrust reduced to zero in the beginning of the third turn the height in which the aircraft must descend is reduced to height less then 100 ft. With only 300 ft to travel before the aircraft must land it is important to reduce the height and speed. During the descent the velocity is decreasing so that ideally the speed at touch down is a bit higher than the stall velocity to minimize ground roll. The simulation calculates the AOA necessary to descend on a linear path that intercepts the runway 300 ft. before the center of the course. When the aircraft touches the runway, ground=1, so the friction can be considered. The rate of decent was directly applied to structural calculation required for landing components of the overall structure.

4.3.10 RAC Calculation

Based on all of the parameters loaded into the simulation code, RAC was calculated using the exact formulas specified in the 2005 rules. RAC was not optimized directly, but was optimized indirectly by reducing the size and weight of the aircraft to decrease mission time.

4.4 Predicted Mission Performance

A visual representation was used to ensure that the simulation was performing correctly. Figure 4.4 is a plot from the simulation code of the SRM. Turns are represented by teal circles at 100 ft. The chart illustrates how the thrust degrades with flight speed. Thrust is measured in lb, Velocity in ft/s, position in ft, and AOA in degrees. Current was integrated in the code to determine energy consumed. Takeoff distance of the third and most critical takeoff was 147 ft as verified on a similar chart. Voltage drop over time was based on a 16 cell 1300mA NiCd pack, with a measured decay rate of -0.034 V/s. This explains why the speed of the aircraft decreases each lap.

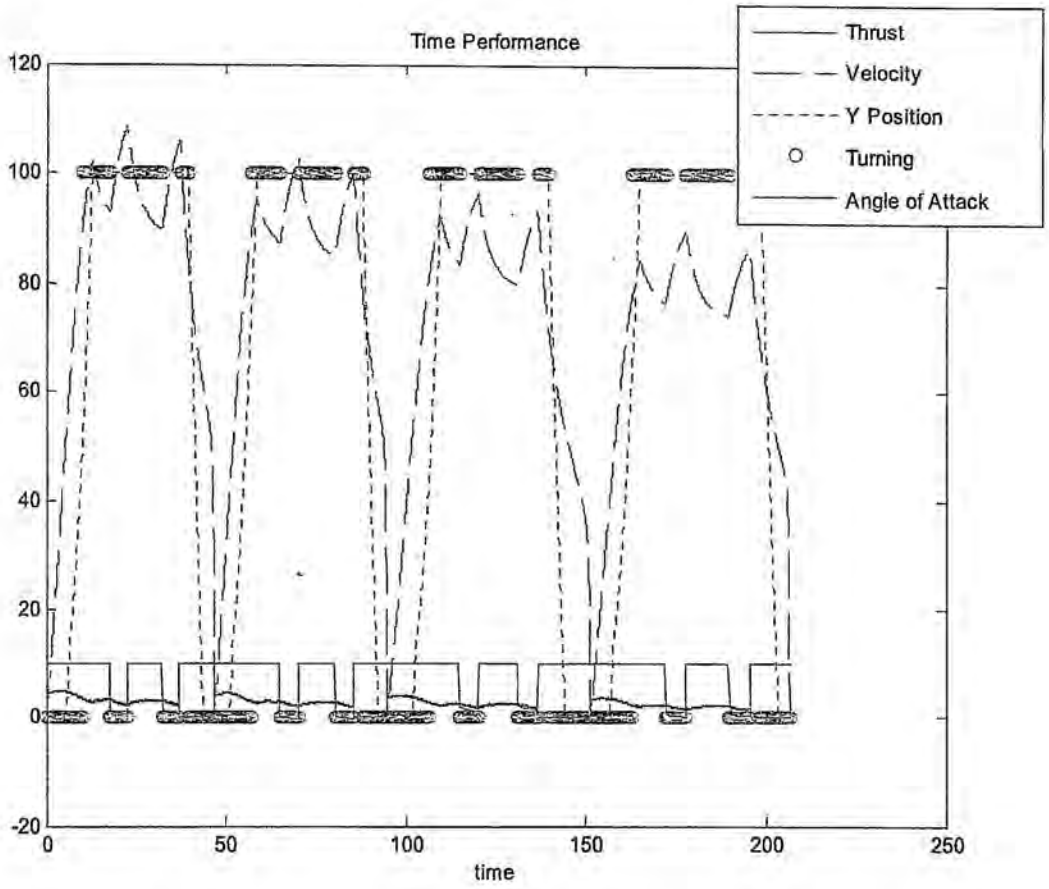

Figure 4.4 Predicted Mission Performance, Re-supply Mission

4.5 Estimates of Performance and Stability

4.5.1 Performance

After running the program through many aircraft configurations, the best designs were analyzed and compared. With many of the general aircraft parameters being predetermined only a limited number configurations had to be tried. The simulation code focused on verification of many primary design parameters, and what propulsion system would be required to complete the SRM. The final preliminary design was the end result of both the general aircraft design and the end propulsion system configuration, and is given in Table 4.5.1.

2005 DBF Best Configuration				
SCORE =	365.47		NUMBER_OF_CELLS =	18.00
SRM_FLIGHT_SCORE =	17.28		WING_SPAN =	5.50
RAC =	7.03		WING_AREA_SQUARE_FT =	4.58
FLIGHT_TIME_S =	201.65		ENERGY_CONSUMED_MAH =	835.67
STATIC_THRUST_OZ =	66.97		TURN_1_VELOCITY_MPH =	55.81
STATIC_PITCH_SPEED_MPH =	58.76		TURN_1_BANKANGLE_DEG =	72.00
STATIC_RPM =	6205.00		TURN_1_LIFT_LBS =	40.07
PEAK_CURRENT_A =	38.00		TURN_1_RADIUS_FT =	67.36
TOTAL_WEIGHT_LB =	12.34		TURN_1_FORCE_G =	3.25
THRUST_TOTAL_WEIGHT_RATIO =	0.34		TURN_2_VELOCITY_MPH =	61.13
TOTAL_WING_LOADING_OZ_PER_SQUARE_FT	43.07		TURN_2_BANKANGLE_DEG =	76.00
STALL_VELOCITY_MPH =	30.97		TURN_2_LIFT_LBS =	48.08
LIFT_OVER_DRAG_MAX =	16.12		TURN_2_RADIUS_FT =	66.03
RATE_OF_CLIMB_FT_PER_MIN =	610.17		TURN_2_FORCE_G =	3.90
CRITICAL_TAKEOFF_DISTANCE_FT =	147.29		TURN_3_VELOCITY_MPH =	59.13
MOTOR =	825.00		TURN_3_BANKANGLE_DEG =	75.00
PROP_DIAMETER_IN =	14.00		TURN_3_LIFT_LBS =	44.98
PROP_PITCH_IN =	10.00		TURN_3_RADIUS_FT =	66.33
			TURN_3_FORCE_G =	3.65

Table 4.5.1 Predicted Mission Performance Results

4.5.2 Stability

After achieving an optimized design, a detailed stability analysis was performed. Table 4.4.2a shows relevant stability and control derivatives for the cruising portion of the mission. The methods used were based on those from Nelson (1989) and Raymer (1999).

Czu	Cxα	Cyβ	Cnβ	Cℓβ
-0.6373	0.0929	-0.2466	0.0824	-0.0002
Czα	Cmα	Cyr	Cnp	Cℓp
-4.0194	-0.9795	-0.1670	-0.0697	-0.6721
Czά	Cmά	Cyδr	Cnr	Cℓr
-0.8431	-1.1417	0.1083	-0.0447	0.1246
Czq	Cmq	Cht	Cnδα	Cℓδα
-2.4058	-6.2550	0.5182	-0.0656	0.6891
Czδe	Cmδe	Cvt	Cnδr	Cℓδr
-0.2313	-0.6014	0.0357	-0.0330	0.0096

Table 4.5.2.a Stability Derivatives, at Cruise Speed, Per Radian

The stability derivatives above are only valid for small deviations from straight and level flight or where the change in forces or moments is linear. The two most important dynamic instabilities are directional divergence, and spiral divergence. Directional divergence is generally caused by a lack of static directional stability; $C_{n\beta}$. $C_{n\beta}$ is the change in yaw due to sideslip angle. Raymer suggests a value for $C_{n\beta}$ should be positive with a magnitude of about 0.06 for very low mach numbers. Raymer explains that NASA suggests a higher value, about 0.1, in NAST TN D-423.

Spiral divergence is generally caused by directional stability that is high and lateral stability that is low. Lateral stability, $C_{\ell\beta}$, is the change in roll due to sideslip angle. Raymer suggests that $C_{\ell\beta}$ should be a negative value about half the magnitude of $C_{n\beta}$. Many of the stability derivatives above are dampening derivatives. These include $C_{\ell p}$, C_{nr}, C_{zq}, C_{mq}, $C_{z\dot{\alpha}}$, and $C_{m\dot{\alpha}}$. The larger the magnitude of the derivative value, the more dampening exists. All of the stability derivatives were compared to stability derivatives of a general aviation aircraft from Nelson, achieving values that varied some in magnitude, but no different in the same sign. Cht and Cvt are not actual derivatives, but are the horizontal and vertical tail volumes. These are parameters used to calculate many of the stability derivatives. General sizing of the empennage based on historical values normally results in an aircraft that has adequate stability.

The rest of the stability derivatives are defined as:

C_{zu} = change in the Z-force due to speed derivative.
$C_{z\alpha}$ = change in the Z-force due to angle of attack.
$C_{z\dot{\alpha}}$ = change in the Z-force due to rate of change in angle of attack.
C_{zq} = change in the Z-force due to pitching velocity.
$C_{z\delta e}$ = change in Z-force due to elevator deflection.
$C_{x\alpha}$ = change in X-force due to angle of attack.
$C_{m\alpha}$ = change in pitching moment due to angle of attack.
$C_{m\dot{\alpha}}$ = change in pitching moment due to rate of change in angle of attack.
C_{mq} = change in pitching moment due to pitching velocity.
$C_{m\delta e}$ = change in pitching moment due to elevator deflection.
$C_{y\beta}$ = change in Y-force due to sideslip angle.
C_{yr} = change in Y-force due to yaw velocity.
C_{np} = change in yaw moment due to roll velocity.
C_{nr} = change in yaw moment due to yaw velocity.
$C_{n\delta a}$ = change in yaw moment due to aileron deflection.
$C_{n\delta r}$ = change in yaw moment due to rudder deflection.
$C_{\ell p}$ = change in roll moment due to roll velocity.
$C_{\ell r}$ = change in roll moment due to yaw velocity.
$C_{\ell\delta a}$ = change in roll moment due to aileron deflection.
$C_{\ell\delta r}$ = change in roll moment due to rudder deflection.

LCDP	TDPF	TDR	URVC	μ
0.088342	4.2348E-04	0.03246	0.013046	5.470223

Table 4.5.2.b Handling Quality Parameters

As defined by Raymer, LCDP is the lateral control departure parameter. LCDP focuses on the relationship between adverse yaw and directional stability. The TDPF is the tail-dampening power factor which is a product of TDR and URVC. TDR is the tail damping ratio and URVC is the unshielded rudder

volume constant. These figures were arrived at by adding an aerodynamic balance to the top of the rudder. This modification was made to the rudder, exposing approximately 12.5 square inches of rudder forward of a 60 degree line drawn from the leading edge of the horizontal stabilizer. This brought the value of TDPF and μ that was off of the chart in Fig 16.32 in Raymer (1999), to a value that was acceptable.

4.6 Results of Optimization Trade Studies Performed

The combination of the simulation code with individual optimizations of the wing, wing spar, propulsion system, and empennage resulted in what the team believes is the best possible aircraft for the SRM and RSM, within the team's financial budget, and within time constraints. The optimizations were combined in the next section to define the details of the aircraft's layout.

5.0 Detail Design

In the preliminary design, the design parameters were to maximize the overall score. This was accomplished by minimizing the rated aircraft cost while maximizing the flight score. Maximization of flight score was determined by choosing the SRM and RSM missions. A Matlab routine was used to perform calculations of various design parameters in order to optimize the specifications of the aircraft and yield the highest possible score. The result of that optimization and the final configuration of the aircraft is the detailed design.

5.1 Rated Aircraft Cost and Sized Aircraft Data

The final design changed little from the conceptual design. The final Rated Aircraft Cost is as follows in Table 5.1a. The final sized aircraft data can be found in Table 5.1b.

University:	Washington State University				
Team Name:	Wazzugar Flieger				
	RAC	6.91			
Empty Weight	6.41				
	REP	1.20			
# Engines	1				
Battery Weight (lb)	1.2				
	MFHR	125.32			
	Wing Subset	56.12		Fuselage Subset	19.20
Wing #1 Span (in)	73.61		Max Length (in)	48.17	
Wing Max Chord (in)	10.00		Max Width (in)	7.25	
Wing #2 Span (in)	0.00		Max Height (in, w/o landing gear)	4.75	
Wing Max Chord (in)	0.00			Empenage Subset	20
Controls Type, Enter "1" in correct type			# verticals w/ no controls	0	
Ailerons	1		# verticals with controls	1	
Flaperons	0		# horizontals (any)	1	
Ailerons+Flaps	0		V-tail (uncheck all others)	0	
Ailerons+Spoilers	0			Flight Systems	30
Ailerons+Flaps+Spoilers	0		#servos (any function)	5	
			#motor controller(s)	1	

Table 5.1a Rated Aircraft Cost

Geometry:	
Length	48.17 in
Span	73.61 in
Height	20.62 in
Wing Area	736.1 in^2
Aspect Ratio	7.325
Control Volume	Cht=.566 Cvt = .036

Preformance:	
CL Max (wing)	1.436
L/D Max (aircraft)	16.1
Maximum Rate of Climb	610 fpm
Stall Speed	27 mph
Maximum Speed	72.5 mph
Take-off Distance (empty)	55 ft
Take-off Distance (gross)	110 ft

Weight:	Lbf
Airframe Weight	3.5
Propulsion Weight	1.9
Control System Weight	0.91
Payload Rel. System Weight	0.1
Payload Weight	6
Empty Weight	6.41
Gross Weight	12.41

Wing:	
Airfoil	SG6042
Aileron Area (per side)	71.25 in^2

Horizontal Stabilizer:	
Airfoil	NACA 0009
Span	18.25 in
Tip Chord	6.75 in
Root Chord	10 in
Area	152.84 in^2
Elevator Area	45.625 in^2

Vertical Stabilizer:	
Airfoil	NACA 0009
Height	9 in
Tip Chord	6 in
Root Chord	13.2 in
Area	86.4 in^2
Rudder Area	31.875 in^2

Systems:	
Radio Used	JR 8103 PCM
Servos Used	Futaba S3102
Battery Config. Used	18 cell NiCd
Motor Used	Master Flight 825G
Propeller (nominal)	APC 14x10E
Gear Ratio	3.69:1

Table 5.1b Final Aircraft Configuration

5.2 Component Design and Selection

The simulation code did not calculate certain parameters because it would make the simulation code too complex. These were separated into different systems, analyzed in detail separately, and include the wing system, empennage system, control system, propulsion system, fuselage system, wing to fuselage interface system, and landing gear system.

5.2.1 Wing System

The wing system consists of three major criteria. These are the airfoil selection, the aileron system, and the wing spar.

5.2.1.1 Airfoil Selection

One of the important parts of designing the Wazzugar Flieger was choosing the airfoil. The aircraft, which has a maximum allowable weight of 13 lb, needs to take off within 150 feet. This means a high coefficient of lift is important. The aircraft will cruise at about 60 mph, so the drag at this cruise lift

coefficient needs to be low. A low RAC is desired for a higher total score, which can be achieved with a smaller wing area. Also, a payload of 3 pounds will be hung from underneath the wingtips and the shorter a wing, the easier it is to make it light and strong. The maximum wing span was therefore set at 6 feet.

Design requirements were made to set a target max lift coefficient of 1.5, with a minimum coefficient of 1.1 allowed. The target stall speed was set at 25 mph, but no more than 30 mph allowed. The coefficient of drag and the wing area were also desired to be a minimum. Two Reynolds numbers were looked at; one for cruise at 60 mph and one for take off at 25 mph. Assuming a 10 inch cord, the Reynolds numbers came to be about 464,000 and 193,000. The airfoils were evaluated at a Reynolds number of about 300,000 to simplify things.

After much searching through databases of airfoil data, the choices were narrowed down to seven profiles: Selig-Giguere SG6042, Selig-Donovan SD7032, Selig-Donovan SD7037, Selig-Donovan SD7062, Wortmann FX 63-137, Wortmann FX 76MP-140, and the Eppler E432. The coefficients of lift, coefficients of drag, and lift to drag ratios for the airfoils are shown in Figures 5.2.1.1a, 5.2.1.1b, and 5.2.1.1c respectively.

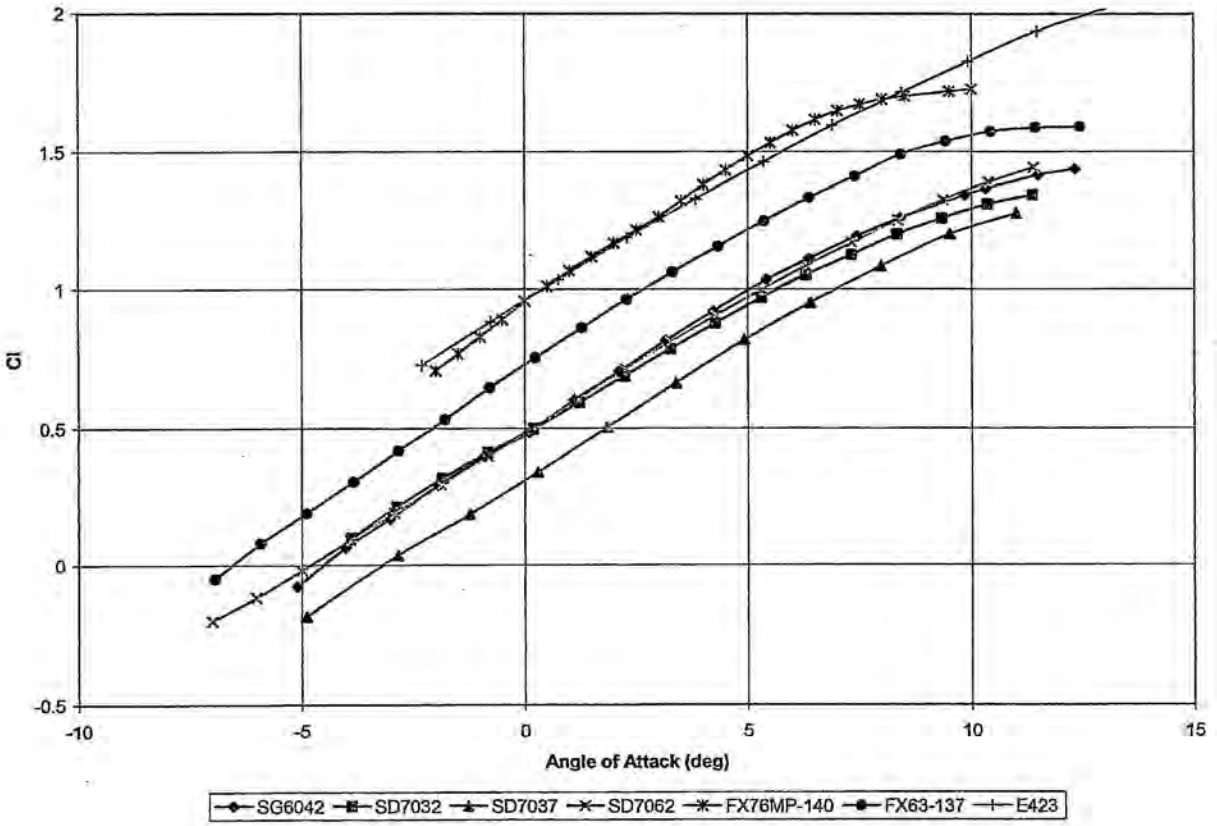

Figure 5.2.1.1a Coefficients of Lift

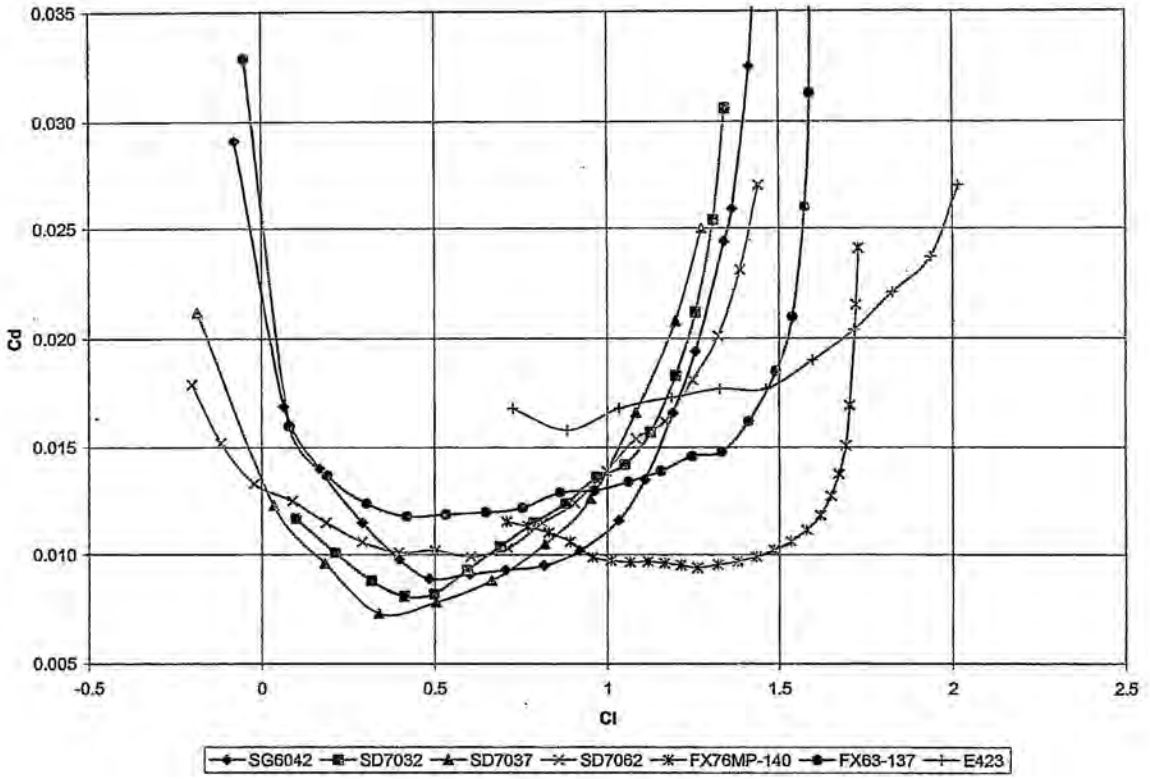

Figure 5.2.1.1b Coefficients of Drag

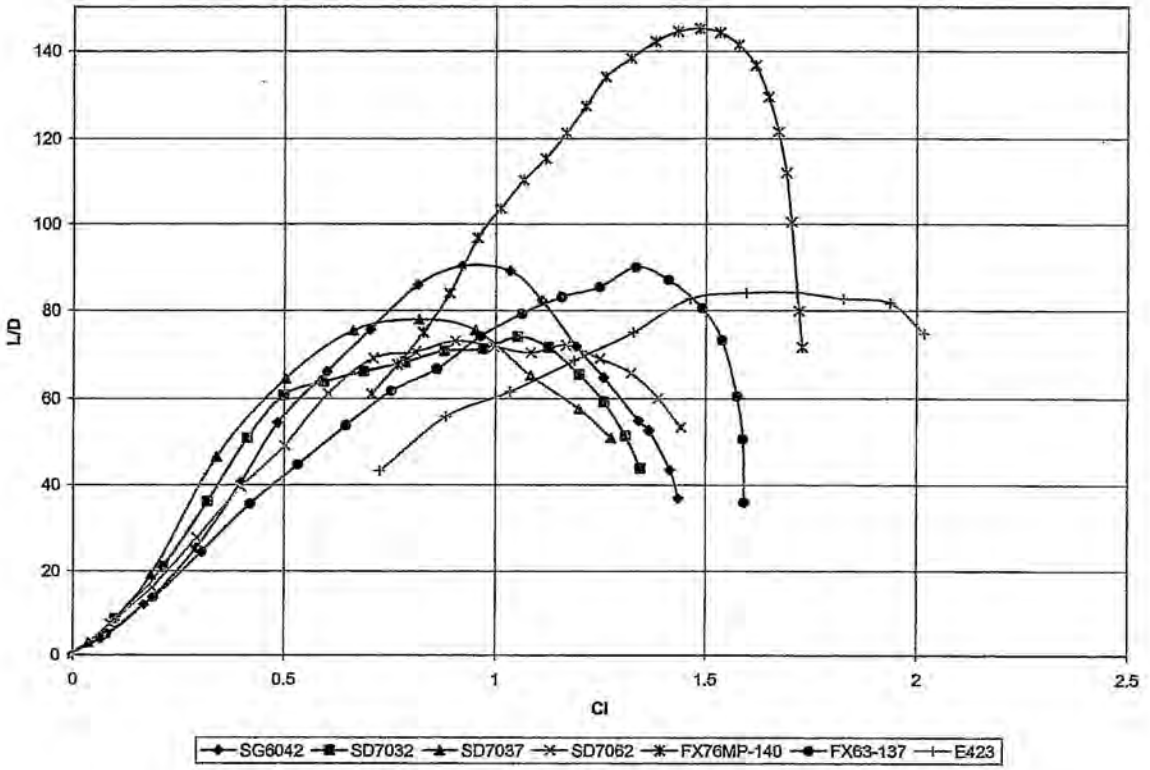

Figure 5.2.1.1c Lift to Drag Ratios

At takeoff, high lift is more important than low drag. At cruise, low drag is more important than high lift. To determine what the coefficient of lift and drag will be at cruise, the area of the wing needed for take off at the max coefficient of lift was calculated. This area was then used to calculate the lift coefficient at cruise. Sample calculations are shown below for the SG6042, and results are shown in Table 5.2.1.1.

$$V_t = 25mph = (25mph)\left(1.4667\frac{ft/s}{mph}\right) = 36.7\,ft/s$$

$$V_c = 60mph = (60mph)\left(1.4667\frac{ft/s}{mph}\right) = 88.0\,ft/s$$

$$\rho_{air} = 0.002377\,slugs/ft^3$$

$$c = 10in$$

$$L = 13lbs$$

$$Cl_{max} = 1.436$$

$$L = \tfrac{1}{2}C_l A\rho V^2 \Rightarrow$$

$$Span = \frac{2L}{Cl_{max}c\rho V_t^2} = \frac{2(13)}{(1.436)\left(\frac{10}{12}\right)(0.002377)(36.7)^2} = 6.80\,ft$$

$$L_t = L_c \Rightarrow \tfrac{1}{2}Cl_{max}A\rho V_t^2 = \tfrac{1}{2}Cl_c A\rho V_c^2 \Rightarrow$$

$$Cl_c = Cl_{max}\frac{V_t^2}{V_c^2} = 1.436\frac{36.7^2}{88.0^2} = 0.249$$

$$Cl_c = 0.292 \Rightarrow AOA_c = -1.94$$

$$\Rightarrow Cd_c = 0.0115$$

Airfoil	Max Cl	Span (ft)	Cruise CL	Cruise AOA	Cruise Cd	L/D	
SG6042	1.436	6.8	0.249	-1.9	0.0115	21.7	
SD7032	1.344	7.26	0.233	-1.9	0.0088	26.5	
SD7037	1.275	7.66	0.221	0.3	0.0073	30.3	
SD7062	1.442	6.77	0.25	-1.9	0.0106	23.6	
FX76MP-140	1.729	5.65	0.3	-2	0.0116	25.9	*
FX63-137	1.592	6.13	0.276	-3.8	0.0124	22.3	*
E423	2.018	4.84	0.35	-2.3	0.0168	20.8	*

*Lowest AOA with available data, actual drag at the appropriate CL may be significantly higher.

Table 5.2.1.1 Lift and Drag Comparisons at Cruise of 60 mph, stall of 25 mph.

As can be seen from the data, the wingspan required for different airfoils varies. Since a smaller span is desired, this gives airfoils with a higher C_L more consideration. The SD7032 and the SD7037 had the lowest drag, but also the largest wing area. The FX76MP-140, FX63-137, and the E423 all had small wing areas, but their problem was that they were designed for high lift. This meant the drag at the lower coefficients of lift was too high (in fact, data didn't even exist for the lower lift values needed at cruise), and so they were also ruled out.

This left the SG6042 and the SD7062. Although they both have similar lift curves, the SD7062 has slightly lower drag at max and min coefficients of lifts. However, since the lift to drag ratios at all of the

angles of attack between take off and landing were higher for the SG6042, we finally selected the SG6042 for our airfoil.

5.2.1.2 Aileron System

The aileron system needed to provide good roll control for maneuvering the aircraft in high speed turns, during low speed takeoff, and landing situations. Most important of all, the aileron size needed to be substantial enough to provide adequate control while carrying a payload total of 6 lb at the wingtips. This extra mass will require much more authority in order to control the aircraft. The sizing for the ailerons was determined by the forces needed in high and low speed situations.

The control system (aileron servo) needed to be sized correctly to deal with the loads experienced by the ailerons plus a safety margin. The ailerons were calculated to an appropriate size, resulting in a 2.5 inch chord and 28.25 inch length giving an overall area of 70.625 square inches. The ailerons were mounted inboard, leaving 4.75 inches on the outboard section of the wing. This was left to avoid aileron interference with the external payload. Also, this section reduces chances of a tip stall and lowers drag. With the extra mass at the wingtips, the effects of a tip stall become more severe. The use of ailerons at the wingtip can induce tip stalls, causing the aircraft to become harder to control.

5.2.1.3 Spar Setup

It was determined that the 33" wing spar would be 0.725" in height, have a carbon thickness of 0.021" on the bottom and top, and would have constant section the whole length. The outer diameter of the carbon tube would be 0.683" and be embedded 3.0" into the spar. These dimensions would allow for a deflection of 0.5" under maximum loading.

5.2.2 The Empennage System

Since the fuselage was required to fit in the 1 ft x 2 ft x 4 ft box quickly, it was sized at 48" long. With this short of a fuselage, the horizontal and vertical stabilizers need to be sized to ensure the stability of the aircraft. In the preliminary design, the aircraft configuration was analyzed for stability. From the results, it was determined that an aerodynamic balance needed to be added to the top of the rudder to put more rudder area in an area with airflow during a spin. The rudder area was sized as 31.875 in^2 on a vertical stabilizer with an area of 74.25 in^2.

5.2.3 The Control System

One aspect that plagued last years aircraft was having a simple, well routed, and reliable wiring system for the aircraft. This year, the aircraft will use as few electrical connections as possible by making a custom wiring harness. With the control surfaces sized, calculations for the loads on the surfaces were performed. The aileron and empennage control surface loads determined by the equation:

*Torque (oz-in) = 8.5E-6 * [(Surface chord (cm)^2 * Speed (MPH)^2 * Length (cm) * sin(ctrl surf. degrees) * tan (ctrl surf degrees)] / tan (servo degrees)*

From this equation, it was determine how much torque would be necessary to deflect each of the aircrafts control surfaces. The load on a servo was based upon the control surface size, which included the chord, length, deflection of the surface, deflection of the servo, and the maximum aircraft speed. In Table 5.2.3, the loads are calculated for all the surfaces at maximum deflection at maximum speed.

	Torque Load	Max Airspeed	Surface Chord	Surface Length	Surface Deflection	Servo Angle	Surface Deflection	Servo Angle
	Oz-In	mph	cm	cm	Radians	Radians	Degrees	Degrees
Aileron	51.92	72.5	6.35	71.76	0.611	1.571	35	90
Rudder	29.12	72.5	6.35	22.86	0.785	1.571	45	90
Elevator	59.05	72.5	6.35	46.36	0.785	1.571	45	90

Table 5.2.3 Control Surface Loads

To control the ailerons, one servo was placed in each wing. It was determined that the reliability of the aileron system would be compromised by having a long, complex linkage connect both ailerons to a single servo. The connection to the control surface was made by using standard servo linkages.

After determining the number of servos and the loads required for the servos, the number of cells and capacity of our receiver battery was determined. It was decided to use a five cell receiver battery because of better servo performance at six volts, and reliability if a cell were to fail (short only). It was determined that the cells needed to handle a worst case servo and receiver load of two amps for a theoretical situation where two flight attempts were made, each lasting at most five minutes. This would require a cell capacity of 0.333 Ah. From this, the best brand and model cells for the receiver battery pack was determined to be a HiCell 350 1/3 AA 6.0V.

5.2.4 The Propulsion System

Based on the simulation code, the final configuration requires 4.5 lbs of static thrust for takeoff on the third lap of the sensory reposition mission, which must be achieved with a partially drained battery. The simulation code models the voltage decay of the batteries as they are discharged. It was determined that the thrust and duration requirements could be met with the correct combination of prop, motor, and battery: an Astro Flight 825G motor, an 18 cell pack of Sanyo CP1300SCR cells, and an APC 14x10E propeller.

5.2.5 The Fuselage System

Since the fuselage needed to contain the payloads, the internal area needed to be large enough to hold both payloads, but minimized to reduce drag. It was determined that a side-by-side payload configuration would work the best. The materials used on the fuselage were desired to be as light and

rigid as possible. For extra rigidity, a center-plate was designed to fit between the top and bottom sections of the fuselage.

5.2.6 Wing to Fuselage Interface

The wing to fuselage interface consists of a wing endplate and reinforced holes in the stressed skin. A rod connects all the parts and runs from one wing, through the fuselage and centerplate, to the other wing. To keep the wing from rotating about the spar, two stabilizer pins were built into the wing assembly and inserted into holes of the fuselage. The pins were made of nylon so that if there was excessive force on landing, they would shear and the wing would hopefully be spared. To provide a quick release for the wing, a plastic card was constructed to provide a locking mechanism between the fuselage and the nylon bolt.

5.2.7 Landing Gear System

The landing gear was attached to a mounting bracket located on the wing spar. Since the payloads have to be mounted on the wingtips, ground stability is an important issue. After many calculations, it was determined that the landing gear should be 37.23 inches wide to give the plane adequate ground stability. The landing gear was sized to provide 1.24 inches of ground clearance for a 16" propeller. It was determined that the landing gear needed to have low drag and be stiff to provide good landing characteristics with little bounce. Steel was the material chosen to construct the landing gear because of its strength properties.

5.3 Drawing Package

The next four pages display the drawing package. Included in the drawing package is a 3-view of the aircraft, an exploded parts detail, a payload system detail, and a fit in box detail.

6.0 Manufacturing Plan

By using figures of merit and some calculations, manufacturing methods for all of the components were investigated and determined. For each component, a material (or combination of materials) and a construction method were selected. A construction plan was then scheduled for each component.

6.1 Manufacturing Processes and Component Selection

The figures of merit, or matrices, were set up with qualities on the top row, and weights for each quality on the next row (all weights adding up to 1). On the left, a column with different construction options was laid out. Matrices for all major components were generated: wings, fuselage, landing gear, and empennage. The team based the different matrices on a minimum of four qualities; Strength to weight, smooth surface, easy to build/rebuild, and durability. Additional qualities were considered on some components.

Strength to weight is the primary concern for this year. Considering the weight problems encountered during 2003-2004, a special effort was made to keep component weight under control. By going overweight, many other parts and systems are compromised. Achieving the weight goals is critical to being able to meet our design goals. For a given propulsion system, components that are as light as possible allow an aircraft to achieve a higher speed and shorter takeoff. Weight is also the most important factor in determining the rated aircraft cost, or RAC. An effort to reduce RAC as low as possible is required to maximize scoring potential.

The next concern is having a smooth surface. A smooth surface can make a noticeable difference in drag. A rough and wavy surface will produce more drag than a glass smooth surface with an accurate profile, and more drag means more motor power is required to maintain speed. This leads to higher drain on the batteries and shorter flight time, yielding a lower score.

Another desired quality was an easy-to-build/rebuild airplane. If a crash occurs during flight testing, components may need to be repaired or replacement parts reconstructed quickly.

The last quality is durability. With the possibility of loosing all the points for a flight mission by having "significant damage", this quality became mission critical. Each matrix quality was weighted differently for each component, since the components have specific needs.

6.1.1 General Material Selection

Many components were designed using fiber reinforced polymer matrix composites, so finding the best fiber material for our application was important. For cloth, the material of choice was determined to be S-glass. If availability was ignored, carbon fiber would have been the best fiber material. The availability of carbon fiber in woven form that was light enough was an issue. To meet weight goals, cloth that was 2.5 oz/yd or less was required. An exception is where load paths were known. In those locations, unidirectional carbon fiber was the material of choice because it was available in thin sheets. This allowed the weight requirements to be achieved. Kevlar, while great in tension and exceptionally tough, is poor in

compression. With a three pound payload on the wing, the torsion stiffness of the wing became an important factor. Concerning fiberglass options, S-glass outperforms E-glass in all significant aspects. While E-glass is offered in more varieties of light cloth than S-glass, one available weave S-glass was sufficient to meet most of the needs for composite lay-ups.

Composite Matls.	Availability	Stiffness	Strength/Weight	Durability	Score	Rank
Weight	0.4	0.2	0.2	0.2		
S-glass	**80**	**75**	**75**	**85**	**79**	**1**
E-glass	100	60	60	65	77	2
Kevlar	70	50	80	100	74	3
Carbon Fiber	0	100	100	60	52	4

Table 6.1.1 Composite Material Matrix

6.1.2 Wings

Wing Construction	Strength/Weight	Surface Quality	EZ Build/Rebuild	Durability	Score	Rank
Weight	0.3	0.3	0.2	0.2		
Foam Core	**100**	**75**	**90**	**85**	**87.5**	**1**
Shell over foam	100	100	40	85	85	2
Spar and Shell	85	100	65	75	83.5	3
Stressed Skin	70	100	60	60	75	4
Built-up Balsa	50	50	50	30	46	5

Table 6.1.2 Wing Construction Matrix

For the wings, it was determined that the best construction method was the simplest; a foam core wing. It is light, fast, easy to make, cheap, and results in a relatively accurate wing profile. If easy-to-build was not as much of an issue, having a shell-over-foam wing would be the second choice, since it would produce better surface quality while remaining strong and light.

6.1.3 Fuselage

Fuselage Construction	Str./Wt.	Surf. Qual.	EZ Build	Low Frontal Area	Door-ability	Score	Rank
Weight	0.3	0.2	0.1	0.1	0.3		
Stressed Skin, Neg. Mold	**100**	**100**	**80**	**100**	**70**	**89**	**1**
Built-Up Balsa	100	75	50	70	90	84	2
Spar and Shell	60	85	65	85	100	80	3
Stressed Skin, Foam Core	75	50	70	70	70	67.5	4

Table 6.1.3 Fuselage Construction Matrix

For the fuselage, it was determined that the best method of manufacturing was a stressed skin using a negative mold. While a bit more skill and time is required in building the molds than in fabricating

the other methods, it produces a very light, low cost fuselage with a great surface finish. In this matrix, low frontal area and "door-ability" were included in the desired qualities. Different construction methods have limitations.

For the fuselage, a PVC pipe payload needs to be loaded and removed through a door. In order to have the smallest frontal area possible (thereby minimizing drag), the fuselage construction needs to have minimal structural thickness. A built up balsa or foam core fuselage would need more internal room for structure. A stressed skin fuselage would be thin and minimize the physical size of the airplane. "Door-ability" was an important evaluation criterion, since the re-supply mission requires the payloads to be inserted to and extracted from the inside of the fuselage. Constructing a door in the fuselage affects the stress distribution in the structure and must be considered in the design.

6.1.4 Landing Gear

Landing Gear	Availability	EZ Build/Rebuild	Energy/Weight	Durability	Smooth Surf.	Value	Rank
Weight	0.2	0.2	0.3	0.2	0.1		
Steel	**100**	**100**	**100**	**90**	**70**	**95**	**1**
Aluminum	100	80	70	70	80	79	2
Titanium	60	80	80	70	80	74	3
Magnesium	40	80	70	60	80	65	4
Carbon fiber	100	60	30	50	70	58	5

Table 6.1.4 Landing Gear Material Matrix

For the landing gear, it was determined that the best material was steel. Landing gear needs to be able absorb energy and steel can absorb the most energy with respect to its weight. Although it doesn't have the highest specific strength or specific stiffness, it is quite resilient. Carbon fiber may have the highest specific strength and specific stiffness, but the elastic strain to failure is very small. Metals can be easily bent into the desired shape, but some have limitations on bend radii. Steel is the easiest of the materials to form, requiring only a vice, a hammer, and some pliers. Steel is also able to tolerate deformation during impact, which is desired in case of a hard landing. Bent landing gear can also be easily straightened. Even though a small, smooth round section produces as much drag as an aerodynamic section several times thicker, an easy fix is constructing a simple, light fairing to cover the wire.

6.1.5 Empennage

Empennage	Strength/Weight	Surface Quality	EZ Build/Rebuild	Durability	Value	Rank
Weight	0.3	0.3	0.2	0.2		
Foam Core	**100**	**75**	**90**	**85**	**87.5**	**1**
Spar and Shell	85	100	65	75	83.5	2
Shell over foam	100	100	30	85	83	3
Stressed Skin	70	100	50	60	73	4
Built-up Balsa	50	75	70	30	57.5	5

Table 6.1.5 Empennage Construction Matrix

The empennage decision matrices were similar to the wing, except that built up balsa was easier to build in this case because of the smaller surface sizes. Stressed skin and shell-over-foam become difficult to build because additional time required. The empennage parts are smaller than the wing, but a similar amount of time is involved with CAD/CAM and cutting the mold. The best method was still a foam core, because it is fast, easy to make, cheap, and relatively accurate. Again, if easy-to-build were not as much of an issue, having a shell-over-foam would produce better surface quality, while remaining strong and light.

6.1.6 Payload Deployment

To produce a small, light, tough, and reliable mechanism for the payload deployment required some brainstorming and trial-and-error. Commercially available RC airplane bomb releases did not meet the needs of our aircraft's payload mechanism, which needed to be manually reloadable and remotely actuated. Since the payloads at each wingtip need to be released separately and the RAC needed to be kept low, finding a method to release one payload independent of the other with only one servo was required. Because of the concentration of stress, we focused on using metals. Pinning together some sheet and square stock aluminum with brass wire and inserting a spring produced an ingenious mechanism. Similar to a gun's trigger mechanism, it had a spring loaded shear pin release that would release the payload when pushed by a wire. A single servo in the fuselage of the plane was used to push a wire in either direction, actuating only one trigger at a time.

6.2 Manufacturing Processes of Major Components

In the past, manufacturing parts has always proven to be more complicated than originally anticipated. To alleviate the amount of problems encountered during the manufacturing process, many sources on manufacturing methods were consulted. After reviewing the research conducted, manufacturing processes for each component were chosen.

6.2.1 Wings

The wings were made with a foam core built around a balsa/carbon fiber/Kevlar spar and covered with a thin sheet of balsa. The foam core was cut using a hot wire and airfoil profile templates. The slot for the wing spar is also created with a hot wire. The wing spar itself consisted of an end-grain balsa core, uniaxial carbon fiber strips on the top and bottom, and Kevlar tape wrapped around all of it. Epoxy was used as the reinforcing matrix and a vacuum bag was used to ensure quality construction. The end closest to the fuselage transitioned to a 3" long carbon fiber tube so that an aluminum tube could be used to connect the two wings to fuselage. A nylon screw with a plastic card keeper was used to keep the wings from sliding out or rotating.

6.2.2 Fuselage

The fuselage construction used a female mold and a vacuum bag. The fuselage runs from the firewall to where the fuselage tapers to the center plate. It was constructed from two halves, top and bottom. The sandwich lay-up was bonded together using epoxy and consisted of 3 layers with balsa as the inner layer, S-glass as the outer. The firewall core was made of balsa and thin plywood was used to strengthen the outside faces. The top front of the fuselage opens like a car hood so that the motor and batteries can be accessed and the rear doors will provide access to other components. A center plate runs along the entire length of the aircraft and serves as a structural I-beam, the tail boom, and also the vertical stabilizer. This center plate is a sandwich a thick balsa core and an S-glass outer layer.

6.2.3 Landing Gear

The landing gear was made by bending a piece of music wire to the desired geometry. A plywood adapter holds one end of the wire and attaches to the wing spar with nylon bolts. This provides a predetermined failure point to absorb energy and minimize damage to the wing in the event of a crash or very hard landing. The wheels are commercially available and made of lightweight foam. The nose gear is also a commercially available unit made from steel wire. In order to reduce drag, the wire has a simple, lightweight fairing.

6.2.4 Empennage

The horizontal stabilizer was manufactured using the same method as the wing. A foam core was hotwired out, covered with balsa, and then covered with S-glass. The center plate of the fuselage transitions into the tail boom and the structure for the vertical stabilizer. A simple spar intersects with the tail boom to provide structure for the horizontal stabilizer. Inside the fuselage, servo control linkages are routed to the control surfaces.

6.2.5 Electronic Components

The radio gear was selected based on the transmitter used to control the aircraft (JR 8103 PCM). It was decided to use the existing JR 8 channel PCM receiver. The only connections are at the receiver, which means there aren't multiple servo extension wires with connections to come loose. The receiver antenna is routed along the center plate of the fuselage. Five servos (rudder/nose wheel, left and right aileron, elevator, and payload release) and an electronic speed control make up the control outputs.

After calculating the required torque in the detailed design, the required loads for the ailerons, rudder, and elevator were found. The servos selected were chosen based on various attributes. The aircraft demanded that the servos not only have sufficient torque, but also gears that would not strip out. The most important requirement was choosing the lightest servos possible. It was determined that the Futaba S3102 would best fit our needs.

To power the receiver and servos, a five cell 350 mAh NiMH battery pack was specified to save on weight. The increase in voltage to the servos allowed operation at higher torque levels. Also, if a cell shorted out, the other four cells could provide the performance of a normal four cell receiver battery.

6.2.6 Payload Deployment System

The payload deployment system consists of a small, high-torque servo with a paddle attached to the servo arm that pushes on the end of a wire rod. Two wire rods go to each of the payload release mechanisms. This setup can independently deploy either the left or right servo, and allowed the wing to be removed quickly.

6.3 Manufacturing Dependencies

During the process of building the plane, certain parts need to be finished before others can begin construction. The table below outlines the production sequence.

Step	Process	Dependencies	Est. MFG time (Man-hrs)
A	Construct and wax fuselage mold		20
B	Construct payload release mechanisms		10
C	Fabricate payloads		8
D	Fabricate landing gear		20
E	Fabricate firewall		2
F	Hot wire foam wing core		3
G	Hot wire foam horiz. & vert. stabilizer		3
H	Construct wing spar		12
I	Form fuselage core	A	6
J	Lay-up fuselage	I, A	30
K	Assemble & vacuum bag wing and spar	H,F	8
L	Install propulsion system	J,E	1
M	Lay-up empennage	G	4
N	Install electronics, batteries, and servos	L, N, O, M	4
O	Install landing gear	K	1
	Total Man hours		132

Table 6.3.1 Manufacturing Dependencies

6.4 Skills Matrix

To effectively predict the time and difficulty of manufacturing a part, a skills matrix was developed to evaluate various tasks. This was necessary to ensure that the most skilled personnel worked on the more difficult components. In table 6.4.1, different components are in the rows, and tasks are in columns. A skill level is assigned to each task for each component. Using the skills matrix, personnel were assigned tasks based on their competency.

Component	CAD modeling	CAM & Construction	Lay-up	Assembly	Controls & wiring
Fuselage	4	4	3	2	1
Payload release mech.	2	3	N/A	3	1
Payloads	2	3	N/A	2	N/A
Landing gear	2	2	N/A	1	N/A
Firewall	1	1	N/A	2	N/A
Wing	3	2	3	1	1
Empennage	3	2	2	1	1
Wing spar	2	2	2	2	N/A
Propulsion System	2	2	N/A	1	1
Skill levels: 1: Easy, 2: Some Skill Req., 3: Moderate Skill Req., 4: Extensive Skills Req., N/A: Not Applicable					

Table 6.4.1 Component Task Skills Matrix

6.5 Manufacturing Milestones

Below is a chart showing the manufacturing schedule. The bars in blue show the planned schedule. The bars in magenta show the actual event.

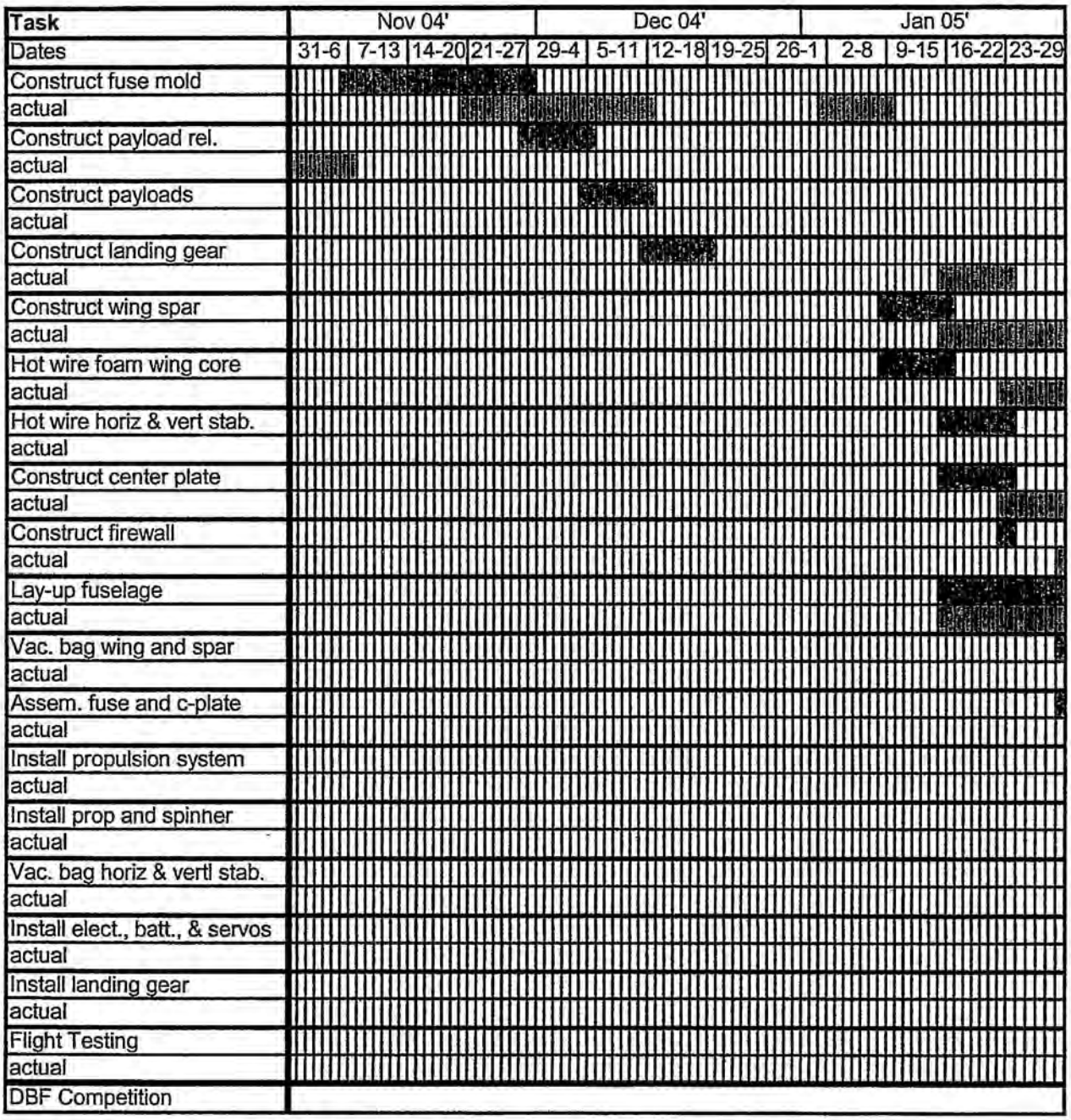

Table 6.5.1 Manufacturing Schedule, November 2004 to January 2005

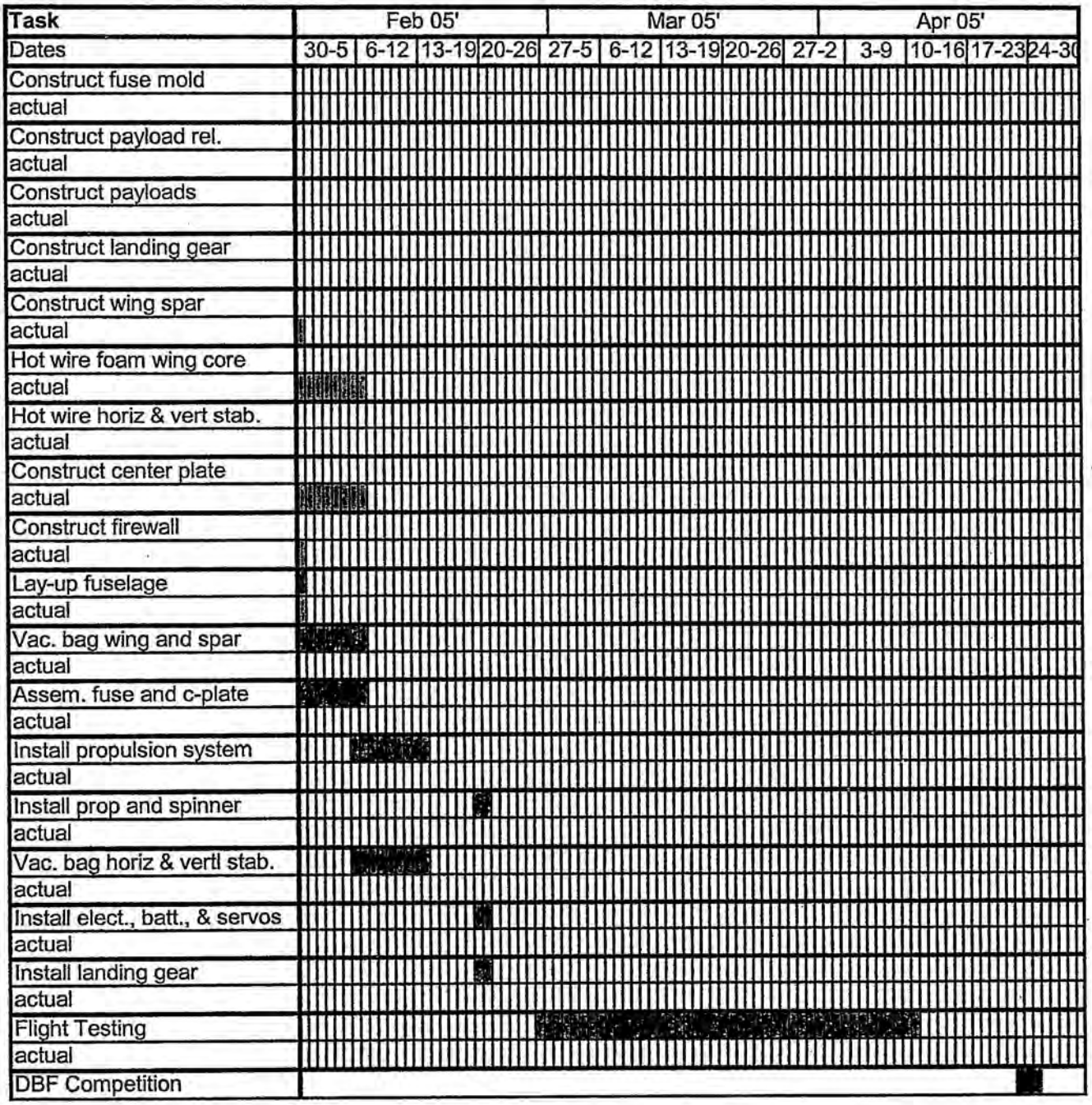

Table 6.5.2 Manufacturing Schedule, February to April 2005

7.0 Testing Plan

Testing is critical to the manufacture of a successful aircraft. Questionable analytical data and calculations can be verified with real world results. Testing can show weaknesses, design flaws, and oversights. Testing can also be used as a method for optimization to find the best combination of components for the aircraft.

7.1 Test Objectives and Schedules

The objective of our tests is to verify calculations made. The first series of tests will be static propulsion system tests. Given a particular propulsion system setup, data is recorded for thrust, current, and voltage. This is compared to data from the simulation code program. From this data, changes to how the simulation code models thrust and current was made. The second test will be the flight test. Checklists for the flight and testing can be found in the tables below.

7.2 Flight Testing Checklists

WING:

[ ] No dents, warps, or any damage
[ ] Control surfaces mounted
[ ] Hinges tight (give control surfaces slight tug)
[ ] Control horns tight, no slop or loose screws
[ ] Clevises threaded on with thread exposed
[ ] Clips on all clevises
[ ] Payload linkage complete
[ ] Covering completely attached

FUSELAGE:

[ ] Fiberglass without dents, cracks, warps, or any damage
[ ] Paint is without cracks or peeling

TAIL:

[ ] Horizontal Stabilizer on securely
[ ] Vertical Stabilizer on securely
[ ] Control surfaces mounted
[ ] Hinges tight (give control surfaces slight tug)
[ ] Control horns tight, no slop or loose screws
[ ] Clevises threaded on with thread exposed
[ ] Clips on all clevises
[ ] Covering completely attached

LANDING GEAR:

[ ] Landing gear attached and strong

[ ] No bends or fatigued areas

[ ] Wheels roll freely and are without damage

[ ] Wheel collars secured properly

ELECTRONICS:

[ ] 2 screws attaching each servo securely

[ ] Servo head screws in securely

[ ] All linkages mounted strongly to fuselage and unable to move

[ ] Speed controller properly attached and without damage

[ ] All wires have shielding intact

[ ] Wiring is mounted to fuselage and unable to interfere with servos

[ ] Connectors show no wire and are connected

[ ] Batteries mounted securely without damage to heat shrink

MOTOR:

[ ] Propeller and spinner balanced and mounted securely

[ ] Motor mounted properly to fuselage

[ ] Gear box oiled with all teeth satisfactory

PREFLIGHT CHECKLIST:

[ ] Voltage with load applied exceeds 6 volts on servo battery

[ ] Voltage with load applied exceeds 19.2 volts on motor battery

[ ] Transmitter voltage exceeds 9.6 volts

[ ] Wing is secured with wing bolts tight

[ ] Center of Gravity is at proper location

[ ] When full throttle is applied motor runs too full

[ ] Record full throttle rpm_____

[ ] When left stick is moved left, rudder moves left

[ ] When left stick is moved right, rudder moves right

[ ] When right stick moves left, left aileron goes up, right aileron goes down

[ ] When right stick moves right, left aileron goes down, right aileron goes up

[ ] When right stick is pulled back, elevator goes up

[ ] When right stick is pushed forward, elevator goes down

[ ] When payload drop switch is activated, payloads drop freely

[ ] Surfaces move freely with no glitches

[ ] Aircraft taxis straight

[ ] Wind is noted in direction and speed by pilot

RANGE CHECK:

(Test to be performed from 100ft with antenna collapsed)

[ ] Servos move in proper directions without glitches at zero throttle

[ ] Servos move in proper directions without glitches at full throttle

[ ] Test radio fail safe

7.3 Flight Testing Procedure

The documented flight test procedure consists of 15 flights to test the capabilities of the aircraft and its ability to carry out the mission objectives. From these flights, improvements will be made which will aid in development of the team and aircraft for competition.

Each flight must be accompanied by a thoroughly completed preflight checklist. These flights will be performed with the safety of people and the aircraft a priority. If at any time, a member determines the test to be unsafe, it shall be immediately cancelled and changed to satisfy the concerns of the team. After each flight, an aircraft flight evaluation will be completed by the pilot. In this evaluation the flight characteristics will be listed as well as anything out of ordinary and suggestions for possible improvements. From this post flight report the aircraft will be refined to perform at the competition as efficiently as possible.

7.3.1 Flight Test #1

Objectives: Basic Aircraft Testing

Payloads: Unattached

Scheduled Date: March 5, 2005

A few high speed taxi tests at reasonable speed will be performed to get an understanding of rolling characteristics. After pilot feels comfortable with the aircraft on the ground, a take off will be performed and the pilot will do several laps to get a basic feeling for the airplane. Once the airplane is trimmed and seems to be flying well, the pilot will climb to a higher altitude and test low speed and stall characteristics. Once pilot has basic understanding for the aircrafts behavior, a landing approach will be attempted, followed by a landing. Upon landing, the checklist will be run through again. All screws and bolts will be checked for tightness and batteries for voltage. Flight time will also be recorded to aid us in understanding the capabilities of the airplane. If problems are noticed, they will be rectified as best as possible and the flight will be repeated.

7.3.2 Flight Test #2

Objectives: Flight Time Evaluation – Full Throttle

Payloads: Unattached

Scheduled Date: March 5, 2005

The pilot will take off with a fully charged battery pack and fly at a high speed in large uniform laps. This path will be maintained until motor seems to slow or lose power. Upon noticing this, the pilot will land the aircraft and the motor battery's voltage with applied load will be checked. If flight time is not

adequate, battery capacity will be rethought. This flight can be repeated as many times as necessary using different components, such as batteries and propellers, to optimize performance.

7.3.3 Flight Test #3

Objectives: Flight Time Evaluation – Low Throttle

Payloads: Unattached

Scheduled Date: March 26, 2005

This test is similar to test #2, except at a lower throttle setting. The pilot should perform the same laps as in test #2 at very low throttle setting. This is an attempt to make the flight time as long as possible. The aircraft will not be flown on the verge of stall but at a smooth controllable speed. Again, when power loss is noticed the aircraft will be landed and voltage checked. If flight time is not adequate, battery capacity will be rethought. This flight can be repeated as many times as necessary using different components, such as batteries and propellers, to optimize performance.

7.3.4 Flight Test #4

Objectives: Testing Aircraft Capabilities

Payloads: Unattached

Scheduled Date: March 26, 2005

To test the capabilities of the airplane, a flight will be performed at high speeds with tight turns. Loops, rolls, and spins will also be done to ensure strength and recovery techniques in case of an emergency. The aircraft is designed to be capable of 6.5 g loading, both negatively and positively. With the ability of the aircraft ensured, load testing can be done. This flight can be repeated as many times as necessary using different components, such as batteries and propellers, to optimize performance.

7.3.5 Flight Test #5

Objectives: Mass Testing

Payloads: Internal

Scheduled Date: April 2, 2005

Taxi and flight characteristics of the aircraft will be tested and noted with two internally mounted payloads of varying weight. Payload test weights will be performed at 1 lb, 2 lb, and 3 lb each. A stall test with each weight will be performed to ensure flight safety and flight time will be noted.

7.3.6 Flight Test #6

Objectives: Mass Testing

Payloads: External

Scheduled Date: April 2, 2005

Taxi and flight characteristics of the aircraft will be tested and noted with two externally mounted payloads of varying weight. Payload test weights will be performed at 0.5lb, 1 lb, 1.5 lb, 2 lb, 2.5 lb, and 3 lb each. A stall test with each weight will be performed to ensure flight safety and flight time will be noted.

7.3.7 Flight Test #7

Objectives: Sensor Reposition Drill

Payloads: External

Scheduled Date: April 9, 2005

The aircraft will perform the sensor reposition mission as instructed in the competition rules. The flight will be timed and everything performed as would be at the contest. This flight will be performed as often as necessary to improve the time, score, and individual and team proficiency.

7.3.8 Flight Test #8

Objectives: Maximum Utilization Drill

Payloads: Internal

Scheduled Date: April 9, 2005

The aircraft will perform the maximum utilization mission as instructed in the competition rules. The flight will be timed and everything performed as would be at the contest. This flight will be performed as often as necessary to improve the time, score, and individual and team proficiency.

7.3.9 Flight Test #9

Objectives: Re-Supply Drill

Payloads: External

Scheduled Date: April 9, 2005

The aircraft will perform the re-supply mission as instructed in the competition rules. The flight will be timed and everything performed as would be at the contest. This flight will be performed as often as necessary to improve the time, score, and individual and team proficiency.

7.4 Summary of Test Results and Lessons Learned

Tests performed to date have shown significant differences between published data for motor performance and data collected in tests. Much of this difference has to do with the voltage drop of the battery packs. Collecting data to accurately model voltage drop was essential to determining the overall performance of the aircraft in mission models. The lesson learned here was that the reliability of manufacturer's data can be suspect. Having an independent analysis of performance can prove to be quite valuable.

References

Raymer, Daniel P., *Aircraft Design: A Conceptual Approach,* 2nd Ed., AIAA, Reston VA, 1999.

Nelson, Robert C., *Flight Stability and Automatic Control*, McGraw-Hill, New York, 1989.

Boucher, Robert J., *The Electric Motor Handbook*, AstroFlight, 1994.

Shigley, J. E. and Mischke, C. R., *Mechanical Engineering Design*, 6th Ed., McGraw-Hill, Boston, 2001.